INFORMATION TO USERS

This manuscript has been reproduced from the microfilm master. UMI films the text directly from the original or copy submitted. Thus, some thesis and dissertation copies are in typewriter face, while others may be from any type of computer printer.

The quality of this reproduction is dependent upon the quality of the copy submitted. Broken or indistinct print, colored or poor quality illustrations and photographs, print bleedthrough, substandard margins, and improper alignment can adversely affect reproduction.

In the unlikely event that the author did not send UMI a complete manuscript and there are missing pages, these will be noted. Also, if unauthorized copyright material had to be removed, a note will indicate the deletion.

Oversize materials (e.g., maps, drawings, charts) are reproduced by sectioning the original, beginning at the upper left-hand corner and continuing from left to right in equal sections with small overlaps. Each original is also photographed in one exposure and is included in reduced form at the back of the book.

Photographs included in the original manuscript have been reproduced xerographically in this copy. Higher quality 6" x 9" black and white photographic prints are available for any photographs or illustrations appearing in this copy for an additional charge. Contact UMI directly to order.

UMI

A Bell & Howell Information Company
300 North Zeeb Road, Ann Arbor MI 48106-1346 USA
313/761-4700 800/521-0600

Université d'Ottawa · University of Ottawa

MODELLING OF POLLUTANT TRANSPORT IN COMPOUND OPEN CHANNELS

By

Jean Georges Chatila

A Thesis*
submitted under the supervision of
Dr. Ron D. Townsend

in partial fulfilment of the
requirements for the degree of
Doctor of Philosophy
in
Civil Engineering

Department of Civil Engineering
University of Ottawa
Ottawa, Ontario
Canada, K1N 6N5
September, 1997

*The Ph.D of Civil Engineering Program is a joint program with Carleton University, administrated by the Ottawa-Carleton Institute for Civil Engineering

To my Parents,

Sisters,

and

Brother

ABSTRACT

An increasing amount of effort in computational hydraulics is being devoted to the simulation of contaminant dispersion in rivers and coastal waters. Many important problems in water resources engineering involve the mass transport of a miscible fluid in a flow. When sewage is discharged into a body of water, it is often desirable to be able to predict the concentration of the materials downstream from the release point. A conservation equation for the discharged material can be used in this prediction. Applying such an equation requires that: (i) the general hydraulics of the stream; (ii) any physical, chemical, biological changes in the material; and (iii) the rates of mixing with respect to the velocity used in category (i) are known. In general, the results of channel-flow simulations are often used as the hydrodynamic basis for water quality analysis and/or modelling. While much work has been carried out in the past on steady and unsteady 1-D flow simulations of pollutant transport in channels of simple cross-section, the literature indicates that there are few papers describing tracer experiments in compound channels. The one-dimensional (1-D) analogy can be useful if one is only interested in the mixing far from the source. However, if one needs to predict the mixing relatively close to a source concentrated at one bank, it may be necessary to employ a two-dimensional (2-D) analysis to obtain useful results. 2-D models are capable of predicting the depth-averaged concentrations anywhere in the cross-section. In developing pollutant transport models for natural watercourses it is important to properly account for complex channel geometry where warranted.

The present research investigates the numerical and experimental modelling aspects of flow in compound channels, with special interest in the transport of inert pollutant aspects. This is examined through developing a 2-D finite difference mathematical model, ***(CHAT: Compound-channel Hydraulics And Transport),*** to solve the flow and transport equations for open channels having compound cross-sections. The numerical computation of open-channel flows requires preparing and processing larger volumes of boundary and bathymetry

data for computer inputs and the development of numerical algorithms for treating complex boundary condition, channel properties, and free surface effects. Derivation of the basic differential equations is based on the Navier-Stokes equations of continuity and fluid motion, in addition to the convection-dispersion equation. These equations are derived in three dimensions (3-D), however, in order to simplify the problem and ease the computational effort, the equations are integrated over the depth (depth-averaged). Most finite difference methods for calculating the convection portion of the transport equation are plagued by artificial (numerical) diffusion. This is sometimes stronger than the physical diffusion and can render the calculations useless. Therefore, as far reliability of the results is concerned, selection of the numerical scheme is critical.

Data for the verification and validation of the developed mathematical model was obtained through dye-tracer experiments performed in a large concrete channel of the Hydraulics Laboratory, University of Ottawa. Consideration was limited to conservative, non-buoyant material. The study investigates the impact on the mixing processes of strong lateral momentum transfer effects associated with severely compound flow fields. The experiments include measurements of dye concentrations downstream from slug-injection or steady-injection point source(s). Longitudinal and transverse mixing coefficients were calculated using the method of moments and by estimation using empirical relationships.

In general, it is not possible to obtain analytical solutions to the dispersion equation in natural waterways with arbitrary boundary conditions. However, a variety of exact solutions exists for idealized situations, which can be useful in obtaining order-of-magnitude estimates. These exact simplified solutions were applied to our experimental data.
The comparison between measured and predicted concentration curves by the developed model shows a level of agreement in the general shape, peak concentrations and time to peak. Different statistical methods were considered in evaluating the simulated results.

ACKNOWLEDGEMENTS

Special and sincere appreciation is expressed to Dr. Ron D. Townsend for his assistance, guidance, and supervision of this research.

The author is grateful to Mr. R. Moore, the Hydraulics Laboratory technician for constructing the experimental facility.

Special thanks are extended to my friends Mr. E. Makhoul, Mr. J. Daoud, and Mr. J. Abou Assaly for their support and encouragement.

The author also wishes to thank his parents, sisters, brother, nephew, and niece for their understanding, patience, and ever-lasting encouragement and overwhelming support.

TABLE OF CONTENTS

ABBREVIATIONS

1-D	:	one-dimensional,
2-D	:	two-dimensional,
3-D	:	three-dimensional,
ADI	:	alternating direction implicit,
ADZ	:	Aggregated Dead Zone,
BE	:	boundary element,
BTCS	:	Backward-Time Centered-Space method,
CORMIX	:	Cornell mixing Zone expert system,
DA	:	depth-averaged,
DO	:	dissolved oxygen concentration,
DISPER	:	convection-dispersion simulation model,
EDS	:	environmental data system,
FD	:	finite difference,
FDE	:	finite difference equations,
FEM	:	finite element method,
FESWMS	:	Finite Element Surface Water Modelling System,
FTCS	:	Forward-Time Centered-Space method,
FV	:	finite volume,
GIS	:	geographical information system,
HPRB	:	Holly-Preissman reach-back,
LMT	:	lateral momentum transfer,
M	:	momentum correction factor,

N & S	:	Nash and Sutcliffe criterion,
ONELAY	:	one layer hydrodynamic model,
PDE	:	partial differential equations,
PEE	:	proportional error of estimate,
POLTRA	:	pollutant transport model,
ppm	:	parts per million,
ppt	:	parts per trillion,
PTM	:	pollutant transport model,
U.S.EPA	:	U.S. Environmental Protection Agency,
REE	:	reduced error of estimate,
RMCC	:	residual mass curve coefficient,
RMSE	:	root mean square error,
SEE	:	standard error of estimate,
SS	:	sum of squares,
TARE	:	total absolute relative error,
TSAA	:	total overall sum of absolute areas of divergence,
TSAR:	:	total overall sum of absolute deviations,
TSSR	:	total overall sum of squared residuals,
USTFLO	:	unsteady flow model.

NOTATIONS

A	=	flow area,
A'	=	stream tube area perpendicular to the flow direction,
a_x	=	coefficient to be calibrated,
a_y	=	coefficient to be calibrated,
c	=	mass concentration of diffusing solute,
C	=	depth-averaged concentration,
C_a	=	cross-sectional average concentration,
C_o	=	dimensional constant, (C_o = 1 for SI units and C_o = 1.49 for English units),
c_v	=	empirical constant,
d	=	flow depth over flood plain,
D	=	flow depth in main channel,
F	=	Coriolis factor,
FR	=	fluorometer reading,
F_x	=	body force per unit mass in the x direction,
F_y	=	body force per unit mass in the y direction,
F_z	=	body force per unit mass in the z direction,
g	=	gravitational acceleration,
H	=	water level refrenced to a datum,
h	=	water depth below a datum,
h_+	=	value of a quantity h just after a grid point,
h_-	=	value of a quantity h just after a grid point,
$h^=$	=	average of any quantity h,
$h^{-t/2}$	=	average, in time, of a quantity h

h^{-x} = average of any quantity h in the x-direction,

h^{-y} = average of any quantity h in the y-direction,

h_x = difference of any quantity h in the x-direction,

h_y = difference of any quantity h in the y-direction,

i = grid indicator in x-direction,

j = grid indicator in y-direction,

K_n = an artificial diffusion coefficient introduced by the approximate nature of FD scheme,

K_x = longitudinal mixing coefficient,

lb = left boundary of the stream tube,

L_r = ratio length in the model to that in the prototype,

m = time level indicator,

MC = measured concentration,

n = Manning's roughness coefficient,

n_m = Manning's roughness in the model,

n_p = Manning's roughness in the prototype,

n_r = ratio of Manning's roughness coefficient in the model to that in the prototype,

P = fluid pressure,

Q = Q(x,y,t) or discharge,

Q_r = ratio of discharge in the model to that in the prototype,

r = reaction coefficient,

rb = right boundary of the stream tube, (facing downstream),

s = sources or sinks present,

S_r = scale distortion,

S_{fx} = friction slope in the x direction,

S_{fy} = friction slope in the y direction,

S_{ox} = bottom slope in the x direction,

S_{oy} = bottom slope in the y direction,

t	=	time,
t_r	=	ratio of time in the model to that in the prototype,
u	=	velocity component in the x direction,
U	=	depth-averaged longitudinal velocity,
$\mathbf{u}$	=	velocity vector with components u, v, and w,
u_*	=	shear velocity,
U_a	=	cross-sectional average velocity,
v	=	velocity component in the y direction,
V	=	depth-averaged transverse velocity,
w	=	velocity component in the z direction,
W_x	=	wind stress in the x direction,
W_y	=	wind stress in the y direction,
x	=	distance in the longitudinal direction,
X_r	=	scale factor in the horizontal direction,
y	=	distance in the transverse direction,
Y	=	distance measured from the outer left edge of the flood plain,
Y_r	=	scale factor in the vertical direction,
z	=	distance in the vertical direction,
ϵ_x	=	empirical mixing coefficient in the x direction,
ϵ_y	=	empirical mixing coefficient in the y direction,
ϵ_z	=	empirical mixing coefficient in the z direction,
ρ	=	fluid density,
ν	=	fluid kinematic viscosity,
υ_t	=	eddy viscosity,
k-ϵ	=	parameters of the turbulence model,
Δt	=	time increment,
Δx	=	longitudinal distance interval,
Δy	=	transverse distance interval,
τ_{bx}	=	bottom shear stress,

$h(i\,\Delta x, j\,\Delta y, m\,\Delta t)$ = a spatial grid point at time level m,

$\delta_x h$ = derivative of any quantity h with respect to x,

$\delta_y h$ = derivative of any quantity h with respect to y,

$\delta_{t/2} h$ = derivative of any quantity h along the time level,

LIST OF TABLES

LIST OF FIGURES

LIST OF PLATES

CHAPTER ONE

INTRODUCTION

1.1 INTRODUCTION

In a surface water system, runoff, floods, droughts, and stream water quality interact very closely. Excessive rainfall from extreme storms results in flooding along rivers whereas shortage of rainfall due to drought causes minimal stream flows, reduced water supply, restricted navigation and poor water quality. Rivers, estuaries, and other waterways have long served many important uses for humankind although they have been subjected to stresses by diverse human activities. Such uses and stresses have made it necessary for hydrologists and hydraulicians to research and understand the complicated behavior of water movement and interaction with its environment, by means of computer simulation and/or experimental verification. Engineers are concerned with the processes that take place between the point where the pollutant is discharged into the water environment and some other sites where the ambient water quality is observed. For a long time, they have had the responsibility for drawing our water supply from natural water bodies; now they must pay equal attention to how it is returned in diminished amounts and of poorer quality.

Flood Routing is the process of tracing by calculation the course of a flood wave along a channel and/or through a reservoir. In large measure, it is the problem of applying

the principles of unsteady flow to open channel systems. Flood Routing can also be defined as a mathematical method (model) for predicting the changing magnitude and celerity of a flood wave as it propagates along a river, (Chatila, 1992). It is employed in practice for the solution of a wide variety of problems associated with water use. Some of these include: (i) predicting flood hydrographs for given or assumed initial conditions, (ii) determining hydrographs modified by reservoir storage, (iii) evaluating past floods for which records are incomplete, (iv) studying the effects of water resources development on the downstream flow conditions, and (v) using results of hydrodynamic models for *water quality and pollutant transport modeling*.

An increasing amount of effort in computational hydraulics is being devoted to the simulation of contaminant dispersion in rivers and coastal waters. The general subject of water quality modeling is a vast one, (Djordjevic, 1993). Although many aspects of water quality modeling can be considered to be completely independent of unsteady flow modeling in open channels, one essential factor links the two disciplines: transport of dissolved or suspended substances. Transport refers to the hydrodynamic process of dispersion or, in other words, the interaction between *differential convection* and *turbulent diffusion* which are both dependent upon the flow velocity field. In general, ***the results of unsteady channel flow simulations are often used as the hydrodynamic basis for water quality models.*** Thus, often the need for water quality models must be taken into account in the construction of hydrodynamic models. In addition, the numerical representation of physical reality in transport models is subject to the same kinds of constraints as in river flow modeling.

Many important problems in water resources engineering involve the mass transport of a miscible fluid in a flow. When sewage is discharged into a body of water, it is important to ascertain how the sewage is dispersed in the receiving water. Velocity is usually defined on an average basis in a finite volume. Actually, the fluid particles are not moving with the same velocity. They tend to separate from one another. Thus, it is necessary to regard the flow as capable of some dispersive action. Mass transport in open channel flow can be

simulated on different levels, (Djordjevic, 1993). These levels range from simple one-dimensional (1-D) models, which should be used only for estimation of the global amounts of given matter in the river, to the rather complicated procedures based on refined turbulence modeling, which enables three-dimensional (3-D) prediction of concentration and velocity fields even in the vicinity of outlet structures, (ibid). It is often desirable to be able to predict the concentration of the materials downstream from the release point. A conservation equation for the discharged material can be used in this prediction. The use of such an equation really requires at least three categories of knowledge; namely, (i) the general hydraulics of the stream, e.g. velocity, depth, cross-sectional shape, ...etc; (ii) any physical, chemical, biological changes in the materials; and (iii) the rates of mixing with respect to the velocity used in category (i).

Computational hydraulics is the reformulation of the hydraulics equations to suit the digital machine process, allowing for algorithmic representation of natural phenomena. Models incorporate differential equations with no direct mathematical solutions. In general, they are solved numerically by replacing the partial differential equations (PDE) with equivalent (approximating) finite difference equations (FDE). However, other solution techniques are available, including finite element methods (FEM) or the boundary element method (BEM).

1.2 STATEMENT OF THE PROBLEM

The growing intensity of land and water resources utilization has renewed efforts towards systematic research in the field of alluvial hydraulics. Drinking water distribution, storm drainage systems, irrigation networks, flood forecasting and pollution control are becoming increasingly important as water resources become scarcer. Many flow phenomena of great importance to the engineer are unsteady in character, variable with time, and cannot be reduced to steady flow. Unsteadiness implies that the velocity may be increasing and the streamlines themselves may be shifting. The equations of motion are not solvable in the most

general case. Explicit solutions are possible in certain cases, which are physically very simple but are real enough to be of engineering importance. For the less simple cases, approximations and numerical techniques can be developed which yield solutions of satisfactory accuracy.

In recent years, one of the problems that has become increasingly important is predicting the ecological consequence of discharged wastes or substances into bodies of water, (Fischer et al., 1979). Modeling of water pollution has advanced from the simple 1-D analyses to the more accurate and complicated 2-D and 3-D approaches. A necessary prerequisite to making ecological predictions is to assess the changes in the concentration distribution of the water body due to effluent discharges. The redistribution of heat or any other substance from a source into a water body occurs through a series of turbulent transport processes. The main mechanisms affecting the redistribution include momentum and buoyancy of the discharge; turbulence, current, and density structure of the ambient fluid; surface transfer; and the solid boundaries. Near the source of discharge it can be expected that momentum and buoyancy of the effluent would be important in influencing the mixing process. On the other hand, far from the source it may be imagined that the ambient current and turbulence would be dominating factors. In between, all mechanisms may contribute to the dispersion process. In general, when the problem of predicting the temperature or substance concentration distribution is concerned, the solution is divided into *far* and *near* fields .

Flood routing and water quality considerations are important in compound channels, particularly when relatively shallow sections (flood plains) adjoin a deep (main) section. A major area of uncertainty in river channel analysis is that of accurately predicting the capacity of compound channels consisting of a central main channel and one or two side flood plains. If the compound section is treated as a single channel, discharge capacity is under-estimated, (Chatila and Townsend, 1996), while if the more common method of dividing the section into main channel and flood plains is employed then the capacity is generally over-estimated,

(ibid). The cross-section is usually divided in such a way as to insure hydraulic homogeneity in flow computations. In general, numerical models developed for predicting the transport and fate of pollutants in rivers assume, for simplicity, that the river can be considered as a single prismatic channel of regular shape. However, during a major flood event the flow field takes on a compound shape. A unique feature of compound channel flows is the lateral momentum transfer (LMT) phenomenon occurring along the interface regions that separate the main channel and flood plain zones, (Zheleznyakov, 1965 and 1971). To the author's knowledge, there are a very few pollutant transport models that take the *compound-channel* effect into consideration. Moreover, these models are based on some simplifying assumptions that limit their generality or applicability. For example, Djordjevic (1993) developed a mathematical model for unsteady transport in compound channel flows and verified it experimentally. He stated that the velocity can be determined using some of the Manning-type equations, taking for granted that the depth-averaged (DA) velocity is proportional to the local depth raised to a certain power (depending on which friction coefficient is used). This method, however, does not take the horizontal momentum transfer into consideration, which leads to rough estimations of the velocity field. As a result, any refined dispersion modelling with a doubtful velocity field is unreasonable. Djordjevic (1993) used the DA x-direction conservation of momentum equation derived by Rastogi and Rodi (1978). Based on the assumption that the flow has insignificant secondary currents, Rastogi and Rodi omitted the so-called ***dispersion*** terms. These terms account for vertical non-uniformities in the longitudinal and transverse velocity components. Furthermore, if the ***inertia*** terms are also neglected then the resulting equation is valid only for ***uniform*** flows. However, it was still applied for the calculation of velocity distribution in ***non-uniform*** flow. In addition, the variation of the DA velocity with time term ($\partial u/\partial t$) and the effects of wind stresses were dropped from the corresponding equation.

In view of the above discussion clearly, there is a need to improve the simulation of open-channel flows and hence pollutant transport processes in rivers having compound cross-sections.

1.3 STUDY NEEDS

1.3.1 NUMERICAL MODELLING

During periods of flood, the wetted perimeter of a river channel increases rapidly as the flow spreads over the flood plain zone(s). This can be catastrophic as flood plains of rivers are considered to be the most productive agricultural lands as well as attractive locations for dwellings and other structures. To alleviate the problem of perennial flooding various flood control measures need to be introduced. These include the construction of storage reservoirs to reduce peak flows, and flood embankments (dikes) to confine flows within the main channel. The design of such flood control structures depends primarily on flood routing techniques and their reliability in predicting, with reasonable accuracy, flows in the resulting compound sections.

The extension of unsteady flow theory to compound channels presents a number of complications and uncertainties, (Lai, 1986). This is due to the different flow phenomena and transport processes associated with this type of flow, which are not yet well understood. In general, a river's composite section may be divided into (i) a deep section, which serves for both storing and conveying water, and (ii) adjacent flood plain(s), largely believed to play a storage role only. However, item (ii) can be justified only under special conditions, i.e. where flow depths on the flood plain(s) are relatively small compared to that in the main channel. Flood plain flow has been shown to depend on channel geometry, boundary roughness, and the flood return period. For the less frequent (extreme flood) events the flood plain flow can be as large as the main channel flow and in these circumstances the composite section can be treated as a single unit, (Bhowmik and Demissie, 1982). In the case where flood plains are believed to contribute to stream conveyance, but not to the extent that the composite section can be treated as a single unit, the generally adopted procedure is to increase the main channel top width to compensate for the flood plain flow contribution, (Liggett and Cunge, 1975). This technique, though simple and easy to use, is very arbitrary and its general use is therefore

questionable. The procedure might be appropriate in the case of shallow flood plains, however, it should not be applied when relatively high flood plain depths are encountered. In fact, based on an analysis of flood flows field data of several streams, Bhowmik and Demissie (1982) observed that the discharge carrying capacity of flood plains reached as much as 80% of the total flow in the system.

During the progression of flood waves the depth varies along the stream and mass exchanges across verticals at the boundary breaks will become more pronounced. The difference in velocities between the main channel and the flood plains results in a deceleration of flow in the deep section and an acceleration in the flood plain zones. The LMT mechanism is too complex to be modeled analytically; however, many empirical procedures are available in the literature to account for it, (Yen and Overton, 1973; Wormleaton et al, 1982; Prinos and Townsend, 1983; Dracos and Hardegger, 1987; and Wormleaton and Merret, 1990). It is worth mentioning that excluding LMT in the simulation process may lead to significant inaccuracies in river stage and discharge calculations, numerical modelling, sediment transport and erosion computations, and water quality and pollutant transport, (Wormleaton and Merrett, 1990). ***Literature on the subject shows that few studies have addressed the numerical modelling aspects of pollutant transport in compound channels. In the case of a severely compound channel, strong LMT will clearly have a marked effect on pollutant transport therein. Since the majority of existing numerical transport models ignore LMT effects in their formulations, in general they may not be accurate for applications involving compound channels.***

Further to what has been stated above, the increasing pollution of seas, estuaries and rivers requires the development of methods simulating quantitatively the propagation of dissolved or suspended material in the water. The same is true for the spreading of heat, (Maier-Reimer, 1982). The most important means is to treat the transport equation (advection-diffusion) numerically. Cunge et al. (1980) recommended that future research should deal with the mathematical modelling of transport of neutrally buoyant conservative

substances by river flows including the time-dependent evolution of pollutant concentration. This can be performed either by a flood propagation model or measured. Also, Cunge et al. (1980) stated that, since the time scale of the mixing phenomena is generally much shorter than the time over which significant changes in water discharge occur, the steady-flow approach, which simplifies the transport equations, is usually justified.

The ASCE Task Committee on Verification of Models of Hydrologic Transport and Dispersion (1987) recommended that an important question for further research relates to the use of automated calibration and/or expert systems approaches. These approaches attempt to relieve the analyst of much of the burden of coefficient tuning. However, no evaluation of the adequacy or accuracy of these procedures has been done for surface water models. One should be aware of the fact that calibrating the *mixing coefficients*, so as to better reproduce observed concentrations, may only be compensating for numerical simulation errors and/or incomplete hydraulic data. The more accurate the numerical method used and the more faithful the schematization of the physical flow field, the better the chance to find mixing coefficients that are representative of the real physical phenomena.

In general, it is not possible to obtain analytical solutions to the dispersion equation in natural waterways with arbitrary boundary conditions. However, a variety of exact solutions exists for idealized situations, which can be useful in obtaining order-of-magnitude estimates. Sauvaget (1985) suggested two areas of research development which are closely related to the subject of inert contaminant dispersion. The first area deals with the application of inert contaminant techniques to the computation of sediment transport in rivers. Most of the numerical techniques are directly transferable. The second area concerns adaptation of numerical techniques for the accurate computation of linear contaminant advection to non-linear momentum advection. Also, Sauvaget (1985) found that the predictive capability of contaminant models is presently severely compromised by the inability of the commonly accepted functional form of the DA transverse mixing coefficient to incorporate the effects of transverse secondary flow, even in straight reaches. He proposed some accurate numerical

methods to be employed to minimize the purely numerical error. Moreover, he stated that there was a need for fundamental research and analysis geared to the development of a complete description of the DA transverse mixing process. ***It can be concluded that future progress in numerical modelling of contaminant transport in surface waters and particularly in rivers will depend more on an improved understanding of the physical processes involved than on improved numerical methods.***

As stated above, many existing transport models have been developed assuming a single regular-shaped channel flow. In addition, they are mostly 1-D steady or unsteady flow models. This research specifically addresses these two modelling limitations, in that: (i) THE NUMERICAL MODEL DEVELOPED, CHAT (Compound-channel Hydraulics And Transport), IS A 2-D UNSTEADY FLOW MODEL, AND (ii) CHAT IS CAPABLE OF SIMULATING TRANSPORT PROCESSES IN CHANNELS HAVING COMPOUND CROSS-SECTIONS.

1.3.2 EXPERIMENTAL VERIFICATION

Physical hydraulic models of rivers have permitted the study of flood waves, and their use as flood predictors has been responsible for the saving of countless lives and untold value of property, (Abida, 1992). Holly (1985) reported that although emphasis is mainly concentrated on numerical models and their theoretical basis, it should be recognized that under certain circumstances reduced-scale physical models offer an alternative means of investigation. However, Fischer and Holley (1971) reported that the primary restriction to the use of physical models is that scale distortion cannot legitimately be used.

Abbott (1976) reported that there has been several notable failures of computational models and these have already led to a discrediting of mathematical modelling in some quarters and even a reversion to physical modelling as a less problematical alternative. However, in some instances mathematical models are unavoidable, especially when wind

stresses, salinity variations or similar influences are important. The literature indicates that modelling practice continues to generate new computational hydraulic problems far faster than it solves them. Many of these problems are profound, difficult and interesting material for significant research. Research should concentrate more on the study of problem fundamentals rather than on building and running mathematical models. It is important that a model gives good and useful outputs. An excellent method to verify the output of a mathematical model is to run it against data obtained from a physically-scaled model of the prototype system. Thus, experimental verification remains a good validation procedure.

Experimental tracer measurements are frequently used to recognize and study certain flow phenomena and to validate and calibrate mass transport mathematical models. It is useful to perform experiments in compound channels in order to understand the complex flow structure and to verify mathematical models. Recently a number of experimental works utilizing straight compound channels have been carried out, (Shiono and Knight, 1991; Tominaga and Nezu, 1991; and Noat et. al, 1993). In light of these investigations, secondary currents are found to be significant in the vicinity of the junctions between the main channel and the flood plain(s) of compound channels. Although these secondary currents are only a few percent of the longitudinal velocity, they may significantly influence solute transport processes because they not only convect solute (or substance), but also affect the exchange coefficients of momentum and solute (or substance).

It is worth noting at this point that the literature indicates that there are still very few research papers dealing with tracer experiments in compound channels, (Arnold et al., 1985). Djordjevic et al. (1989) reported an experimental tracer investigations in a compound laboratory channel. However, the authors state that the analysis has been made for a rather narrow cross section. The width/depth ratios adopted were close to the limit under which depth-averaging is not reasonable. Thus, the extrapolation of the above conclusions to other channel geometries is not straightforward. The width of their experimental facility was 68 cm and the depth ranged between 23.7 and 26.4 cm. Thus, the aspect ratio ranged between 2.58

and 2.87. Prinos and Townsend (1984) reported that when the main channel was made narrow, their mathematical model did not reproduce the observed isovel patterns satisfactorily. Sauvaget (1985) stated that in river flow, the width is great in comparison to the depth, and homogeneous distribution is reached more quickly vertically than horizontally over the river's cross-section. Consequently, it is often possible to assume that the contaminant is uniformly mixed over the depth. All of the above comments were considered in developing this experimental programme at the University of Ottawa. For example, among the novel aspects introduced, the present channel width to depth ratios ranged between 4.2 and 6.0, (in order to ensure that depth-averaging of the equations was valid). Moreover, the conditions under which the current experimental programme was performed, were more realistic, re: the assumptions in the model development. For these reasons, the present research relied on an important experimental component.

1.4 STUDY OBJECTIVES

The literature on the subject indicates that 1-D models are not able to fully describe the pollutant transport process in rivers. Moreover, very few publications deal with the transport of pollutants or contaminants in rivers with compound sections. It can be argued that a 3-D model is required for more precise simulation of the flow field. However, the effort and cost of developing a 3-D model would likely outweigh the improvement gained over a 2-D model simulation. Thus, a 2-D model is generally considered to be a reasonable compromise between the simplified 1-D simulation and the difficult to model 3-D version.

The Objective of this study was to develop a 2-D DA FD model, (CHAT), to solve the complete conservation of mass and momentum equations and the convection-dispersion equation describing the transport of inert pollutants in compound channels, without introducing major simplifications. LMT effects, which are specific to compound channel flows, are

accounted for through the eddy viscosity terms rather than applying the k-ϵ model. A semi-implicit semi-explicit FD method is used to solve the discretized PDEs in a multi-operational manner to reduce numerical errors. Important related objectives of this research were model calibration and verification. ***Data for these exercises were obtained from dedicated laboratory studies of dye tracer (pollutant) transport in compound-channel flows.*** The cross-section of a 1.5m wide by 0.76m deep by 29m long rectangular-shaped flume in the Civil Engineering Department's Hydraulics laboratory was converted to an asymmetrical compound shape for this purpose.

It is important to search for a suitable numerical method or scheme, which involves either selecting one among numerous existing schemes or developing a new one tailored to the purpose. Also, it is important to check the method or scheme of choice for its *adequacy, reliability, and efficiency.* Sound knowledge of numerical techniques is a basis for these tasks.

1.5 THESIS DESCRIPTION

Chapter two deals with the major related research contributions of past years. The literature review is presented in a thematic as well as chronological order.

Chapter three deals with the theoretical and mathematical formulation of the flow and transport problems with all pertinent assumptions and simplifications.

Chapter four reviews possible numerical schemes that can be used in solving the PDEs. Also, a proper scheme is selected in this instance that minimizes artificial diffusion.

Chapter five deals with the experimental data that was measured for the purpose of calibrating the new mathematical model and checking its capabilities. This chapter also addresses the question of steady-state dispersion in compound open channels.

Chapter six compares the mathematical model outputs to the experimental data sets. Also, model calibration and performance are discussed along with an error analysis.

Chapter seven presents conclusions and recommendations for future research.

Chapter eight provides a list of references consulted during the research.

CHAPTER TWO

LITERATURE REVIEW

2.1 INTRODUCTION

It is important to have a complete picture of what has been previously presented in the literature in order to address the need for further research. Available results that are satisfactory can continue to be used in practical considerations and results that pose problems should be studied in future research.

When materials are discharged into rivers, it is often desirable to be able to predict the concentration of the materials downstream from the release point. A conservation equation for the discharged material can be used in this prediction. The problem of unsteady flow modelling of pollutant transport in compound channels can be divided into two major parts: (I) unsteady modelling of compound channel flows, with LMT effects taken into consideration, and (ii) pollutant transport in rivers with compound cross-sections. In this thesis, the literature review will be subdivided accordingly. Simons and Lam (1986) noted that in pollutant transport modelling usually hydrodynamic computations are completed before the water quality calculations are started. Output results from the flow problem should

be used as input in the mathematical modelling of the transport problem. In their pollutant transport model (POLTRA) Simons and Lam (1986) used the depth array and the calculated water transports from the hydrodynamic model (ONELAY) and carried out the desired water quality computations.

2.2 UNSTEADY FLOW PROBLEM

2.2.1 INTRODUCTION

Discharge estimation is vitally important in the regulation, development, and management of river systems. Until recently, most laboratory studies involving open channel flows have been performed in single regular-shaped channels with discharges estimated using either the Manning or Chezy formulae. While this approach greatly simplifies matters, it has its limitations concerning accurate representation of river channel geometry. This is especially true in times of flooding when the bankfull stage of the river's main channel is frequently exceeded and adjacent flood plain zones are inundated. If the flood plain depth (d) to main channel depth (D) ratio is in the range $0.0 < d/D < 0.3$, LMT is strong in the interface regions separating the deep and shallow zones and, as stated earlier, this feature can impact significantly on system conveyance, (Myers, 1978). Applying traditional discharge estimation methods in these circumstances generally results in over-estimation of system discharge, (Wormleaton et al., 1982).

2.2.2 LATERAL MOMENTUM TRANSFER (LMT)

Flow in the *mixing regions* of channels of compound cross-section is a complex, 3-D phenomenon. An important aspect of this particular flow is the LMT between the fast moving part of the stream (main channel) and the adjacent slower moving parts (flood plains). LMT results from the strong lateral gradient of longitudinal velocity in the *mixing regions*. Because of these gradients, banks of vortices rotating about vertical axes are present along the

interface. LMT may be envisaged to occur through the action of turbulent shear stresses which act to transfer streamwise momentum from the main channel to the flood plain(s).

In general, methods for numerical modelling of rivers during floods utilize the De Saint Venant (1871) equations of motion which ignore the influence of turbulent shear stresses on the transfer of momentum. The phenomenon may affect the predicted water surface elevations, velocity distributions and bed shear distributions with obvious consequences in such areas as flood plain modelling, and detailed sediment transport studies. Although the existence of the phenomenon is not explicitly accounted for in existing numerical flood models, its effect is implicitly lumped with the bed resistance coefficient when models are calibrated against existing data. Errors then arise when such models are used to predict flood events very different from the calibration data, since the relative influences of the bed shear stress and the turbulent shear stresses on the flow pattern are very different.

The interface between main channel and flood plain flows has been investigated in a number of experimental studies, (Wormleaton et al., 1982; Yen and Overton, 1973, Chatila and Townsend, 1996; Dracos and Hardeggar, 1987). In most of these studies, consideration was limited to channels of compound rectangular section in which the flood plain was considered as a shallow rectangular section adjacent to a rectangular main channel. From the experimental data, relationships were developed which expressed such parameters as the percentage of total flow on the flood plain in terms of geometry and flow parameters. Such relationships have limited applications due to the small range of experimental conditions studied. The importance of the phenomenon has given impetus to the search for a more universal method of predicting the influence of the interaction phenomenon on compound channel flow characteristics.

Sellin (1964) appears to have been the first to recognize the existence of the LMT phenomenon. He presented photographic evidence of the complex flow features (vortex sheets) associated with LMT by dusting aluminium powder on the water surface of his

experimental compound channel. The interaction between the fast main channel flow and the slower flood plain flows results in a tangential force, which amounts to a drag force on the main channel flow and a propulsive force on the over-bank flow. Many research efforts, aimed at determining this tangential force, have been reported in the literature (Chow, 1959 and 1964; Posey, 1967; Wright and Carstens, 1970; Yen and Overton, 1973; Wormleaton et al., 1982; Prinos and Townsend, 1983).

Similar studies confirmed the existence of the unique feature of compound channel flow fields, namely the *kinematic effect*. Zheleznyakov (1965, 1971), demonstrated that at low flood plain depths ($d/D < 0.3$), flow velocities within the main channel portions of the mixing regions were significantly lowered by LMT. This, in turn, produced a corresponding reduction in system conveyance. Zheleznyakov also showed that, at large flood plain depths, ($d/D > 0.3$), channel velocities in the vicinity of the mixing regions approached bankfull values, which was an indication of weak LMT in these circumstances.

Zheleznyakov (1965), Cruffs (1965), and Myers (1978) have investigated LMT and related phenomena in various-shaped laboratory compound channels using different methods to account for flood plain conveyance. Once the main channel bankfull stage is exceeded, the wetted perimeter increases dramatically as flow spreads onto the flood plain(s). Liggett (1968) and Baltzer and Lai (1968) view flood plains as *storage* zones only. On the other hand, Tingsanchali and Ackermann (1976) suggest that if the velocities on the flood plain zones are high, it is important to assess the dynamic effect of the flood plain flow when modeling system conveyance.

If a compound channel is treated as a *single* channel, that is, if LMT effects are ignored entirely, system discharge is generally under-estimated, (Wormleaton et al., 1982). On the other hand, if the cross-section is subdivided into hydraulically homogeneous main channel and flood plain zones, system discharge is generally over-estimated, (Ibid). Standard methods employed to sub-divide the cross-section differ only in the assumptions made

regarding the arrangement of *imaginary* interface planes used to effect the division, (Ibid). Wright and Carstens (1970) proposed that these interfaces should be included in the wetted perimeter calculation for the main channel portion only. Yen and Overton (1973) produced an empirical relationship between the angle of inclination of *inward* diagonal interfaces and flood plain depth. When comparing the effectiveness of *horizontal, vertical, and inward-diagonal* interfaces Wormleaton et al. (1982) noted that the most commonly used method of calculating discharge in rectangular-shaped compound channels is the *vertical* interface method, (figure 2.1). A standard uniform flow equation (Manning or Chezy) is usually applied to calculate the discharge in each sub-section of the cross-section. Sub-section discharges are then summed to give total or *system* discharge.

Because of the complexity of the LMT phenomenon (and its associated turbulence) most of these past studies were experimental. In their experiments dealing with flow in two joined rectangular channels, Wright and Carstens (1970) observed a linear momentum transfer from the major to the minor channel. They also demonstrated that the apparent shear stress at the junction interface plane was of the same order of magnitude as the boundary shear stress in the major channel. Therefore, to properly account for the *drag* effect on the major channel flow by the slower moving minor channel flow, the authors recommended that the (imaginary) junction plane be included in the major channel's wetted perimeter calculation.

Rajaratnam and Ahmadi (1979) also confirmed, through experiments, the transport of longitudinal momentum from a main channel to its flood plain. The bed shear in the flood plain near the junction interface with their compound channel's main channel was observed to increase considerably, while a decrease occurred in the main channel bed shear because of the LMT effect. A method to estimate the loss in flow capacity of their compound channel, due to LMT, was also recommended.

Yen and Overton (1973) approached the problem in a different way. They considered that it was impossible to determine shear stresses on arbitrary division lines (that divide the

composite section into subsections) and instead determined the plane of zero shear stress. In their experimental study the conveyance of their compound channel's main channel was shown to significantly decrease once the water surface exceeded the bank-full stage. This would imply that the main channel portion of a compound channel conveys water less effectively than the equivalent rectangular channel. Based on this finding, an empirical relationship was suggested for estimating discharge in the main portion of compound channels. Another equation for estimating the flood plain discharge, which was simply a modified version of Manning's equation, was also developed. Discharges computed using this procedure were compared with observed flows and a reasonably good agreement was noted.

Generally, methods for discharge assessment in compound channels assume vertical interface planes between the deep and shallow sections. Some of these methods, however, include the interface plane in the wetted perimeter computations (assuming the fluid shear stress at the junction is the same as the average boundary shear stress) and others exclude it (assuming zero apparent shear stress), (Wright and Carstens, 1970; Yen and Overton, 1973; Wormleaton et al., 1982; Prinos and Townsend, 1983; Dracos and Hardegger, 1987; Chatila and Townsend, 1996). Wormleaton et al. (1982) proposed a parameter they called the *apparent shear stress ratio*, defined as the ratio of apparent shear stress to the average boundary shear stress, to compare between the two stresses.

Observations, that LMT effect is strongest at low flood plain depths, were made by Myers (1978) and Prinos and Townsend (1983). It has been established that, in the case of vertical interface planes, the apparent shear stress is large at low flood plain depths, (Wormleaton et al., 1982). Therefore, it would be useful to examine other possible division planes (where the apparent shear stress is lower) and hence can be ignored or equated to the local boundary shear stress. Indeed, the diagonal and horizontal interface planes did not show the dramatic increase of the apparent shear stress ratio values obtained for vertical interface planes at low flood plain depths, (ibid).

Krishnappan and Lau (1986) have developed a 3-D calculation method which permits

the simulation of such details as the turbulence-driven secondary motions evolving in the channel by utilizing a refined algebraic stress model. However, in the case of straight channel, these motions are unlikely to influence significantly the flow parameters of practical interest such as streamwise velocity and bed shear stress distribution. Even 3-D calculation procedures employing less refined turbulence models, which do not allow the resolution of the turbulence-driven secondary motion, would, in most cases, go beyond what is called for in practical applications where the resolution of vertical distributions is rarely of interest. For such calculations there is considerable merit in having available a 2-D DA model which resolves only the horizontal distributions. Keller and Rodi (1984) appear to have been the first to adopt this approach, incorporating a DA k-ϵ model of turbulence in a preliminary numerical study to predict some existing laboratory data. A similar approach has since been adopted by Radojkovic and Djordjevic (1985). In an attempt to predict relative discharge percentages between main channel and flood plain, Pasche et al.(1985) predicted, with some success, velocity and bed shear stress distributions in a laboratory flume modeling a compound channel with a heavily vegetated flood plain.

It is likely impossible to develop a universal flood routing model capable of handling all practical situations. However, for certain applications, the selection of a model would depend, to a large extent, on whether to account for the flood plain contribution to system conveyance or assume that flood plains are *storage* zones. Chatila and Townsend (1995) proposed outward-facing diagonal interface planes to define the flood plain hydraulic boundaries, (figure 2.1). They presented a relationship between the angle of inclination of the interface plain and the ratio of flood plain depth to main channel depth. Chatila and Townsend (1996) also compared different discharge estimation methods in a steady flow compound channel application. They concluded that the outward-facing diagonal interface as well as the vertical interface methods produced relatively better results than other methods involved in their applications, specifically for flood plain depths up to approximately 35 % of main channel depths. Bhowmik and Demissie (1982) showed that flood plain carrying capacity depends mainly on the nature of the flood plain, the main channel, and the flood frequency. Decreased flow velocities (resulting from LMT) in the main channel of compound

sections at low flood plain depths were observed by many investigators. Rajaratnam and Ahmadi (1979) showed that, for small flood plain depths, there is a sharp discontinuity of velocity and bed shear at the sides of the main channel due to strong LMT effects. However, as flood plain depth increases, the LMT effect gradually diminishes, resulting in a smoother transition of velocity and bed shear from the deep section of the channel to the flood plains. The same phenomenon was also observed by Bhowmik and Demissie (1982) while analysing field data from the Sanganon River near Oakford and from the Salt Creek near Greenview, Illinois. They also found that the average velocity of the compound section decreased until a minimum was reached at an average flood plain depth of about 35% of the average depth in the main channel. In a similar study, Karasev (1969) reported that the minimum average velocity for the composite section of a laboratory channel was reached at a stage where average depth on the flood plain was about 30 to 40% of the average depth in the main channel.

As depth on flood plains increases beyond ~35% of the main channel depth, mean flood plain velocities increase substantially. In these circumstances the average velocity in the flood plain zone is observed to approach a value close to the average velocity in the compound section, (Bhowmik and Demissie, 1982). Accordingly, the flow can be considered effectively homogeneous throughout the entire cross-sectional area. It should be noted, however, that the aforementioned 35% relative depth value is not universal but rather expected to vary from one reach to another as the carrying capacity of flood plains depends upon the size, shape, width, depth, and nature of the flood plains and main channel and on the frequency of the flood event. Based largely on experimental studies, many researchers (Wormleaton et al., 1982; Yen and Overton, 1973; and Prinos and Townsend, 1983) have developed empirical relationships to account for the aforementioned LMT when flood plain depths are shallow (i.e. less than 35 % of the average depth in the main channel).

2.2.3 NUMERICAL DEVELOPMENTS

In past years most of the numerical models developed for flow in compound channels

are either finite element (FE) or finite difference(FD) solutions of the equations of motion. Vreughenhill and Wijbenga (1982) used a FD method, of the alternating-direction-implicit (ADI) type, to solve the appropriate shallow-water equations. The eddy viscosity was not prescribed in advance but was calculated as part of the calibration process, thereby ***having a numerical rather than a physical sense.*** It should be noted that secondary flow was not simulated in their model. The authors, in applying their model to prototype conditions, attribute its poor performance to boundary roughness effects among other things.

Demuren (1983) used a 3-D numerical procedure for *developing* flow in channels with flood plains. The PDE governing the steady-state turbulent flow field were solved with the standard k-ϵ model of turbulence. Their model was incapable of predicting turbulence-induced secondary currents; however, this was not considered a serious defect for *developing flows*. The model was applied to the data collected by Rajaratnam and Ahmadi (1981) and gave satisfactory results, but it was found to be computationally very expensive.

Prinos and Townsend (1984) used a FE model based on the classical Ritz or Galerkin method to determine isovel patterns in their compound channel. The method is based on a variational technique in which the governing function for steady turbulent flow is minimized with respect to velocity. With this approach the distribution of longitudinal velocity U in the vertical and lateral directions can be obtained. For *wide* central channel conditions, the differences between predicted and observed velocity distributions were considered unimportant from a practical viewpoint. However, when the main channel was made *narrow*, the mathematical model did not reproduce the observed isovel patterns satisfactorily. This modeling deficiency was attributed to LMT effects which were only partly accounted for in the model.

2.2.4 IMPROVED LMT MODELING

One of the very few studies that considered the dynamic effect of flood plain or *berm* flow when modeling river stage and discharge is that of Tingsanchali and Ackermann (1976).

First, a momentum correction factor (M) was introduced to relate momentum flux through a composite section with the summation of momentum fluxes through each individual subsection. This momentum correction factor is unity for in-bank flow (no flood plain flow) and greater than unity for overbank flow during flood periods. Under conditions where the flood plain is considered to play only a storage role (no conveyance), M becomes very large and can be approximated by the ratio of the compound channel cross-sectional area to that of the main channel flow area. Tingsanchali and Ackermann (1976) applied their model to determine flow conditions of the Bicol River in the Philippines for a flood that occurred in 1970. When compared to observed data, their model performed better than the *off-channel storage* model, which over-estimated peak stages and underestimated peak discharges.

Based on laboratory tests, Nicollet and Uan (1979) developed an empirical relationship between discharge in the main channel of a composite section and the discharge in an equivalent regular section. This empirical model was used to account for LMT between the flood plain and main channel flows in their proposed gradually-varied unsteady flow equations. A momentum equation was developed for the composite section, in terms of the flow parameters in both main channel and flood plain sub-sections. Another momentum equation, describing motion in the equivalent main channel was also established. The continuity equation simply stated that summation of discharges in the sub-sections was equal to the total flow through the composite section. Nicollet and Uan (1979) developed another procedure for describing average flow conditions in a compound channel. The related momentum equation was coupled with expressions for equivalent conveyance of the composite section, an average composite momentum coefficient, and the distribution of flow between main channel and flood plain to describe unsteady gradually-varied flows in compound channels.

Kolovopoulos (1990) proposed a 1-D unsteady flow model for the simulation of flows in looped and branched open channels. The author evaluated different steady-state models that account for LMT and concluded that the Prinos-Townsend (1984) equation gives accurate results for apparent shear stresses at the main channel-flood plain interface.

Accordingly, this equation was incorporated in the Kolovopoulos' unsteady flow model to account for LMT effects. Applying this model showed that LMT results in: (1) an attenuation of discharge hydrographs at low depths, (2) a delay in the falling of water stages, (3) a shift in the loop rating curve, and (4) an increase in flood plain flow accompanied by a decrease in main channel carrying capacity. Kolovopoulos (1990) stated that, for the most part, the phenomenon of main channel-flood plain interaction can safely be ignored and any conventional flood routing models can be applied. He applied his model to eight test cases and concluded that it performed well for a wide range of unsteady flows, tidal flows, and regulated flows frequently encountered in practice. The author also analyzed other unsteady flow models currently in use. He compared the performance of the *Single Channel* and the *Off-Channel Storage* models in regards to computed hydrograph peaks and attenuation times. The *Storage* model was found to underestimate discharges and overestimate peak water surface elevations.

Forrest and Holley (1983) developed a stream-tube dispersion model approach and calibrated it using on-site measurements. The model was used to plan a field study in which measurements of tracer diffusion from a continuous source were supplemented by detailed velocity and depth observations. The authors stated that the calibrated (adjusted) non-dimensional coefficients were so large as to suggest that secondary currents play an important role in transverse mixing, and thus weakening the generality of the calibration and pointing out the need to account for secondary circulation explicitly.

Pezzinga (1994) used the k-ϵ model to predict uniform turbulent flow in compound channels with secondary currents. He reported that the energy slope, after the convergence, does not coincide with the imposed slope in the momentum equation in the x-direction. This was explained by the numerical viscosity that was introduced by the computational procedure. The model was applied to reproduce the experimental data of Tominaga et al. (1989). The primary velocity component, secondary circulation, and the discharge distribution were predicted accurately.

Cokljat and Younis (1995) used a complete Reynolds-stress transport model of turbulence to predict the effects of asymmetry, surface roughness and side-wall inclination on the behavior of turbulent flows in compound open channels. They concluded in their parametric study that the model reproduced the main features of the compound channel flows.

Thomas and Williams (1995) performed a large eddy simulation of a symmetric trapezoidal channel with flood plains at a Reynolds number of 430 000. In their simulations, they predicted the bed stress and velocity distribution, as well as secondary circulations across the flood plain. Good agreement was obtained when they compared their simulations to observations from the SERC flood Channel facility at the Hydraulics Research Ltd., Wallingford, England.

Lambert and Sellin (1996) used the mixing length concept to predict discharge in straight compound channels in their applications to two different experimental sets. They applied a variation of Prandtl's mixing length hypothesis to calculate apparent shear stresses and introduced the mixing length approximation to determine the correction for momentum interaction effects that are neglected when the traditional divided channel approach is used.

2.3 UNSTEADY TRANSPORT PROBLEM

2.3.1 INTRODUCTION

Many important problems in water resources engineering involve the mass transport of a miscible fluid in a flow. When sewage is discharged into a body of water, it is important to ascertain how the sewage is dispersed in the receiving water. Velocity is usually defined on an average basis in a finite volume. Actually, the fluid particles are not moving with the same velocity. They tend to separate from one another. Thus, it is necessary to regard the flow as capable of some dispersive action. Mass transport in open channel flow can be simulated on different levels. These levels range from simple 1-D models, which are to be

used only for estimation of the global amount of given matter in the river, to the rather complicated procedures based on refined turbulence modeling, which enables 3-D prediction of concentration and velocity fields even in the vicinity of outlet structures, (Djordjevic, 1993).

2.3.2 HISTORICAL PREVIEW

Mixing of pollutants in rivers is accomplished by the process of mechanical dispersion. Physically, dispersion may be considered as a hydraulic mixing process, by which the *waste concentrations are attenuated while the waste pollutants are being transported downstream.* Turbulent diffusion and velocity gradients are the two main mechanisms in dispersion.

2.3.2.1 Field Testing

The disposal of human wastes and other organic refuse without creating a nuisance is an ongoing problem. Moses was one of the foremost early sanitarians who framed a very striking and comprehensive code of health regulations for the ancient Israelites. At that time, the difficulty in disposal of human waste products was surmounted by resorting to the burial of the wastes rather than dumping them in rivers and water bodies, (Old Testament in Duet xxiii, 12-13). More recently, Armstrong and Gloyna (1968) presented two methods of evaluating the effects of stream pollution. These methods furnish valuable information regarding the condition and stability of ecological systems in receiving waters, and may ultimately become design criteria. Bagdasar'yan (1968) investigated the presence of cytopathogenic viruses in the Moskva, Skhodnya, and Yauza Rivers within the city boundaries of Moscow. Cytopathogenic agents were isolated from 34.1% of all the samples and from 45.4% of the samples from the Skhodnya which was the most heavily contaminated river, probably owing to discharges of sewage effluent from a biological treatment plant near the confluence with the Moskva.

Burdiyan (1968) studied the pollution of rivers in the Ob-Irtysh Basin, Siberia. He reported that industrial wastewater had caused severe depletion of fish stocks during the previous 15 years, young fish being the most susceptible. Regulations for the treatment of effluents existed, but enforcement was lacking. Aragon et al. (1969) performed some studies on the chemical, physical and bacteriological aspects of the River Duero and some of its tributaries, Spain. These studies showed that the river system was well oxygenated, allowing self-purification of local incidences of pollution. A relatively high level of ammonia was found at certain points, and at Valladolid, where the lowest DO concentration occurred, this was a cause for concern.

Buscemi (1969) analyzed the chemical and detrital aspects of Palouse River, Idaho. Water and sediment samples were collected at four stations established on the river. The results showed influence of rainfall, melt water, stream inflow, and mill pond on seston concentration. Variations in chemical composition of water indicated the effect of either melt water runoff or subterranean discharge. The increased pollution of water and sediment enrichment in organic matter were correlated with locations of lumber camps and cattle grazing.

2.3.2.2 Numerical Modeling

Cleary and Adrian (1973) presented an integral transform method to solve the differential equation governing the concentration of dye released as an instantaneous source and subject to the *no-flux boundary* conditions of the river banks, bottom, and surface. The solutions were obtained for a constant average river velocity, constant but different turbulent eddy diffusivities and an arbitrary source location. They recommended that spatial, or time dependency, or both, of the longitudinal river velocity and the turbulent diffusivities be considered in future models. Martin (1974) proposed some numerical representations which model properties of the solution to the diffusion equation. He based the solution on the integral form of the equation by imposing certain restrictions to guarantee that the numerical

solution will *conserve mass*, produce no negative masses, and have the same low-order moments as the analytical solution to the diffusion equation. Martin (1974) concluded that this method was highly successful on sample tests according to the various criteria used.

Verboom (1975) used the *fractional-step* method to solve the 1-D advection-dispersion equation for an anisotropic medium. He demonstrated that the *fractional-step* method is highly suitable because the numerical scheme used to solve a certain step is independent of the scheme used for the other steps. As a consequence, the method can be used with great advantage if some coefficients are of the order of magnitude larger than others, whereas the transport mechanism can not be neglected. In his applications, mainly because of *accuracy*, Verboom (1975) preferred *explicit schemes* over the *implicit Crank-Nicolson* formula. However, he stated that using *accuracy* to select a certain scheme is not applied in the *same sense* for the case of the fractional-step method.

Yeh and Tsai (1976) solved analytically the *transient 3-D turbulent diffusion* equation describing the concentration distribution of a substance or heat in a time-dependent flow field. In their search for solutions, the method of Green's function was utilized to the optimum advantage. They investigated two models: the first considered both depth and width of a water body as finite, while the second dealt with finite depth and infinite width. They assumed the velocity as the sum of a constant and a harmonic component with no limitation on the type of source condition. Comparing model results with field measurements showed that the models were capable of simulating both space and time variation of dye concentrations in tidal water bodies. They recommended that... *the present model (3-D) shall provide a quick and easy way of predicting the whereabouts of effluent discharges.*

Holly and Preissmann (1977) presented a *numerical method* for the calculation of advection and diffusion in 1- and 2-D. Their method was based on the fact that interpolating polynomials of higher order may be constructed between only two points if not only the dependent parameter, but also its derivatives, were known at each point. This method

characterized the transport process in the following manner: a neutrally buoyant marked fluid, assumed to be uniformly distributed over the depth, was subjected to turbulent diffusion and differential advection in a 2-D, time-dependent velocity field that is assumed to be known. Changes in concentration of the marked fluid were assumed to occur only as a result of mechanical dilution.

Komatsu et. al. (1985) reported that the high accuracy of the *two-point fourth-order Holly-Preissmann* method for numerical calculation of contaminant advection was obtained by treating the spatial derivatives of concentration as dependent variables. In a *split-operator* approach for dispersion modeling, diffusion of both the concentration and its spatial derivatives must be computed, leading to a rather complicated algorithm in 2-D. Holly-Komatsu proposed the *eight-point* method as an alternative approach which retained high accuracy but treated only the concentration as a dependent variable. However, there were some practical difficulties in 2-D implementation of the *eight-point* scheme. Komatsu et al. (1985) described the search for an improved approach which had almost the same accuracy but used values of concentration at only six points. Some treatments of the boundary conditions in 1- and 2-D were described in detail and their performance was evaluated through applications to schematic test cases.

Costa et. al. (1987) developed a new *water quality model* for dynamic simulation of the transport, dispersion and degradation of pollutants in rivers, channels and well-mixed reservoirs. Their model's formulation for transport and dispersion was based on the aggregated *dead zone* theory, and not on the traditional Fickian theory. The aggregated *dead zone* theory considered that in natural channels and rivers, dispersive effects were due not only to the Fickian type of dispersion but also to the effect of *eddies created by natural obstacles in both the bottom and banks*. The model parameters and inputs were described *deterministically or stochastically.*

Vasil'ev (1987) proposed a *nonlinear differential scheme* to solve numerically the

problem of pollutant transport in rivers with an unsteady flow regime. In order to ensure the conservative nature of the scheme, he assumed the mean concentration in the segment did not exceed the limits of the concentrations at its ends. Without lowering the calculation accuracy, the scheme allowed coarser grids in smooth areas than with schemes of first-order accuracy of approximation. At the same time it remained monotonic with the concentration gradients under sharp variations. The problems of convection and dispersion were solved separately with the use of dissociation in terms of physical processes.

Hayter and Pakala (1988) developed a *FE model* capable of simulating 3-D transport and interaction of cohesive sediments and inorganic pollutants in rivers and estuaries. This modeling system included a *hydrodynamic* module, *a cohesive sediment transport* module, and both *dissolved* and *particulate pollutant transport* modules. They used the model to simulate sediment and pollutant transport in a 11.3km-long partially-stratified tidal river.

Seo (1990) investigated the non-Fickian nature of the longitudinal dispersion in natural channels during low flow. He used both laboratory experiments and numerical solution of the proposed mathematical model, which was based on a set of mass balance equations describing the dispersion and mass exchange of mechanisms. Laboratory experiments, which involved collection of channel geometry, hydraulic, and dye dispersion test data, were conducted to obtain sets of experimental data on a model of four *pool and riffle* sequences in a 161 ft long tilting flume in the Hydro-systems Laboratory at the University of Illinois at Urbana-Champaign. The experimental results indicated that flow over the model *pool-riffle* sequences was highly nonuniform; concentration-time curves were significantly skewed with long tails. The mixing and dispersion in the laboratory channel was simulated using a numerical solution of the mathematical model, in which the FD method developed by Stone and Brian (1963) was used as a solution technique. A comparison between measured and predicted concentration-time curves showed that there was a good level of agreement in the general shape, peak concentration, and time to peak. The proposed model showed significant improvement over the conventional Fickian model in predicting dispersion processes in natural channels under low-flow conditions.

Al-Kadi and Fattah (1991) developed an *exact analytical solution for the 2-D unsteady convective-dispersive equation.* The solution described the concentration distribution for a conservative pollutant or substance injected as a pulse (not continuous) into a river by a diffuser pipe installed normal to the direction of the river bank. The river had a constant mean velocity and a relatively large discharge in comparison to the pollution discharge. The solution was developed using *Laplace and Finite Fourier Transforms.* The distribution of the transporting concentration of the pollutant in the river due to such disposal was developed in terms of error functions, exponential, and trigonometric series. Variations in the location of the diffuser pipe in the river were examined. The concentration distribution was determined across and along the river as a function of time. The effects of variations in river velocity, and both lateral and longitudinal dispersion coefficients on the mixing patterns were presented. The solution presented variations in concentration distribution in the river with time during and after the pulsing injection period of the pollutant. Sensitivity analysis was performed and determined significant variations in the solution due to changes in various parameters.

Yang et al. (1992) introduced a *water quality model* which is capable of carrying out the simulation of unsteady flow and pollutant transport for a *looped-channel* network and the simulation of *non-point* source pollutant washed out by the runoff from a watershed. In addition, the model can be used to study the impact of the *non-point* source pollutant to the water quality of complex river systems. The applicability of this model was demonstrated through a case study performed for the Ta-Han River system, which is located in the Taipei area of Taiwan. *The results were quite convincing although the model was not completely calibrated.*

Datsenko et al. (1993) developed a *hydrodynamic model of pollutant transport* in water bodies for the Volga water supply system of Moscow, which includes five reservoirs and a channel. The model solves practical problems, including calculation of pollution concentration reduction due to the dilution. Jirka and Akar (1993) formulated a *buoyant*

spreading model for a current-advected plume, including several distinct mechanisms: convective spreading, interfacial friction spreading, entrainment at the density front, shear flow entrainment, wind-induced entrainment, and surface heat exchange. The buoyant spreading model was implemented within the Cornell Mixing Zone Expert System (CORMIX), and comparisons with available laboratory and field data demonstrated the substantial role of density currents in pollutant transport and mixing.

Lin and Shiono (1995) developed a 3-D numerical model to predict solute transport processes in compound open channels. They used linear and non-linear k-ϵ models along with the Navier Stokes equations to describe the flow problem. Predicted values of the velocity and eddy viscosity were used to compute solute transport rates. They applied the developed model to the data of Wood and Liang (1989) and obtained comparable results clarifying the effects of secondary currents on mixing processes.

2.3.2.3 Statistical Modeling

Bird and Holley (1985) used *2-D, temporal moment*, numerical calculations in a natural curvilinear coordinate system to simulate the longitudinal and transverse distributions of concentration resulting from a slug or instantaneous release of pollutants in rivers. The already existing temporal moment analysis was transformed for the curvilinear coordinates and modified to include the longitudinal dispersive effects associated with the vertical distribution of velocity. This dispersion term was included in the analysis in an approximate fashion, based on the analytical solution for the change of moments due to dispersion. A Pearson Type III distribution was used to obtain a predicted concentration distribution from the calculated moments. Dye experiments were performed for two separate release locations in a meandering laboratory channel with cross-sectional shapes which varied in the longitudinal direction in a manner to simulate the variation in natural rivers.

Lafe (1986) derived a *boundary integral equation* for the pollutant transport problem in surface flows. The new formulation was obtained when the turbulent convective-diffusive equation governing the species transport problem in a binary system was transformed, in a Laplace domain, into an integral equation with two different kernels one of which was unknown a priori. The unknown kernel was a function of the appropriate convective-diffusive coefficients. By representing the spatial distribution of the latter by a polynomial, an analytical expression for the unknown kernel was obtained. The formulation provided estimates for the effective transport coefficient for an equivalent binary system in which the diffusion coefficient was independent of space. The method was applicable to both 2-D/3-D species transport problems in surface flows.

Al-Masri et al. (1989) used different *regression models* to evaluate the variations of various pollutants in the River Tigris at Baghdad. Some of the models used gave an excellent estimates of pollutant variations in terms of distance, flow rate, and reference point concentration. Comparisons between estimated and actual values of pollutants were also made.

Bensabat and Zeitoun (1990) proposed a *least-squares formulation* associated with a *conjugate gradient algorithm* for the solution of transport problems. In this procedure the advection-diffusion equation was first discretized in time using an implicit scheme. At each time step the resulting partial differential equation was replaced by an optimal control problem. This minimization problem involved the minimization of a functional defined via a state equation. This functional was chosen in order to force the numerical solution of the advection-diffusion equation to be equal to the hyperbolic advective part of this equation. The effectiveness of the method was shown through a 1-D example involving advective and diffusive transport. No oscillation and high accuracy had been obtained for the entire range of Peclet numbers with a Courant number well in excess of unity.

2.3.2.4 Model Applications

McCorquodale et al. (1986) applied the U. S. Environmental Protection Agency (EPA) TOXIWASP fate transport model to simulate the response of the St. Clair River system to a spill of perchloroethylene (PERC). The spill occurred from August 13 to 16, 1986 at the Dow Chemical of Canada Inc. site. The estimated quantity of the spill was 18,000 kg of which approximately 10,000 kg initially settled out in the vicinity of the Dow Chemical outfalls. At the end of 30 days the model indicated that about 12,600 kg had been discharged to Lake St. Clair, while 4500 kg and 90 kg remained on the river bed and in temporary storage in the water column, respectively. Approximately 5% of the original spill was volatilized in the river during the 30 days after the spill.

Schumann et al. (1991) reported that as a result of the general improvement of waste water treatment facilities, point sources of pollutants have become less important than non-point sources for the water quality of many rivers. One important source of pollutants is urban areas. Routine water quality monitoring usually is insufficient to describe the dynamics of short-term variations in the water quality of rivers affected by the transport of pollutants from urban areas during storms. To better understand the processes governing the transport and transformation of pollutants, Schumann et al. (1991) proposed that runoff components generated in urban areas be identified using a hydrologic model. By estimating the storm runoff from urban areas and the corresponding chemical loads, the river pollution could be estimated. This analysis was useful in demonstrating the influence of urban areas on water quality conditions and in developing strategies for improving the water quality of rivers.

Stronach et al. (1992) reported that the Niagara River plume in Lake Ontario and the Fraser River plume in the Strait of Georgia were of similar spatial dimensions, and arose from rivers with comparable discharge. Both rivers received significant loads of toxic wastes. Hydrodynamic models of the Niagara River plume and the Fraser River plume were combined with a generalized pollutant transport model to simulate the horizontal distributions of

pollutants. The model partitioned the pollutant between a dissolved fraction and a fraction adsorbed onto the ambient suspended sediment. To simulate this partitioning, the pollutant transport module separately computed suspended sediment concentration and total pollutant concentration. The Niagara River plume simulations compared reasonably well with observations. For the Fraser River plume, observational data was presently unavailable. In both cases, the suspended sediment load had a significant effect on the pollutant transport distribution.

Pollutants transport and management in the river Rhine basin is of international concern and deals with a variety of functions and environmental aspects of the river Rhine, its delta and the coastal waters along the Dutch coast. Sweerts et al. (1992) described an internationally developed integral approach which enabled the assessment of impacts of managerial actions on the quality of water, sediment and biota in the river Rhine and the coastal waters. The project *Chemical Pollution and its Sources in the Basins of the Rhine and Meuse* included the quantification of the input of nutrients, heavy metals and organic micro-pollutants into the water system as a function of human activities. All major natural, point and diffusive sources could be distinguished in a Geographic Information System (GIS). The transport of the pollutants through the rivers, estuaries and their dispersion in the coastal waters of the Netherlands was analyzed, evaluated and predicted using a mathematical framework. The sedimentation of pollutants and related accumulation in bottom sediments in the downstream regions of the rivers received special attention because of the implications for water management. The study covered the entire catchment area of two large rivers and receiving coastal waters in western Europe. The results could be used to quantify the efficiency of managerial actions aimed at reducing the discharges of pollutants on an European scale. Due to the fact that all major point and diffusive sources were identified, it was possible to determine the impact of managerial actions for specific sources. The development of Cadmium pollution in the Rhine over the last two decades was presented as a case study.

2.3.2.5 Numerical Improvements

Cadena (1989) reported that the number of significant digits stored by personal computers during calculation of exponential and complementary error functions in pollutant transport models was frequently insufficient, even when double-precision was used. A numerical simplification overcame this limitation and increased output precision. Cadena (1989) presented a QUICKBASIC program to illustrate the use of this numerical simplification.

Yang and Hsu (1991) introduced a new interpolating technique for incorporation with the Holly-Preissmann *two-point* method. The method was referred to as the *Holly-Preissmann Reach-Back (HPRB)* method and allowed the characteristics to project back several time steps beyond the present time level. Through stability analyses it had been observed that the increase of the reach-back time step numbers for the characteristics indeed reduced the numerical damping and dispersive phenomena. A schematic model had been constructed to demonstrate the merits of this new technique for the calculation of the pure advection and dispersion equations. Numerical experiments and comparisons with analytical solutions, which supported and demonstrated this new technique, were presented.

Casulli et al. (1993) discussed a *semi-implicit FD formulation* for the numerical solution of *3-D tidal circulation*. The governing equations are the 3-D Reynolds equations, in which the pressure was assumed to be hydrostatic. A minimal degree of implicitness had been introduced in the FD formula, so that the resulting algorithm permitted the use of large time steps at a minimal computational cost. This formulation included the simulation of flooding and drying of tidal flats, and was fully vectorizable for an efficient implementation on modern vector computers. The high computational efficiency of this method had made it possible to provide the fine details of circulation structure in complex regions that previous studies were unable to obtain. For proper interpretation of the model results suitable interactive graphics was also an essential tool.

Moeller and Adams (1994) compared an *Eulerian-Lagrangian, a random walk, and a hybrid model*, in terms of their accuracy and efficiency, in simulating 2-D pollutant transport. Computer simulations indicated that the *hybrid* approach, which used particles to model the *near* field and the *Eulerian-Lagrangian* method to model the *far* field, was the most accurate overall. The *Eulerian-Lagrangian* model performed best in simple flow fields without shear, but the *hybrid* model performed better than the *Eulerian-Lagrangian* model in moderate and heavy shear flows, because it modeled the *near* field much more accurately. The *random walk* model did not compare well in terms of accuracy, which suggested the most appropriate role for particles in surface water modeling may be in a *hybrid* approach.

2.4 NUMERICAL SCHEMES

Different methods have been proposed in the literature to solve the partial deferential equations (PDE). These methods involve:

- Development of a network of characteristics (Lai, 1965-a; Amein, 1966; Fletcher and Hamilton, 1967; and Baltzer and Lai, 1968),

- Explicit finite-differencing of characteristic equations on a rectangular network in the x-t plane (Stoker, 1957; Amorocho and Strelkoff, 1965; and Strelkoff and Amorocho, 1965),

- Direct, explicit finite-differencing of the equations of continuity and momentum in a rectangular net (Isaacson, Stoker and Troesch, 1954),

- Direct, implicit finite-differencing of the equations of continuity and momentum in a rectangular net (Lai, 1965-b; and Vasilev et al., 1965),

- Finite element (FE) techniques, and

- Boundary integral (element) method.

2.4.1 FINITE ELEMENT

The river reach under investigation is divided into a number of elements, and the PDE are integrated at the nodal points of the elements. Cooley and Moin (1976) applied the FE method to solve the complete De St. Venant equations. Hicks and Steffler (1995) showed the advantages of the FE method when applied to 1-D flows. In general, the FE method is advantageous when applied to 2-D unsteady flow problems. Hinwood and Wallis (1975, a, b) and Abbott (1976-b), among others, applied 2-D models in their complete form, whereas Cunge (1975) and Vicens et al (1975) used the simplified forms. 2-D models are more complex than 1-D models, and their use is limited to applications where a large amount of flow information is desired in complex unsteady flow problems.

FE is attractive for simulating flow of water in natural streams and water bodies having irregular boundaries and complex topography. It has a flexibility that allows the choice from a wide array of linear and higher order elements which can be combined to give the best representation of complex domains using an unstructured mesh. With the FE method it is possible to concentrate nodes in regions of complex geometry and/or interesting flow features and have a more sparse layout in areas which are more uniform. FE allows integration by parts of the governing equations facilitates a natural implementation of boundary conditions. It requires less nodes than FD and FV methods to achieve similar accuracy. Models based on this approach include: the Finite Element Surface Water Modelling System (FESWMS), (Froehlich, 1989), RMA-2 (King and Norton, 1987), Leclerc et al., (1990), and FASTTABS (Boss Corporation and Brigham Young University, 1992). The success of this technique to suppress spurious oscillations has been attributed to error

consistency (Lee and Froehlich, 1986). Walters (1983) explained that the use of mixed interpolation cuts off the short wave lengths for the depth at 4 times the nodal grid spacing, and thereby eliminates the spurious oscillation mode.

2.4.2 FINITE DIFFERENCE (FD)

In the FD method the partial derivatives are replaced by FD approximations, and the resulting algebraic equations are then solved to determine the unknowns. Liggett and Woolhiser (1967) presented a comprehensive study dealing with FD solutions of the shallow water equations. They concluded that experience with each of the above solution categories will show the best-suited for a specific application. In addition, the advent of high-speed computers have made it possible to obtain solutions of the complete PDE.

2.4.2.1 Explicit FD Methods

Explicit methods, as the term indicates, solve directly the algebraic linear equations for the unknowns. The unknown conditions at a point at the end of a time step are expressed in terms of the unknown conditions at the beginning of the time step. These methods advance the solution, point by point from one time line to the next in the x-t domain until all the unknowns associated with the time line are evaluated. Explicit methods were applied as early as the 1950's by Stoker (1953) and Isaacson et al. (1954, 1958) to route floods in the Ohio River. Dronkers (1969) and Thatcher and Harleman (1972), among others, used explicit methods to analyze tidal movements in estuaries. On the other hand, Johnson (1974) and Garrison et al (1969) applied this method for flood routing in reservoirs.

Many variations of the explicit schemes were introduced. Richtmyer and Morton (1957) reported the Lax-Wendroff two-step scheme to successfully obtain solutions of the gas dynamics equations. However, disappointing results were obtained when Liggett and Woolhiser (1967) applied this scheme to shallow water equations with particular boundary

conditions. A second popular scheme is the Leap-Frog which led to the same result as the Lax-Wendroff schemes when applied to shallow water equations. A third one is the Diffusion Scheme, which proved empirically stable for all cases except the rising part of the hydrograph under certain conditions.

Although simple in formulation, the explicit method has a restriction on the size of the computational time step due to numerical stability considerations. The Courant Condition ($C_r = U \Delta t/\Delta x$, where U = velocity, Δt = time step, and Δx = distance step) is necessary for numerical stability. However, satisfying the Courant condition does not guarantee that the method is stable. In general, the time step is substantially reduced as the hydraulic depth increases. The stability requirement imposes that the time step size should be in the order of seconds or few minutes as a maximum. Correspondingly, the explicit method is inefficient in the use of computer time.

Strelkoff and Amarocho (1965) found that even if the method is empirically stable, the equation of continuity may not be satisfied. In other words, over a long period of time, inflow may be greater or less than outflow plus accumulation of storage. Liggett and Woolhiser (1967) state: *In general, this method (explicit) is completely unsatisfactory for even rough and approximate calculations.*

2.4.2.2 Implicit FD Methods

Implicit methods advance the solution of the PDEs from one time line to the next simultaneously for all points along the time line. Implicit methods are ideally applied to solutions of problems requiring computations over a long time period. Ponce et al. (1978) report that implicit numerical schemes are generally preferred over explicit schemes because they allow larger time steps and consequently reduce the computational effort. Amein and Fang (1970) state that implicit methods give the same results as those obtained using any other numerical scheme; however, they provide the results much faster.

Cunge and Wegner (1964), Amein and Fang (1970), and Fread (1974), among others, used the *Four-Point implicit* FD scheme to solve the unsteady flow equations. This scheme, also referred to as Preissmann's scheme, has received wide attention. A weighting factor is introduced to approximate the spatial derivatives by a FD quotient positioned between two adjacent lines. Baltzer and Lai (1968) and Amein and Chu (1975) used a weighting factor of 1.0, which resulted in the formation of a fully implicit scheme. Amein and Fang (1970) used a weighting factor of 0.5, which led to a "box" scheme. Fread (1974) examined the influence of the weighting factor on stability and convergence properties. He concluded that accuracy decreases as the weighting factor departs from 0.5 and approaches 1.0, and that this effect becomes more pronounced as the time step size increases. A value of 0.55 is often used to minimize loss of accuracy while avoiding weak or pseudo-instability, as reported by Baltzer and Lai (1968) when a weighting factor of 0.5 was used. Cunge (1966), Abbott and Ionescu (1967), Gunaratnam and Perkins (1970), Fread (1974), and Ponce et al. (1978), among others, analyzed the numerical stability of the various implicit techniques. Chaudry and Contractor (1973) and Fread (1974) showed that instability can occur if the time step is too large. In addition, the time step is chosen in such a way as to satisfy accuracy requirements.

In an implicit scheme, a system of 2N algebraic equations is generated from the equations applied simultaneously to the N cross-sections along the x-axis. This system could be linear or non-linear depending on the type of implicit scheme adopted. Linear implicit schemes require only one solution of the system of equations at each time step; (Chen et al., 1957). The time step should be small enough to satisfy accuracy requirements for rapidly changing transient flows using linear methods. On the other hand, non-linear implicit schemes require an iterative solution where the system of equations is solved once or more at each time step. The Newton-Raphson method is efficient for solving non-linear systems which are effective when applied to waterways with non-prismatic geometry.

Abbott and Ionescu (1967) and Vasilev et al. (1965) proposed a six-point implicit scheme. However, this scheme requires the use of regular Δx intervals whereas the four-point schemes allow variable Δx spacing. Amein and Fang (1970) state two factors that work in

favour of implicit methods: (i) the method is stable for large time steps with no loss of accuracy, (ii) Although the system of equations is large, each equation by itself contains at most only four unknowns. In addition, they state: *The implicit method can also handle varying channel geometry even where the changes from section to section and in the bottom slope are quite significant.*

2.5 NUMERICAL DIFFICULTIES

Each of the schemes or solution methods are plagued by some difficulties in their application. In this section a discussion of some of the numerical schemes with their advantages and difficulties will be presented.

Benque et al. (1982) used the split operator FD technique together with the ADI method to simulate tidal currents. However, they found that the scheme was not suitable for rapidly varying or highly nonlinear velocities. Jenkins and Keller (1990) developed a 2-D FD model using a boundary fitted coordinate system with subregion grid generation to simulate flow in a hypothetical river with flood plain. They used first order upwinding for the convective terms together with the ADI method. Hirsch (1988) used the Finite Volume (FV) method, which is based on the integral form of the conservation equations, and has the advantage of having good conservation properties. Soulis (1992) developed a 2-D FV model to solve dambreak problems using body fitted non-orthogonal local coordinates. In his development he assumed the main flow to be in the positive x-direction and employed a first order upwind scheme. Other FV techniques classified under the approximate Riemann solvers, such as Flux Vector Splitting and Flux Difference Splitting have been proposed by Stager and Warming, (1981), Van Leer (1982), Roe (1981), and Hirsch (1988). Glister (1988), proposed a Flux Difference Splitting Scheme to solve the shallow water equations. Zhou et al. (1994) dealt with domain irregularity. They used an unstructured mesh of triangles and quadrilaterals together with the explicit FV method. This method suffered from the requirement of small computational time steps, excessive numerical damping, no domains having discontinuities and shocks.

Some limitations face the FD and FV methods. A Few examples of these limitations will be cited. The boundary conditions are imposed artificially. Derivative boundary conditions require the use of fictitious nodes and/or a reduced accuracy at the boundary. Lee and Froehlich (1986) concluded that although the FD method is usually easier to program than the FE method, it generally requires more nodes and computational time to achieve accuracy comparable to the FE method. FD is usually unable to operate on an unstructured grid greatly limits its applicability to simulate flow in natural water bodies, whereas the FV can be used. The FV is used on unstructured grids (Zhou et al., 1994). It is important to note the advantage of ease of implementation attributed to the FV method as compared to the FE method starts becoming debatable in this class of FV methods.

The numerical techniques have their disadvantages as large values of diffusion could have a distorting effect on the simulated flow, as they would smear out any interesting flow features. Norton and King (1976 and 1978), Walters and Cheng, (1980), and Froehlich (1989) reported conservation problems, especially at no flow boundaries with sharp corners. Problems in satisfying continuity were also reported by Gee and McArthur (1978) and Bates et al. (1992). Walters and Cheng, (1980) noticed difficulties in applying head-type boundary conditions. Some remedies were suggested but often led to problems in convergence. Wang and Adeff (1987) applied a Petrov Galerkin technique to solve the depth-integrated 2-D Navier-Stokes equations and Katopodes (1987) applied a similar technique to simulate the surge resulting from a breached dam.

2.6 STATISTICAL CRITERIA

The representation of a hydraulic phenomenon by some mathematical relationships (or models) inevitably introduces some degree of inaccuracy. Other inaccuracies occur when representing the system of mathematical equations by FD and in producing the results. It is generally accepted that no single simulation model output will be identical in all respects to the physical phenomenon it aims to represent. However, it is required that this output be

sufficiently close to its physical counterpart in order for the model simulation to be considered acceptable.

The principle of *goodness-of-fit* is a measure of the degree to which the output conforms to the corresponding observed data. *Goodness-of-fit* techniques may range from purely subjective graphical (visual) methods to purely objective techniques using mathematical and statistical relationships. These relationships usually portray the difference between simulated and observed variables.

Prior to any calibration or model application, the user should establish criteria for comparing simulated and observed variables. However, if too many criteria are used and are frequently switched, the assessment of the model performance becomes difficult. For example, if the model is intended to design sewers, then the primary variable of interest is the peak flow and calibration would be best made on a comparison between modelled and observed peak flows. On the other hand, in designing a storm detention basin, run-off volumes and possibly the hydrograph shape are important and calibration must be based on a comparison of simulated and observed volumes and hydrograph shapes. In a hydrodynamic flood routing and pollutant transport application, both the peak flow rates (or peak depths) and hydrograph shapes would be the criteria for comparison in the modelling exercise, in addition to pollutant concentration values in a water quality application.

Related to model simulation assessment is the graphical method for calibration. It consists of plotting the observed and simulated hydrographs on the same graph. A visual comparison is then made of peak flows and hydrograph shapes. The importance of the graphical method should not be overlooked. Although subjective, it provides a rough appreciation of the model capabilities. Johnston and Pilgrim (1976) emphasized the importance of subjective impressions, based on the fact that even the choice of the form of a statistical fitting technique is still a subjective decision.

With a good understanding of the physical problem (and the effect of each model parameter on the simulation), the user can re-adjust parameters to obtain a better fit. Even though time consuming, this method is very instructive to the model user and helps in understanding the model performance under different conditions. This methodology is often used when there is only a limited number of measured events. However, it is usually thought to be highly subjective and difficult when comparing the performance of similar models. In these instances the user can only resort to statistical *goodness-of-fit* techniques.

While the graphical calibration method is often referred to as a *trial and error* procedure, statistical *goodness-of-fit* techniques are more often associated with automatic optimization of parameters. A statistical goodness-of-fit procedure implies a method to measure, in some way, the deviation of a simulated output to that observed; the measurement thus obtained being an end in itself. On the other hand, a statistical fitting procedure employs this measure of deviation of the simulated output to assist in the calibration process; the objective being a simulated output more closely resembling that observed.

Statistical fitting procedures were used by Dawdy and O'Donnel (1965) to demonstrate the usefulness of automatic optimization for parameter calibration. Automatic optimization means systematic adjustment of model parameters, or sets of parameters, in such a way that the corresponding model output agrees more closely with the observed data after the adjustment. In this context, the statistical *goodness-of-fit* equation is called an objective function. For example, let G(x) be an objective function of the error in a model prediction which results from x_1, x_2, x_3, ..., x_n model input parameters. It would be required to minimize (or optimize) the value of G(x) by assigning a suitable choice of values to the individual elements in the vector x. A search must be employed to determine the location of the overall global minimum over the surface where G(x) is defined.

Several search methods are available. Nelder and Mead (1965) used the *Direct Search Simplex* method, whereas Fletcher and Powell (1963) used the *Steepest Descent*

procedure. The optimization (or minimization) of the objective function G(x) can be achieved by changing several values of x until no significant reduction of the G(x)-value is recognized. Therefore, the goal of calibration would be to find the combination of model parameters that would minimize the objective function.

Different objective functions would ordinarily give more weight to a certain aspect of disagreement between observed and simulated results. In general, the choice and role of the objective functions are aspects which offer serious difficulties to the model user. In a comparative study, Diskin and Simon (1977) concluded that the choice of the most appropriate objective function must be based on the nature of the problem to which the model is to be applied. Furthermore, this study favoured the consideration of more than one objective function when assessing the *goodness-of-fit* of a particular model for a given application. Ibbitt and O'Donnell (1971) expressed similar sentiments with regard to statistical fitting procedures. Aitken (1973) stated that the simulation model should have the ability to reproduce the mean and standard deviation of the observed values.

No single statistical goodness-of-fit criterion is sufficient to assess adequately the measure of fitness between simulated and observed hydrographs. Ultimately, the selected objective function should depend on the objective of the modelling exercise, as different criteria are weighted in favour of different hydrograph variables. For the present research, different statistical *goodness-of-fit* techniques were employed to evaluate the performance and validation of the new hydrodynamic model. The graphical assessment technique was employed occasionally. Simulated results were compared with observed data on the same graphs and a visual check was performed. This method gives a good appreciation of the effect of parameter variation on model performance. However, it may be misleading on some occasions when a visual check is made for the rising and recession parts of the hydrograph. A visual check may appear to have an excellent fit, but the actual relative error at a particular point might rise to 30 % in some instances, (Chatila, 1992). Statistical *goodness-of-fit* techniques used in this research to evaluate model performance included: sum of squares

criteria, Nash and Sutcliffe (N & S) method, RMSE, SEE, REE, and PEE. An alternative method, which determined the relative percent error at every point of the simulated hydrograph, is relied on. Absolute values of the corresponding relative percent errors at every point are then summed to give the total absolute percent relative error or the total absolute relative error (TARE). In general, hydrographs with the least total absolute relative errors would give the best-fit. Therefore, except for N&S criteria which should approach 1, the goal is to minimize the objective function to obtain the best-fit hydrograph.

2.7 SUMMARY

In the literature a wide spectrum of mathematical models are available for ***unsteady flow*** and ***water quality*** computations. The variability can be attributed to the fact that the phenomenon is very important from the physical point of view.

The construction of the mathematical model of a flooded area sets up a series of problems, concerning both representation of the physical reality and the numerical methods. Different alternatives can be employed to define the main channel-flood plain interaction process. Further discussion will be cited in chapter 4. In general, extensive simplifications are applied for the case of the equations of continuity and motion in order to obtain a solution, (Cunge, 1975; and Radojkovic and Ivetic, 1982). An example of these major simplifications is the case of splitting the compound channel into a series of stream tubes. Another example is determining the distribution of the eddy viscosity (υ_t) by a turbulence model such as the depth-averaged k-ϵ model and neglecting inertia terms, (Prinos, 1984). After neglecting several terms the PDE are restricted to parabolic flows only. The velocity components are governed only by the continuity and the x-momentum equations, whereas the DA y-momentum is not needed and the vertical z-momentum equation is therefore reduced to the hydrostatic pressure relation. As a result of DA, the x-momentum equation contains the local bottom shear stress whereas the surface shear stress is neglected, (Prinos, 1984).

Djordjevic (1993) developed a mathematical model for unsteady transport in compound channel flows and conducted an experimental verification. His method does not take the horizontal momentum transfer into consideration, which leads to rough estimations of the velocity field. As a result, any refined dispersion modeling with a doubtful velocity field is unreasonable. The equation developed was valid only for uniform flows. However, it was still applied for the calculation of velocity distribution in ***non-uniform*** flow. In addition, the variation of DA velocity with time term ($\partial u/\partial t$) and the effects of wind stresses were dropped from his equation.

In summary, (i) the majority of existing pollutant transport models were developed for either steady or unsteady flow in single, regular-shaped channels, and (ii) these models are mostly 1-D models that are based on simplified (or over-simplified in some cases) versions of the governing equations. In view of these limitations there is a need to develop a 2-D model to solve the continuity equation, the momentum equations, and the convection-dispersion equation describing the transport of pollutants or contaminants in compound river channels. ***THE MAIN PRODUCT OF THIS RESEARCH IS THE DEVELOPMENT OF A 2-D FLOW MODEL, CHAT, DESIGNED SPECIFICALLY FOR SIMULATING POLLUTANT TRANSPORT IN CHANNELS HAVING COMPOUND CROSS-SECTIONS.***

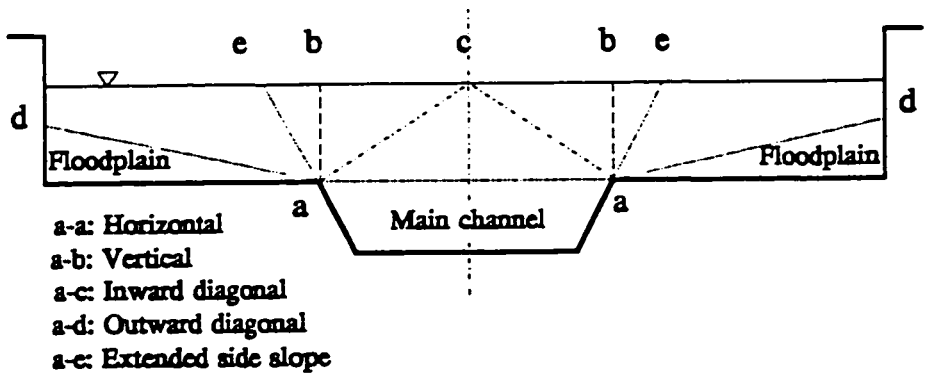

Figure 2.1 Alternatives to Define Main Channel-Flood Plain zones.

CHAPTER THREE

THEORETICAL CONCEPTS

3.1 MODELLING PROCESS

Computational hydraulics is the application of numerical methods for the solution of problems of hydraulic flows. The computational modelling process consists of describing an object with a set of numbers and simulating the laws acting upon it with a set of operations upon these numbers. Abbott (1976) states that to any one object there corresponds an infinite number of possible descriptions and to any one law there corresponds an infinite set of operations, or schemes, that describe its action. Therefore, the mathematical modeller should make the model as accurate as his/her knowledge of the prototype geometry and its physical laws. He/she should strive for a compromise between accuracy, computational effort and cost involved. In general, computational hydraulics models are built based on conservation laws of mass, momentum, and/or energy. It is important to select a proper scheme for the solution of the governing equations to avoid the falsification of any of the conservation laws. This falsification will generally worsen when abrupt and rough changes occur from one point to the next in the model.

Physical and mathematical models are very suitable for basic research within a wide range of boundary conditions and for the development of general design rules. However, on-site investigations, evaluation of experience, and large-scale (prototype) tests are needed to verify the final results because river flow is a complex process. The similarity between a river and its model can usually be verified only partially. The results obtained by the model, using different sets of parameters and different transport formulae, can then be used to assess the future situation of the river and suggestions made with regards to the design. The model parameters should be estimated based on field and/or laboratory measurements. Thus, a model can be efficient only if it relies on data and if its predictions can be verified by measurable data. Also, measurements should concentrate on those data only, which are used in the model. Modellers often include as many parameters as possible to satisfy the theoretical requirements of simulating the system, even if some of their values are not directly measurable (e.g. defining the turbulence of a stream). Investigations should aim at reducing the number of non-measurable factors by improved techniques and methods of measurements, including new sets of relevant physical data to be used in the model, (Bruk, 1988).

3.2 SPATIAL DIMENSIONS

River flow is a 3-D time-dependent problem. It requires a great deal of schematization in order to *make* a mathematical description, leading to a mathematical model that can be used for morphological predictions such as the case of water quality and transport processes. Regarding the number of spatial dimensions the flow simulation approach can be classified as 1-, 2- or 3-D. 1-D models view the stream as a number of cross-sections. They provide results in the form of cross-section-averaged values as functions of time and space, where the longitudinal coordinate along the flow direction is the spatial dimension. This approach is usually used to analyse long reaches of rivers extending over many kilometres, where the variation of flow across the channel is not of much interest. Hicks and Steffler (1990) provide an overview of different approaches and approximations to solve the 1-D open channel flow equations.

For some practical applications, the velocity distribution across a stream might be important, for example, flows in estuaries and river deltas, or flows in a meandering river with wide flood plains. Also, environmental impact assessment models often require the distribution of the velocity across the stream as input to other (chemical or biological) models. In these situations, solution of the 2-D shallow water equations can provide relatively good estimates of flow features in the horizontal plane, such as re-circulation, flow around islands and obstructions, and flow in braided channels. The approach is a 2-D horizontal DA approximation to the real flow. Such models are based on the 2-D flow equations in the x- and y-directions. Also, the 2-D vertical approach in the x-z planes can be used. Computing time for 2-D models is great, thus preventing them from being used for long river reaches or rivers with long flow duration. The 2-D model is often used over short reaches of a long river channel. However, because of the DA feature of the 2-D equations, 2-D models are not able to resolve, accurately, flow phenomena of a 3-D nature. For example, when simulating a river bend, a 2-D model would be able to predict the redistribution of longitudinal velocity reasonably well, but it would not be able to represent the *helical vortex* feature usually associated with *bend* flows. As this vortex has a large effect on the mixing characteristics and local bathymetry of the river, the direct application of a 2-D model to simulate water quality or sediment transport would provide only limited success.

The 3-D approach provides the complete definition of flow, including the secondary currents, (Rodi, 1984). The complexity and computing time consumption associated with 3-D models have so far prevented them from being used for rivers of any significant length. ***Most 3-D models only cover the hydraulics of flow but not bed sediment motion or pollutant transport.*** A general review of these models is given by The ASCE Task Committee on Turbulence Models in Hydraulic Computations (1988). Solution of the 3-D Reynolds equations could account for secondary flows and other flow features, such as horseshoe vortices in the vicinity of bridge piers, and flow details around obstructions and bed forms, however, it is not an easy task to obtain valid solutions. The equations are comprised of one conservation of mass and three conservation of momentum equations applied in the

directions of the three space dimensions. The turbulent fluctuations of the flow are time-averaged to yield additional turbulent stress in the momentum equations. The resulting system of four equations has a total of *ten unknowns*, and therefore, *closure models* are required to relate the turbulent stresses to mean flow parameters. Further, the resolution required to obtain numerically stable solutions in a typical reach of a stream or river would involve an enormous number of computational nodes, having four unknowns each. The free water surface would further complicate the problem, as the 3-D mesh would have to change continually with time.

3.3 MATHEMATICAL FORMULATION OF FLOW PROBLEM

The growing intensity of land and water resources utilization has renewed efforts towards systematic research in the field of alluvial hydraulics. In general, it is not possible to obtain analytical solutions to the conservation of mass equation, conservation of momentum equations and the advection-diffusion equation in natural waterways with arbitrary boundary conditions. However, a variety of exact solutions exists for idealized situations, which can be useful in obtaining order-of-magnitude estimates. Future progress in numerical modelling of contaminant transport in surface waters and particularly in rivers should depend not only on an improved understanding of the physical processes involved but also on improved numerical methods.

The simulation of the flow of water in natural streams and rivers is of importance to many disciplines. Hydraulic models are required for flood forecasting and designing of flood protection measures, for the design of dams and power stations, and for the analysis and design of stream diversions and water intakes. *A correct understanding of the flow characteristics is also important for analysing processes related to the flow of water, such as sediment transport, water quality, and aquatic habitat protection.*

3.3.1 GOVERNING EQUATIONS

The derivation of the basic differential equations begins from the general equations of continuity and motion for an incompressible fluid in classical hydrodynamics, (Streeter, 1948; Rouse, 1959). These equations, which are referred to as the Navier-Stokes equations, are derived in 3-D in Appendix A. With reference to a Cartesian orthogonal system (x,y,z), the equations have the following form:

$$\frac{\partial u}{\partial x} + \frac{\partial v}{\partial y} + \frac{\partial w}{\partial z} = 0 \qquad \textbf{(3-1)}$$

$$\frac{\partial u}{\partial t} + u\frac{\partial u}{\partial x} + v\frac{\partial u}{\partial y} + w\frac{\partial u}{\partial z} = F_x - \frac{1}{\rho}\frac{\partial P}{\partial x} + \nu\nabla^2 u \qquad \textbf{(3-2)}$$

$$\frac{\partial v}{\partial t} + u\frac{\partial v}{\partial x} + v\frac{\partial v}{\partial y} + w\frac{\partial v}{\partial z} = F_y - \frac{1}{\rho}\frac{\partial P}{\partial y} + \nu\nabla^2 v \qquad \textbf{(3-3)}$$

$$\frac{\partial w}{\partial t} + u\frac{\partial w}{\partial x} + v\frac{\partial w}{\partial y} + w\frac{\partial w}{\partial z} = F_z - \frac{1}{\rho}\frac{\partial P}{\partial z} + \nu\nabla^2 w \qquad \textbf{(3-4)}$$

$$\nabla^2 = \frac{\partial^2}{\partial x^2} + \frac{\partial^2}{\partial y^2} + \frac{\partial^2}{\partial z^2} \qquad \textbf{(3-5)}$$

where:

x, y, and z = distances in the longitudinal, transverse, and vertical directions respectively,

u, v, and w = velocity components in the x-, y-, and z-directions respectively,

t = time,

F_x, F_y, and F_z = body forces per unit mass in the x-, y-, and z-directions respectively,

P = fluid pressure,

ρ = fluid density, and

ν = fluid kinematic viscosity.

The fluid flow in a river is 3-D and time-dependent. Hydrostatic pressures can be safely assumed in the case of a river flow because the flow is nearly horizontal. In addition, only shear stresses from horizontal velocity components are important. In the classical approach, it is further assumed that gross motions only are considered and the effects of small-scale velocity fluctuations are aggregated into shear stress terms. Furthermore, it will be assumed that the mass densities of the substances transported in the river are very small compared to the density of water. In such a case, the density of water is considered constant in the whole region under investigation and is not influenced in time and/or space by changes in the mass density of the transported substances.

3.3.2 MODEL REPRESENTATION

A review of the literature on existing 1-D FD flow models indicated several areas of difficulties which prevent them from providing accurate solutions. Examples of these difficulties are *the inability to represent complex topography and boundaries, poor conservation properties, excessive artificial diffusion, and instabilities occurring when attempting to simulate domains containing wet and dry areas.* The basic formulation of the St. Venant equations, for a channel with lateral inflow or outflow, is given as, (Chaudhry, 1993):

- Conservation of mass equation:

$$\frac{\partial A}{\partial t} + \frac{\partial Q}{\partial x} = - q \qquad \textbf{(3-6)}$$

where:

A = cross-sectional area of flow,

Q = discharge, and

q = lateral inflow or outflow.

and a conservation of momentum equation:

$$\frac{\partial Q}{\partial t} + \frac{\partial (Q\ U_a)}{\partial x} + g\ A\ \frac{\partial h}{\partial x} = g\ A\ (S_o - S_f) - U_{xq} \qquad (3\text{-}7)$$

where:

U_a = cross-sectional average velocity,

g = gravitational acceleration,

h = flow depth,

S_o = bed slope,

S_f = resistance slope, and

U_{xq} = convective momentum transport between the main channel and the flood plain.

As the 2-D model provides a good representation of the flow field, it can serve as a tool to analyse the complex flows encountered in typical fish habitat reaches. The good conservation properties of the model make it suitable for further development to simulate the transport phenomena and flow under ice cover. In view of the enormous data and computer requirements involved in solving 3-D equations for flow in rivers, the solution of 2-D DA equations is generally attempted.

Several difficulties arise when solving 2-D equations for natural streams. First, there are the challenges which are also encountered in the 1-D approach, such as the simulation of *shocks*, and the production of *wiggle-free* solutions. In addition, new difficulties, related to the 2-D nature of the problem, have to be overcome. For example, the problem of cross-wind diffusion appears, which requires special treatment, (Brooks and Hughes, 1982). Other difficulties are introduced by the complex boundaries often encountered in 2-D domains. The computational grid should be able to conform well to complex geometrical shapes. Another difficulty in 2-D modelling is the treatment of boundary conditions. In the 1-D approach, if the water level drops and the cross section is only partially full, the area at that cross section remains positive. On the other hand, any drop of water level in a 2-D domain usually results in exposing nodes and elements. These *dry areas* result in mathematical complications and require special treatment.

Analytical solutions do not exist for the set of 3-D equations. Also, numerical solutions of these equations in their complete form is very difficult to accomplish due to several problems. These problems include, among many others, the capabilities of available computers in the public domain, and the complexities in defining river boundaries and geometry. It can be argued that a 3-D model is required for proper simulation of the flow field. However, the effort and cost of developing a 3-D model would outweigh the improvement gained over a 2-D model. ***Thus, a 2-D model is a reasonable compromise between the over-simplified 1-D and the difficult to model 3-D processes.*** In this instance, in order to simplify the problem and ease the computational efforts and complexities, ***the Navier-Stokes equations are integrated over the water depth to give the DA 2-D equations.***

3.3.3 2-D DA EQUATIONS

Consider a water column of unit-square cross-section and depth h, extending from the (fixed) bottom $z = Z_b(x,y)$ to the surface $z = Z(x,y,t)$; i.e., $h = Z - Z_b$. The equation of continuity for this column can be obtained by integrating the 3-D continuity equation (eq. 3-1) over the vertical, (Chen and Chow, 1971; and Lai, 1977) and noting that:

$$U = \frac{1}{H} \int_{Z_b}^{Z} u \, dz$$

$$V = \frac{1}{H} \int_{Z_b}^{Z} v \, dz \qquad \textbf{(3-8)}$$

where: U and V = DA longitudinal and transverse velocities respectively. Therefore, vertical integration of the continuity and momentum equations yields the following basic equations for vertically DA 2-D flow, (Lai, 1986):

3.3.3.1 Continuity Equation

$$\frac{\partial H}{\partial t} + U \frac{\partial H}{\partial x} + V \frac{\partial H}{\partial y} + h \frac{\partial U}{\partial x} + h \frac{\partial V}{\partial y} + U S_{ox} + V S_{oy} = 0 \quad \textbf{(3-9)}$$

where:

H = water surface elevation,

S_{ox} and S_{oy} = bottom slopes in the x-, and y-directions respectively.

3.3.3.2 Momentum Equations

$$\frac{\partial U}{\partial t} + U \frac{\partial U}{\partial x} + V \frac{\partial U}{\partial y} + g \frac{\partial H}{\partial x} - F V + g S_{fx} - W_x = 0 \quad \textbf{(3-10)}$$

$$\frac{\partial V}{\partial t} + U \frac{\partial V}{\partial x} + V \frac{\partial V}{\partial y} + g \frac{\partial H}{\partial y} + F U + g S_{fy} - W_y = 0 \quad \textbf{(3-11)}$$

where:

S_{fx} and S_{fy} = friction slopes in the x-, and y-directions respectively,

W_x and W_y = wind stresses in the x-, and y-directions respectively, and

F = Coriolis factor.

S_{fx} and S_{fy} are usually determined from a steady-state friction formula such as Chezy's or Manning's equation. In this case, Manning's equation is used to quantify S_{fx} and S_{fy} as follows:

$$S_{fx} = \frac{n^2 U \sqrt{U^2 + V^2}}{k_o^2 h^{\frac{4}{3}}}$$

$$S_{fy} = \frac{n^2 V \sqrt{U^2 + V^2}}{k_o^2 h^{\frac{4}{3}}} \qquad \textbf{(3-12)}$$

where:

n = Manning's roughness coefficient, and

k_o = dimensional constant, (= 1 for SI units and = 1.49 for English units).

The above set of equations is based on the assumptions of constant fluid density, hydrostatic pressure distributions, and relatively uniform bottom slopes. The unsteady flow equations are nonlinear PDE that defy analytical solution except in their very simplest form. When their numerical solutions are attempted, since the digital computer is a discrete-type calculating machine the actual flow computation must be carried out in discrete form rather than in continuous form. This implies that infinitesimal quantities dx, dy and dt must be represented by finite quantities Δx, Δy and Δt for calculations to be performed on the computer.

3.3.4 COMPOUND CHANNEL FLOWS

Construction of the mathematical model of a flooded river channel sets up a series of problems, concerning both representation of the physical reality and the numerical methods. The problem is reduced to 2-D, i.e., there are three independent variables: two spatial ones, (x and y) and the time variable t. The two unknown dependent variables are the discharges Q(x,y,t) and the water levels above the datum z(x,y,t). The governing equations of the flow problem constitute a system of nonlinear hyperbolic partial differential equations (PDE). From a mathematical point of view, this is not the Cauchy problem but a mixed one, because it involves a set of initial conditions at time t = 0 and a set of boundary conditions, specified as

functions of time. The numerical solution of this system of equations raises difficulties, particularly because of the uncertainty about what sort of boundary conditions should be imposed upon the system.

Different alternatives can be employed to define the main channel-flood plain interaction process. Some of these procedure are cited in the following sections, including a discussion of their advantages and disadvantages.

3.3.4.1 Stream Tubes, (Cunge, 1975)

In 2-D problems involving flood propagation over inundated flood plains, the flood build-up is relatively slow (except when dikes break) and the resistance terms (friction slopes) prevail in the flow equations. Cunge (1975) reported that it is logical to drop the inertia terms from the PDE because they are of small importance as compared to the water surface and friction slopes. In his derivation, Cunge (1975) assumed that, (I) bottom slopes are not very important, (ii) Coriolis centrifugal acceleration due to the earth's rotation can be neglected, (iii) uniform distribution of the velocity exists within the section, (iv) vertical pressure distribution is hydrostatic, and (v) inertia terms are dropped. Based on those assumptions, the system of equations is still nonlinear but it becomes *parabolic* instead of being *hyperbolic*. In order to ensure the existence and uniqueness of its solutions one only needs to specify the set of initial and boundary conditions. It is sufficient to prescribe the water levels at time t = 0 and their evolution in time along the boundaries.

Even if the inertia terms are disregarded, the numerical solution of a mixed problem of this type still involves great difficulties. Furthermore, it cannot be generally assumed that the flood plain remains completely submerged and that depths are everywhere of the same order of magnitude. Even during the flood peak the flood plain zone still forms a system of cells or compartments separated by dikes and the depths are never so great that the effects of the plain topography can be ignored. These cells are laced by irrigation channels, low

dikes, culverts, etc., all of them influencing the direction of flow. Suppose that the flood plains, as well as the actual bed of the river and its tributaries can be divided into a certain number of cells. Each cell communicates with its neighbouring cells and the links between them correspond to an exchange of flow in the physical reality. The breakdown of the given area into cells is not arbitrary but is based as far as possible on natural boundaries, such as roads, dikes, natural bank levees, etc. The absence of natural obstacles leads to cells of unwieldy size, where the separation is no longer based on natural features but is merely used to allow for the slope of the flood plain. Each cell is assigned a characteristic water level value, for example, the level z_c taken at the centre of cell I. It is assumed that this water level is horizontal throughout the cell. Any cell is connected to all other cells sharing a common boundary with it. Therefore, the cell centres must be defined in such a way that the directions of flow are correctly allowed for at any time during the flood. The slope of the water surface is discretely defined by the levels z_c.

Consider a part of the inundated flood plain shown in figures 3.1 and 3.2. The area AA'B'B can be considered as one cell but since a horizontal water surface was assumed within the cell then the model would not reproduce the slope between cross-sections AA' and BB'. Thus, the only known level within area AA'B'B is z_c. If one desires to reproduce on the model the natural slope of the reach between the two sections AA' and BB', the area should be represented at least by two cells: AA'D'D and DD'B'B. Then, two water levels will be computed: one, z_c' at the centre of the upstream cell and another, z_c'' at the centre of the cell DD'B'B. The slope of the water surface will thus be defined by $(z_c' - z_c'')/l'$.

In order to derive the continuity equation for a cell, it is assumed that the water surface is horizontal within the cell boundaries and that its elevation above the datum is z. There are two fundamental hypotheses on which the governing equations are based:

- The volume V_i of water stored in cell I is directly related to the level z_i^k in this cell,

- The discharge $Q_{i,j}^{k}$ between two adjacent cells I and j at the given time $k\Delta t$ is a function of the levels z_i^k and z_j^k only. ***This means that any forces of inertia which might act on the flow between these two cells are disregarded.***

These hypotheses enable one to write the continuity equation for any cell I. There are as many continuity equations as there are cells I in the model and, also, as many unknown water levels $z_i(t)$. Thus, for N cells the system of N ordinary differential equations is established for N unknown functions z_i of the independent variable t. The solution to this system exists and is unique if the set of initial conditions z_i (t=0) is prescribed. Once this set is known, the functions $z_i(t)$ may be computed numerically and the discharges $Q_{i,k}$ can be found as they only depend upon the water levels z_i and z_k. It is obvious that the system of boundary conditions varying in time must be prescribed too if the problem is to be well posed. The continuity equations may be written in a form suitable for numerical solution, but then the functional dependence of discharges $Q_{i,k}^{n}$ upon levels z_i^n and z_k^n must be given explicitly. Two types of exchange relationships between cells are generally assumed:

(I) River type links: there are no local obstacles to the flow (no singular head losses) and a mean resistance coefficient for a given cross section of the flow can be used in Strickler's (Manning's) formula.

(ii) Weir type links: the roads or dikes form a boundary that can be represented by a singular head loss between two cells. In this case the classical discharge formulae for broad-crested weirs are used. When the weir is of compound type, the discharge is computed separately for each of the cross-sectional components. These component discharges are then added to give the total discharge.

Again, extensive simplifications are applied for the case of the equations of motion in order to obtain a solution, (Cunge, 1975). ***Based on the fact that major simplifications are involved in order to reach at a solution, the option of splitting the channel into a series of stream tubes will not be investigated any further as far as the flow problem is concerned.***

3.3.4.2 2-D DA k-ϵ Model

The distribution of the eddy viscosity (υ_t) can be determined by a turbulence model such as the depth-averaged k-ϵ model, (Prinos, 1984). ***In order to ease the computations and reach a solution, inertia terms are usually neglected.***, (ibid) In this instance, the PDE are restricted to parabolic flows only. The velocity components are governed only by the continuity and the x-momentum equations. The DA y-momentum is not needed and the vertical z-momentum equation is therefore reduced to the hydrostatic pressure relation. As a result of DA process, the x-momentum equation contains only the local bottom shear stress; (the surface shear stress is neglected), (Prinos, 1984). The x-momentum equation, in its discretized form, can be derived using a control-volume formulation. The calculation domain is divided into a number of non-overlapping control volumes and the differential equation is integrated over each control volume. The discretized equation is applied to any subsection of the compound channel. For the main channel, the velocity differential with the flood plain generates additional internal shear and a continuous transfer of momentum (due to turbulence diffusion) from the main channel to the flood plain zone.

In his applications, Prinos (1984) determined υ_t at each point in the flow field by means of a turbulence model that accounts for both bottom and free shear influences on the eddy viscosity distribution and therefore permits a much wider range of flows to be calculated without changing the empirical parameters involved. He employed the DA k-ϵ model, which characterizes the local DA state of turbulence through two parameters: (I) the turbulence kinetic energy, and (ii) the rate of dissipation of turbulence kinetic energy. The variations of the turbulence parameters k and ϵ are determined from the transport equations.

In past years most of the numerical models developed for flow in compound channels involved simplifications. Radojkovic and Ivetic (1982) applied a numerical model to *fully-developed* flows in compound channels. The governing equations were simplified by combining convection and shear stresses in an *effective shear stress* parameter, the latter

being calculated from a length-scale model. The resulting differential equation was then solved by a FE techniques. In most computational methods the turbulent or eddy viscosity is assumed constant over the flow field and therefore this was adjusted to suit a particular condition after calibration, which limited the effectiveness of those methods. Puri and Kuo (1983) used a constant eddy viscosity distribution to determine the velocity field associated with a side discharge into an open channel. The results did not show a clearly defined deflection region and the accompanying re-circulation zone was suppressed. They obtained better results using a variable eddy viscosity distribution based upon the Prandtl *mixing length* hypothesis and an assumed seventh power law velocity profile. For the same problem, Rodi (1982) used a constant eddy viscosity ($\upsilon_t = 200\nu$) and obtained results very similar to those obtained using the k-ϵ model. Lean and Weare (1979) used an expression for viscosity derived from 2-D shear layer concepts, first proposed by Rodi (1980).

Djordjevic (1993) developed a mathematical model for unsteady transport in compound channel flows and performed an experimental verification. He stated that the velocity distribution can be determined using some of the Manning-type equations, assuming that the DA velocity is proportional to the local depth raised to a certain power (depending on which friction coefficient is used). This method does not take the horizontal momentum transfer into consideration, which leads to rough estimations of the velocity field. Accordingly, any refined dispersion modelling with a doubtful velocity field is unreasonable. Djordjevic (1993) used the DA x-direction conservation of momentum equation derived by Rastogi and Rodi (1978) as follows:

$$U \frac{\partial U}{\partial x} + V \frac{\partial U}{\partial y} = - g \frac{dH}{dx} + \frac{1}{h} \frac{\partial}{\partial y}\left[h \upsilon_t \frac{\partial U}{\partial y}\right] - \frac{\tau_{bx}}{\rho h} \qquad \textbf{(3-13)}$$

where τ_{bx} = bottom shear stress.

Based on the assumption that the flow has insignificant secondary currents, Rastogi and Rodi (1978) omitted the so-called dispersion terms. These terms account for vertical

non-uniformities in the longitudinal and transverse velocity components. Furthermore, if the left-hand side terms are also neglected then the resulting equation is valid only for uniform flows. However, it was still applied for the calculation of velocity distribution in ***non-uniform*** flow. In addition, the variation of DA velocity with time term ($\partial u/\partial t$) and the effects of wind stresses were dropped from the above equation.

The eddy viscosity is not a real DA value, but it is introduced, (by analogy with its definition), as the coefficient of proportionality between the DA turbulent stress and transverse DA velocity gradient. By the constant dimensionless (or relative) eddy viscosity model, it is expressed as:

$$\upsilon_t = c_v \, h \, u_* \qquad \textbf{(3-14)}$$

where:

c_v = empirical constant, and

u_* = shear velocity, ($\sqrt{[\tau_o/\rho]}$).

As it does not require any additional equations, using the eddy viscosity model is simpler than employing the k-ϵ model. Moreover, Radojkovic and Djordjevic (1985) showed that in many situations, especially in the case of compound channel flows, ***the constant eddy viscosity model may give better agreement that the DA k-ϵ model with its standard empirical constants.***

3.3.5 PROPOSED GOVERNING PDE

The governing 2-D DA equations of continuity and momentum are presented in this section along with the introduction of the constant eddy viscosity terms to account for LMT. The wind stress in the x- and y-directions is neglected throughout. In addition, terms of the continuity equation are grouped together using the rules of differentiation. Thus, the equations to be solved are:

$$\frac{\partial H}{\partial t} + \frac{\partial (H\ U)}{\partial x} + \frac{\partial (H\ V)}{\partial y} = 0 \qquad \textbf{(3-15)}$$

$$\frac{\partial U}{\partial t} + U\ \frac{\partial U}{\partial x} + V\ \frac{\partial U}{\partial y} + g\ \frac{\partial H}{\partial x} - F\ V$$

$$+ g\ \frac{n^2\ U\ (U^2 + V^2)^{\frac{1}{2}}}{k_o^{\,2}\ h^{\frac{4}{3}}} - \frac{1}{h}\ \frac{\partial}{\partial y}\left[h\ \upsilon_t\ \frac{\partial U}{\partial y}\right] = 0 \qquad \textbf{(3-16)}$$

$$\frac{\partial V}{\partial t} + U\ \frac{\partial V}{\partial x} + V\ \frac{\partial V}{\partial y} + g\ \frac{\partial H}{\partial y} + F\ U$$

$$+ g\ \frac{n^2\ V\ (U^2 + V^2)^{\frac{1}{2}}}{k_o^{\,2}\ h^{\frac{4}{3}}} - \frac{1}{h}\ \frac{\partial}{\partial x}\left[h\ \upsilon_t\ \frac{\partial V}{\partial x}\right] = 0 \qquad \textbf{(3-17)}$$

3.4 MATHEMATICAL FORMULATION OF TRANSPORT PROBLEM

In recent years hydraulic engineers have frequently been asked to analyse and predict mixing in natural bodies of water. It is no longer sufficient to deal only with water quantities because of the growing concern over water quality. Engineers are concerned with the processes that take place between the point where the pollutant is discharged into the water environment and some other sites where the ambient water quality is observed. They are often called upon to make the interfaces between man's activities, involving water and wastewater, and the natural environment. For a long time, they have had the responsibility for drawing our water supply from natural water bodies; now they must pay equal attention to how it is returned in diminished amounts and of poorer quality.

3.4.1 GENERAL DEFINITIONS

Several terms that relate to the transport problem will be defined in this section.

Point source: is the discharge from a structure which is specifically designed for the outflow of wastewater from some industrial process or municipal sewerage system. Point sources have been the target of most of the laws and regulations of water pollution control. The accidental spill of oil from a ship and the release of radioactive wastes from a power plant can be considered as point sources.

Non-point sources: are defined as widely distributed points where pollutants are introduced into the hydrologic cycle. In such cases, water treatment is usually not feasible. Examples are the runoff of salts used for deicing highways in winter, soil erosion, acid rainfall and street drainage.

Advection: is transport by an imposed current system.

Convection: is the vertical transport induced by hydrostatic instability, such as the flow over a heated plate, or below a chilled water surface in a lake.

Molecular Diffusion: is the scattering of particles by random molecular motion, which may be described by Fick's Law and the classical diffusion equation.

Turbulent Diffusion: is the random scattering of particles by turbulent motion, considered roughly analogous to molecular diffusion, but with eddy diffusion coefficients which are much larger than molecular diffusion coefficients.

Shear: is the advection of fluid at different velocities and positions; this may be simply the normal velocity profile for a turbulent flow where water flows faster with increasing elevation

above the bed of the stream; or shear may be the changes in both magnitude and direction of the velocity vector with depth in complex flows, such as estuaries or coastal waters.

Dispersion: is the scattering of particles or a cloud of contaminants by the combined effects of shear and transverse diffusion.

Mixing: is diffusion or dispersion as described above; turbulent diffusion in buoyant jets and plumes; any process which causes one parcel of water to be mingled with or diluted by another. For example, for a thermal discharge we may neglect heat loss from the water surface in the near field, where the initial jet and plume mixing occurs. Hydraulic modelling might be used here. However, in the far field, where heat loss is a dominant factor, the results from the near field are used as input for the hydraulic or computer model.

Laminar and Turbulent Flows: in laminar flow a filament of dye makes a straight streak along the centerline, but in turbulent flow the streak is quickly broken up and spreads across the section. Figures 3.3 and 3.4 show a dye introduced at the upstream end of a pipe in both laminar and turbulent flows along with the deformation of the dye surface.

3.4.2 GOVERNING EQUATION

Starting with a certain elemental volume and applying the conservation of mass, one can obtain a second relationship in addition to Fick's Law. This relationship is true irrespective of the type of the transport process. Combining these two results leads to a PDE that describes the diffusion processes where the fluid is assumed to be stationary and the mass is transported by diffusion alone. However, in most cases the fluid is moving with a velocity vector **u** with components u, v, and w in the x, y, and z directions respectively. **The transport by the mean motion of the fluid is referred to as advection.** It is assumed that the transport by advection and by diffusion are separate entities and they are additive processes. This is equivalent to assuming that diffusion takes place within the moving fluid

just as though the fluid were stationary. Based on the derivation shown in ***appendix B*** the general advection-diffusion equation in 3-D, and accounting for the presence of a source or sink or if one of the constituents undergoes a certain chemical reaction, has the following form:

$$\frac{\partial c}{\partial t} + \frac{\partial (u\ c)}{\partial x} + \frac{\partial (v\ c)}{\partial y} + \frac{\partial (w\ c)}{\partial z} - \frac{\partial}{\partial x}\left(\epsilon_x \frac{\partial c}{\partial x}\right) - \frac{\partial}{\partial y}\left(\epsilon_y \frac{\partial c}{\partial y}\right) - \frac{\partial}{\partial z}\left(\epsilon_z \frac{\partial c}{\partial z}\right) = \pm r\ c \pm s \qquad \textbf{(3-18)}$$

where:

c = mass concentration of diffusing substance,

ϵ_x, ϵ_y, and ϵ_z = empirical mixing coefficient in the x-, y-, and z-directions, respectively,

r = reaction coefficient, and

s = sources or sinks present.

The first term on the left hand side of the above equation (eq. 3-18) expresses the rate of change of the mass concentration with time. The next three terms represent the advective transport, and the last three terms express the turbulent diffusive transport. Furthermore, the right hand side of eq. 3-18 represents the rate of production or decay of the substance and the presence of any sources or sinks.

The 3-D mass balance equation (eq. 3-18) of a certain pollutant can be reduced into a 1- or 2-D form. In this instance, the following sections will discuss the advantages and limitations of using 1- or 2-D analogies.

3.4.7 DIFFICULTIES IN TRANSPORT MODELLING

The selection of the numerical scheme is critical as far as the reliability of the results

is concerned. For example, modelling of convection or transport of material in a stream is thought to be simple. It involves a particle at point x_0 at time t_0 and is convected with a velocity U_a. The same particle will be at $x_0+U_a(t-t_0)$ at time t. Despite its apparent simplicity, modelling of this transport phenomenon introduces many difficulties. One of these difficulties is the numerical dispersion introduced by the transport scheme, which may be at least of the order of magnitude of the physical dispersion. It is possible to add some terms to remedy the situation but some errors will always exist. In such a case the modeller has to find solutions to harder problems than the one he/she started with. Therefore, care should be taken in the selection of the numerical scheme, or combination of schemes.

3.4.7.1 1-D Modelling

The theoretical basis for 1-D modelling was elaborated by Taylor (1954). He showed that in the case of fully-developed pipe flow, the longitudinal dispersion of a tracer which is fully mixed over the cross-section should behave as a Fickian diffusion process, at least at large distances from the point at which the tracer is injected simultaneously. The dispersion equation has the following form:

$$\frac{\partial (A\ C_a)}{\partial t} + \frac{\partial (A\ U_a\ C_a)}{\partial x} = \frac{\partial (A\ K_x \frac{\partial C_a}{\partial x})}{\partial x} \qquad \textbf{(3-19)}$$

where:

C_a = cross-sectional average concentration,

U_a = cross-sectional average velocity,

A = flow area, and

K_x = longitudinal mixing coefficient.

The numerical solution of the 1-D dispersion equation must be approached with a great deal of care. Mechanically speaking, it is not difficult to formulate a solution to the equation, which is a linear parabolic PDE requiring one upstream and one downstream

boundary condition as well as an initial state (or condition). The transport equation represents two physical mechanisms: convective longitudinal transport and longitudinal diffusion.

Most FD methods for the calculation of the convection portion of the transport equation are plagued by artificial, or numerical, diffusion which is sometimes stronger than the physical diffusion, rendering the calculation useless. FD approximations to the convective portion of the transport equation actually represent a different equation of the following form, (Cunge et. al, 1980):

$$\frac{\partial C_a}{\partial t} + U_a \frac{\partial C_a}{\partial x} = K_n \frac{\partial^2 C_a}{\partial x^2} \qquad \textbf{(3-20)}$$

where K_n = an artificial diffusion coefficient introduced by the approximate nature of FD scheme.

If $K_n << K_x$, the artificial diffusion does not compromise the simulation results. But if $K_n \approx K_x$, the simulation results may well appear plausible but be unrelated to the natural phenomena being modelled. Land (1978) suggests that $K_x = 0$ if $K_n > K_x$. But if such drastic action must be taken, there is no point in performing a numerical simulation of the dispersion process, since the essential physical process is suppressed. For implicit schemes solving the transport equation requires an initial and upstream boundary condition, in addition to a downstream boundary condition.

3.4.7.2 2-D Modelling

The prediction of mass transport in a 2-D environment, by means of the numerical solutions of the governing equations, must be approached with care and an awareness of the possibilities of numerical errors. Errors in the calculation of pure advection can be severe if large variations in the ambient current occur in the region involved. The total mass transport is the combined effect of turbulent diffusion and gross advection. Holy and Preissmann (1977)

reported that the **smoothing effect tends to mask errors in the advective portion of a numerical advection-diffusion calculation if turbulent diffusion is relatively strong. Transport calculations of turbulent river flow benefit from this fact.**

3.4.8 DA 2-D MODELLING

The 1-D analogy can be useful if one is only interested in the mixing far from the source of a tracer or contaminant dumped in a river. However, if one needs to predict the mixing relatively close to a source which is concentrated at one bank, or distributed over only part of the cross-section, it may be necessary to employ a 2-D model to obtain useful results. 2-D models are capable of predicting the DA concentration anywhere in the cross-section. In some instances, water quality standards apply to certain portions of the cross-section, which cannot be studied with 1-D models. Also, it should be noted that the form of eq. 3-18 implies that the velocities and concentrations are time-averaged values at a point, (Bird et al., 1960). In collecting data in diffusion tests, grab samples may not satisfy this requirement. In order to obtain a 2-D equation representing the variation of the DA concentration in the transverse and longitudinal directions, eq. 3-18 may be integrated over the water depth. In this instance, integrating between the channel bottom and the free surface, interchanging the order of integration and differentiation, and accounting for the fact that the limits of integration are functions of spatial distances (using Leibniz's Rule) yields the following 2-D DA form of the transport equation:

$$\frac{\partial(H\,C)}{\partial t} + \frac{\partial}{\partial x}\left(H\,u\,C\right) + \frac{\partial}{\partial y}\left(H\,v\,C\right) = \frac{\partial}{\partial x}\left(H\,\epsilon_x\,\frac{\partial C}{\partial x}\right) + \frac{\partial}{\partial y}\left(H\,\epsilon_y\,\frac{\partial C}{\partial y}\right) + r\,H\,C + H\,s \qquad \textbf{(3-21)}$$

where: C = DA concentration. When the transport of and reaction between several soluble constituents are considered, the basic mass balance equation (eq. 3-15) can be extended into a vector form. In this instance, C, r and s become matrices (vectors) containing m

constituents. The empirical mixing coefficients incorporate dispersion as well as turbulent diffusion, and these are required as data in addition to the velocity field.

In the case of a straight prismatic channel, the velocity V will be identically zero provided that the secondary motions associated with shape of the cross-sectional geometry can be neglected. Under these conditions, the only transport in the y-direction is turbulent diffusion and thus, eq. 3-15 may be written for straight, prismatic channels as:

$$\frac{\partial(H\ C)}{\partial t} + \frac{\partial}{\partial x}\left(H\ u\ C\right) = \frac{\partial}{\partial x}\left(H\ \epsilon_x \frac{\partial C}{\partial x}\right) + \frac{\partial}{\partial y}\left(H\ \epsilon_y \frac{\partial C}{\partial y}\right) + r\ H\ C + H\ s \qquad \textbf{(3-22)}$$

3.4.9 ESTIMATION OF MIXING COEFFICIENTS

In the absence of secondary circulation perpendicular to the mean flow direction, the transverse transport due to differential advection associated with any secondary flow is zero everywhere. In this instance, the mixing coefficients in the x and y directions can be represented as:

$$\epsilon_x = a_x\ u_*\ h$$
$$\epsilon_y = a_y\ u_*\ h \qquad \textbf{(3-23)}$$

where: a_x and a_y = coefficients to be calibrated or estimated.

Elder (1959) provided the experimental and theoretical basis for estimating ϵ_x and ϵ_y. The essential conclusion of his work was that for a uniform flow in a wide open channel, a_x = 5.93 and a_y = 0.23. In this respect, ϵ_x is much larger than ϵ_y. In fact, ϵ_x incorporates differential convection due to the logarithmic vertical velocity profile in established flow. Subsequent work by many investigators has led to a consensus that a_y should range from 0.1

to 0.2 in uniform flow where lateral mixing is due only to bed-generated turbulence, as fully described by the parameter u.h, (Lau and Krishnappan, 1977). In addition, investigators reported a wide range of values of a_x, from 0.2 - 0.3 in irrigation canals, (Yotsukura and Cobb, 1972) to 0.5 - 5.0 or more in natural rivers, (Lau and Krishnappan, 1980). Recognizing that some of this variation is undoubtably due to advective effects which were not separated from diffusive ones in the analysis of data, several researchers, including Krishnappan and Lau, 1977; Lau and Krishnappan, 1977; Lau and Krishnappan, 1981; Okoye, 1970; and Webel and Schatzmann, 1980, have attempted to explain the variation by correlating a_x and a_y with the overall channel characteristics such as width to depth ratio, sinuosity, meander amplitude to wavelength ratio, bed friction factor, ...etc. Various researchers have tried to propose different formulations of the ϵ_x and ϵ_y equations. These analyses have met with varying degrees of success in reducing the range of uncertainty in the variation of the mixing coefficients. Holly (1971) proposed several possible alternative formulations of the mixing coefficients. Holly (1975) reported that although the results are not conclusive, it would appear that the variation of the mixing coefficients across a section is unimportant compared to its variation from one section to another. Djordjevic (1993) used values of $a_x = 6.0$ and $a_y = 0.20$ for his experimental channel although it was narrow. Those adopted values proved to produce good agreement between the observed and model-simulated concentrations, (ibid).

3.4.10 SIMPLIFIED APPROACHES

3.4.10.1 Stream Tubes

A 2-D model could be developed by writing a FD algorithm to solve for convection and diffusion in the longitudinal and transverse directions. A simpler and more economic approach makes use of the fact that the transverse velocity v is small compared to the longitudinal velocity u. In this instance, the river is divided into a series of adjacent stream tubes with constant discharges and assuming steady river flow conditions, (Fischer, 1966).

Once the dimensions and discharges of each tube are fixed at the upstream flow section, their depths, widths, and velocities vary longitudinally so as to maintain the same discharge in each tube through the changing cross-sectional shapes and velocity distributions encountered at different points along the river. The lateral shifting of each tube's position with respect to the banks takes into account the DA transverse velocity. Thus, an algorithm can be developed to simulate 2-D mixing as the simultaneous occurrence of three mechanisms: (I) longitudinal convection in each stream tube, (ii) longitudinal diffusion in each stream tube, and transverse diffusion between adjacent stream tubes.

Integrating eq. 3-15 (mass-conservation of a tracer or contaminant at a point) over the width of a stream tube gives:

$$A' \frac{\partial C}{\partial t} + \frac{\partial(A' U C)}{\partial x} = \frac{\partial (A' \epsilon_x \frac{\partial C}{\partial x})}{\partial x} + (H \epsilon_y \frac{\partial C}{\partial y})_{lb} - (H \epsilon_y \frac{\partial C}{\partial y})_{rb} \qquad \textbf{(3-24)}$$

where:

A' = stream tube area perpendicular to the flow direction,

lb = left boundary of the stream tube, and

rb = right boundary of the stream tube, (facing downstream).

The transverse velocity no longer appears explicitly in the above equation. However, it implicitly governs the dimensioning of stream tubes. Due to the simplifying assumptions, the 2-D stream tube approach will not be selected and ***the full 2-D DA equation will be solved along with the equations of continuity and motion using the eddy viscosity model.***

3.4.10.2 Steady State Assumption

Most pollution problems are of short duration. In such a case, the stream flow may

be assumed to be steady over the period of interest. But for some predictions, such as long-term build up of concentrations in a reservoir as a result of continuous discharge of pollutants from an upstream source, it may be necessary to incorporate time-varying (unsteady) velocities and depths into the mathematical model. The dimensions of the stream tubes in any FD formulation would vary as the water surface rises and falls at a cross-section, making the numerical solution of the problem quite complex.

An alternative approach would be to divide the annual hydrograph into discrete periods of constant discharge. Then, a numerical solution of the appropriate diffusion equation could proceed under the assumption of steady flow in each period. In this instance, the concentration field computed during the previous period is used as an initial condition for the subsequent run. Using an efficient numerical scheme produces satisfactory predictions as long as the water flow changes slowly with time. In this research because of limitations in the laboratory facility and because of time constraints, steady-state conditions were assumed throughout.

3.5 SUMMARY

An increasing amount of effort in computational hydraulics is being devoted to the simulation of contaminant dispersion in rivers and coastal waters. Literature recommend that future research should deal with mathematical modelling of neutrally buoyant conservative substances by the river flow. The 1-D analogy can be useful if one is only interested in the mixing far from the source of a tracer or contaminant dumped in a river. However, if one needs to predict the mixing relatively close to a source which is concentrated at one bank, distributed over only part of the cross-section, it may be necessary to employ a 2-D model to obtain useful results. 2-D models are capable of predicting the DA concentration anywhere in the cross-section. In some instances, water quality standards apply to certain portions of the cross-section, which cannot be studied with 1-D models.

There is a need to develop a 2-D model to solve the convection-dispersion equation describing the transport of pollutants or contaminants in rivers with compound channel flows. It is true that a 3-D model will simulate the problem more accurately, however, the effort and numerical cost of developing a 3-D model would outweigh the improvement over a 2-D model. Thus, a **2-D model is a reasonable compromise solution between the over simplified 1-D and the difficult to model 3-D versions.**

The 3-D Navier Stokes equations are integrated over the depth to produce the 2-D DA equations. Recent literature on the subject indicates that, in order to reach at a feasible solution, some of the terms should be dropped from the equations of motion. However, simplifications like dropping the unsteady flow term and the inertia terms, among others, have introduced significant errors in the analysis. **In this research, the complete DA equations are solved without introducing major simplifications. Furthermore, the LMT effects which are specific to compound channel flows are accounted for through the eddy viscosity terms rather than applying the k-ϵ model.**

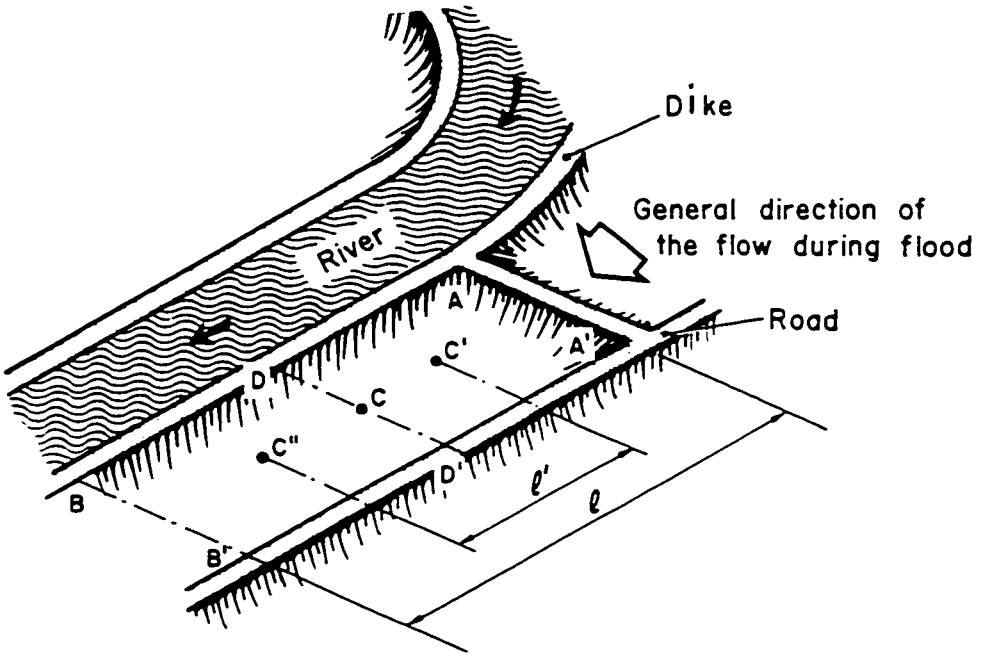

Figure 3.1 Diagram of a Discretized Flooded Plain, (after Cunge, 1975).

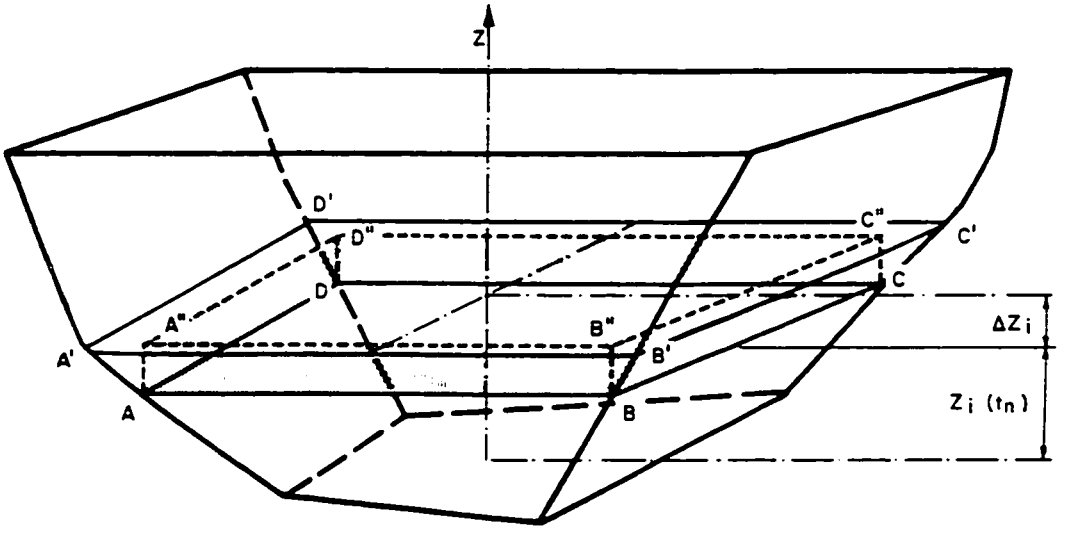

Figure 3.2 Definition Sketch for Deriving the Continuity Equation of a Cell, (after Cunge, 1975).

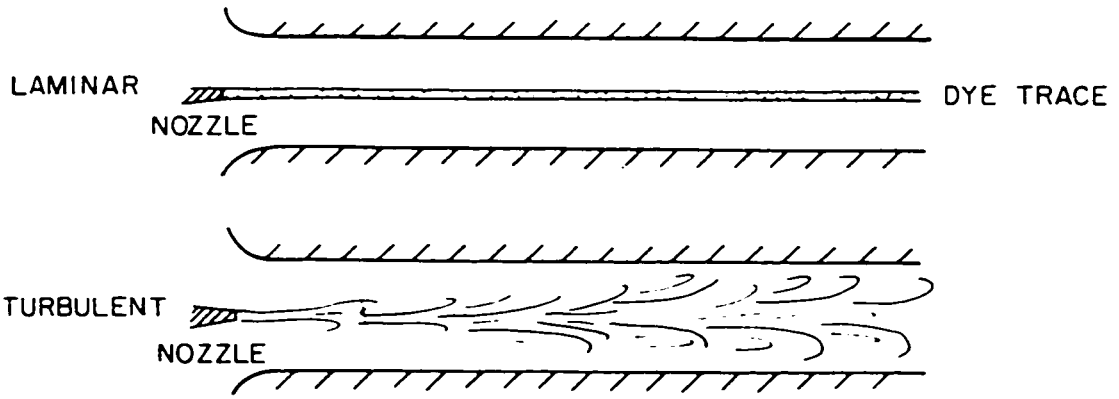

Figure 3.3 Dye Introduced at the Upstream End of a Pipe.

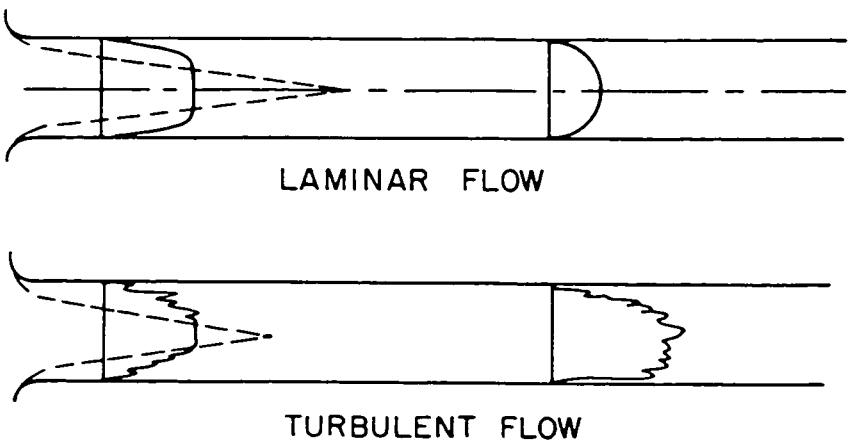

Figure 3.4 Schematic Representation of a Deformation of a Dye-Tracer, (after Cunge, 1975).

CHAPTER FOUR

NUMERICAL DESCRITIZATION AND APPROXIMATIONS

4.1 INTRODUCTION

In general, modelling hydraulic applications involves nonlinear terms in the governing equations. Thus, a *closed-form* solution of these PDE is not available, except for very simplified cases. An alternate solution is to integrate these equations numerically, which is the domain of *computational hydraulics*. The computational modelling process consists of describing an object with a set of numbers and simulating the laws acting upon it with a set of operations upon these numbers. Abbott (1976) stated that to any one object there corresponds an infinity of possible descriptions and to any one law there corresponds an infinity of sets of operations, or schemes, that describe its action. Therefore, the mathematical modeller should make the model as accurate as his/her knowledge of the prototype geometry and its physical laws. He/she should strive for a compromise between accuracy, computational effort and cost involved. The computer modelling of unsteady flow today encompasses a much broader scope than mere numerical solutions of the basic transient flow equations. It includes the development of the real-world algorithm for flow simulation in natural environments; it deals with the computer science and engineering technology of building a simulation model; it involves the disciplines of model implementation, application, and utilization; and it should include the work on specific areas that are vital to the operation of a flow model.

Several researchers have expressed concern at the quality of many computational models currently used in hydraulic research and hydraulic and coastal engineering practice. Liggett (1987) classified the difficulties in computational hydraulics into about six categories: *geometric description, excessive problem size, turbulence, physics, data, and numerical difficulties*. All of these troubles are related in obvious ways. The geometrical detail of many problems defies practical description. In general, computational hydraulics models are built based on conservation laws of mass, momentum, and energy. It is important to select a proper scheme for the solution of the governing equations to avoid the falsification of any of the conservation laws. This falsification will generally worsen when abrupt and rough changes occur from one point to the next in the model.

4.2 NUMERICAL SCHEMES

The continuity and momentum equations describing the flow problem are hyperbolic PDE. There are a number of numerical schemes which could be applied to solve the system of equations. Numerical methods to the flow equations has been the subject of intense research for many years, (Priessmann, 1961; Amein, 1968, Liggett and Cunge, 1975; Hicks and Steffler, 1992; to name only a few). However, as the primary objective was to explore the formulation itself that would produce the necessary and reliable data for solving the transport problem, the numerical technique may be considered as merely a vehicle to obtain a solution of the flow equations with much care to avoid any falsification of the physical properties. This does not mean that any formulation can be implemented to solve the hyperbolic flow equations. In this instance, it was desirable to select a numerical scheme that is computationally robust as well as accurate in order to ensure that the evaluation of the performance and validity of the proposed compound channel flow formulation was not obscured by limitations of the numerical scheme.

The advection-diffusion equation applies to problems dealing with transport of mass, momentum, energy, or neutron. It is a parabolic PDE although the convection is represented by a first-order term. Convection has a major influence on the numerical solution procedure. Being a transient problem, an initial condition has to be supplied. In addition, since the equation is second-

order in the space coordinate, two boundary conditions are required. These boundary conditions may be of the Dirichlet type (specified values of the concentration), the Neumann type (specified values of the derivative of concentration with respect to space coordinates), or the mixed type (specific combinations). The space coordinates must be a closed physical domain. In general, the solution of the unsteady problem approaches the asymptotic steady state solution as time increases. This fact can be used to obtain the solution of steady state problems.

Different numerical methods for solving the convection-diffusion equation are proposed in the literature. These methods include: *Forward-Time Centred-Space method (FTCS), Lax and Richardson (Leapfrog) methods, Upwind methods, Leonard method, Dufort-Frankel method, Lax-Wendroff type methods, MacCormack method, Backward-Time Centred-Space method (BTCS), Crank-Nicolson method, Keller box method, and Hopscotch method, as well as the FE and Boundary Element methods,* (Hoffman, 1993).

In general, explicit FD schemes, as typified by the FTCS method, are conditionally stable and require a relatively small time step size in the marching direction to satisfy stability criteria. On the other hand, implicit FD schemes, as exemplified by BTCS method, are unconditionally stable. The marching time step size is restricted by accuracy requirements, rather than stability. However, to obtain accurate solutions the marching time step size can not be very much larger than the stable step size for explicit methods. In some cases, depending upon the scheme and the problem, a large time step can be used safely in the case of steady state problems. Hoffman (1993) states that accurate solutions of transient problems can be obtained by explicit methods. Also, nonlinear differential equations can be solved directly by explicit methods.

Several important properties of FD approximations to the parabolic and hyperbolic PDE must be considered before selecting the appropriate approach. These include: consistency, order, stability, and convergence, (Hoffman, 1993).

(i) A finite difference equation (FDE) is consistent with a PDE if the difference between the FDE and the PDE (i.e. the truncation error) vanishes as the sizes of the grid spacings go to zero independently.

(ii) The order of a FD approximation of a PDE is the rate at which the global error of FD solution approaches zero as the sizes of the grid spacings approach zero.

(iii) When applied to a PDE that has a bounded solution, a FDE is stable if it produces a bounded solution and is unstable if it produces an unbounded solution.

(iv) A FD method is convergent if the solution of the FDE approaches the exact solution of the PDE as the sizes of the grid spacings go to zero.

(v) Finally, the Lax equivalence theorem (Lax, 1954) states that: given a properly posed linear initial-value problem and a FD approximation to it that is consistent, stability is the necessary and sufficient condition for convergence.

4.3 ILLUSTRATIONS ON ARTIFICIAL DIFFUSION

4.3.1 EXAMPLE 1

Assume we are dealing with the convection equation in 1-D with a constant area:

$$\frac{\partial C_a}{\partial t} + U \frac{\partial C_a}{\partial x} = 0 \qquad \textbf{(4-1)}$$

Consider the numerical scheme by Dobbins and Bella (1968) and analysed in detail by Chevereau and Preissmann (1971). Figure 4.1 shows a space-time grid (or domain) for FD solution. For the convection problem:

- a particle departs point p at time m,
- it arrives at point i+1 at future time m+1,
- its trajectory is as shown in the figure,
- the concentration of marked particles is fixed (pure convection): C_a (i+1, m+1) = C_a (p, m).

Recall: at previous time step n, concentrations are known at p-1, p, p+1,.. etc. If p coincides with I: U $\Delta t = \Delta x$, then C_a (i+1, m+1) = C_a (i, m), (figure 4.1-a). In general, U is not the same, UΔt is not equal to Δx, (figure 4.1-b). Interpolate linearly between C_a (i-1, m) and C_a (i, m) to obtain C_a (p, m), (basis of Dobbins and Bella scheme).

This interpolation yields numerical diffusion,

$$C_a(i+1,m+1) = C_a(p,m) = \frac{(\Delta x-\alpha)C_a(i,m) + \alpha C_a(i-1,m)}{\Delta x} \qquad \textbf{(4-2)}$$

Expanding C_a (i+1,m+1), C_a (i,m) and C_a (i-1,m) in a Taylor series around the point (i+1,m), and dropping terms higher than second order gives:

$$C_a(i+1,m+1) \approx C_a(i+1,m) + \frac{\partial C_a}{\partial t}\Delta t + \frac{\partial^2 C_a}{\partial t^2}\frac{\Delta t^2}{2}$$

$$C_a(i,m) \approx C_a(i+1,m) - \frac{\partial C_a}{\partial x}\Delta t + \frac{\partial^2 C_a}{\partial x^2}\frac{\Delta x^2}{2} \qquad \textbf{(4-3)}$$

$$C_a(i-1,m) \approx C_a(i+1,m) - \frac{\partial C_a}{\partial x}(2\,\Delta x) + \frac{\partial^2 C_a}{\partial x^2}(2\,\Delta x^2)$$

Using:

$$\Delta x + \alpha = U\,\Delta t \quad \text{and} \quad \frac{\partial^2 C_a}{\partial t^2} = U^2\frac{\partial^2 C_a}{\partial x^2} \qquad \textbf{(4-4)}$$

Manipulating eqs. 4-3 and 4-4 and simplifying gives:

$$\frac{\partial C_a}{\partial t} + U \frac{\partial C_a}{\partial x} = \frac{\alpha\ (\Delta x - \alpha)}{2\ \Delta t} \frac{\partial^2 C_a}{\partial x^2} \qquad \textbf{(4-5)}$$

Thus, for this scheme:

$$K_n = \frac{\alpha\ (\Delta x - \alpha)}{2\ \Delta t} \qquad \textbf{(4-6)}$$

In terms of the Courant Number:

$$K_n = \frac{\Delta x^2}{2\ \Delta t} (1 - C_r)\ (C_r - 2) \qquad \textbf{(4-7)}$$

$K_n = 0$ for $C_r = 1$ or 2, and $K_n = \max = \Delta x^2/(8\Delta t)$ for $C_r = 1.5$. The same analysis applies for $C_r << 1$.

4.3.2 EXAMPLE 2

A river has a mean velocity of 1 m/s and a depth of 5 m. It is necessary to use $\Delta x = 1$ km to minimize cost of simulation and it is required to perform a 1-D dispersion analysis. The worst case occurs when $C_r = 0.5$, this means that: $\Delta t = 500$ s, and $K_n = \Delta x^2/(8\Delta t) = 250$ m^2/s. By comparison, observations by Fischer (1973) suggest that: $K_x/(RU_*) = 250$. Assuming $R \approx h$ and $U_* \approx U/20 = 0.05$ m/s leads to $K_x = (250)(5)(0.05) = 62.5$ m^2/s.

Thus, $K_n >> K_x$ and the solution is dominated by **NUMERICAL** rather than **PHYSICAL DIFFUSION.**

4.3.3 EXAMPLE 3

A rectangular section, 2 m wide and 1 m deep, slope 0.1 %, Strickler coefficient (1/n) of 25, discharge 1 m^3/s, velocity 0.5 m/s. The channel's 10 km length was divided into 50 computational

reaches of $\Delta x = 200$ m each. The upstream concentration distribution shown as curve 0, (figure 4.2), was transported downstream for approximately 3 hours using the conditions given in table 4.1. Only case 1 reproduces pure convection with no artificial diffusion, (C_r is integer), other curves demonstrate strong diffusion by numerical scheme, (figure 4.2). This numerical diffusion can be taken as physical diffusion if the user is not aware of the numerical problem and the choice of Δx and Δt accordingly. Chevereau and Preissman (1971) recommended:

- use Δx as small as possible within the time and cost of study,

- use Δt as large as possible without losing resolution,

- choose Δt and Δx such that $\Delta x \approx (U\Delta t)/e$ where e = positive integer.

4.4 GOVERNING PDE

The governing 2-D DA equations of continuity and momentum as well as the advection-diffusion equation, are presented in this section along with minor simplifications introduced to those equations in an attempt to solve them numerically. In this instance, the wind stress in the x- and y-directions, reaction rate constants, sources (and/or sinks) are assumed negligible. In addition, terms of the continuity equation are grouped together using the rules of differentiation. Thus, the equations to be solved are:

$$\frac{\partial H}{\partial t} + \frac{\partial (H\ U)}{\partial x} + \frac{\partial (H\ V)}{\partial y} = 0 \qquad \textbf{(4-8)}$$

$$\frac{\partial U}{\partial t} + U \frac{\partial U}{\partial x} + V \frac{\partial U}{\partial y} + g \frac{\partial H}{\partial x} - F V$$

$$+ g \frac{n^2 U (U^2 + V^2)^{\frac{1}{2}}}{k_o^2 h^{\frac{4}{3}}} - \frac{1}{h} \frac{\partial}{\partial y}\left[h \upsilon_t \frac{\partial U}{\partial y}\right] = 0 \qquad \textbf{(4-9)}$$

$$\frac{\partial V}{\partial t} + U \frac{\partial V}{\partial x} + V \frac{\partial V}{\partial y} + g \frac{\partial H}{\partial y} + F U$$

$$+ g \frac{n^2 V (U^2 + V^2)^{\frac{1}{2}}}{k_o^2 h^{\frac{4}{3}}} - \frac{1}{h} \frac{\partial}{\partial x}\left[h \upsilon_t \frac{\partial V}{\partial x}\right] = 0 \qquad \textbf{(4-10)}$$

$$\frac{\partial (H C)}{\partial t} + \frac{\partial}{\partial x}(H U C) + \frac{\partial}{\partial y}(H V C)$$

$$- \frac{\partial}{\partial x}(H \epsilon_x \frac{\partial C}{\partial x}) - \frac{\partial}{\partial y}(H \epsilon_y \frac{\partial C}{\partial y}) = 0 \qquad \textbf{(4-11)}$$

Chezy's equation can be used instead of Manning's equation. Manning's roughness coefficient is related to Chezy's coefficient (CC) by:

$$n = \frac{k_o H^{\frac{1}{6}}}{CC} \qquad \textbf{(4-12)}$$

Substituting in the expressions for the friction slopes and simplifying gives:

$$S_{fx} = \frac{U (U^2 + V^2)^{\frac{1}{2}}}{CC^2 H}$$

$$S_{fy} = \frac{V (U^2 + V^2)^{\frac{1}{2}}}{CC^2 H} \qquad \textbf{(4-13)}$$

The advantage of using Chezy over Manning's equation is basically computational in that no fractional powers are involved in the calculation of depths. Furthermore, inspecting the channel bed material results in a rather good estimate of the Chezy's coefficient. Variations in Chezy's coefficient do not significantly affect the simulations.

In addition to representing the boundary roughness, the Manning's n is used to indicate whether a particular grid point is *dry* or *wet*. A value of zero represents land, while a positive value designates water. If calculating a new water level leads to a negative volume of water then that particular grid point is removed from the computations. This is accomplished by setting n = 0 and the current values of the velocity components leading to that grid point. Then, the previous row or column in the grid of recursion formulas, velocities, and water levels is recalculated with the point now taken as *dry*. In order to avoid any falsification of the conservation of mass principle, a thin layer of water is still assumed over a *dry* grid point. The thickness of this layer is set equal to the water level calculated at the previous time step. Although it is physically impossible to obtain a negative cross-sectional area or a negative volume at any time step, it is numerically possible. A check is made at each time step to avoid incorrect transport of water and constituent mass. At any *dry* grid point, each of the four surrounding grid points adjacent to it is checked to see whether it is under water. If one or more of the surrounding grid points are wet, then the water levels of those surrounding grid points that are under water are averaged.

4.5 FD APPROXIMATIONS

In the FD approximation, a space-staggered scheme is used where velocities, water levels, and depths are described at different grid points, (figure 4.3). This scheme, first used by Platzman (1959), has the advantage that in the formula for the variable operated upon in time, there is a centrally located spatial derivative for the linear term. In the modelling exercise, H values are described at integer values of the spatial grid coordinates, whereas U is assigned at integer and a half value of the x-grid coordinate and integer value of y-coordinate. However, V is described at integer values of the x-grid coordinate and integer and a half value of y-coordinate. h values are

defined at integer and a half values of grid coordinates. A double time step operation is used in such a manner that the terms containing space derivatives are generally taken alternating backward and forward. Thus, the time interval is considered over two successive operations, and these terms are either central in time or averaged in time over that interval. The same value of time step was employed for the computation of the flow model as well as the transport model. This was done not only to circumvent difficulties with the conservative properties of the computational method, but also in anticipation of developing a predictive model. Two arrays were used for the two velocity components and three arrays for the water levels, since three time levels are involved. One array is used for the depth data and one for the Manning's coefficient. The depth or elevation data for each point in the field were interpolated from adjacent data if not directly available at the point. The sequential use of the FD approximation to the continuity equations results in the use of the spatial derivatives alternatingly forward and backward. The use of this procedure over the whole time step results in terms that are either central in time or averaged over that time interval.

The following notations are used in the approximation of the PDE to transform them into FDE (averages and differences). A quantity h is represented by h(i Δx, j Δy, m Δt) as a spatial grid point at time level m, where i or j = 0, ±½, ±1, ±3/2, ...etc. and m = 0, ½, 1, 3/2, 2, ...etc. The same approximations apply to any other quantity including U, V, H, ...etc.

In the approximation process, **averages** of any quantity h in the x- or y-directions are represented in the following manner:

$$\bar{h}^{x} \doteq \frac{h[(i+\frac{1}{2})\Delta x,\ j\Delta y,\ m\Delta t] + h[(i-\frac{1}{2})\Delta x,\ j\Delta y,\ m\Delta t]}{2}$$

$$\bar{h}^{y} \doteq \frac{h[i\Delta x,\ (j+\frac{1}{2})\Delta y,\ m\Delta t] + h[i\Delta x,\ (j-\frac{1}{2})\Delta y,\ m\Delta t]}{2} \qquad \textbf{(4-14)}$$

Differences of any quantity h in the x- or y-directions are expressed using the following notations:

$$h_x \doteq h[(i+\tfrac{1}{2})\Delta x,\ j\Delta y,\ m\Delta t] - h[(i-\tfrac{1}{2})\Delta x,\ j\Delta y,\ m\Delta t]$$
$$h_y \doteq h[i\Delta x,\ (j+\tfrac{1}{2})\Delta y,\ m\Delta t] - h[i\Delta x,\ (j-\tfrac{1}{2})\Delta y,\ m\Delta t] \qquad \textbf{(4-15)}$$

The **derivative** of any quantity h with respect to x or y can be written as:

$$\delta_x h \doteq \frac{h[(i+\tfrac{1}{2})\Delta x,\ j\Delta y,\ m\Delta t] - h[(i-\tfrac{1}{2})\Delta x,\ j\Delta y,\ m\Delta t]}{\Delta x}$$
$$\delta_y h \doteq \frac{h[i\Delta x,\ (j+\tfrac{1}{2})\Delta y,\ m\Delta t] - h[i\Delta x,\ (j-\tfrac{1}{2})\Delta y,\ m\Delta t]}{\Delta y} \qquad \textbf{(4-16)}$$

The **average** of any quantity h can be expressed as:

$$\bar{\bar{h}} \doteq \frac{1}{4}\left[h[(i+\tfrac{1}{2})\Delta x,(j+\tfrac{1}{2})\Delta y,m\Delta t] + h[(i+\tfrac{1}{2})\Delta x,(j-\tfrac{1}{2})\Delta y,,m\Delta t]\right]$$
$$+ \frac{1}{4}\left[h[(i-\tfrac{1}{2})\Delta x,(j+\tfrac{1}{2})\Delta y,m\Delta t] + h[(i-\tfrac{1}{2})\Delta x,(j-\tfrac{1}{2})\Delta y,m\Delta t]\right] \qquad \textbf{(4-17)}$$

In addition to the above mentioned operators, the following will also be used in the descritization of the PDE. The **derivatives** of any quantity h along the **time** level is represented by:

$$\delta_{+\frac{1}{2}t} h \doteq \frac{2}{\Delta t}\left[h[i\Delta x,\ j\Delta y,\ (m+\tfrac{1}{2})\Delta t] - h[i\Delta x,\ j\Delta y,\ m\Delta t]\right] \qquad \textbf{(4-18)}$$

The value of a quantity h **just after** (h_+) or **just before** (h_-) a grid point on the time line is approximated as:

$$h_+ \doteq h[i\Delta x,\ j\Delta y,\ (m+\tfrac{1}{2})\Delta t]$$
$$h_- \doteq h[i\Delta x,\ j\Delta y,\ (m-\tfrac{1}{2})\Delta t] \qquad \textbf{(4-19)}$$

The **average, in time**, of a quantity h is described as:

$$\overline{h}^{\,t}_{\frac{1}{2}} \doteq \frac{h[i\Delta x,\ j\Delta y,\ (m+\frac{1}{2})\Delta t] + h[i\Delta x,\ j\Delta y,\ m\Delta t]}{2} \tag{4-20}$$

In selecting the time levels m and (m+1/2), the sets of FD approximations of the PDE describing the problem under consideration can be written for different grid points in the same sequence as the calculations are performed:

At grid point (i+1/2, j, m) the momentum equation in the x-direction is presented as:

$$\delta_t U - F\,\overline{\overline{V}} + U_{\cdot}\,\overline{\delta_x U_{\cdot}}^{x} + V\,\overline{\delta_y U_{\cdot}}^{y} + g\,\overline{\delta_x H}^{t} + g\,\frac{\overline{U}^{t}\,(U_{\cdot}^{\,2} + \overline{\overline{V}}^{2})^{\frac{1}{2}}}{(\overline{h}^{y} + \overline{H}^{x})\,(\overline{CC}^{x})^{2}} - \frac{1}{\overline{h}^{y}}\,\overline{\delta_y\left[\overline{h}^{y}\,\upsilon_t\,\overline{\delta_y U}^{y}\right]}^{y} = 0 \tag{4-21}$$

At grid point (i, j, m) the continuity equation is presented as:

$$\delta_{\cdot\frac{1}{2}t}\,H + \delta_x\left[(\overline{h}^{y} + \overline{H}^{x})\,U_{\cdot}\right] + \delta_y\left[(\overline{h}^{x} + \overline{H}^{y})\,V\right] = 0 \tag{4-22}$$

At the same grid point (i, j, m) the advection-diffusion equation is approximated as:

$$\delta_{\cdot\frac{1}{2}t}\left[C(\overline{\overline{h}}+H)\right] + \delta_x\left[(\overline{h}^{y}+\overline{H}^{x})\,U_{\cdot}\,\overline{C_{\cdot}}^{x}\right] + \delta_y\left[(\overline{h}^{x}+\overline{H}^{y})\,V\,\overline{C}^{y}\right] - \delta_x\left[(\overline{h}^{y}+\overline{H_{\cdot}}^{x})\,\epsilon_x\,\delta_x C_{\cdot}\right] - \delta_y\left[(\overline{h}^{x}+\overline{H}^{x})\,\epsilon_y\,\delta_y C\right] = 0 \tag{4-23}$$

At grid point (i, j+1/2, m+1/2) the momentum equation in the y-direction is presented as:

$$\delta_t v + F\,\overline{\overline{U}} + U\,\overline{\delta_x V_{\cdot}}^{x} + V_{\cdot}\,\overline{\delta_y V_{\cdot}}^{y} + g\,\overline{\delta_y H}^{t} + g\,\frac{\overline{V}^{t}\,(\overline{\overline{U}}^{2} + V_{\cdot}^{\,2})^{\frac{1}{2}}}{(\overline{h}^{x} + \overline{H}^{y})\,(\overline{CC}^{y})^{2}} - \frac{1}{\overline{h}^{x}}\,\overline{\delta_x\left[\overline{h}^{x}\,\upsilon_t\,\overline{\delta_x V}^{x}\right]}^{x} = 0 \tag{4-24}$$

At grid point (i, j, m+1/2) the continuity equation is presented as:

$$\delta_{t,\frac{1}{2}} H + \delta_x\left[(\overline{h}^y + \overline{H}^x)\, U\right] + \delta_y\left[(\overline{h}^x + \overline{H}^y)\, V_{\cdot}\right] = 0 \qquad \textbf{(4-25)}$$

At the same grid point (i, j, m+1/2) the advection-diffusion equation is approximated as:

$$\begin{aligned} &\delta_{t,\frac{1}{2}}\left[C(\overline{\overline{h}} + H)\right] + \delta_x\left[(\overline{h}^y + \overline{H}^x)\, U\, \overline{C}^x\right] + \delta_y\left[(\overline{h}^x + \overline{H}^y)\, V_{\cdot}\, \overline{C_{\cdot}}^y\right] \\ &- \delta_x\left[(\overline{h}^y + \overline{H}^x)\, \epsilon_x\, \delta_x C\right] - \delta_y\left[(\overline{h}^x + \overline{H_{\cdot}}^y)\, \epsilon_y\, \delta_y C_{\cdot}\right] = 0 \end{aligned} \qquad \textbf{(4-26)}$$

4.6 FD DESCRITIZATION

At the time level (m+1/2), the continuity equation has the following unknowns: U[(i-1/2)Δx, jΔy, (m+1/2)Δt], H[iΔx, jΔy, (m+1/2)Δt] and U[(i+1/2)Δx, jΔy, (m+1/2)Δt]. In addition , the momentum equation in the x-direction has the following unknown values: H[iΔx, jΔy, (m+1/2)Δt], U[(i+1/2)Δx, jΔy, (m+1/2)Δt] and H[(i+1)Δx, jΔy, (m+1/2)Δt].

Upon substituting the FD approximations in the continuity equation at time level m, expanding and simplifying, results in the following equation (neglecting to repeat Δx, Δy, and Δt, for simplicity):

$$\frac{2}{\Delta t}\left[h_{i,\,j,\,(m+\frac{1}{2})} - h_{i,\,j,\,m}\right]$$

$$+\left[h_{i+\frac{1}{2},\,j+\frac{1}{2},\,m} + h_{i+\frac{1}{2},\,j-\frac{1}{2},\,m} + H_{i+1,\,j,\,m} + H_{i,\,j,\,m}\right]\frac{U_{i+\frac{1}{2},\,j,\,m+\frac{1}{2}}}{2\,\Delta x}$$

$$-\left[h_{i-\frac{1}{2},\,j+\frac{1}{2},\,m} + h_{i-\frac{1}{2},\,j-\frac{1}{2},\,m} + H_{i-1,\,j,\,m} + H_{i,\,j,\,m}\right]\frac{U_{i-\frac{1}{2},\,j,\,m+\frac{1}{2}}}{2\,\Delta x} \qquad \textbf{(4-27)}$$

$$+\left[h_{i+\frac{1}{2},\,j+\frac{1}{2},\,m} + h_{i-\frac{1}{2},\,j+\frac{1}{2},\,m} + H_{i,\,j+1,\,m} + H_{i,\,j,\,m}\right]\frac{V_{i,\,j+\frac{1}{2},\,m}}{2\,\Delta x}$$

$$\left[- h_{i+\frac{1}{2},\,j-\frac{1}{2},\,m} + h_{i-\frac{1}{2},\,j-\frac{1}{2},\,m} + H_{i,\,j,\,m} + H_{i,\,j-1,\,m}\right]\frac{V_{i,\,j-\frac{1}{2},\,m}}{2\,\Delta x} =$$

This form of the expanded continuity equation can be written in a concise manner as follows:

$$- r_{i-\frac{1}{2}}\,U_{i-\frac{1}{2},\,j,\,m+\frac{1}{2}} + H_{i,\,j,\,m+\frac{1}{2}} + r_{i+\frac{1}{2}}\,U_{i+\frac{1}{2},\,j,\,m+\frac{1}{2}} = A_{i,\,j,\,m} \qquad \textbf{(4-28)}$$

The coefficients of the variables in the continuity equation can be written as:

$$r_{i-\frac{1}{2}} = \left[\,h_{i-\frac{1}{2},\,j+\frac{1}{2},\,m} + h_{i-\frac{1}{2},\,j-\frac{1}{2},\,m} + H_{i-1,\,j,\,m} + H_{i,\,j,\,m}\right]\frac{\Delta t}{4\,\Delta x} \qquad \textbf{(4-29)}$$

$$r_{i+\frac{1}{2}} = \left[\,h_{i+\frac{1}{2},\,j+\frac{1}{2},\,m} + h_{i+\frac{1}{2},\,j-\frac{1}{2},\,m} + H_{i+1,\,j,\,m} + H_{i,\,j,\,m}\right]\frac{\Delta t}{4\,\Delta x} \qquad \textbf{(4-30)}$$

$$A_{i,j,m} = H_{i,j,m}$$

$$+ \left[h_{i+\frac{1}{2},j-\frac{1}{2},m} + h_{i-\frac{1}{2},j-\frac{1}{2},m} + H_{i,j,m} + H_{i,j-1,m} \right] V_{i,j-\frac{1}{2},m} \frac{\Delta t}{4\,\Delta x} \qquad \textbf{(4-31)}$$

$$- \left[h_{i+\frac{1}{2},j+\frac{1}{2},m} + h_{i-\frac{1}{2},j+\frac{1}{2},m} + H_{i,j+1,m} + H_{i,j,m} \right] V_{i,j+\frac{1}{2},m} \frac{\Delta t}{4\,\Delta x}$$

In a similar manner, the momentum equation is written at grid point (i+1/2, j, m) as:

$$- r_i H_{i,j,m+\frac{1}{2}} + rr_{i+\frac{1}{2}} U_{i+\frac{1}{2},j+\frac{1}{2},m+\frac{1}{2}}$$

$$+ r_{i+1} H_{i+1,j,m+\frac{1}{2}} = B_{i+\frac{1}{2},j,m} \qquad \textbf{(4-32)}$$

where the coefficients of the above equation are derived in a similar manner. They are not listed here for simplicity to avoid any lengthy presentation of equations.

Eqs. 4-28 and 4-32 can be solved for the unknown values of velocities and water levels on each row j once boundary conditions are specified at either end of the row. The boundary conditions can be specified so that there are open (water) or closed (water-land) boundaries at either side of the computational field, and given values of velocities or water levels can be used as input conditions. In the modelling process an open boundary is assumed at the left and right-hand side of the grid system and a closed boundary is assumed at the top and bottom sides. Incorporating the boundary conditions into the system, eqs. 4-28 and 4-32 can be written in the matrix form. Then, the unknowns can be calculated at time level (m+1/2) using a series of recursion formulas.

The solution of eqs. 4-28 and 4-32 yields H and U values for the time level m+1/2. These values, along with V values at time level m, are used to solve for the concentration at time level (m+1/2). The numerical procedure is similar to that used in the flow computations. The advection-diffusion equation can be written in a concise form as a recursion formula:

$$a_i\, C_{i-1,\, j,\, m+\frac{1}{2}} + b_i\, C_{i,\, j,\, m+\frac{1}{2}} + cc_i\, C_{i+1,\, j,\, m+\frac{1}{2}} = D_i \qquad \textbf{(4-33)}$$

where a_i, b_i, cc_i, and D_i are recursion coefficients. These coefficients are not listed hereafter to avoid any lengthy equations. Eq. 4-33 is solved for the concentration at each grid point along the row j by a process of elimination of unknowns. Boundary conditions are incorporated into the eq. 4-33 by setting the coefficients equal to values at the boundary. For example, a closed boundary at the left implies that $a_1 = 0$. If the closed boundary is at the right side then $cc_i = 0$.

For the second half time step, the momentum equation in the y-direction, continuity as well as the advection-diffusion equations are written in a similar form as the above mentioned equations with the necessary changes to the corresponding variables.

The FD equations are solved in an implicit multi-operational manner. The solution proceeds between two time levels of difference half a time step. The sequence of the solution is described hereafter. The first operation is performed at time level m where the solution marches from time t to (t+1/2 Δt). In this process, the momentum equation in the x-direction as well as the continuity equation are solved first for the water levels and velocities in the x-direction at time level (m+1/2). The result of this calculation is then used in the advection-diffusion equation to obtain the concentration of pollutant at time level (m+1/2). After this operation is completed, the results are used at time level (m+1/2) to determine the unknowns in the second half time step. This constitutes going to time level (m+1/2) or basically marching from (t+1/2Δt) to (t+Δt). In this instance, the momentum and continuity equations are solved first to give water levels and velocities in the y-direction at time level m+1. The calculated values are then used in the discretized advection-diffusion equation to obtain the pollutant concentration at level m+1. This completes a time step in the solution procedure. Then, iteration over other time steps to obtain values over the whole domain. The numerical solution of the FD equations leads to a stable solution in both time and space.

4.7 EVALUATION OF MODEL PERFORMANCE

Some of the confusion regarding characterization of model performance results from differences in perspective within the technical community. Three groups (modellers, model users, and decision makers) need to evaluate the model from different viewpoints. An evaluation of model performance cannot be carried out in an abstract or problemless context. A number of questions should be asked regarding the model and the processes it simulates. The essential elements of model evaluation performance are divided into:

- **Problem Identification**: the identification of the specific problem to be solved is an important step in model performance evaluation. Two important questions should be addressed. First, what are the dominant physical processes at work? Second, what are the spatial and temporal scales of these processes?

- **Relation of Model to Problem**: the question of the relation between the model and the problem is another important consideration in model evaluation performance. It addresses the physical processes that the model represents and those ignored. It also deals with the way these physical processes are included in the model.

- **Solution Scheme Examination**: clear documentation of the numerical scheme, including equations and DESCRITIZATION as well as results of tests on the scheme is necessary. Explicit discussion of the relationship between grid size, time step, stability, and accuracy of the solution is also important. In addition, problem-specific tests should be performed.

- **Model Response Studies**: model response studies provide valuable information to both modeller and user and may save later effort in interpreting model performance. Problems with analytical solutions can be used for response studies. Various limiting cases may provide good model response study subjects for models oriented towards solving more complex problems.

- **Model Calibration**: calibration refers to the adaptation of a model to the problem configuration and the identification of coefficient values by application to an existing relevant data set. Calibration data should correspond closely with conditions during the application to a specific problem. For example, if the purpose of the model is to predict currents for pollutant transport, the calibration against tidal elevations provides little assurance that predicted events are accurate. Calibration of parameters is a typical optimization problem, as the aim of any procedure is to minimize the errors between known natural states of a system, and the results of numerical computations by the variation of parameters. Different optimization algorithms have already been proposed by several authors to perform calibration. Neuman (1980) developed an automatic way using computer programs. Januszewski (1980) presented and applied successfully an optimization algorithm based on the direct minimum search method of Powell to tidal computations in estuaries. To reduce the computational costs of calibration, Meissner et al. (1982) approached river flow and transport problems in a deterministic manner. This approach was suitable for problems where non-linearities in the differential equations are not dominant.

- **Validation Studies**: validation refers to comparison between model output and *real world* data. Such validation is instructive only if it is independent of previous calibration. Acquisition of field data to compare with model output requires care.

4.8 SUMMARY

The numerical solution of the 1-D dispersion equation must be approached with great deal of care. Mechanically speaking, it is not difficult to formulate a solution to the equation, which is a linear parabolic partial differential equation requiring one upstream and one downstream boundary condition as well as an initial state (or condition). The transport equation represents two physical mechanisms: convective longitudinal transport and longitudinal diffusion. Most FD methods for the calculation of the convection portion of the transport equation are plagued by an artificial, or numerical, diffusion which is sometimes stronger than the physical diffusion, thereby rendering the calculation useless.

The 1-D analogy can be useful if one is only interested in the mixing far from the source of a tracer or contaminant dumped in a river. However, if one needs to predict the mixing relatively close to a source which is concentrated at one bank, or distributed over only part of the cross-section, it may be necessary to employ a 2-D model to obtain useful results. 2-D models are capable of predicting the DA concentration anywhere in the cross-section. In some instances, water quality standards apply to certain portions of the cross-section, which cannot be studied with 1-D models.

Table 4.1 Different Conditions for Computing the Concentration Downstream.

Curve	Δt (s)	C_r	K_n (m^2/s)	Calculation Interval (s)
1	400	1.0	0.0	11400
2	360	0.9	5.0	11520
3	200	0.5	25.0	11400
4	600	1.5	8.33	11400
5	3800	9.5	1.32	11400

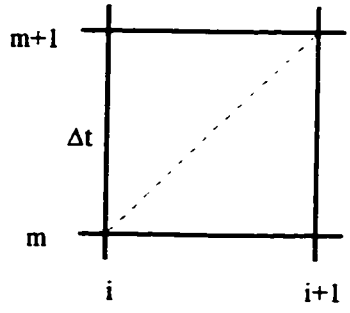

(a)

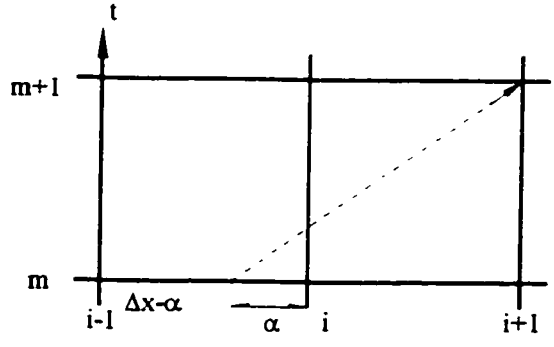

(b)

Figure 4.1 Convection Scheme of Dobbins and Bella (1968), (a) $\Delta x = U\,\Delta t$, (b) $\Delta x \neq U\,\Delta t$.

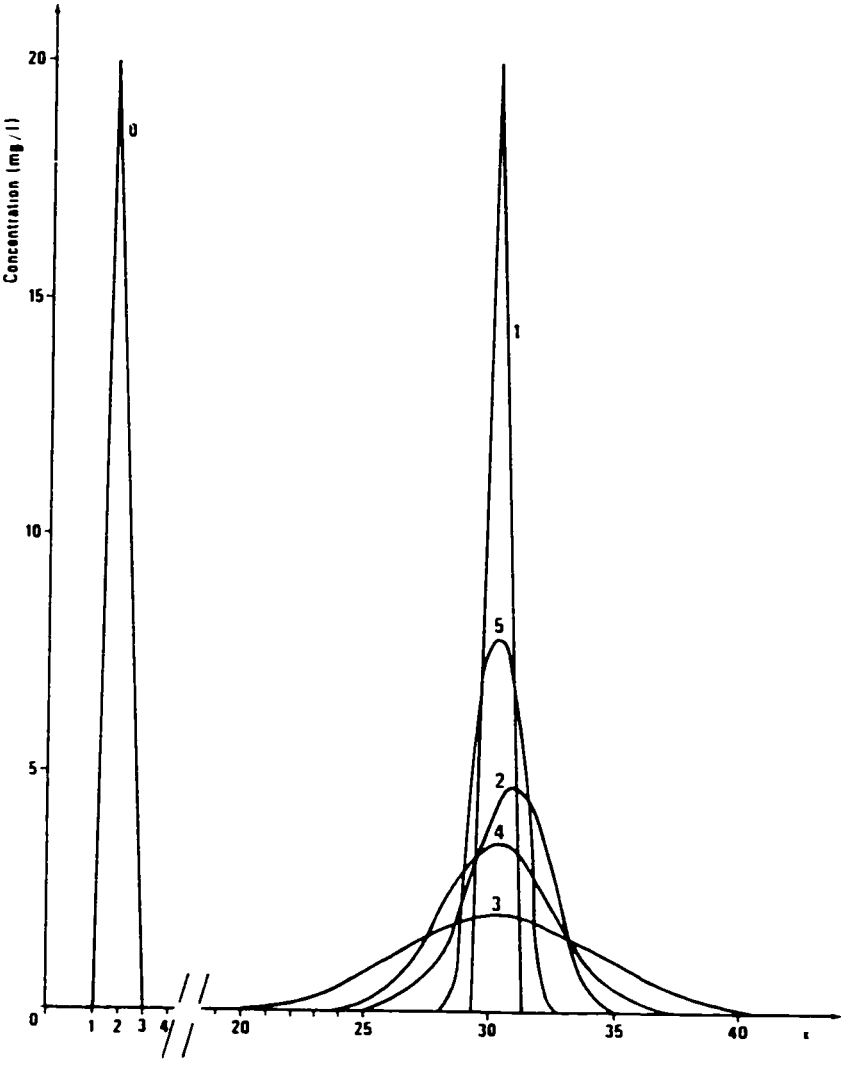

Figure 4.2 Numerical Diffusion of the Dobbins and Bella (1968) Scheme. Case 0 Represents Initial Concentration Distribution; Cases 1, 2, 3, 4, and 5 are Shown in Table 4.1, (after Cunge et al., 1980).

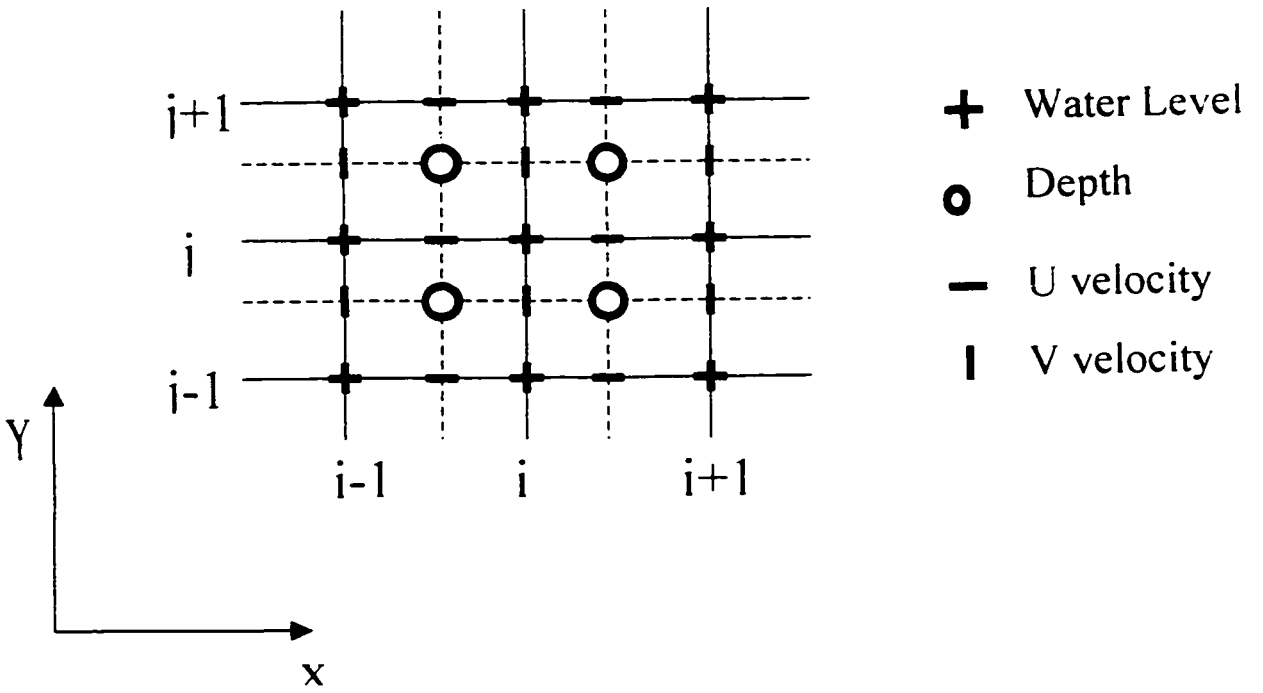

Figure 4.3 A Space-Staggered Grid System Used in the FD Approximations.

CHAPTER FIVE

THE EXPERIMENTAL STUDY

5.1 NEEDS FOR EXPERIMENTAL VERIFICATION

In recent years there has been an increasing interest in predicting solute transport processes in compound channel flows for controlling pollution levels in rivers. Recently a number of experimental works utilizing compound channels have been carried out , (Shiono and Knight, 1991; Tominaga and Nezu, 1991; Noat et al., 1993; Lambert and Sellin, 1996; Nezu et al., 1994). In light of these investigations, secondary currents are found to be significant in the vicinity of the junctions between the main channel and the flood plain(s) of compound channels. Although these secondary currents are only a few percent of the longitudinal velocity, they may significantly influence solute transport processes because they not only convect solute, but also affect the exchange coefficients of momentum and solute. Although many hydraulic engineering problems can be solved through equations and analytical procedures, many problems remain that rely on experimental data for their solution. In reality, very few problems involving real fluids can be solved by analysis alone. It is usually preferable to have a combination of analysis and experimentation. In this instance, we resort to similitude to construct physical models and to make sure that the scale measurements made on one system (model) can be used to describe the behaviour of other system (prototype).

The mathematical model should be checked if it adheres to the conditions of the problem it is simulating. It is important to build a model that gives good and useful outputs. An excellent method to verify the output of a mathematical model is to run it against data obtained from a physically-scaled model of the prototype.

5.2 DIMENSIONAL ANALYSIS

5.2.1 SIMILITUDE ANALYSIS

Based on the Froude (Fr) scaling law and using Manning's equation, the boundary roughness scale in a single-scale model is expressed as $\mathbf{n}_r = \mathbf{L}_r^{1/6}$ where n_r and L_r = respective ratios of Manning's roughness coefficient and length in the model to those in the prototype. This equation states that the length ratio is not arbitrary but is constrained by n_r. Not only is this restrictive, but for relatively smooth prototype channels it may be impossible to satisfy. For example, a river with $n_p = 0.020$ is modelled with a smooth concrete channel of $n_m = 0.012$ then according to the above equation $L_r = 0.047$ or approximately 1:20 which is considered small in river modelling. Another problem with physical modelling arises from the fact that when a river 130 m (400 ft) wide is modelled using a channel 0.65 m (2 ft) wide, this would give a scale ratio $L_r = 1/200$; however, applying the same L_r to the depth of 3 m (10 ft) would reduce the model depth to 0.015 m (0.05) ft. The major problem is that flow at this depth is barely turbulent. In addition, surface tension effects (normally neglected in the prototype) may influence the flow in the model and satisfactory similitude becomes unlikely. Both of these problems can be circumvented through the use of a distorted model by exaggerating the vertical scale relative to the horizontal scale. Although this may introduce some scaling effects, the kinematic similitude is not seriously affected and the distorted model still provides useful quantitative results, (Prasuhn, 1992).

This distortion is intended to solve the depth scaling problem and perhaps will solve the resistance problem. Let X_r and Y_r denote the scale factors in the horizontal and vertical

directions respectively. Since the velocity ratio (V_r) is based on Fr, which is, in turn, based on the depth ratio, Y_r, then $V_r = Y_r^{1/2}$. Since time is usually considered with respect to distances traversed in the flow direction then $t_r = X_r/V_r$, where t_r = ratio of time in the model to that in the prototype. The ratio of discharge in the model to that in the prototype (Q_r) is written as $Q_r = V_r X_r Y_r = X_r Y_r^{3/2}$. Since channel slope is based on the ratio of the vertical dimension to the horizontal dimension, then S_r, which is usually referred to as the distortion scale, can be expressed as $S_r = Y_r/X_r$. Substituting the above identities in Manning's equation gives $V_r = (R_r^{2/3} Y_r^{1/2})/(n_r X_r^{1/2})$.

5.2.2 THE MODEL DIMENSIONS

Applying the basic principles of dimensional analysis to a river model, one can see that our experimental channel's dimensions are reasonable enough to overcome any scaling effects. Those dimensions are as follows: 29.26 m long (96 ft), 0.787 m deep (31 in), and 1.498 m wide (59 in). Although the channel is 0.787 m deep, not all the depth was used since it was important to maintain the ratio of flood plain to main channel depth less than 0.35. In this instance, the maximum depth used was in the range of 32 cm. Thus, in the analysis an ultimate depth of 40 cm was selected. If one selects a horizontal scaling factor of 320 and a vertical scaling factor of 16, this would result in a distortion factor of 20. Considering an average river channel that is 6.40 m (21 ft.) deep, and 480 m (1575 ft) wide and applying the scaling factors in the respective dimensions gives a channel typical of the one used in this study. Also, applying the above mentioned equations gives the following scale factors: X_r = 0.00312, Y_r = 0.0625, V_r = 0.250, S_r = 0.050, t_r = 0.0125, and n_r = 0.3550. A Manning's roughness coefficient for a typical large river channel of 0.040 is equivalent to a model n-value of 0.014, which is appropriate for a smooth concrete laboratory channel, (Chow, 1959).

5.3 EXPERIMENTAL INVESTIGATION

Experimental tracer measurements were used to recognize and study certain flow

phenomena and to validate and calibrate mass transport mathematical models. It is useful to perform some tests in compound channels in order to understand the complex flow structure and to verify mathematical models. This is particularly important when shifting from simple geometry to natural conditions in the development of transport models. With all of the above in mind, it is worthwhile to mention that the literature indicates there are still very few papers that present tracer experiments in compound channels, (Arnold et al., 1985). Also, the aspect ratio in this study ranges between 4.2 to 6.0 which is higher than that of Djordjevic (1993). It is for these reasons that the present research included an important laboratory component.

5.3.1 EXPERIMENTAL CHANNEL

The experimental channel employed in this investigation was 29.26 m long x 0.787 m deep x 1.498 m wide on a bed slope of 0.00069. The channel has a simple rectangular cross-section, however, this was modified using aluminum sheeting to produce an asymmetrical compound shape. The main channel of the compound section is 0.787 m wide and the right-side flood plain is 0.711 m wide. The compound channel is shown in figure 5.1. The channel bottom is concrete and is painted with black asphalt to ensure uniform water tightness at the bottom or sides of the channel. The experiments involved measuring the concentration distribution downstream of an instantaneous injection or a steady point source of tracer (Rhodamine WT) discharging into steady, uniform compound channel flows. The function of the inlet multi-port diffuser pipe was to supply, with minimal disturbance, smooth entrance flow to the main channel and flood plain sections of the channel. Screens (mesh) and baffles were installed downstream of the diffuser to dissipate large-scale turbulence and secondary circulation in the entrance channel. The downstream end of the channel contained a transition section which conveyed the flow smoothly from the flood plain to the channel exit. While the discharge was varied in the various experiments, the depth (d) on the flood plain was maintained at values below 0.35 of the main channel depth (D) throughout.

A description of the various measurements and parameters involved in the study as well as results are presented in the following sections.

5.3.2 EXPERIMENTAL PARAMETERS

5.3.2.1 Depth

Depths were measured with a point gauge mounted on the channel's instrument carriage, (plate 5.1). Although depth measurements were accurate to 0.1 mm, the unevenness of the flume floor demanded some degree of subjective judgement. Due to the small slope in the channel bottom, any error in setting uniform flow could cause substantial errors in the measurements and the consequent calculations. Precise elevation readings were taken at 8 representative sections along the channel and a best-fit line gave an average bottom slope of 0.0007 for the channel. It is noted that meeting the criterion used to determine the existence of uniform flow, namely a uniform flow depth, was not without its difficulties . In the case of a compound channel, attaining a uniform flow with the velocity vectors parallel to the junction is extremely difficult. It was also important to have the velocity contours at two sections within the test reach similar. The downstream variable-height weir was used to adjust the water surface profile in order to have equal depth measurements at one station just upstream and another just downstream of the test section. This process was lengthy and required considerable patience and preciseness on the experimenter's part. Once nearly uniform flow was established in the vicinity of the test section, the other parameters were then measured.

5.3.2.2 Velocity

Velocity measurements were performed at two stations, one 12.24 m and the other 22.76 m from the channel entrance. At each station, the cross-section was subdivided into 11 panels and velocities were measured at the edge of each panel. (figure 5.2). Table 5.1 shows the cross-stream distances of velocity measurements. Where depth allowed, velocities were measured at 0.2D and 0.8D below the free surface. Otherwise, velocities were measured at 0.6D below the free surface. The point velocities were measured using either a

propeller-type current meter or a pitot-static tube. Rotation of the propeller was estimated by counting the beeps over a certain period of time and calculating the number of revolutions per second. Where depth permitted, velocities were averaged over the depth; otherwise, velocity at 0.6D was considered as the DA velocity of the panel. The cross-stream variation of the average velocity at the upstream and downstream stations, for some typical experimental runs, is shown in tables 5.2 and 5.3, respectively. It can be seen that the distributions are essentially similar for all the locations provided that the depth ratio (d/D) is less than 0.30.

5.3.2.3 Discharge

Discharge was calculated by using *stream guaging* procedure, (Chow, 1959; and Prasuhn, 1992). Table 5.4 shows cross-stream variation of panel discharge for some typical experimental runs.

5.3.2.4 Tracer Selection

Fluorescent tracers are measured with an instrument called a fluorometer. Tracers can be used to identify the origin and destination of contaminated water, as well as its influence on other bodies of water. A lesser known but valuable use of tracers is in measuring velocities and discharge rates. Fluorescent tracer methods are simple, fast, accurate, and work in situations where factors such as turbulence or unknown cross-section render other methods inaccurate or impossible. The ideal tracer would be nontoxic, usable in small quantities, cost-effective, invisible, easy to measure at low concentrations, specific, and stable during the course of the study. Since Rhodamine WT meets all the above requirements it was used as the tracer in this study. Rhodamine WT is so safe that the U.S. Environmental Protection Agency (U.S. EPA) and most states approve its use in potable water. It is usually detectable in very small concentrations (in the order of ten parts per trillion) as compared to non-fluorescent tracers (with detectability in the range of 0.1 to 0.001 part per million). For

example, a water body 32 km long, 16 km wide, and only 2.7 m (8 ft) deep would require 12 tons of non-fluorescent tracer, while it would require only a few kilograms of Rhodamine WT to have detectible concentrations. Rhodamine WT absorbs green light and emits red light. It is sufficiently stable in sunlight. However, it is affected by oxidizing agents such as chlorine.

5.3.2.5 Tracer Injection

For the mixing tests, the Rhodamine WT tracer solution, which is neutrally buoyant and conservative, was released at different rates and locations as specified in each test case. Release points were varied across the transverse direction and the vertical dimension of the compound channel to check the effect of point of release on the mixing properties of the tracer. The tracer solution was not mixed with any other material but was used in the *pure* state. Tracer injections were done at a station 7.76 m from the channel entrance where the inflow effect was relatively considered negligible. Different flow conditions and injection points were considered. The tracer was introduced into the channel by sudden release from a 120 ml test bottle, or by continuous steady injection. Two plastic drums, each having a diameter of 0.286 m and a height of 0.508 m (giving an individual capacity of 32.58 litres), were installed above each other on a holding column. The two drums were installed at heights of 0.27 m and 0.70 m from the top concrete edge of the channel, respectively, (plate 5.2). The dye tracer flows from the top drum to the lower one in order to maintain a constant head in the latter. This apparatus kept the injection speed and rate constant as it produced a constant head in the supply drum. The tracer solution was introduced directly, by gravity, into the circulating water system through a set of vinyl tubing. The tubes were connected to tees and angles to supply the tracer to four stainless steel injectors, facing downward, and located at different points across the injection station. The tracer flow rate in the tubes was controlled by miniature screw-valves. This dye-injection rig permitted variation of the dye injection points in both the transverse and vertical direction. For continuous steady injections, the dye injection was performed at different points (at Y m from the right edge of the flood

plain facing upward) in the main channel, near the main channel/flood plain interface, over the flood plain, or a combination of injectors where more than one injector was used and the injection rates were measured in each.

5.3.2.6 Test Descriptions

Table 5.5 gives the details of the various dye-injection experiments performed in the compound channel. Also, table 5.6 shows the hydraulic parameter-computations for typical test runs. The Reynolds numbers over the main channel and the flood plain zone were always in the ***fully-developed turbulent*** range.

5.3.2.7 Tracer Sampling

Although the aspect ratio in the channel under consideration ranged up to 6.0, this cannot be considered as a *wide* channel. In this instance, dye dispersion is not expected to be vertically uniform, but stratification would not be expected either. Consequently, a certain distance (4.48 m from the point of injection) was allowed for complete vertical mixing to take place before any samples were collected. Fischer et al. (1979) proposed the following empirical relationship to estimate the distance (L) from the sources at which mixing is complete and only longitudinal dispersion takes place:

$$L = \frac{0.1\ U_a\ W^2}{\epsilon_y} \qquad \textbf{(5-1)}$$

where W = distance from the source to the farther bank. Although eq. 5-1 is empirical and limited in applications due to the inherent assumptions, it was applied to estimate the distance for complete mixing. These mixing distances were calculated to be 3.51, 0.87, 4.23, 4.15, 4.29, 4.67, and 3.71 m for test runs 1, 4, 12, 15, 20, 23, and 26, respectively. Samples were collected by direct pumping. The upstream and downstream sampling stations were located

12.24 m and 22.77 m from the channel entrance, respectively. Four variable-speed pumps were used and each pump had two sampling ports, (plate 5.3). Four samples were collected at each station at different time intervals using stainless steel sampling tubes. The sampling tubes, which had a 3 mm inside diameter and a 4 mm outside diameter, faced upstream. The intake velocity was adjusted, by trial and error, to a value approximately equal to the average local stream velocity. In order to obtain a time-averaged concentration, the sampling bottle was filled over a 20 s time interval. Table 5.7 shows the cross-stream distances of concentration measurements.

5.3.2.8 Fluorometer Unit

A Turner Designs Model 10-AU fluorometer was used in the study. This model has several unique features, including: direct digital readout, without the need for calculations; automatic temperature compensation for on-line samples; a condensate-proof sample compartment; auto-ranging over a wide range of sensitivity; operation with both analog and serial data collection devices simultaneously. For example, the florescence of Rhodamine WT decreases 2.6 % for each degree Celsius rise in temperature. However, the 10-AU model eliminates this possible source of error by correcting for it automatically. Moreover, with the 10-AU-005 model field fluorometer samples can be pumped directly through flow cells for continuous accurate readings. This particular fluorometer can be configured to log data, which can be easily transferred to a computer. This means it is possible to get reliable data collection without the inconvenience of external devices. Data can be manipulated and plotted using a spreadsheet program supplied with the 10-AU model.

The fluorometer had to be calibrated in order to change the readings from absorbance into real concentrations of dye, measured in mg/l. This task was accomplished by diluting some dye concentration in distilled water samples in order to obtain solutions of known concentration. These samples, which covered a wide range of concentrations, were tested using the fluorometer. The resulting data were reduced and plotted in terms of concentration

versus fluorometer reading, (figure 5.3). A *straight line* relationship appeared when concentration values were plotted versus fluorometer readings on a semi-log scale, (figure 5.4). A linear regression analysis, which resulted in $r^2 = 0.9946$, was applied to the data to obtain the following relationship:

$$\ln (MC) = 0.005786984\ FR - 1.71609 \qquad \textbf{(5-2)}$$

where:

MC = measured concentration, (mg/l), and

FR = fluorometer reading.

Eq. 5-2 can be written in exponential form as:

$$MC = e^{(0.005786984\ FR\ -\ 1.71609)} \qquad \textbf{(5-3)}$$

5.3.2.9 Sample Analysis

Following each experiment, samples were analysed for dye concentration using the Turner 10-AU Fluorometer. Samples of channel water outside of the dye plume were taken to determine background readings. Some fluctuations of concentration were observed in the fluorometer readings, (tables 5.8 to 5.18). The fluctuations were caused primarily by the large scale eddies associated with the flow interaction between the main channel and the flood plain zones. The magnitude of the fluctuations decreased further downstream from the dye release point as the transverse concentration difference became smaller.

Concentrations of the dye tracer were plotted for the four sampling tubes at the upstream and downstream stations, respectively. The main purpose was to investigate the propagation of the dye tracer as the flow moves downstream. Tables 5.8 to 5.18 show the cross-stream variation of the dye concentration with time.

5.4 COMPUTATIONS

5.4.2 DISPERSION MECHANISM

Consider a tracer introduced at the centre-line of a stream in the form of a line source. Let the concentration of the tracer, which is constant over the depth, be C_0. Due to the combined effect of diffusion and dispersion, the tracer spreads laterally and is also stretched in the longitudinal direction. The concentration of the tracer decreases downstream until it becomes constant across the width at some point further downstream. Two cases are considered. First, the tracer is introduced only for a limited period of time *t* as a slug where the concentration decreases continually in the downstream direction because of mixing with increasing volumes of water. Second, the tracer is injected continuously which can be viewed as one of a combination of a series of slug injections, one after the other.

5.4.2 CLASSICAL ANALYTICAL SOLUTIONS

In general, it is not possible to obtain analytical solutions to the dispersion equation in natural waterways with arbitrary boundary conditions. However, a variety of exact solutions exists for idealized situations, which can be useful in obtaining order-of-magnitude estimates. The effects of confining boundaries are taken into account by introducing *image sources*, the effect of which is to nullify any mixing across solid boundaries. Extension of the 1-D solution to 2- and 3-D follows the same general pattern. If further simplifications are made in eq. 3-18, some analytical solutions may be obtained, (Sayre and Chang, 1968; Carslaw and Jaeger, 1959). In particular, first consider the case of an infinitely wide 2-D flow (constant h, u, ϵ_x and ϵ_y), with instantaneous release of a mass M of tracer as a ***slug injection at x = 0, y = 0, and t = 0*** with boundary conditions defined as: $C(\infty,t) = 0$ and $C(x,0) = M\,\delta(x)$, where δ is the dirac delta function. In this instance, the solution is:

$$C = \frac{M}{4\,\Pi\,\sqrt{\epsilon_x\,\epsilon_y\,t}}\; e^{-\frac{(x - U\,t)^2}{4\,\epsilon_x\,t} - \frac{(y - U\,t)^2}{4\,\epsilon_y\,t}} \qquad \textbf{(5-3)}$$

Second, consider a ***continuous injection at x = 0, y = 0, and t = 0*** with boundary conditions defined as: $C(0,t)=C_0$ for $0 < t < \infty$, and $C(x,0)=0$ for $0 < x < \infty$. In this case, the solution can be formulated as:

$$C\,(x,y,t) = \frac{C_o}{4}\left[erfc\left(\frac{x - U\,t}{\sqrt{4\,D_x\,t}}\right) + erfc\left(\frac{x + U\,t}{\sqrt{4\,D_x\,t}}\right)\; e^{\frac{U\,x}{D_x}}\right] \times \left[erfc\left(\frac{y - V\,t}{\sqrt{4\,D_y\,t}}\right) + erfc\left(\frac{y + V\,t}{\sqrt{4\,D_y\,t}}\right)\; e^{\frac{V\,y}{D_y}}\right] \qquad \textbf{(5-4)}$$

where erfc = complementary error function. For V = 0 eq. 5-4 reduces to:

$$C\,(x,y,t) = \frac{C_o}{2}\left[erfc\left(\frac{x - U\,t}{\sqrt{4\,D_x\,t}}\right) + erfc\left(\frac{x + U\,t}{\sqrt{4\,D_x\,t}}\right)\; e^{\frac{U\,x}{D_x}}\right] \times \left[erfc\left(\frac{y}{\sqrt{4\,D_y\,t}}\right)\right] \qquad \textbf{(5-5)}$$

If the tracer is released at some point $x = x_o$, $y = y_o$, instead of x = 0 and y = 0, then x and y in the above equations should be replaced by $(x - x_o)$ and $(y - y_o)$, respectively.

5.4.3 DETERMINATION OF ϵ_x AND ϵ_y

As discussed in section 3.4.9, a_x and a_y were assumed based on some earlier work, (Djordjevic, 1993; and Elder, 1959).

5.5 SUMMARY

This study addresses the mixing experiments of inert pollutant transport in rectangular compound open channels. Consideration is limited to conservative, non-buoyant material hereafter referred to as *tracers*. Experiments aimed at investigating, under uniform flow conditions, the influence of flood plains and lateral momentum transfer on mixing in a compound channel. For all the tests, the test number, flow conditions, injection points and rates, collection points, sampling times, and concentrations were indicated. The experiments include measurements of dye concentrations downstream of a slug-injection or steady-injection *point* sources. In reducing the data and performing the necessary computations, it was difficult to determine the mixing coefficients.

Table 5.1 Cross-Stream Distances of Velocity Measurements.

Panel No.	Distance, Y (mm)
1	75
2	225
3	375
4	525
5	675
6	825
7	975
8	1125
9	1275
10	1425

Table 5.2 Cross-Stream Average Velocity Variation at the Upstream Station.

Distance (m)	Test 2 (m/s)	Test 4 (m/s)	Test 11 (m/s)	Test 16 (m/s)	Test 20 (m/s)	Test 23 (m/s)	Test 27 (m/s)
1.500	0.0000	0.0000	0.0000	0.0000	0.0000	0.0000	0.0000
1.425	0.5017	0.0838	0.3683	0.3467	0.3302	0.4610	0.3480
1.275	0.5105	0.0900	0.3833	0.3569	0.3302	0.5093	0.3505
1.125	0.5080	0.0970	0.3833	0.3518	0.3505	0.5334	0.3797
0.975	0.4877	0.0955	0.3798	0.3391	0.3378	0.5410	0.4216
0.825	0.4661	0.0813	0.3420	0.3048	0.3061	0.5156	0.4115
0.675	0.4928	0.0610	0.2440	0.2032	0.1829	0.5486	0.4064
0.525	0.5080	0.0560	0.2340	0.1981	0.1829	0.5283	0.3962
0.375	0.4775	0.0510	0.2340	0.1778	0.1727	0.5182	0.3658
0.225	0.4674	0.0410	0.2180	0.1727	0.1626	0.5080	0.3353
0.075	0.4166	0.0360	0.1980	0.1524	0.1321	0.4470	0.2946
0.000	0.0000	0.0000	0.0000	0.0000	0.0000	0.0000	0.0000

Table 5.3 Cross-Stream Average Velocity Variation at the Downstream Station.

Distance (m)	Test 2 (m/s)	Test 4 (m/s)	Test 11 (m/s)	Test 16 (m/s)	Test 20 (m/s)	Test 23 (m/s)	Test 27 (m/s)
1.500	0.0000	0.0000	0.0000	0.0000	0.0000	0.0000	0.0000
1.425	0.5211	0.0860	0.3765	0.3480	0.3505	0.5080	0.3581
1.275	0.5499	0.0993	0.3923	0.3683	0.3556	0.5271	0.3607
1.125	0.5385	0.1030	0.3938	0.3632	0.3658	0.5334	0.3835
0.975	0.5245	0.0918	0.3758	0.3454	0.3404	0.5347	0.4140
0.825	0.4851	0.0798	0.3493	0.3086	0.3124	0.5156	0.4064
0.675	0.4775	0.0610	0.2340	0.2134	0.1829	0.5385	0.3861
0.525	0.4572	0.0510	0.2340	0.1930	0.1626	0.5283	0.3861
0.375	0.4369	0.0460	0.2180	0.1626	0.1524	0.4978	0.3556
0.225	0.4470	0.0360	0.2180	0.1676	0.1524	0.5182	0.3454
0.075	0.4013	0.0300	0.1780	0.1372	0.1321	0.4470	0.3048
0.000	0.0000	0.0000	0.0000	0.0000	0.0000	0.0000	0.0000

Table 5.4 Cross-Stream Variation of Average Panel Discharge.

Panel Width (m)	Test 3 (m^3/s)	Test 5 (m^3/s)	Test 13 (m^3/s)	Test 17 (m^3/s)	Test 21 (m^3/s)	Test 24 (m^3/s)	Test 25 (m^3/s)
0.0750	0.0283	0.0036	0.0148	0.0132	0.0127	0.0230	0.0160
0.0750	0.0293	0.0041	0.0154	0.0138	0.0132	0.0246	0.0161
0.0750	0.0289	0.0043	0.0154	0.0136	0.0125	0.0253	0.0173
0.0750	0.0280	0.0040	0.0150	0.0131	0.0142	0.0256	0.0190
0.0750	0.0328	0.0043	0.0171	0.0146	0.0007	0.0305	0.0231
0.0750	0.0086	0.0005	0.0015	0.0010	0.0009	0.0064	0.0041
0.0750	0.0115	0.0006	0.0019	0.0013	0.0009	0.0085	0.0054
0.0750	0.0109	0.0006	0.0019	0.0011	0.0009	0.0081	0.0050
0.0750	0.0109	0.0004	0.0018	0.0011	0.0007	0.0082	0.0047
0.0750	0.0097	0.0004	0.0016	0.0010	0.1321	0.0072	0.0042

Table 5.5 Summary of Test Conditions and Related Data.

Test #	Sampling Time (min)	Average Depth (m)	Depth Ratio d/D	Injection Type	Injection Rate	Injector Number	Injection Point (x,y,z)
1	40	0.3683	0.431	Continuous	N/A	1	(7.76,1.350,0.178)
2	5	0.3683	0.431	Slug	120 ml	N/A	Whole Width
3	5	0.3683	0.431	Slug	60 ml	N/A	Main Channel
4	33	0.2858	0.266	Continuous	N/A	2	(7.76,1.000,0.140)
5	28	0.2858	0.266	Continuous	N/A	3	(7.76,0.780,0.038)
6	26	0.3148	0.333	Continuous	0.100 ml/s	3	(7.76,0.780,0.025)
7	14	0.3148	0.333	Continuous	0.580 ml/s	3	(7.76,0.780,0.025)
8	3	0.3148	0.333	Slug	100 ml	N/A	Flood Plain
9	15	0.2966	0.292	Continuous	1.000 ml/s	4	(7.76,0.337,0.254)
10	12	0.2966	0.292	Continuous	0.250 ml/s	4	(7.76,0.337,0.254)
11	12	0.2651	0.209	Continuous	2.083 ml/s	3	(7.76,0.780,0.132)
12	10.5	0.2651	0.209	Continuous	0.667 ml/s	3	(7.76,0.780,0.132)
13	2.5	0.2651	0.209	Slug	80 ml	N/A	Main Channel
14	2.5	0.2651	0.209	Slug	100 ml	N/A	Main Channel

Test #	Sampling Time (min)	Average Depth (m)	Depth Ratio d/D	Injection Type	Injection Rate	Injector Number	Injection Point (x,y,z)
15	10	0.2542	0.175	Continuous	0.367 ml/s	3	(7.76,0.780,0.178)
16	7.5	0.2542	0.175	Continuous	0.622 ml/s	3	(7.76,0.780,0.178)
17	2.5	0.2542	0.175	Slug	56 ml	~ 3	N/A
18	3.0	0.2542	0.175	Slug	75 ml	~ 2	N/A
19	3.0	0.2462	0.148	Slug	100 ml	N/A	Whole Channel
20	10.5	0.2462	0.148	Continuous	1.244 ml/s	2	(7.76,1.000,0.159)
21	10.0	0.2462	0.148	Continuous	0.300 ml/s	2	(7.76,1.000,0.159)
23	9.0	0.3167	0.338	Continuous	1.533 ml/s	2	(7.76,1.000,0.159)
24	10.0	0.3167	0.338	Continuous	2.000 ml/s 1.000 ml/s	1 4	(7.76,1.350,0.159) (7.76,0.340,0.263)
25	8.5	0.3026	0.307	Continuous	0.917 ml/s	5	(7.76,0.064,0.256)
26	9.5	0.3026	0.307	Continuous	1.300 ml/s	1	(7.76,1.350,0.042)
27	2.5	0.3026	0.307	Slug	50 ml	N/A	Main Channel

Table 5.6 Hydraulic Parameters of Different Test Runs.

Test #	1	4	12	15	20	23	26
d (m)	0.159	0.076	0.055	0.044	0.036	0.107	0.093
D (m)	0.369	0.286	0.265	0.254	0.246	0.317	0.303
d/D	0.431	0.266	0.209	0.175	0.148	0.338	0.307
A_{fp}	0.113	0.054	0.039	0.032	0.026	0.076	0.066
A_{mc}	0.290	0.225	0.209	0.200	0.194	0.249	0.238
Q_{fp}	0.053	0.003	0.009	0.006	0.004	0.039	0.024
Q_{mc}	0.143	0.020	0.077	0.068	0.064	0.128	0.091
V_{fp}	0.470	0.048	0.224	0.181	0.166	0.508	0.357
V_{mc}	0.493	0.089	0.0370	0.338	0.330	0.512	0.384
Re_{fp}	**73108**	**3580**	**12116**	**7848**	**5920**	**53145**	**32437**
Re_{mc}	**177870**	**24877**	**96025**	**84208**	**79482**	**158839**	**113638**

A_{fp} and A_{mc} = respective areas of the flood plain and main channel,

Q_{fp} and Q_{mc} = respective flow rates of the flood plain and main channel,

V_{fp} and V_{mc} = respective average velocities of the flood plain and main channel,

Re_{fp} and Re_{mc} = respective Reynolds Numbers of the flood plain and main channel,

Table 5.7 Cross-Stream Distances of Concentration Measurements.

Upstream		Downstream	
Sampler	Distance, Y (mm)	Sampler	Distance, Y (mm)
1	455	1	410
2	685	2	673
3	913	3	900
4	1255	4	1240

Table 5.8 Cross-Stream Variation of Concentration (mg/l), (Run # 1).

	UPSTREAM				DOWNSTREAM			
Time(min)	Sampler 4	Sampler 3	Sampler 2	Sampler 1	Sampler 4	Sampler 3	Sampler 2	Sampler 1
0.0	0.000	0.000	0.000	0.000	0.000	0.000	0.000	0.000
1.0	0.001	0.000	0.718	1.519	0.001	0.002	0.004	0.003
2.0	0.000	0.002	0.170	0.339	0.000	0.000	0.003	0.004
3.0	0.001	0.000	0.147	0.277	0.065	0.177	0.548	0.356
4.0	0.001	0.001	0.135	0.271	0.002	0.018	0.135	0.122
5.0	0.001	0.002	0.058	0.196	0.008	0.039	0.143	0.118
6.0	0.000	0.000	0.044	0.201	0.001	0.031	0.102	0.108
7.5	0.001	0.001	0.057	0.137	0.002	0.014	0.089	0.100
10.0	0.000	0.002	0.051	0.132	0.002	0.012	0.069	0.081
12.0	0.000	0.007	0.040	0.091	0.001	0.015	0.066	0.079
14.0	0.001	0.003	0.049	0.170	0.004	0.014	0.066	0.075
18.0	0.002	0.002	0.035	0.093	0.002	0.009	0.057	0.071
25.0	0.004	0.005	0.034	0.102	0.005	0.018	0.057	0.056
30.5	0.006	0.007	0.008	0.011	0.001	0.006	0.007	0.007
33.0	0.007	0.008	0.007	0.007	0.006	0.006	0.007	0.008
35.0	0.007	0.006	0.008	0.007	0.005	0.006	0.006	0.006
40.0	0.009	0.007	0.008	0.008	0.007	0.007	0.007	0.007
190.0	0.008	0.008	0.008	0.008	0.008	0.008	0.008	0.008

Table 5.9 Cross-Stream Variation of Concentration (mg/l), (Run # 2).

	UPSTREAM				DOWNSTREAM			
Time(min)	Sampler 4	Sampler 3	Sampler 2	Sampler 1	Sampler 4	Sampler 3	Sampler 2	Sampler 1
0.000	0.000	0.000	0.000	0.000	0.000	0.000	0.000	0.000
0.500	0.029	0.060	0.116	0.009	0.008	0.005	0.009	0.005
1.000	0.065	0.290	1.338	0.789	0.073	0.008	0.106	0.043
1.500	6.141	3.122	0.844	1.471	0.105	0.047	0.087	0.038
2.000	0.128	0.040	0.033	0.063	0.137	0.086	0.069	0.034
2.500	0.011	0.000	0.006	0.008	1.232	0.869	2.687	3.200
3.000	0.009	0.003	0.001	0.004	4.855	5.646	6.521	6.215
3.500	0.007	0.003	0.002	0.002	0.133	0.141	0.084	0.077
4.000	0.004	0.003	0.003	0.001	0.021	0.017	0.014	0.009
5.000	0.001	0.016	0.003	0.000	0.035	0.017	0.011	0.002

Table 5.10 Cross-Stream Variation of Concentration (mg/l), (Run # 3).

	UPSTREAM				DOWNSTREAM			
Time(min)	Sampler 4	Sampler 3	Sampler 2	Sampler 1	Sampler 4	Sampler 3	Sampler 2	Sampler 1
0.000	0.000	0.000	0.000	0.000	0.000	0.000	0.000	0.000
0.500	0.000	0.000	0.000	0.000	0.000	0.000	0.000	0.000
1.000	0.038	0.006	1.123	0.040	0.000	0.006	0.030	0.000
1.500	0.048	5.921	0.816	4.735	0.000	0.000	0.047	0.001
2.000	0.006	0.068	0.394	0.421	0.000	0.000	0.157	0.005
2.500	0.006	0.040	0.202	0.215	1.448	0.341	4.091	4.192
3.000	0.006	0.013	0.009	0.009	6.596	6.919	5.080	6.287
3.500	0.007	0.010	0.009	0.009	0.121	1.677	6.557	0.690
4.000	0.008	0.008	0.009	0.009	0.011	0.059	0.190	0.046
5.000	0.008	0.008	0.009	0.009	0.011	0.012	0.016	0.011

Table 5.11 Cross-Stream Variation of Concentration (mg/l), (Run # 5).

	UPSTREAM				DOWNSTREAM			
Time(min)	Sampler 4	Sampler 3	Sampler 2	Sampler 1	Sampler 4	Sampler 3	Sampler 2	Sampler 1
0.0	0.000	0.000	0.000	0.000	0.000	0.000	0.000	0.000
0.5	0.000	0.017	0.017	0.017	0.017	0.017	0.017	0.017
1.0	0.009	0.062	0.139	0.017	0.017	0.017	0.017	0.017
2.0	0.009	0.245	2.515	0.030	0.030	0.053	0.090	0.053
3.0	0.009	0.321	2.369	0.030	0.035	0.090	0.315	0.572
4.0	0.004	0.989	3.755	0.090	0.094	2.789	5.912	2.015
5.0	0.009	0.239	3.729	0.026	0.076	3.266	4.634	0.810
7.0	0.009	1.861	2.748	0.062	0.190	3.678	4.077	1.314
9.0	0.013	0.251	4.333	0.053	0.062	2.369	3.041	0.666
11.0	0.017	0.139	2.669	0.190	0.076	2.871	3.312	0.940
13.0	0.022	0.819	3.335	0.044	0.119	1.436	3.577	0.485
15.0	0.017	0.104	4.105	0.044	0.124	1.314	3.335	0.792
16.0	0.004	0.285	3.833	0.109	0.196	2.144	3.335	0.828
18.0	0.009	0.666	3.833	0.017	0.212	2.144	3.220	0.698
19.0	0.009	0.626	3.335	0.017	0.212	2.144	3.220	0.626
19.5	0.013	0.104	1.070	0.017	0.228	2.315	3.243	0.478
21.0	0.022	0.017	0.017	0.022	0.403	3.755	3.335	0.256
21.5	0.009	0.022	0.022	0.022	0.410	3.577	3.335	0.228
22.5	0.009	0.022	0.035	0.013	0.104	0.698	0.535	0.109
23.0	0.026	0.022	0.017	0.048	0.073	0.312	0.251	0.073
27.0	0.032	0.028	0.026	0.044	0.044	0.030	0.030	0.039
28.0	0.039	0.035	0.035	0.039	0.057	0.053	0.048	0.053
29.0	0.026	0.026	0.039	0.030	0.053	0.053	0.053	0.053

Table 5.12 Cross-Stream Variation of Concentration (mg/l), (Run # 9).

	UPSTREAM				DOWNSTREAM			
Time(min)	Sampler 4	Sampler 3	Sampler 2	Sampler 1	Sampler 4	Sampler 3	Sampler 2	Sampler 1
0.0	0.000	0.000	0.000	0.000	0.000	0.000	0.000	0.000
0.5	0.040	0.023	0.011	0.000	0.057	0.057	0.057	0.057
1.0	4.437	4.500	0.292	0.000	5.533	5.495	1.158	0.307
1.5	4.858	5.063	0.162	0.006	5.063	5.608	0.938	0.300
2.5	3.933	4.926	0.182	0.011	5.385	5.723	0.683	0.307
3.5	4.960	5.276	0.322	0.011	5.421	5.762	0.655	0.215
5.0	4.660	5.240	0.093	0.028	5.919	5.495	0.564	0.285
6.0	5.421	5.385	0.017	0.000	5.458	5.840	0.609	0.314
7.5	5.240	5.421	0.011	0.011	5.608	5.240	0.470	0.257
8.5	4.628	5.385	0.093	0.052	4.892	5.348	0.618	0.462
10.5	4.758	5.312	0.081	0.069	5.421	4.858	0.702	0.422
11.0	5.133	5.495	0.087	0.087	5.312	5.133	0.751	0.479
11.5	5.348	5.801	0.137	0.093	3.349	5.133	0.702	0.438
12.0	0.182	0.182	0.137	0.112	1.473	1.284	0.182	0.169
13.5	0.182	0.182	0.137	0.118	0.137	0.137	0.137	0.130
15.0	0.182	0.169	0.137	0.137	0.149	0.149	0.143	0.169

Table 5.13 Cross-Stream Variation of Concentration (mg/l), (Run # 10).

	UPSTREAM				DOWNSTREAM			
Time(min)	Sampler 4	Sampler 3	Sampler 2	Sampler 1	Sampler 4	Sampler 3	Sampler 2	Sampler 1
0.0	0.000	0.000	0.000	0.000	0.000	0.000	0.000	0.000
0.5	0.039	0.039	0.000	0.046	0.249	0.249	0.100	0.100
1.0	3.672	2.371	0.093	0.087	0.524	0.534	0.100	0.107
1.5	3.672	2.311	0.122	0.100	3.509	3.126	0.217	0.143
2.5	3.812	2.556	0.122	0.114	2.664	2.935	0.363	0.172
3.5	3.005	1.637	0.187	0.080	2.686	2.599	0.264	0.180
4.5	2.888	1.606	0.093	0.080	2.009	2.494	0.256	0.165
5.5	2.730	1.767	0.100	0.087	2.195	2.009	0.217	0.107
6.5	2.708	1.767	0.100	0.087	2.009	1.784	0.172	0.150
8.0	2.101	1.187	0.107	0.107	1.513	1.338	0.272	0.114
8.5	2.119	1.109	0.107	0.100	1.574	1.380	0.249	0.122
9.0	1.920	0.672	0.087	0.107	1.637	1.409	0.187	0.122
10.0	0.114	0.122	0.107	0.100	0.066	0.073	0.172	0.052
12.0	0.114	0.093	0.107	0.114	0.059	0.100	0.093	0.122

Table 5.14 Cross-Stream Variation of Concentration (mg/l), (Run # 13).

	UPSTREAM				DOWNSTREAM			
Time(min)	Sampler 4	Sampler 3	Sampler 2	Sampler 1	Sampler 4	Sampler 3	Sampler 2	Sampler 1
0.000	0.000	0.000	0.000	0.000	0.000	0.000	0.000	0.000
0.250	0.000	0.070	0.046	0.106	0.070	0.035	0.130	0.094
0.500	0.035	0.000	0.046	0.142	0.046	0.058	3.136	3.409
1.000	0.106	3.286	4.035	3.317	2.174	4.734	1.941	1.241
2.500	0.011	0.011	0.000	0.082	0.070	0.058	0.142	0.070

Table 5.15 Cross-Stream Variation of Concentration (mg/l), (Run # 15).

	UPSTREAM				DOWNSTREAM			
Time(min)	Sampler 4	Sampler 3	Sampler 2	Sampler 1	Sampler 4	Sampler 3	Sampler 2	Sampler 1
0.000	0.000	0.000	0.000	0.000	0.000	0.000	0.000	0.000
0.500	0.006	0.009	0.037	0.049	0.005	0.005	0.016	0.028
1.000	0.005	0.695	4.249	1.003	0.012	0.009	0.138	0.323
1.500	0.049	1.535	2.191	1.555	0.064	1.347	3.355	1.872
2.000	0.053	1.110	1.997	1.894	0.307	1.970	2.517	1.427
2.500	0.058	0.685	1.802	2.233	0.550	2.593	1.679	0.983
3.000	0.098	0.943	1.312	0.758	0.542	1.180	0.904	1.045
3.500	0.090	1.338	1.226	0.676	0.357	1.048	0.943	0.959
4.000	0.083	1.734	1.141	0.594	0.172	0.917	0.983	0.873
4.500	0.112	1.445	0.941	0.627	0.173	0.911	0.993	0.797
5.000	0.140	1.156	0.742	0.660	0.174	0.904	1.003	0.720
5.500	0.140	1.149	0.663	0.627	0.159	0.780	0.857	0.690
6.000	0.140	1.141	0.585	0.594	0.144	0.655	0.710	0.660
6.500	0.120	0.886	0.561	0.505	0.123	0.607	0.685	0.557
7.000	0.100	0.631	0.538	0.416	0.102	0.559	0.660	0.455
7.500	0.103	0.670	0.534	0.385	0.101	0.534	0.645	0.474
7.750	0.106	0.710	0.344	0.286	0.061	0.366	0.416	0.485
9.000	0.000	0.005	0.002	0.004	0.044	0.071	0.008	0.007
10.000	0.001	0.003	0.001	0.002	0.001	0.002	0.002	0.002

Table 5.16 Cross-Stream Variation of Concentration (mg/l), (Run # 20).

	UPSTREAM				DOWNSTREAM			
Time(min)	Sampler 4	Sampler 3	Sampler 2	Sampler 1	Sampler 4	Sampler 3	Sampler 2	Sampler 1
0.000	0.000	0.000	0.000	0.000	0.000	0.000	0.000	0.000
0.500	0.003	0.008	0.078	0.001	0.004	0.004	0.004	0.004
1.000	0.015	0.587	7.056	5.680	0.003	0.008	0.050	0.037
1.500	0.003	1.008	6.847	7.098	0.009	0.835	6.847	5.061
2.000	0.005	0.324	6.847	7.270	0.121	3.127	6.972	5.962
2.500	0.002	0.247	6.605	7.812	0.627	3.146	6.256	6.034
3.000	0.008	0.538	6.809	7.607	0.630	3.051	6.219	5.962
3.500	0.014	0.829	7.014	7.402	0.632	2.955	6.181	5.890
4.000	0.033	0.454	6.487	7.447	0.612	2.349	6.181	6.107
4.500	0.019	0.489	6.506	7.230	0.347	2.606	6.126	5.981
5.000	0.006	0.524	6.526	7.014	0.082	2.863	6.071	5.854
5.500	0.005	0.331	6.545	6.889	0.548	3.005	5.841	5.767
6.000	0.003	0.137	6.565	6.765	1.015	3.146	5.612	5.680
6.500	0.010	0.203	6.565	6.765	1.637	3.146	6.030	5.931
7.000	0.016	0.268	6.565	6.765	2.259	3.146	6.448	6.181
7.400	0.020	0.271	6.565	6.765	1.538	2.955	6.370	6.181
7.500	0.094	0.274	6.847	6.725	0.484	2.569	5.854	5.544
8.000	0.012	0.390	6.448	6.685	0.074	0.166	0.056	0.107
9.000	0.020	0.390	3.127	5.477	0.007	0.094	0.321	0.493
10.000	0.007	0.006	0.025	0.026	0.007	0.009	0.013	0.032

Table 5.17 Cross-Stream Variation of Concentration (mg/l), (Run # 21).

	UPSTREAM				DOWNSTREAM			
Time(min)	Sampler 4	Sampler 3	Sampler 2	Sampler 1	Sampler 4	Sampler 3	Sampler 2	Sampler 1
0.000	0.001	0.010	0.008	0.036	0.000	0.000	0.000	0.000
0.500	0.002	0.019	0.017	0.072	0.000	0.000	0.000	0.000
1.000	0.002	0.278	1.457	2.728	0.001	0.002	0.007	0.000
1.500	0.002	0.163	1.462	3.193	0.001	0.217	0.864	0.886
2.000	0.002	0.047	1.468	3.659	0.007	0.437	1.734	1.772
2.500	0.040	0.166	1.352	2.024	0.072	0.530	1.383	1.637
3.000	0.007	0.089	1.784	2.260	0.124	0.452	1.362	1.579
3.500	0.002	0.055	0.989	1.928	0.066	0.371	1.107	1.383
4.000	0.007	0.047	0.844	1.969	0.050	0.311	0.926	1.332
4.500	0.008	0.057	0.840	1.735	0.059	0.301	0.930	1.145
5.000	0.010	0.066	0.837	1.500	0.069	0.290	0.934	0.957
5.500	0.010	0.055	0.819	1.367	0.070	0.284	0.783	0.832
6.000	0.010	0.045	0.801	1.234	0.072	0.278	0.633	0.707
6.400	0.012	0.045	0.669	1.116	0.069	0.271	0.609	0.669
6.500	0.012	0.032	0.615	1.005	0.045	0.271	0.609	0.669
6.750	0.012	0.029	0.609	0.949	0.050	0.271	0.586	0.663
8.000	0.019	0.019	0.024	0.027	0.010	0.029	0.027	0.032
9.000	0.022	0.017	0.022	0.027	0.012	0.017	0.019	0.019
10.000	0.019	0.017	0.019	0.022	0.019	0.017	0.017	0.022

Table 5.18 Cross-Stream Variation of Concentration (mg/l), (Run # 26).

	UPSTREAM				DOWNSTREAM			
Time(min)	Sampler 4	Sampler 3	Sampler 2	Sampler 1	Sampler 4	Sampler 3	Sampler 2	Sampler 1
0.0	0.000	0.000	0.000	0.000	0.000	0.000	0.000	0.000
0.5	0.084	0.015	0.038	0.030	0.076	0.076	0.076	0.076
1.0	0.007	0.076	0.898	3.205	0.305	0.287	0.627	0.520
1.5	0.038	0.045	0.361	3.639	0.061	0.251	1.984	4.054
2.0	0.038	0.045	0.342	2.919	0.057	0.172	1.423	4.329
2.5	0.038	0.045	0.324	2.199	0.053	0.092	0.861	4.604
3.0	0.022	0.038	0.479	3.583	0.030	0.116	1.356	4.242
3.5	0.022	0.068	0.520	3.842	0.045	0.124	1.055	4.178
4.0	0.038	0.038	0.191	2.280	0.022	0.092	1.180	3.872
4.5	0.038	0.084	0.251	2.625	0.045	0.191	1.529	5.518
5.0	0.030	0.068	0.216	2.833	0.045	0.100	1.513	4.503
5.5	0.030	0.038	0.221	3.352	0.057	0.108	1.505	4.071
6.0	0.030	0.007	0.225	3.872	0.068	0.116	1.497	3.639
6.5	0.030	0.038	0.531	3.992	0.061	0.116	1.433	3.842
7.0	0.038	0.045	0.849	3.128	0.045	0.124	1.082	4.023
7.8	0.038	0.038	0.038	0.157	0.000	0.076	0.165	1.628
9.5	0.076	0.092	0.053	0.053	0.038	0.053	0.068	0.038

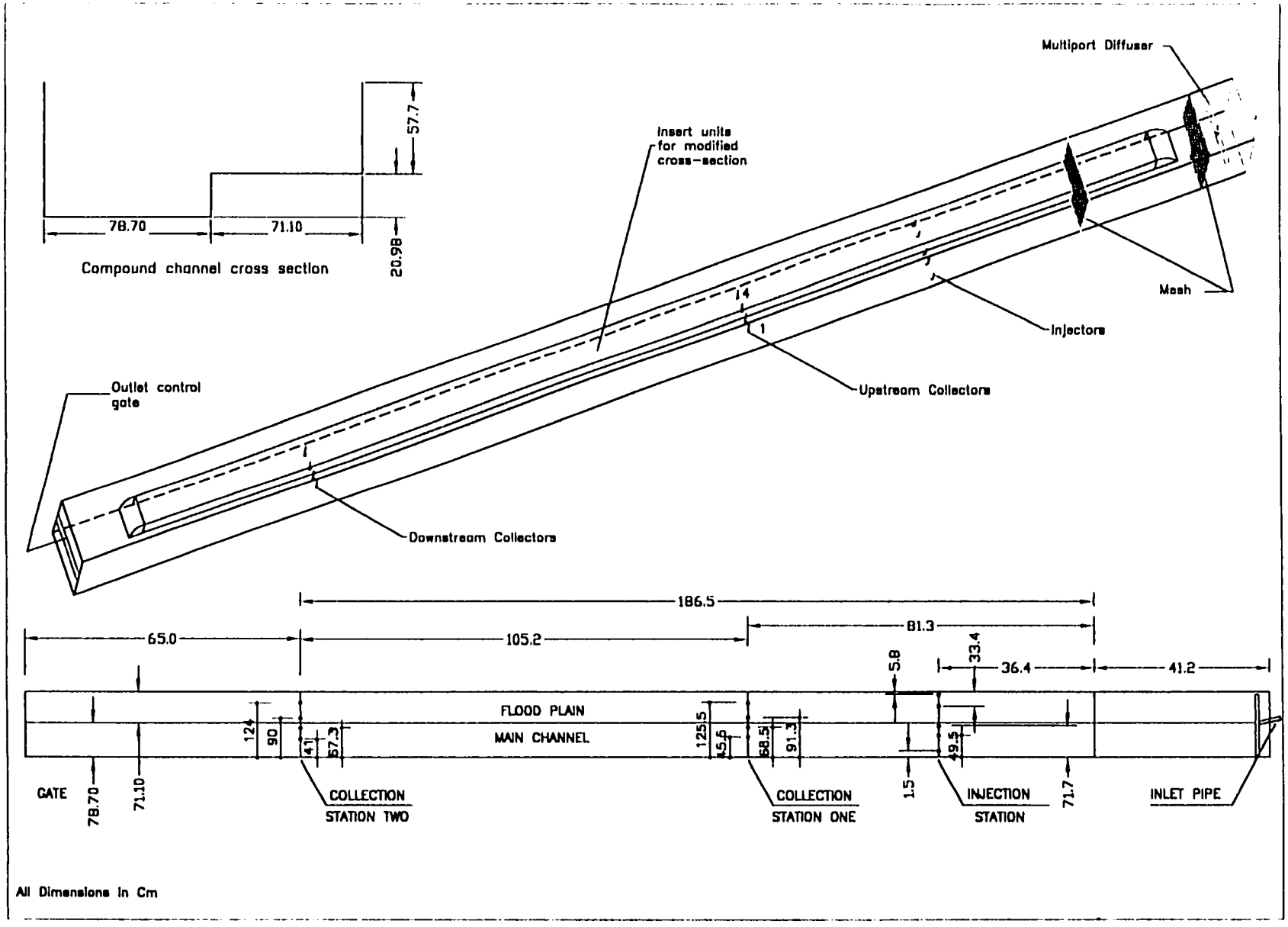

Figure 5.1 Schematic Representation of the Experimental Channel.

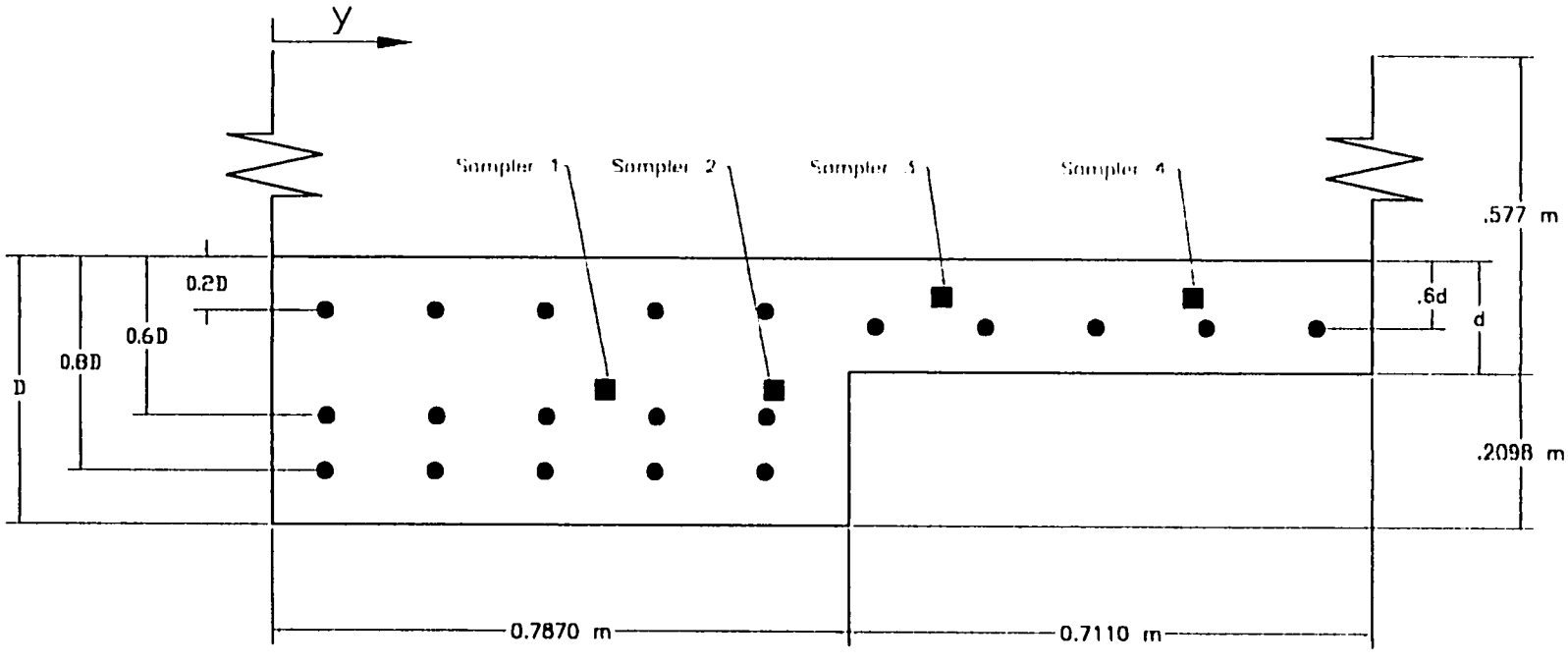

Figure 5.2 Points of Velocity and Concentration Measurements.

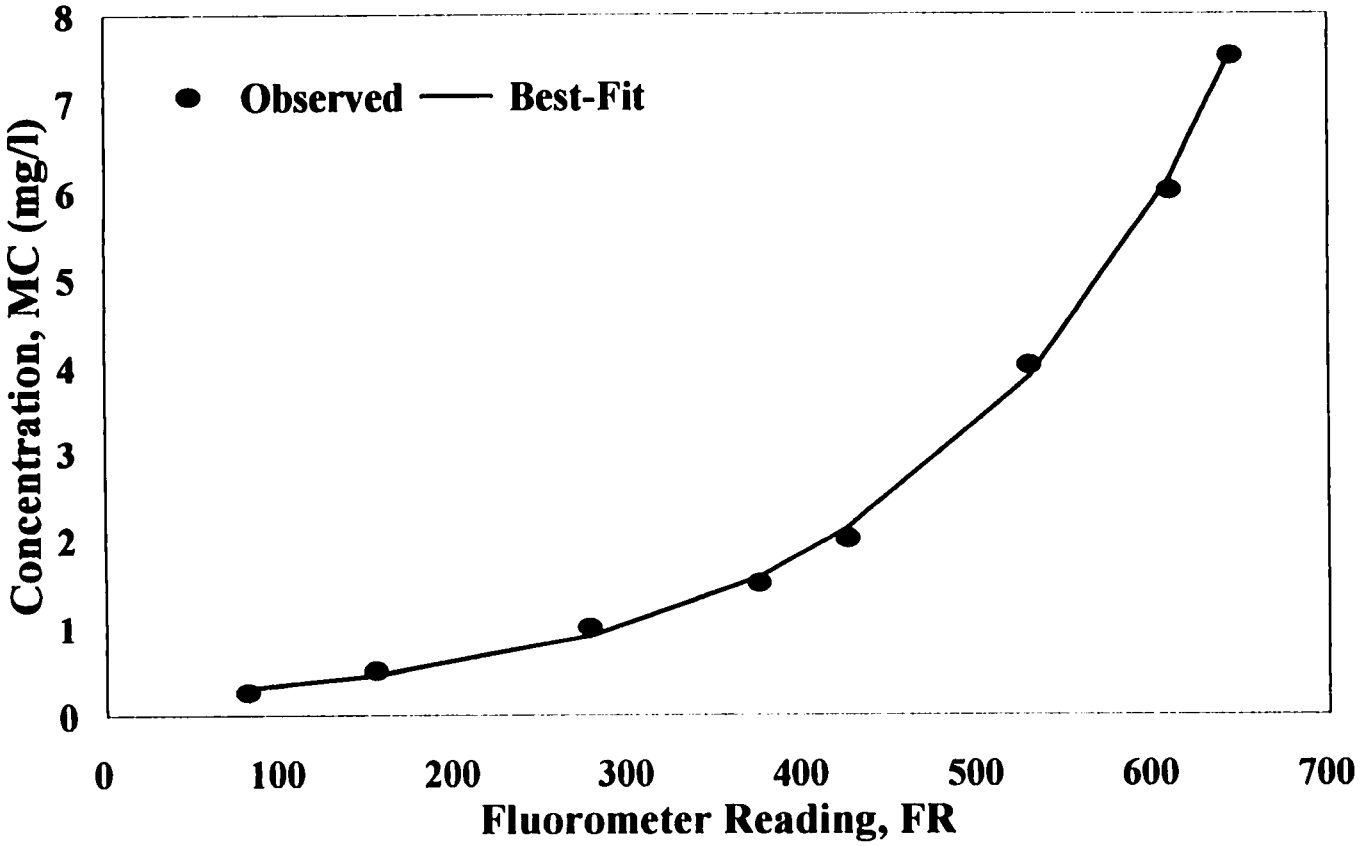

Figure 5.3 Variation of Concentration with Fluorometer Reading.

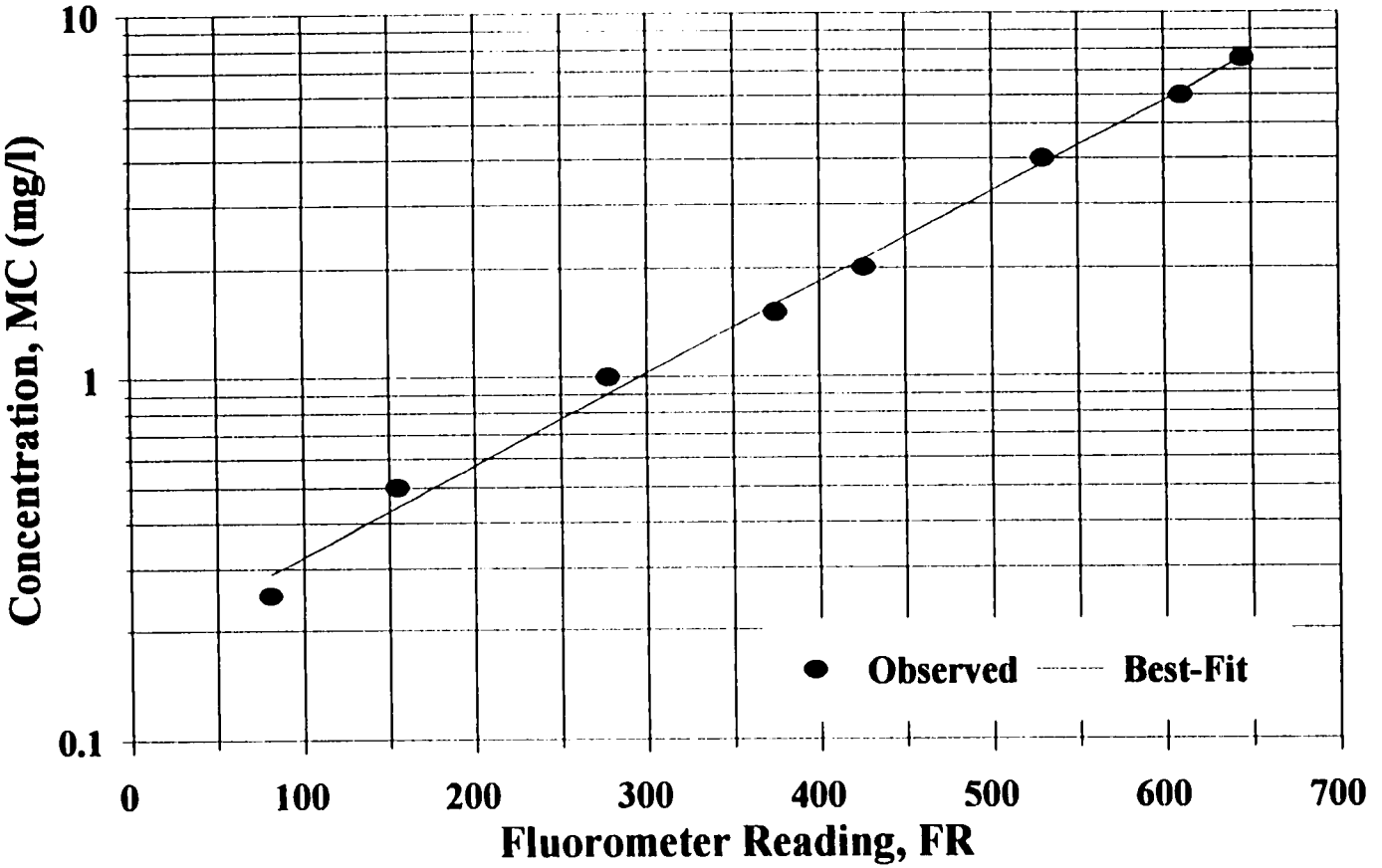

Figure 5.4 Best-Fit Line of Concentration vs. Fluorometer Reading, (semi-log scale).

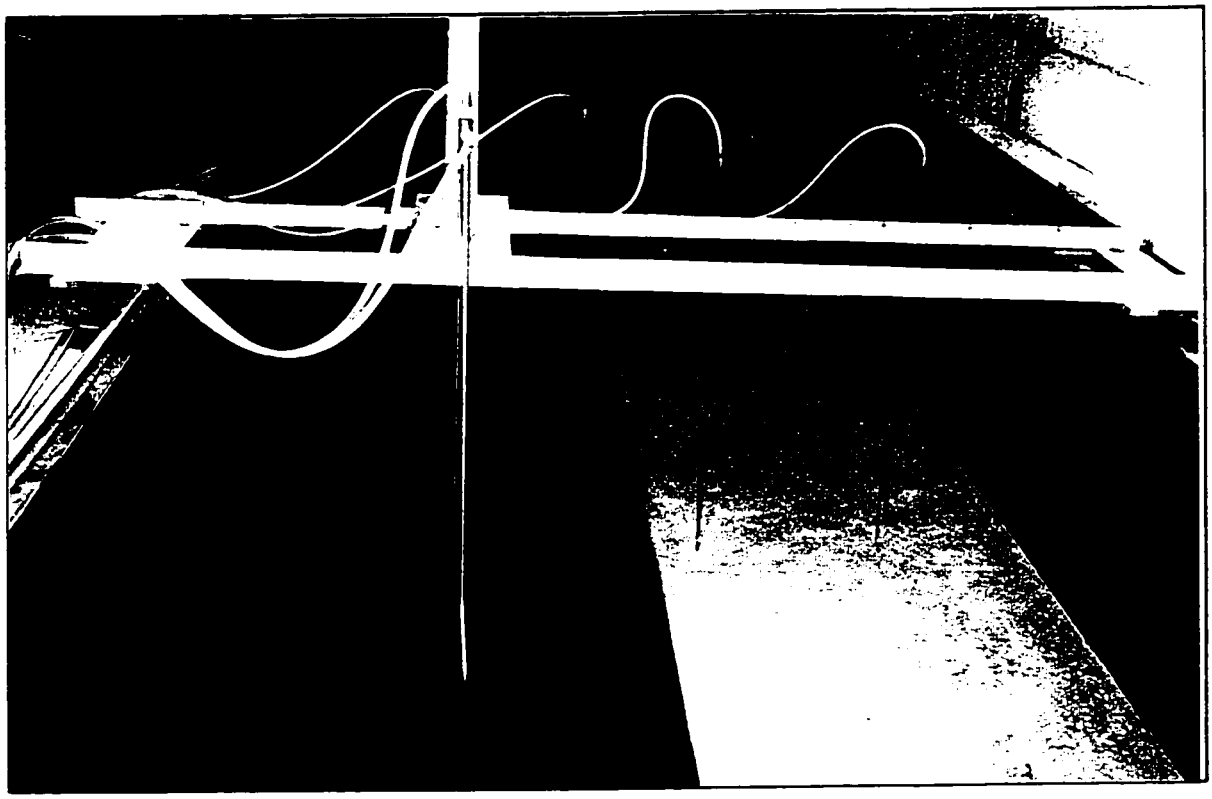

Plate 5.1 Point Gauge, Pitot Tube, and Sample Collectors.

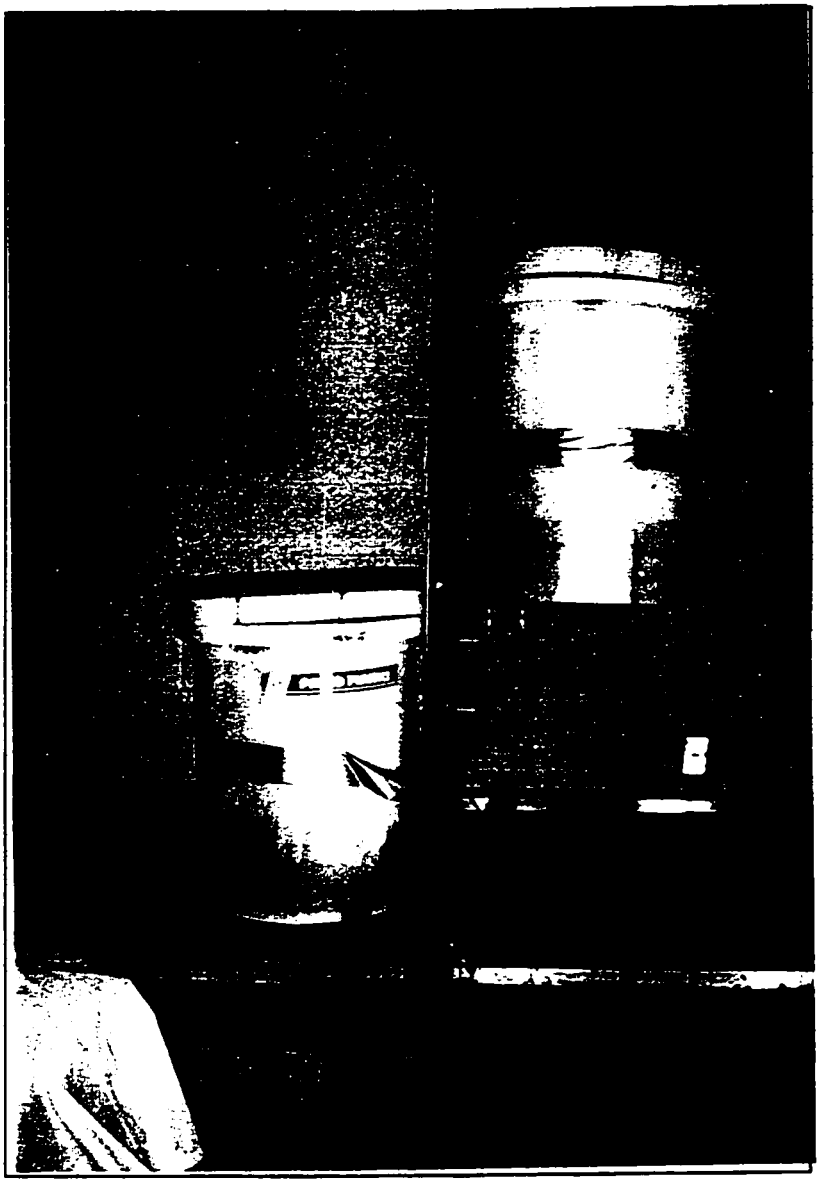

Plate 5.2 Gravity Injection System of the Dye.

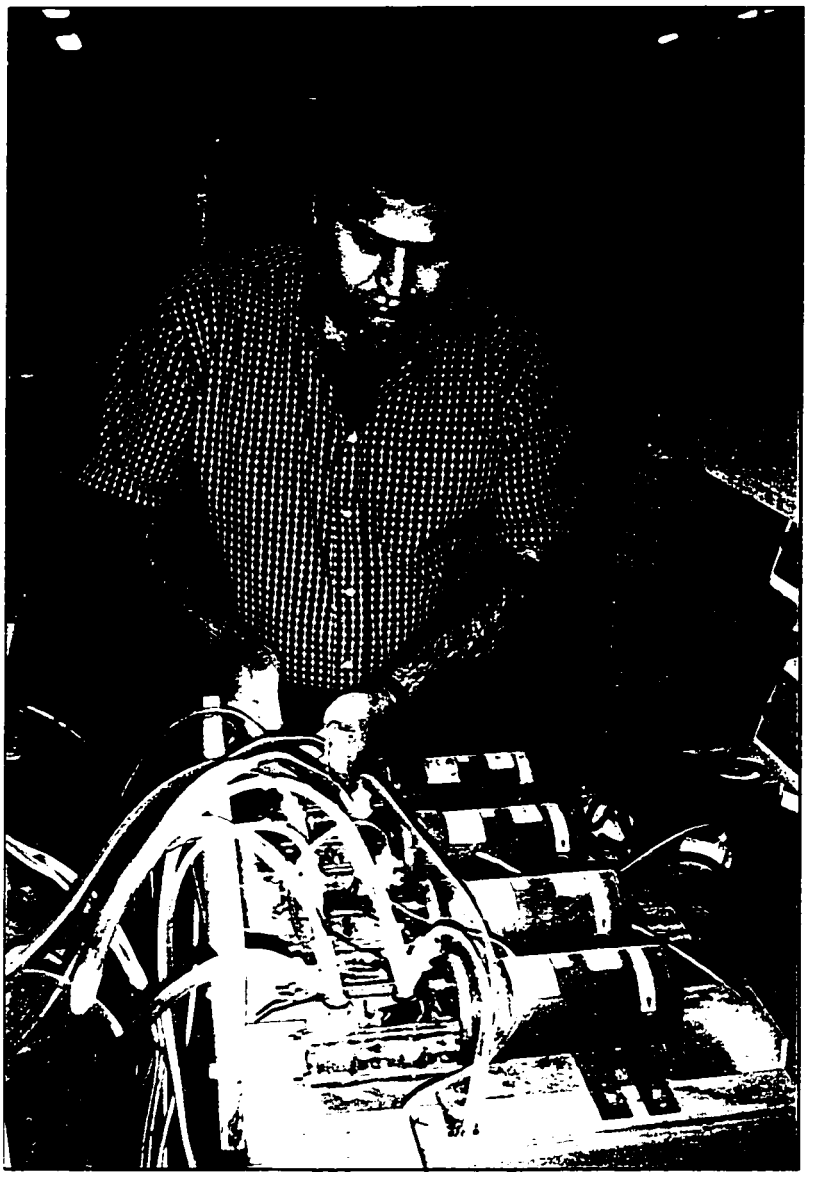

Plate 5.3 Pumps Apparatus Used for Sample Collection.

CHAPTER SIX

DATA ANALYSES, SIMULATIONS, AND DISCUSSIONS

6.1 INTRODUCTION

Unsteady flow and water quality models have the reputation of being difficult to apply. It is critical that proper initial and boundary conditions are established, or models will not execute. In addition, modifications to existing data sets may be introduced. A critical task in the application of hydrodynamic models is the determination of the roughness parameter in the friction slope terms of the momentum equations. Manning's n is adjusted to reproduce historical observations or measured values. However, in the absence of necessary data, Manning's n can be approximated. Similarly, an important task in water quality and dispersion modeling is determining properly the dispersion coefficients. The adjustment process is referred to as calibration. Calibration may be either a trial-error process or an automatic iteration procedure.

In general, the mathematical model should be checked if it adheres with the conditions of the problem it is simulating. It is important to build a model that gives good and useful outputs. An excellent method to verify the output of a mathematical model is to run it against

data obtained from a physically scaled model of the prototype. In a modeling exercise consideration is not only given to the problem to solve, but also to the inherent assumptions and the errors resulting from the numerical approximations. In the present study, the newly developed model, CHAT, is checked using experimentally measured data in a compound channel at the Hydraulics Laboratory, University of Ottawa.

6.2 INPUT DATA REQUIREMENTS

6.2.1 GRID SIZE AND TIME STEP

In this current application, the bathymetry is modeled in a grid. Since a FD approximation is used to solve the PDEs on a grid it is important to select a proper computational grid size. The FD approximation requires a small grid size and consequently a large storage memory. The selection of a grid size (or distance step) in both the x- and y-directions affects the dimensions of the computational arrays. This selection is subject to many restraints including accuracy. In general, accuracy is directly related to grid size. In a FD approximation, a large grid size would imply inaccurate discretization of the flow field and consequently a higher tendency for inaccurate prediction or calculation of parameters especially in the vicinity of the main channel-flood plain zone(s). However, a smaller grid size may lead to a considerable increase in the computational effort although it improves accuracy. In addition to accuracy, convergence to a proper solution and the dispersive properties of the computational method used in the discretization are directly related to the ratio of the time step to the spatial grid size. Thus, a small grid size means a small time step. Although this may increase the computational effort, it improves the accuracy and the solution properties. It is always important to maintain a compromise between numerical accuracy and run time. The grid size was varied in order to reach a proper value beyond which no significant improvement is noticed in the simulation exercise. In this instance, a grid size of 15 cm was selected in the simulation exercise in both the x- and y-directions,($\Delta x = \Delta y$). Thus, the computational arrays are 70 x 12 points. Two arrays were used for the two velocity

components and three arrays for the water levels, since three time levels are involved. One array is used for the depth data and one for the Manning or Chezy coefficients. The depth or elevation data for each point in the field were interpolated from adjacent data if not directly available at that point. Values of the water levels are computed on a Cartesian grid with same distances in the x- and y-directions. Data, including the geometry of the channel, is required before discretizing the channel into grids. In addition to accuracy and convergence, selecting a smaller distance step results in more computations to be performed on grid points.

Although the grid size plays an important role in the simulation exercise, the orientation of the grid system is also critical. Thus, it is advisable to have the grid directed and oriented parallel to the major dimensional lengths of the channel. Land-water boundaries were taken through lines in which the local velocity components were set to zero. Figure 6.1 shows the computational grid.

Different time steps were tried in the simulation exercise and since the dispersive properties of the computational method are related to the ratio of the time step to the spatial grid size, a small time step of 5 seconds was selected. Given the alternating implicit-explicit nature of the numerical solution scheme, time steps were selected based on accuracy as well as stability. The same time step and grid size were used in the solution of the continuity and momentum equations as well as the advection-diffusion equation.

6.2.2 INITIAL AND BOUNDARY CONDITIONS

CHAT simulates problems that are unsteady in nature and therefore, it is important to select proper initial and boundary conditions. Since computations are done on a grid, and given the nature of the PDE, then time and/or space variations of velocity, water level, and concentrations were needed at open boundary points of the grid and supplied as boundary conditions (equations are second-order in the space coordinates). In addition, initial conditions had to be specified at every point in the grid. In solving the momentum equations the velocity at the open boundary appears in the advective term and thus, has to be specified

as input. These velocity values are used in the computation of water levels at grid points. However, in the experimental channel, the velocity gradients are small, which means that the advective terms at the open boundary can be eliminated or omitted from the computations. Nevertheless, longitudinal velocity values were still input as data at the open boundary.

In the modeling exercise, the water levels and concentration values are required as input at open boundary grid points. This gives rise to another problem. In general, time-varying values of water levels and concentrations are usually measured at several points that may not coincide with grid points at the open boundary. In this case, some boundary points do not have specified values of input. Consequently, information is inferred from available laboratory measurements and interpolating functions are introduced for that purpose. Depth data (or elevations) are input at each grid point within the laboratory as initial conditions. Land is assumed at a particular grid point if no depth value is inserted at that particular point. At the beginning of the computation, initial values of the constituent concentrations at each grid point are input. If these values are not given, a specified default value is used for each test run modeled.

In general, the equations of motion include a Coriolis parameter to account for the curvature and rotation of the earth. As a result, the water-level gradient should be specified at the open boundary. However, the Coriolis effect is small in a laboratory channel of several metres length and thus in this application water levels are not modified at the open boundary in this application.

6.2.3 CALIBRATION

Calibration of the hydraulic component of CHAT was performed by applying it to our experimental data sets. The frictional effects have been varied by changing Manning's n in the momentum equations and the diffusion coefficients in the advection-diffusion equation for several test runs, including test runs 7, 16, and 21. The calibrated model was then applied to

other experimental data in order to check its performance.

Although it is computationally faster and easier to utilize Chezy's coefficient to represent boundary roughness, Manning's n was used instead in the present application. A default value of 0.014 was specified at all grid points. However, after performing the calibration process, different values were input at selected grid points to reflect the applicability of the model input data to the physical domain it is representing. These values ranged between $0.012 < n < 0.018$.

Diffusion coefficients were then computed based on the velocity components using the following equations: $\epsilon_x = a_x u_* h$ and $\epsilon_y = a_y u_* h$, where a_x and a_y = coefficients to be calibrated or estimated. Djordjevic (1993) used values of $a_x = 6.00$ and $a_y = 0.20$ and obtained relatively good match between simulated and observed concentrations. Different formulations of the ϵ_x- and ϵ_y-equations have been proposed. These approaches have met with varying degrees of success in reducing the range of uncertainty in the variation of the mixing coefficients. In the current simulation exercise, the adopted values are $a_x = 5.93$ and $a_y = 0.23$. The calibrated value of the eddy viscosity constant is 0.23, based on test runs 7, 16, and 21, which is equal to the transverse mixing coefficient constant.

Finally, the calibrated model CHAT was run for other data sets to check the validity of the model calibration.

6.3 RESULTS

With regards to the experimental data, investigating the cross-stream variation of the measured longitudinal velocity shows that the velocity is high in the main channel and decreases across the flood plain until it reaches a minimum close to the edge wall of the flood plain, (figures 6.2 to 6.9). It is noticed that for small flood plain depths, there is a sharp discontinuity of velocity at the junction of the main channel and the flood plain, due to strong

LMT effects, (figure 6.5). However, as flood plain depth increases, the LMT effect gradually diminishes, resulting in a smoother transition of velocity from the deep section of the channel to the flood plain, (figure 6.2). The same phenomenon was also observed by Bhowmik and Demissie (1982) and Rajaratnam and Ahmadi (1979). As depth on the flood plain increases beyond ~35% of the main channel depth, mean flood plain velocities increase substantially. In these circumstances the average velocity in the flood plain zone is observed to approach a value close to the average velocity in the compound section. Accordingly, the flow can be considered effectively homogeneous throughout the entire cross-sectional area of flow. It should be noted, however, that the aforementioned 35% relative depth value is not universal but rather expected to vary from one reach to another, as the carrying capacity of flood plains depends upon the size, shape, width, depth, and nature of the flood plains and main channel. Figures 6.10 to 6.17 show the cross-stream variation of average panel discharge. Clearly, a large portion of the discharge is carried in the main channel, especially at low flood plain depths.

In practice, because of changing flow conditions, it is not always clear whether a flood plain zone acts as a storage reservoir or carries a significant portion of the flood flow. Moreover, the interaction between the fast moving flow in the main channel and the relatively slower flow of the flood plain is not thoroughly understood. It is likely impossible to develop a universal flood routing model capable of handling all practical situations. However, the choice of such a model would depend to a large extent on whether to account for the flood plain contribution to system conveyance or assume this zone to be just a storage area. The flood plain carrying capacity depends mainly on the flow conditions and parameters over the flood plain and the main channel. To test whether the flood plain and the main channel act as a single unit with uniform characteristics, analysis was performed based on the laboratory data set. In this instance, the channel cross-section was subdivided into several panels and the panel discharge was determined based on the *Stream-Gauging* procedure. Figure 6.18 shows the variation of the ratio of flood plain area (A_{fp}) to total cross-sectional area (A) with the ratio of the flood plain discharge (Q_{fp}) to total discharge (Q). If the characteristics of the

entire flow area had been uniform, then all the points should have plotted on a 45°-line. However, it is apparent that for low flood plain depths part of the flood plain area acts as *storage*. It is also clear from the same figure that the points converge towards the 45°-line as the area over the flood plain increases. Under these conditions the main channel and the flood plains can be treated as a *single* unit. Figure 6.19 shows the variation of the ratio of the main channel discharge (Q_m) to total discharge (Q) with the ratio of flood plain depth (d) to main channel depth (D).

For low flood plain depth ratios, figures 6.3, 6.5, 6.6, and 6.7 show that the velocity gradient is generally too steep, compared to that of higher flood plain depth ratios, especially in the vicinity of the junction between the main channel and flood plain. This indicates that there is significant transverse mixing, which in turn means that turbulence and especially the eddy viscosity are expected to be high. In general, the under-prediction of transverse mixing in regions with an abrupt change in depth is due to the fact that turbulence production at vertical submerged walls cannot be accounted for correctly.

Although the main assumption in developing a 2-D DA model is uniformity in flow properties along the vertical (depth-averaged), however, the aspect ratio is not very high. Thus, concentrations are not expected to be fully uniform vertically, but stratification would not be expected either. Consequently, a certain distance was allowed for vertical mixing to take place upstream of the sampling stations. Examining the cross-stream concentration variation with time, it can be concluded that proper mixing is generally not occurring across the transverse direction as shown in figures 6.20 to 6.32. High concentrations are noted at the first and second sampling stations (in the main channel) and rather low concentrations were observed at the other two sampling stations provided that injection was in the main channel. For run 23, injection occurs at tube 2 in the main channel at a distance of 16.1 cm from the bottom of the channel (depth = 31.67 cm). Clearly, figure 6.30 shows that proper mixing does not occur as the dye traveled downstream, except for some change in concentration occurring at sampler 3 and minor changes at sampler 4. In addition, as shown

in figure 6.32 for test run 26, injecting the dye tracer in the main channel at a distance of 25.75 cm below the water surface from injector 1, (depth = 30.26 cm) indicates that complete mixing is still not achieved. The upstream and downstream transverse concentration variations indicate that at samplers 3 and 4 a slight change occurred as the dye moved downstream. Consider test run 9, as figure 6.24 shows, introducing the dye using injector 4 over the flood plain did not change notably the concentration downstream especially in the main channel. For test run 15, injecting the dye with tube 3 at half the depth allowed the tracer to increase in concentration at sampler 3 and not at 1 and 4. Based on the test runs, changing the location of the injection point significantly affected the dispersion of the dye along and across the channel.

Examples of tracer movement across the channel are shown in plates 6.1 to 6.5. These plates confirm that mixing was not occurring properly especially across the junction separating the main channel and flood plain zone. Considerable transverse or lateral fluctuations were observed in that zone. Plate 6.3 shows how the dye is approaching the sampler and then departing from its collection zone. It is worth mentioning that the speeds of injection and withdrawal (collection) were adjusted to match the corresponding channel velocities in order to avoid any unwanted disturbances in the flow or transport field.

Dye concentrations were predicted using eqs. 5-3, 5-4 and 5-5 presented in chapter 5. These equations are usually applied for limited situations where many simplifying assumptions are involved. The predicted values of concentrations are very far from the measured and the model simulated values. Figures 6.33 to 6.37 compare the predicted and measured concentrations. Clearly, concentrations are over-estimated in the main channel and considerably under-predicted over the flood plain zone.

As far as the numerical simulations are concerned, the comparison between measured and predicted concentration curves by CHAT shows a good level of agreement in the general shape of the curves, peak concentrations and time to peak, (figure 6.38 to 6.41; and tables

6.1 to 6.4). Inspection of the simulated concentrations indicates that CHAT slightly over-estimated observed peak concentrations, (figures 6.38 to 6.41). Tables 6.1 to 6.4 show the result of statistical goodness-of-fit criteria for model simulations. The model simulations did not indicate any time delay or phase shift between the corresponding pollutographs. The observed and simulated concentrations have close times to peak.

Inspection of figure 6.42 shows that the time step variation has minimal effect on the stability of the numerical scheme used in the modeling exercise. This figure confirms that selection of the time step size depends on *accuracy* rather than *stability* in this alternating implicit-explicit technique. A 5-second time step was used in the simulation of the laboratory data. The relative errors did not considerably change when the time step was reduced to 33 % (5 seconds). Therefore, as table 6.5 indicates, when applying our *selected* numerical scheme, changing the time step did not significantly improve the simulations. On the other hand, the computer run time was shortened by an increase in the time step.

The problem of numerical stability was also investigated in the simulation exercise. It has been established elsewhere that selection of the time step in an implicit formulation is based on *accuracy* rather than *stability*, (Fread, 1987). Figure 6.42 shows that instability did not occur around the peak of the concentration graph. Also, there is no phase shift or time delay between the observed and simulated values.

6.4 STATISTICAL CRITERIA

In general, no single statistical *goodness-of-fit* criterion is sufficient to adequately assess the measure of fit between simulated and observed hydrographs. Different *goodness-of-fit* criteria are weighted in favor of different hydrograph components (volumes, peak flows, maximum depths ...etc). Thus, no single criterion is universally the best and the criteria ultimately selected should depend on the objective of the modeling exercise. The criteria selected to assess the *goodness-of-fit* of the simulated hydrographs are presented in Appendix

C. In this study the following criteria were applied: graphical techniques, sum of squares (SS), Nash and Sutcliffe (N & S), root mean square error (RMSE), standard error of estimate (SEE), reduced error of estimate (REE), proportional error of estimate (PEE), and total absolute relative error (TARE). Except for N & S, which should approach 1.0 for better simulations, the main goal is to minimize all of the above objective functions, (tables 6.1 to 6.5). Tables 6.1 to 6.5 show that CHAT-simulated results produced the lowest objective functions. Furthermore, the percent error at peak concentration was relatively low.

Table 6.1 Statistical Goodness-of-Fit Criteria for Model Evaluation, (Run #15).

	SAMPLER 1			SAMPLER 4		
	Observed	CHAT-Simulated	Closed-Form	Observed	CHAT-Simulated	Closed-Form
C_p (mg/l) (% Error)	1.870 (0.00)	1.580 (-15.51)	2.103 (+12.40)	2.590 (0.00)	2.900 (+11.96)	0.160 (-93.80)
T_p (min) (delay)	1.500 (0x)	1.500 (0x)	7.500 (5x)	2.500 (0x)	2.500 (0x)	7.500 (3x)
Graphical	N/A	Good	Bad	N/A	Good	Bad
SS	N/A	0.325	21.411	N/A	2.093	18.457
N & S	N/A	0.926	-3.875	N/A	0.755	-1.162
RMSE	N/A	0.131	1.062	N/A	0.332	0.986
SEE	N/A	0.138	1.122	N/A	0.351	1.042
REE	N/A	0.272	2.208	N/A	0.495	1.470
PEE	N/A	0.162	1.312	N/A	0.327	0.972
TARE	N/A	2.506	147.484	N/A	106.919	34.179

Table 6.2 Statistical Goodness-of-Fit Criteria for Model Evaluation, (Run #20).

	SAMPLER 1			SAMPLER 2		
	Observed	CHAT-Simulated	Closed-Form	Observed	CHAT-Simulated	Closed-Form
C_p (mg/l) (% Error)	6.034 (0.00)	6.936 (+14.94)	9.740 (+61.40)	6.970 (0.00)	8.440 (+17.41)	1.738 (-75.07)
T_p (min) (Delay)	2.500 (0x)	2.500 (0x)	0.500 (0.2x)	2.000 (0x)	1.500 (0.66x)	7.400 (3.7x)
Graphical	N/A	Good	Bad	N/A	Good	Bad
SS	N/A	7.557	360.978	N/A	8.975	320.993
N & S	N/A	0.946	-1.571	N/A	0.944	-1.004
RMSE	N/A	0.615	4.248	N/A	0.670	4.006
SEE	N/A	0.648	4.478	N/A	0.706	4.223
REE	N/A	0.232	1.603	N/A	0.237	1.415
PEE	N/A	0.125	0.864	N/A	0.129	0.769
TARE	N/A	12.046	3057.285	N/A	2.164	45.083

Table 6.3 Statistical Goodness-of-Fit Criteria for Model Evaluation, (Run #21).

	SAMPLER 1			SAMPLER 4		
	Observed	CHAT-Simulated	Closed-Form	Observed	CHAT-Simulated	Closed-Form
C_p (mg/l) (% Error)	1.772 (0.00)	1.900 (+6.74)	1.793 (+1.10)	0.124 (0.00)	0.110 (+11.29)	0.002 (-98.39)
T_p (min) (Delay)	2.000 (0x)	2.000 (0x)	6.400 (3.2x)	3.000 (0x)	3.000 (0x)	6.400 (2.1x)
Graphical	N/A	Good	Bad	N/A	Good	Bad
SS	N/A	0.935	8.445	N/A	0.008	0.055
N & S	N/A	0.849	-0.361	N/A	0.655	-1.321
RMSE	N/A	0.222	0.667	N/A	0.021	0.054
SEE	N/A	0.234	0.705	N/A	0.022	0.057
REE	N/A	0.388	1.167	N/A	0.587	1.523
PEE	N/A	0.231	0.694	N/A	0.381	0.988
TARE	N/A	3.750	78.589	N/A	3.719	12.697

Table 6.4 Statistical Goodness-of-Fit Criteria for Model Evaluation, (Run #26).

	SAMPLER 1			SAMPLER 2		
	Observed	CHAT-Simulated	Closed-Form	Observed	CHAT-Simulated	Closed-Form
C_p (mg/l) (% Error)	5.518 (0.00)	5.073 (-8.06)	6.190 (+12.18)	1.984 (0.00)	1.945 (-1.96)	5.272 (+165.72)
T_p (min) (Delay)	4.500 (0x)	4.500 (0x)	6.500 (1.44x)	1.500 (0x)	1.500 (0x)	6.500 (4.3x)
Graphical	N/A	Good	Bad	N/A	Good	Bad
SS	N/A	13.723	55.908	N/A	2.427	133.599
N & S	N/A	0.751	-0.014	N/A	0.522	-25.321
RMSE	N/A	0.899	1.814	N/A	0.378	2.803
SEE	N/A	0.957	1.931	N/A	0.402	2.984
REE	N/A	0.499	1.007	N/A	0.691	5.131
PEE	N/A	0.249	0.503	N/A	0.319	2.368
TARE	N/A	10.176	54.772	N/A	8.659	63.7641

Table 6.5 Goodness-of-Fit Criteria for Effect of Time Step Variation, (Run # 26).

Criterion	Observed	CHAT-Simulated $\Delta t = 5$ sec.	CHAT-Simulated $\Delta t = 15$ sec.	Closed-Form Solution
C_p (mg/l) (% Error)	5.52 (0.00)	5.02 (-9.06)	5.07 (-8.15)	6.38 (+15.58)
T_p (min) (Delay)	4.50 (0x)	4.50 (0x)	4.50 (0x)	6.50 (1.44x)
Graphical (Relative)	N/A	Best	Better	Good
SS	N/A	11.89	13.79	57.90
N & S	N/A	0.78	0.75	0.05
RMSE	N/A	0.84	0.90	1.85
SEE	N/A	0.89	0.96	1.96
REE	N/A	0.46	0.50	1.02
PEE	N/A	0.23	0.25	0.51
TARE	N/A	9.78	10.18	14.69

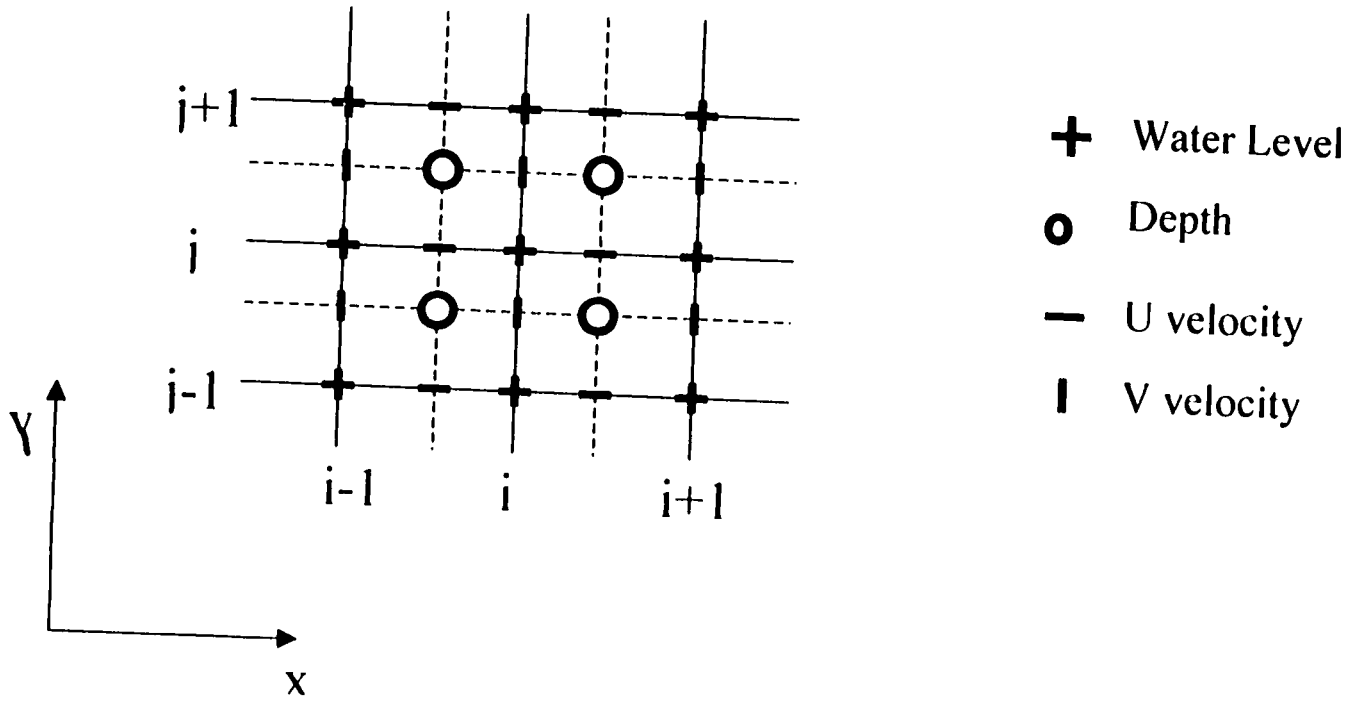

Figure 6.1 Definition Sketch of the Computational Grid.

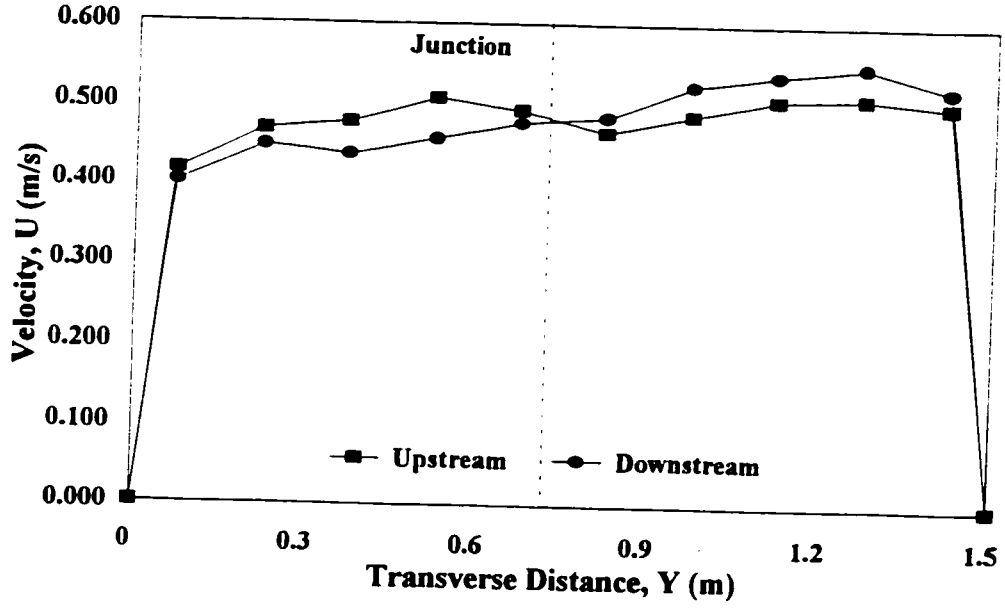

Figure 6.2 Cross-Stream Variation of Longitudinal Velocity, (Run # 1).

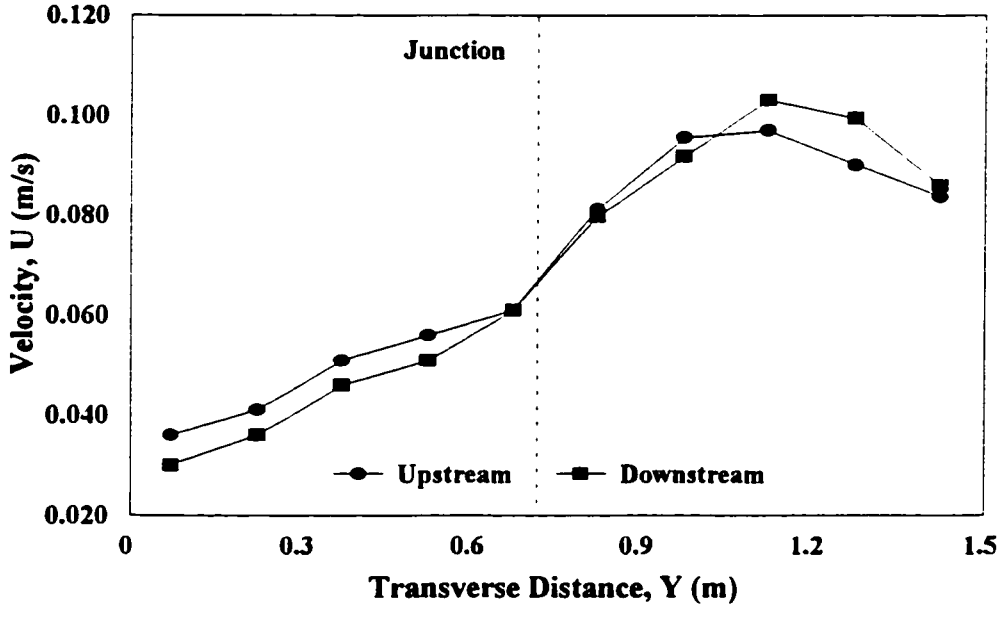

Figure 6.3 Cross-Stream Variation of Longitudinal Velocity, (Run # 4).

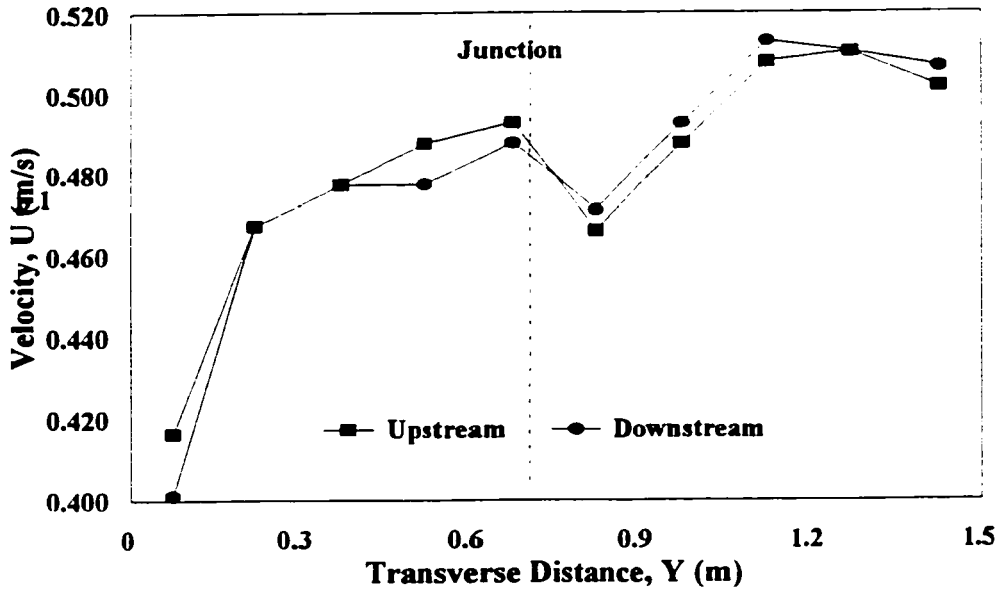

Figure 6.4 Cross-Stream Variation of Longitudinal Velocity, (Run # 10).

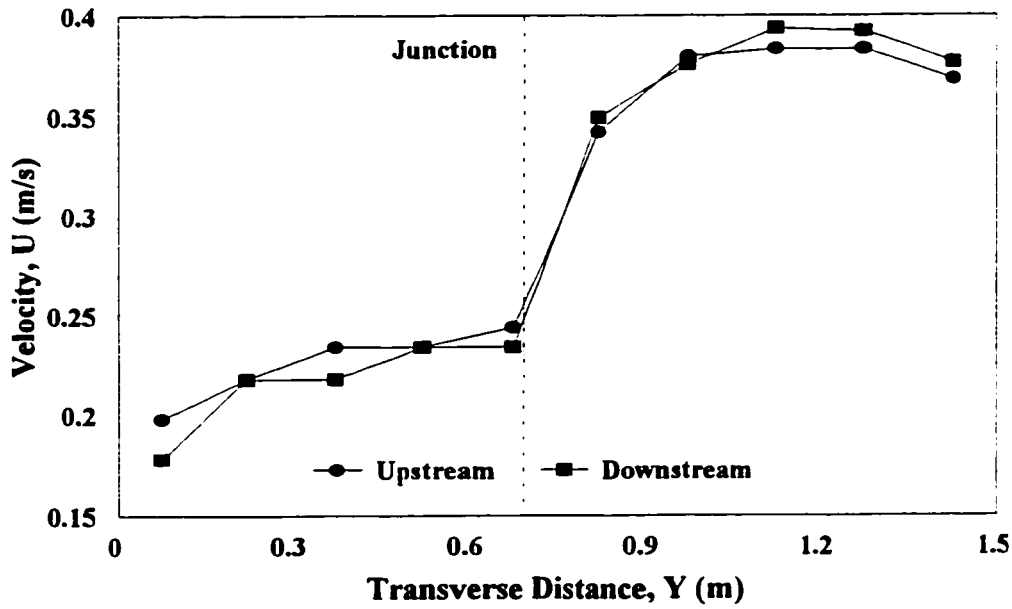

Figure 6.5 Cross-Stream Variation of Longitudinal Velocity, (Run # 12).

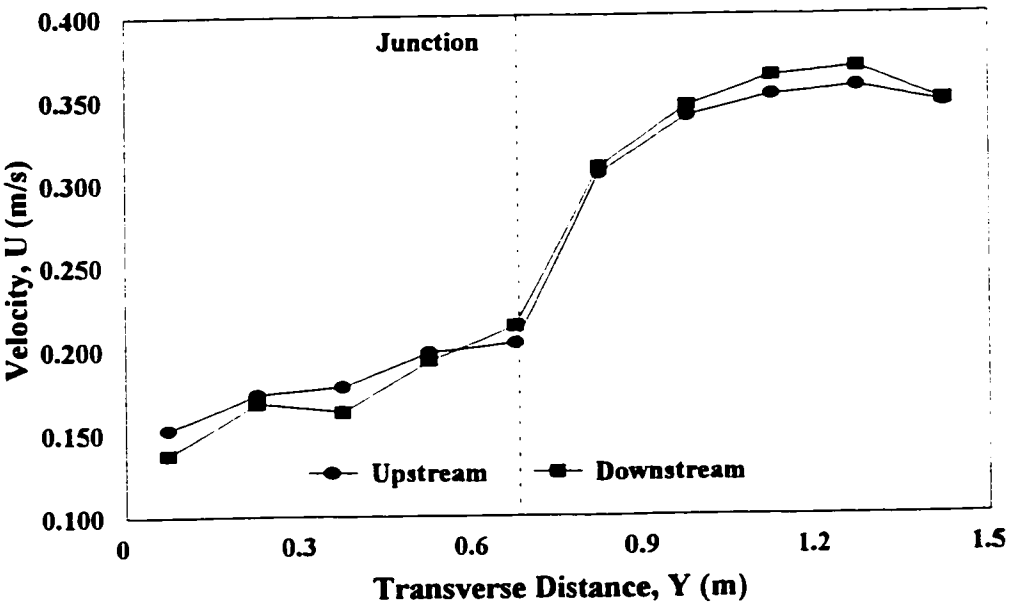

Figure 6.6 Cross-Stream Variation of Longitudinal Velocity, (Run # 15).

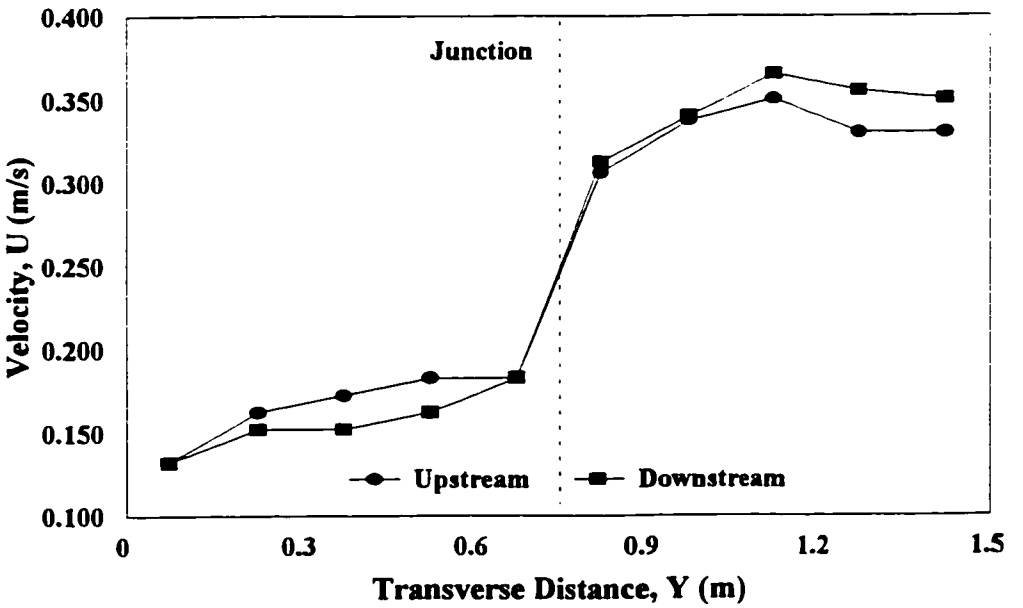

Figure 6.7 Cross-Stream Variation of Longitudinal Velocity, (Run # 20).

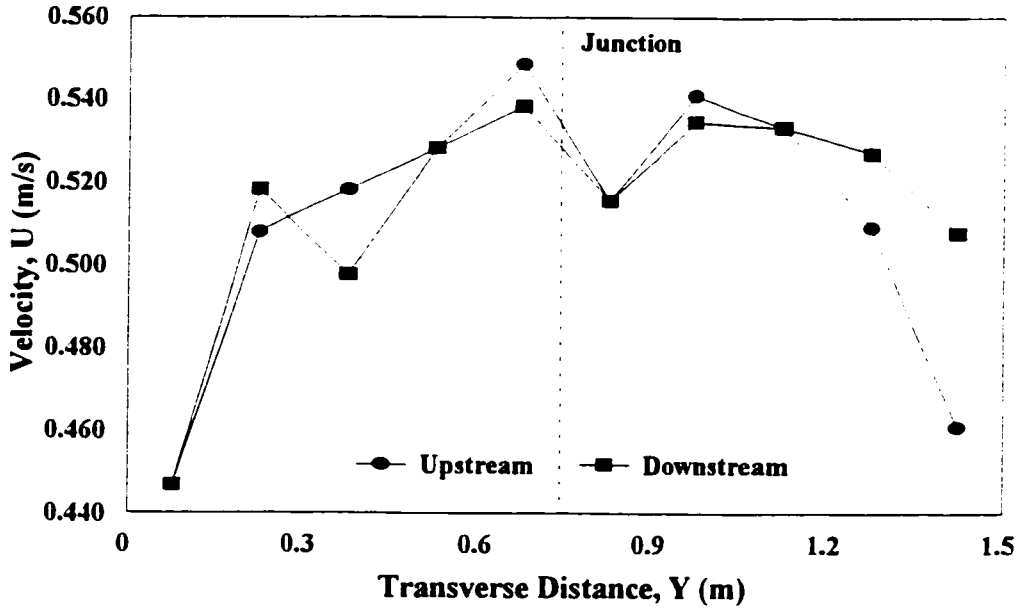

Figure 6.8 Cross-Stream Variation of Longitudinal Velocity, (Run # 23).

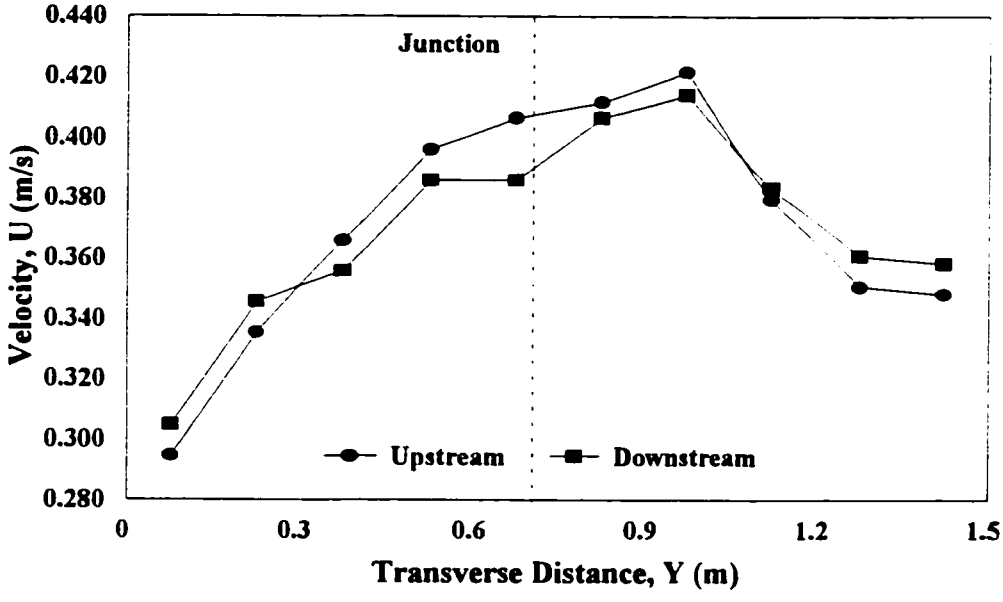

Figure 6.9 Cross-Stream Variation of Longitudinal Velocity, (Run # 26).

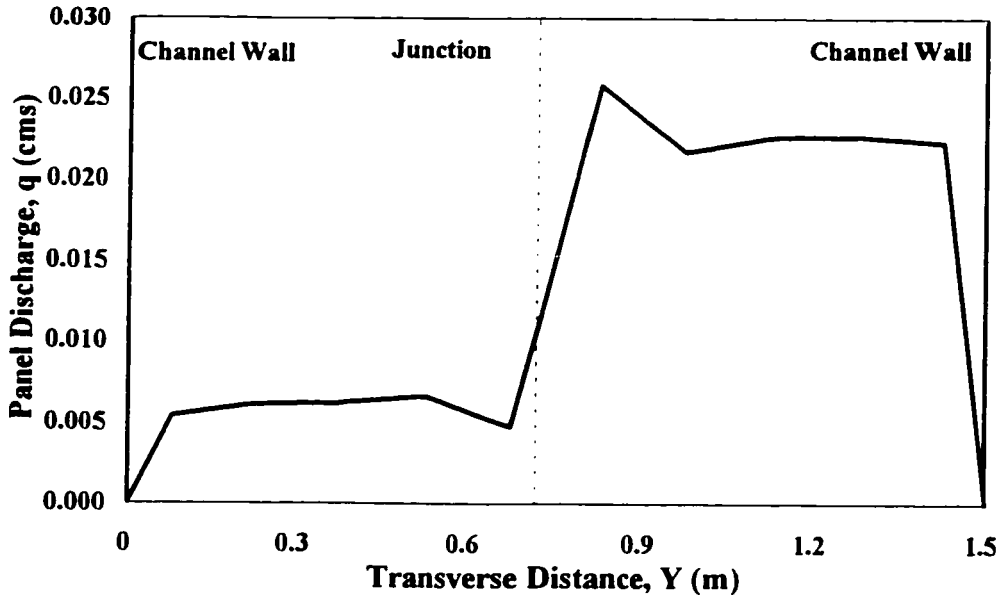

Figure 6.10 Cross-Stream Variation of Discharge, (Run # 1).

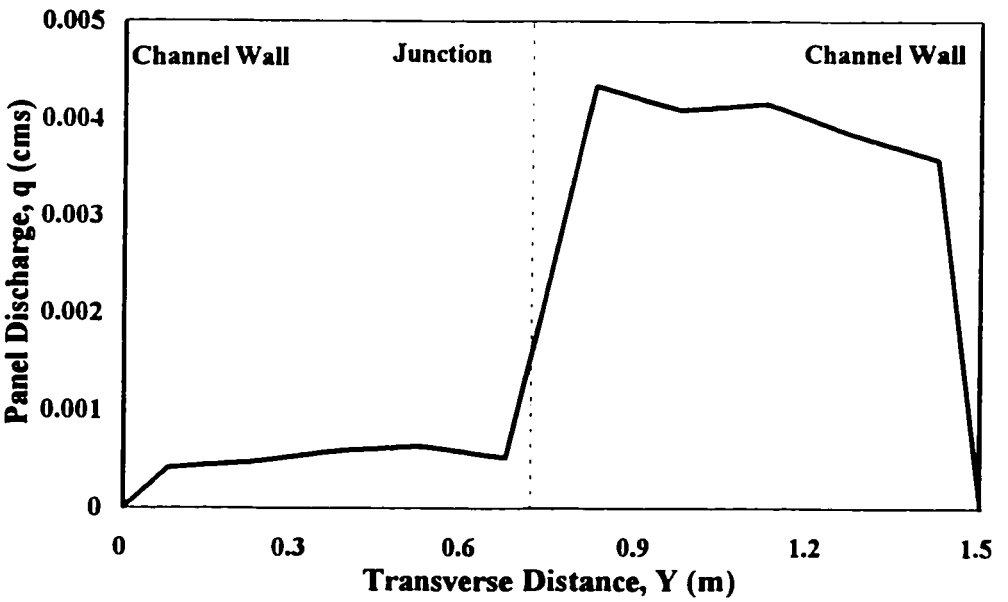

Figure 6.11 Cross-Stream Variation of Discharge, (Run # 4).

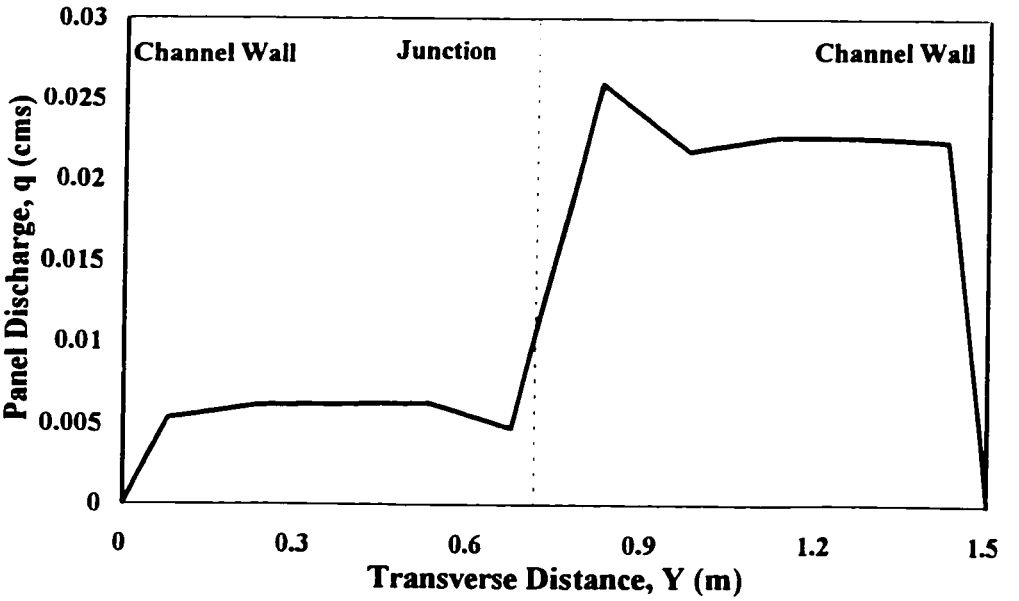

Figure 6.12 Cross-Stream Variation of Discharge, (Run # 10).

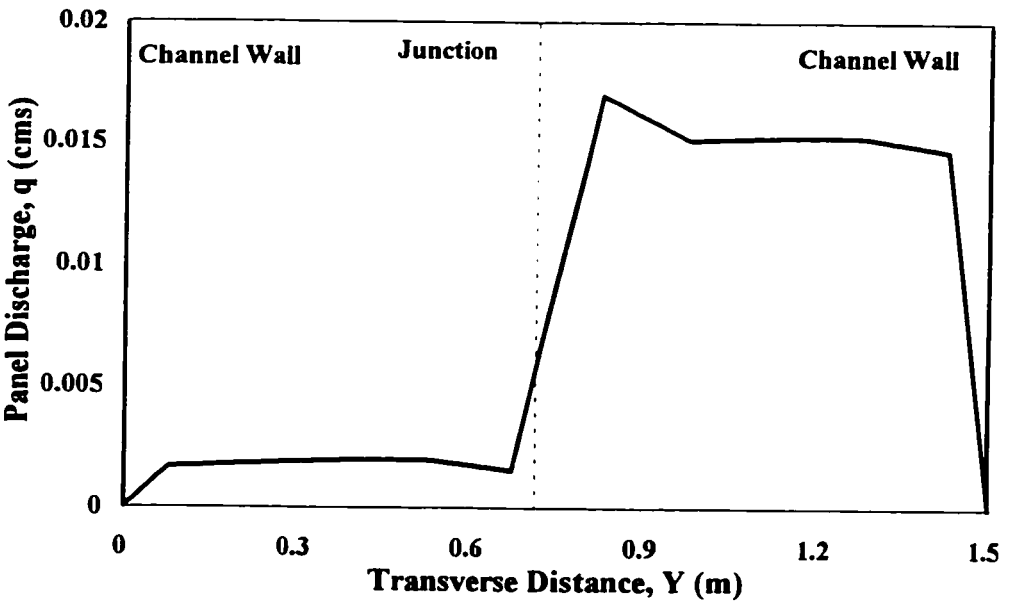

Figure 6.13 Cross-Stream Variation of Discharge, (Run # 12).

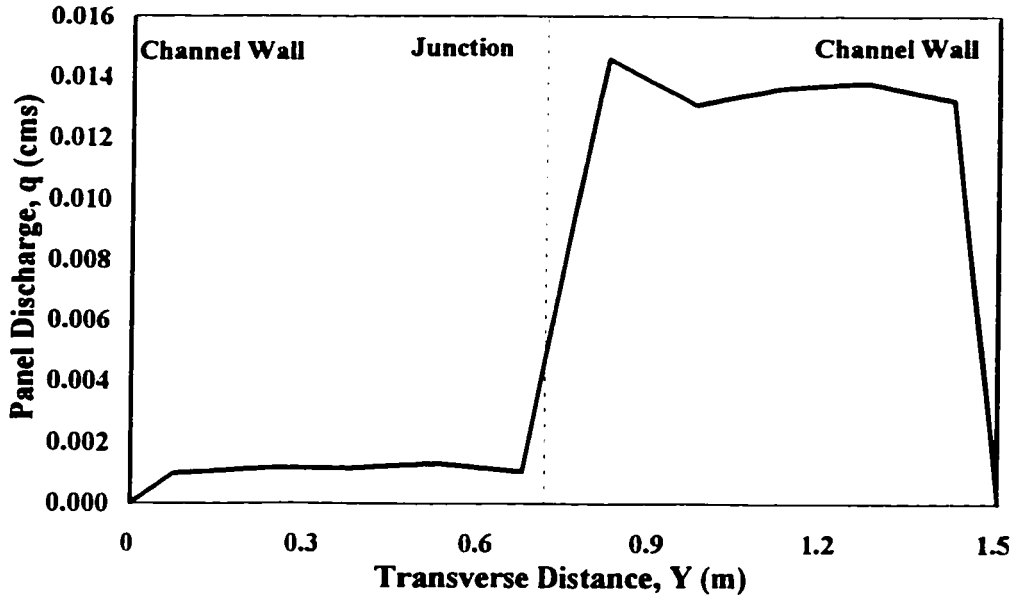

Figure 6.14 Cross-Stream Variation of Discharge, (Run # 15).

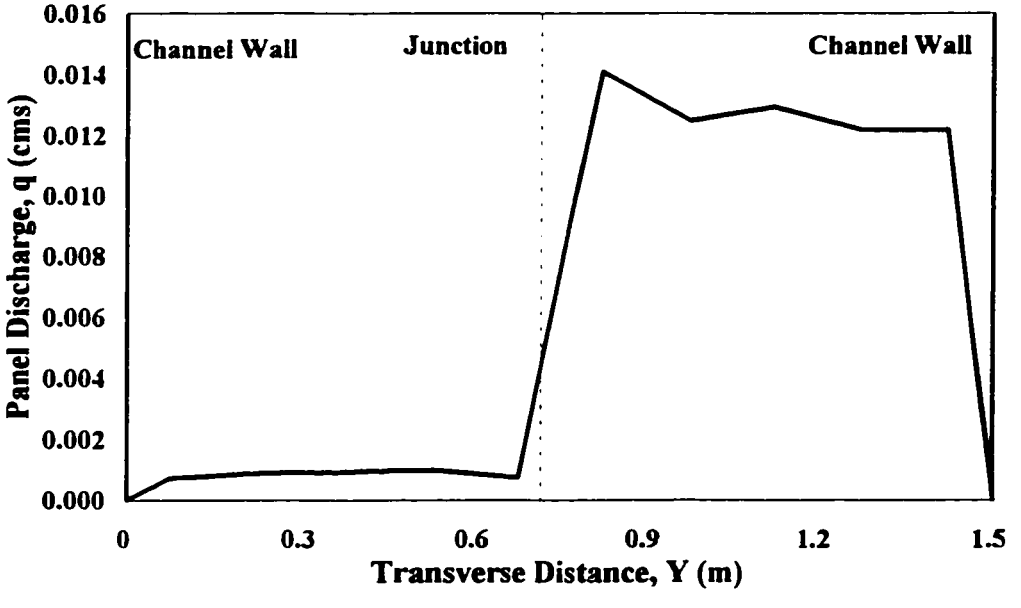

Figure 6.15 Cross-Stream Variation of Discharge, (Run # 20).

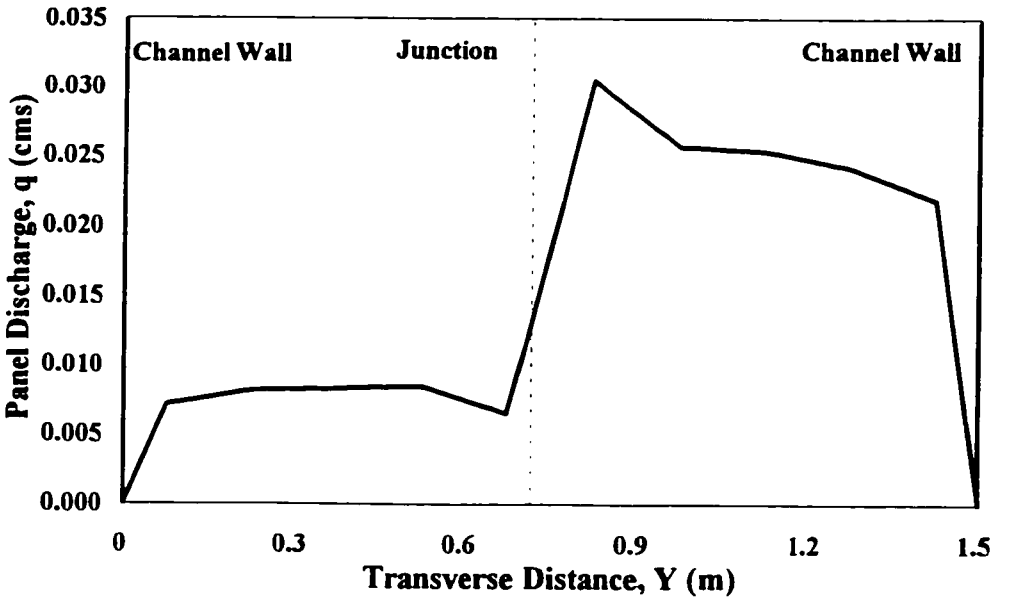

Figure 6.16 Cross-Stream Variation of Discharge, (Run # 23).

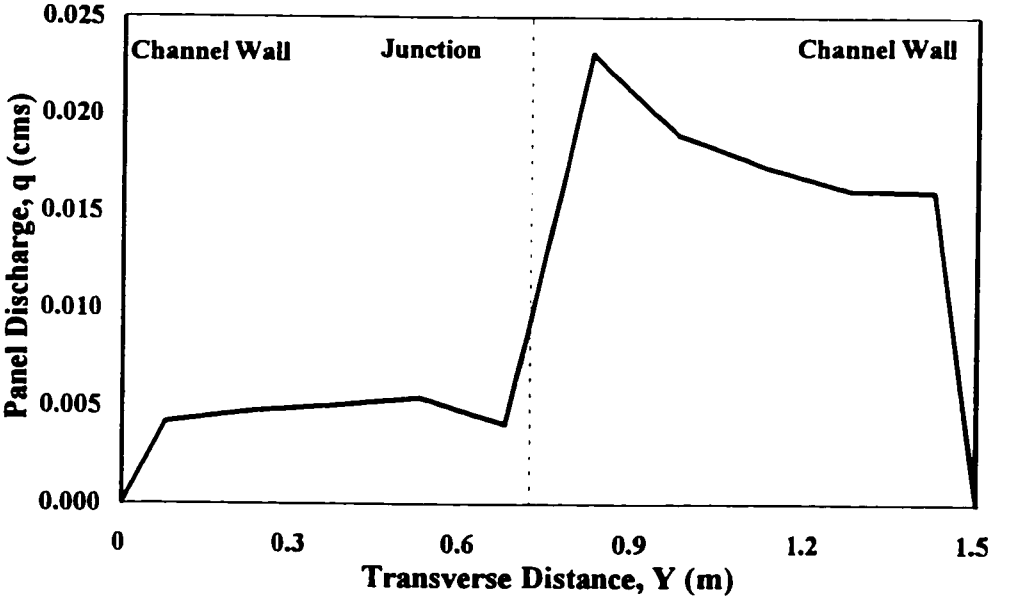

Figure 6.17 Cross-Stream Variation of Discharge, (Run # 26).

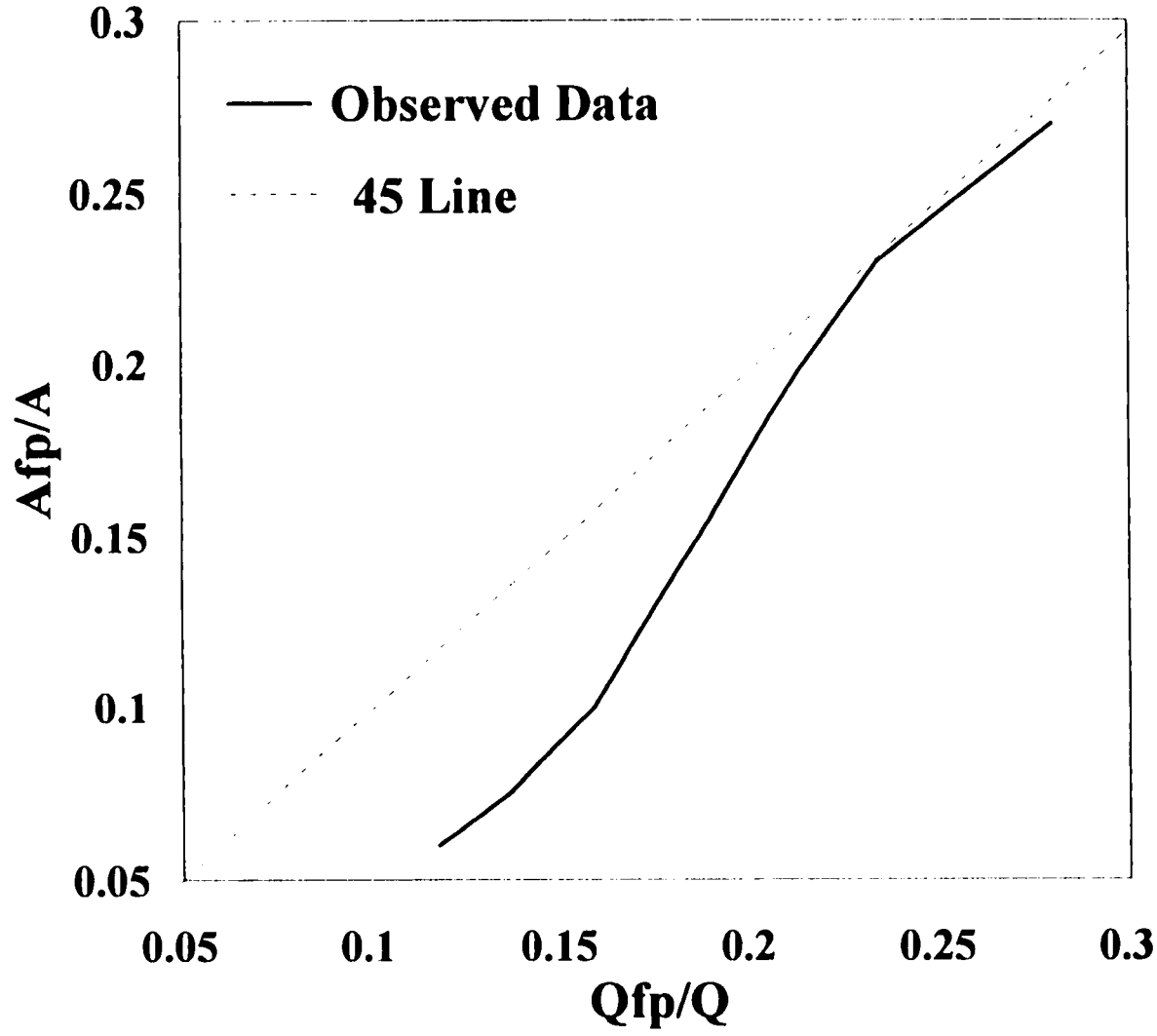

Figure 6.18 Variation of the Ratio of Flood Plain Area to Total Cross-Sectional Area with the Flood Plain Discharge to Total Discharge

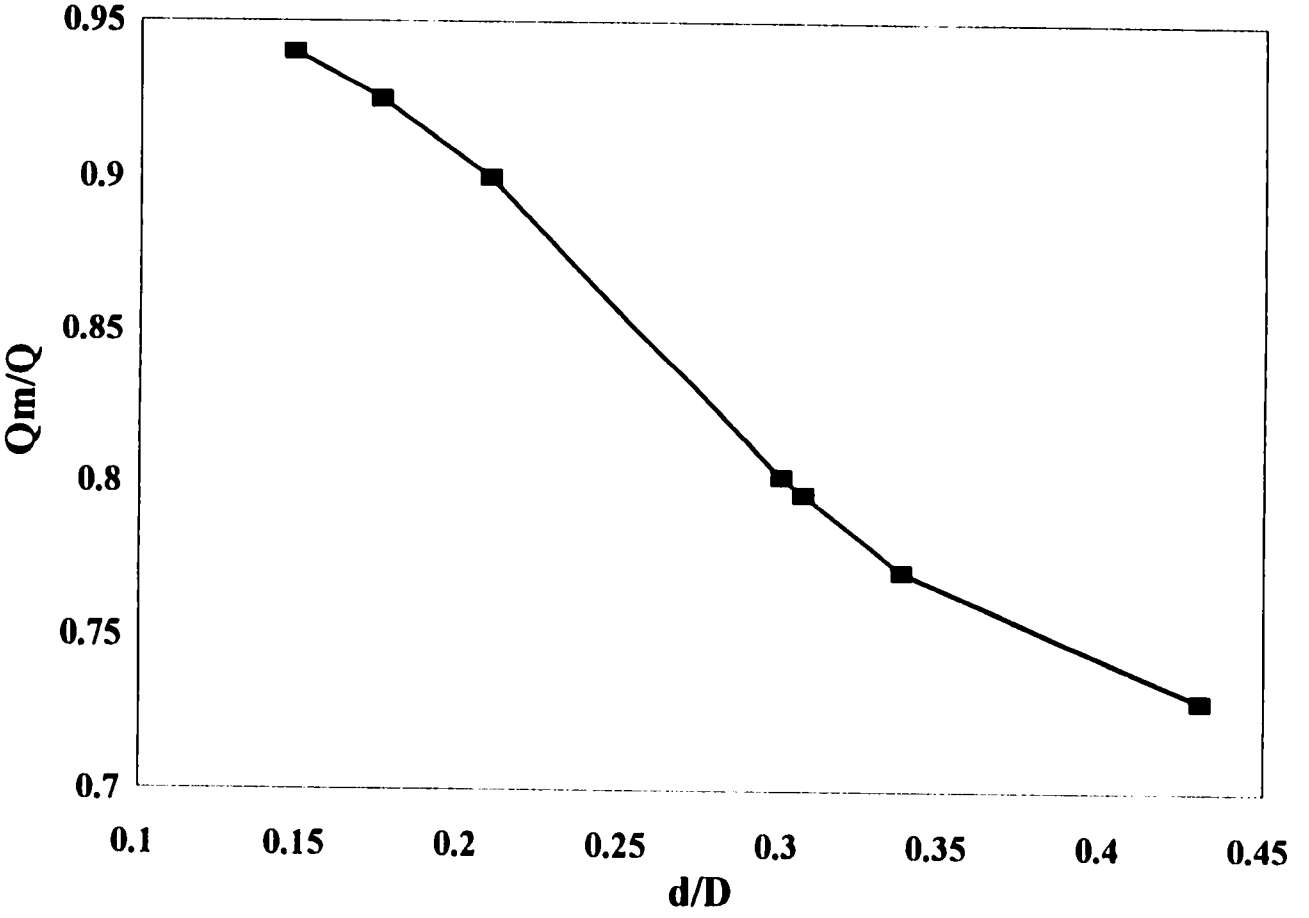

Figure 6.19 Variation of the Main Channel Discharge to Total Discharge Ratio with the Ratio of Flood Plain Depth to Main Channel Depth.

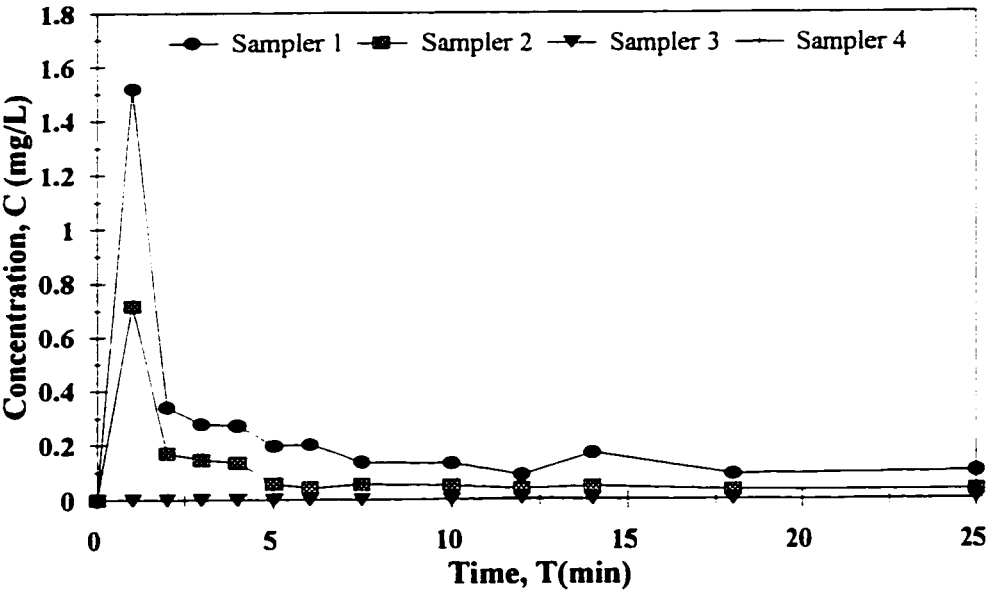

(a) Upstream

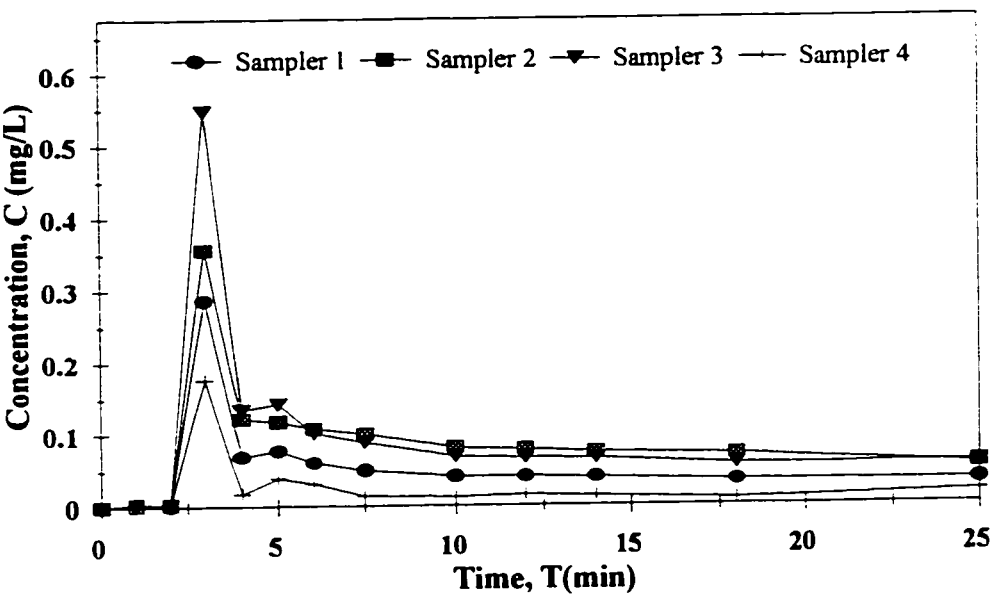

(b) Downstream

Figure 6.20 Cross-Stream Variation of Concentration with Time at Different Sampling Points, (Run # 1).

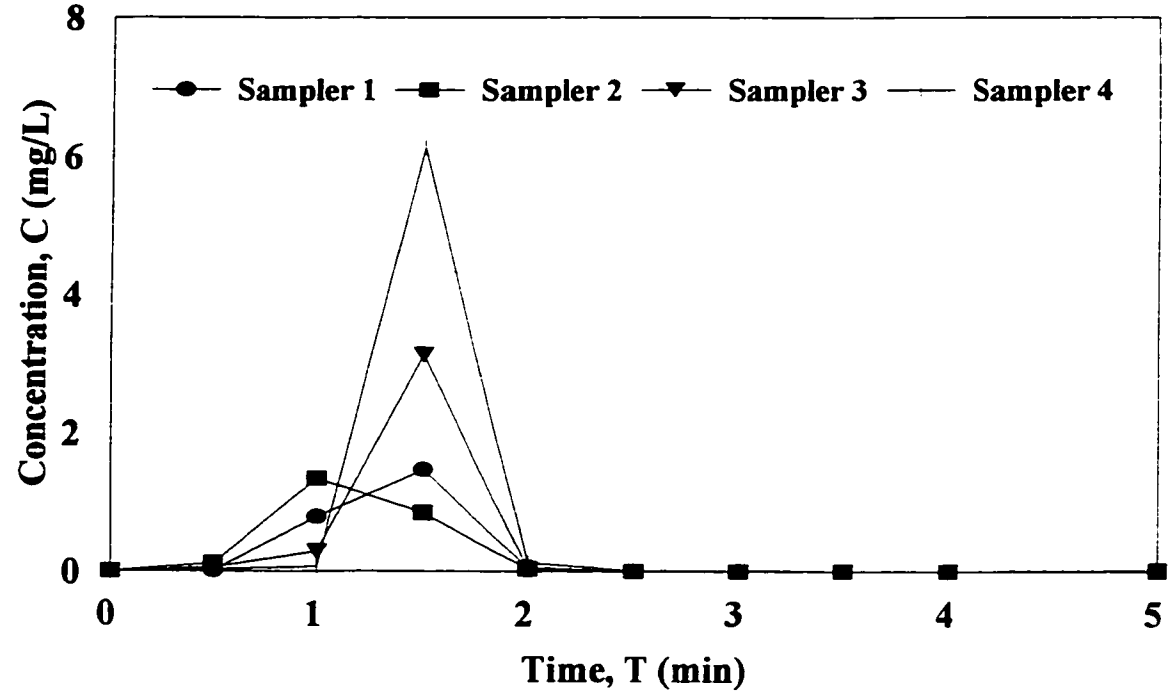

(a) Upstream

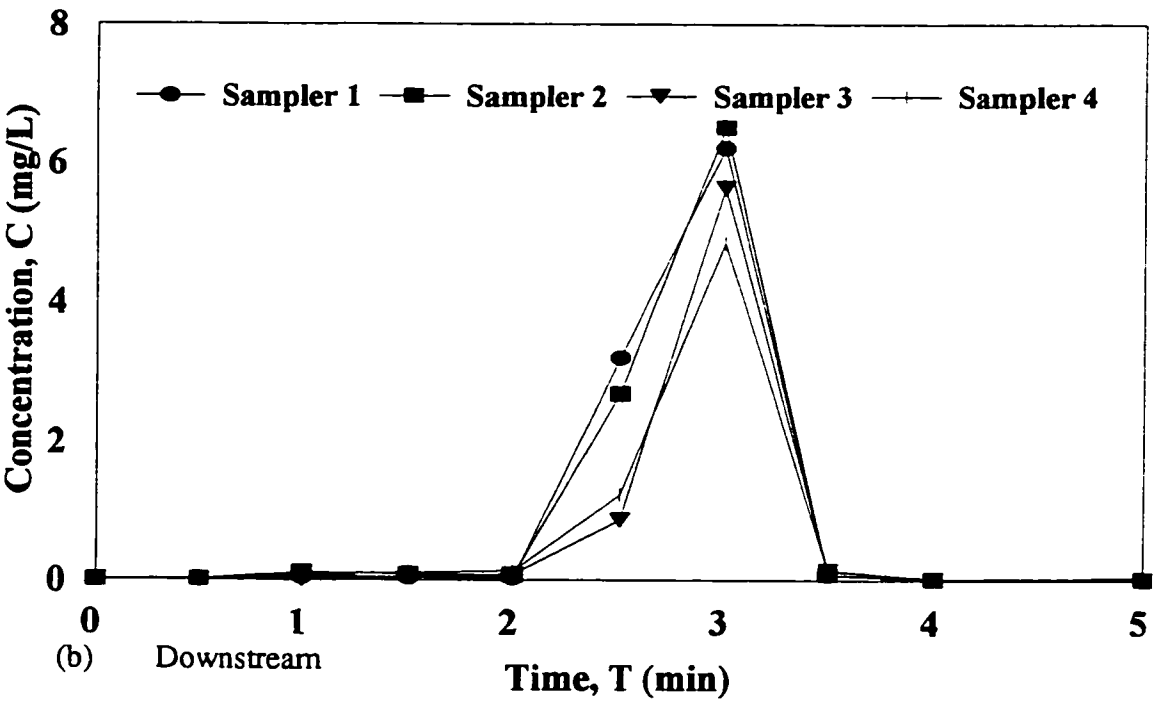

(b) Downstream

Figure 6.21 Cross-Stream Variation of Concentration with Time at Different Sampling Points, (Run # 2).

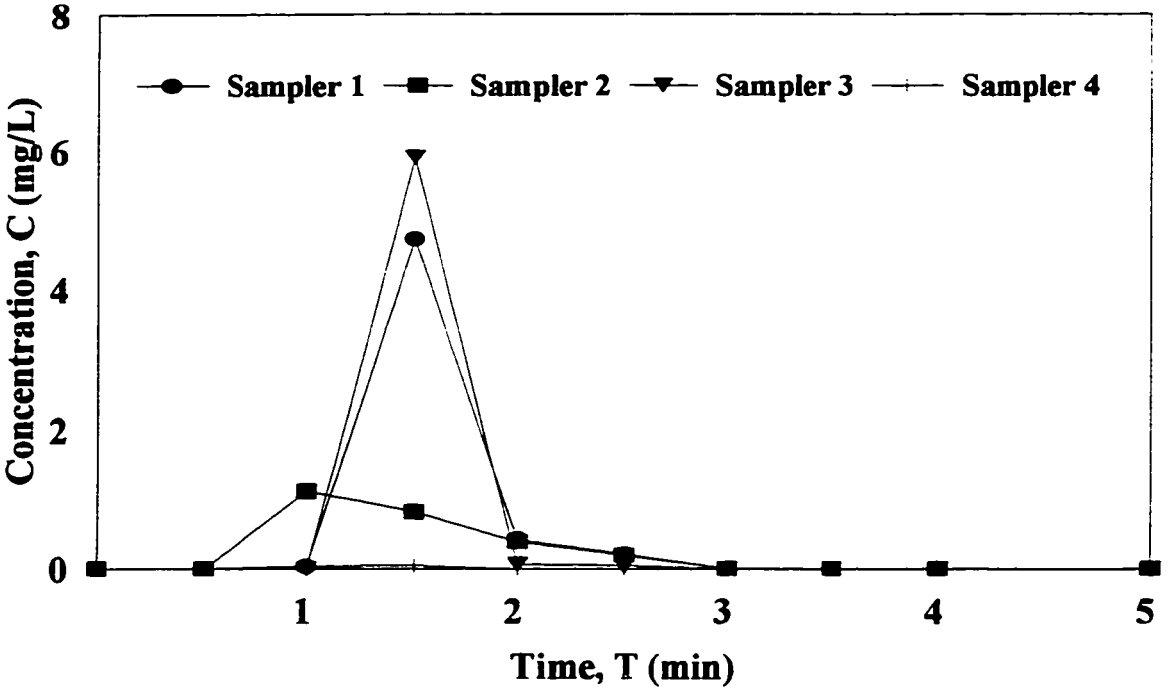

(a) Upstream

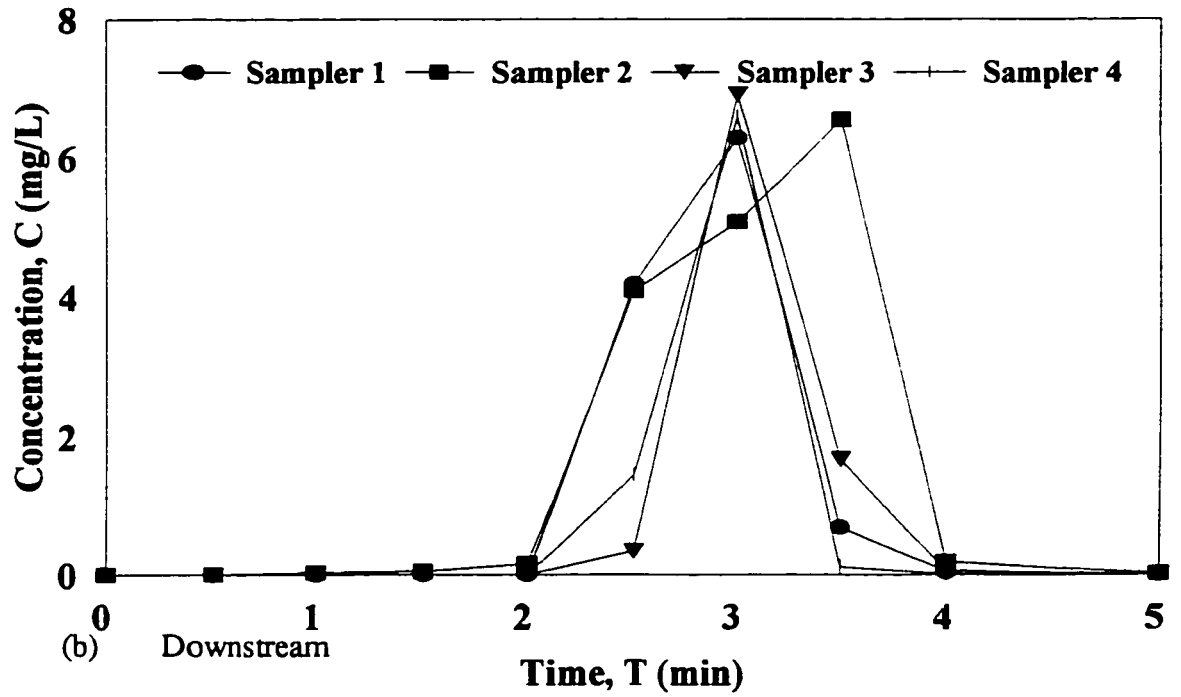

(b) Downstream

Figure 6.22 Cross-Stream Variation of Concentration with Time at Different Sampling Points, (Run # 3).

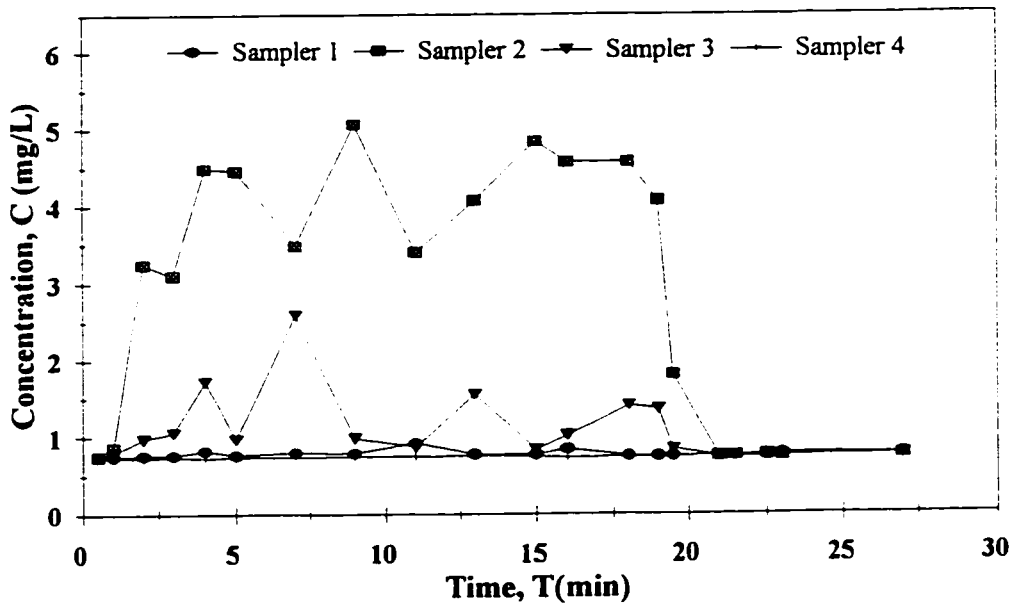

(a) Upstream

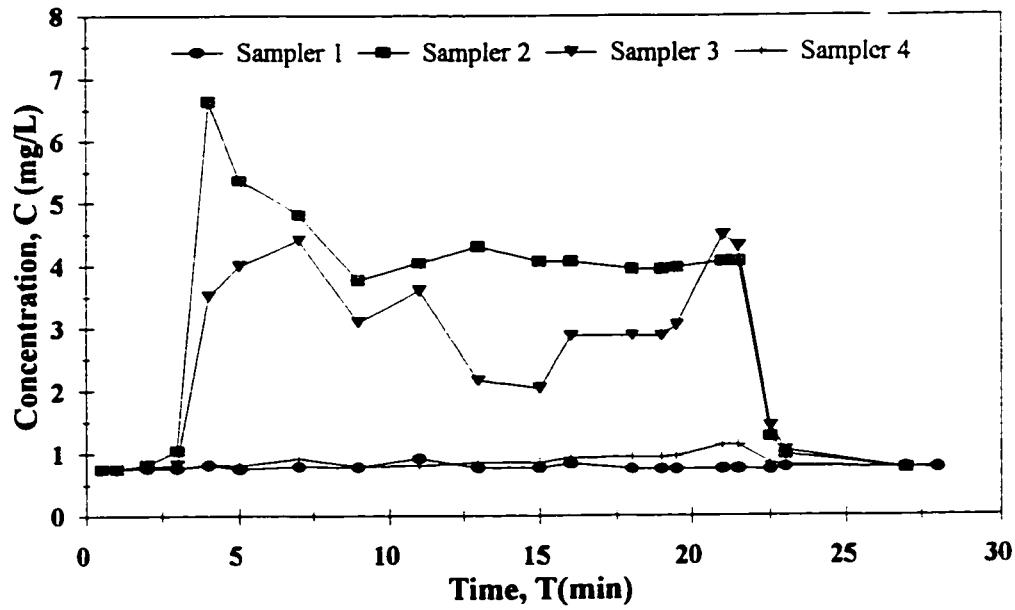

(b) Downstream

Figure 6.23 Cross-Stream Variation of Concentration with Time at Different Sampling Points, (Run # 5).

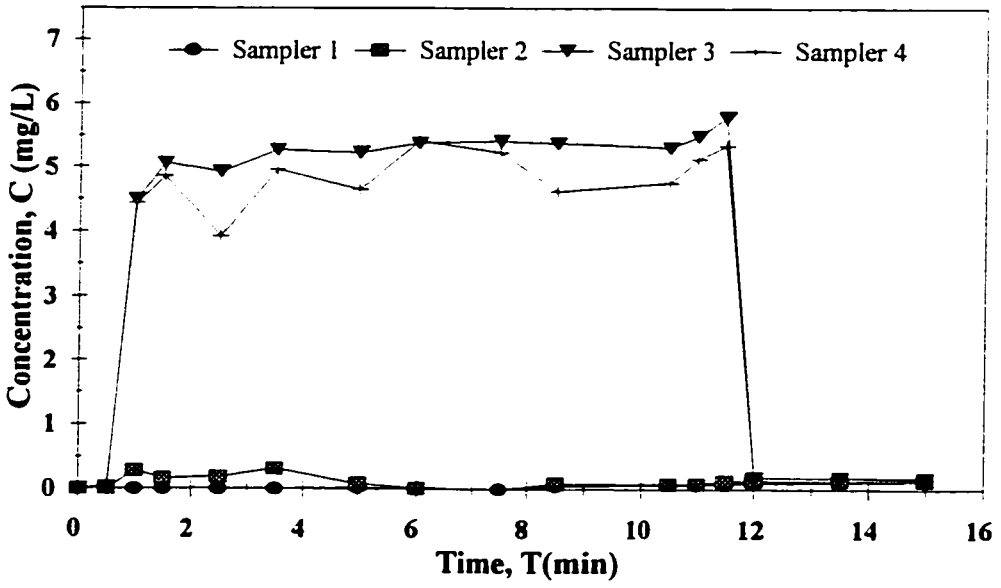

(a) Upstream

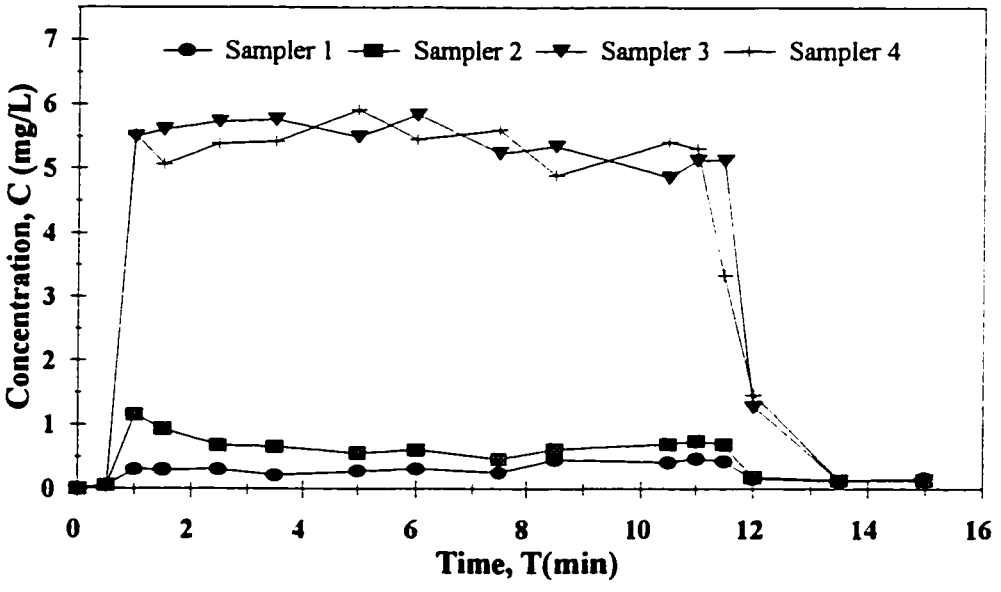

(b) Downstream

Figure 6.24 Cross-Stream Variation of Concentration with Time at Different Sampling Points, (Run # 9).

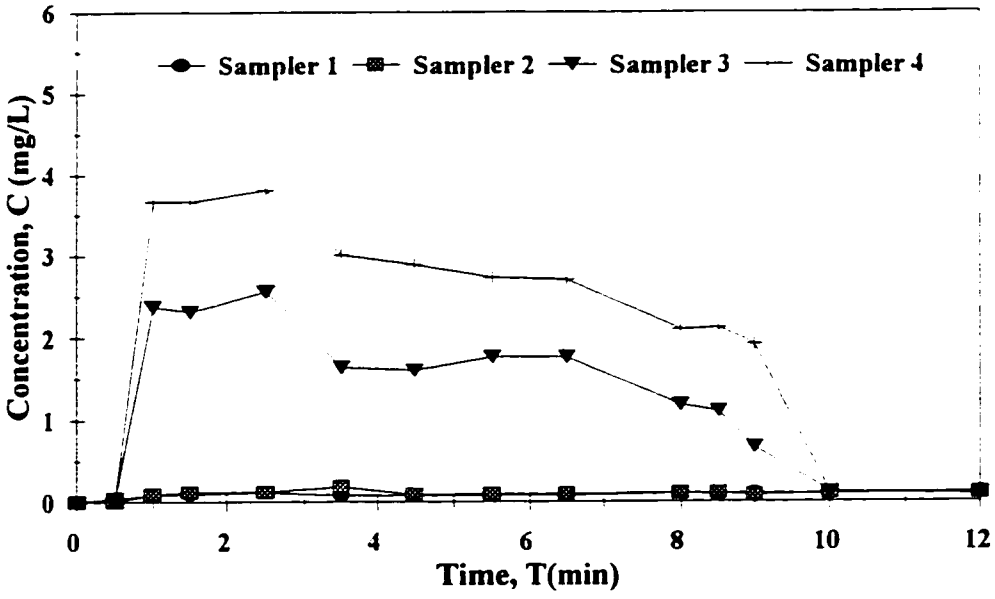

(a) Upstream

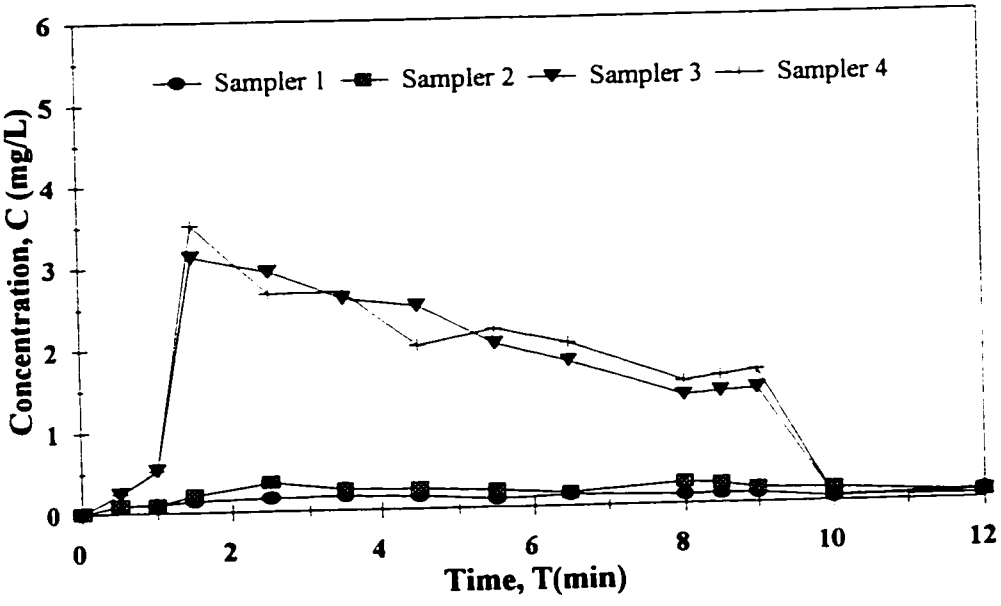

(b) Downstream

Figure 6.25 Cross-Stream Variation of Concentration with Time at Different Sampling Points, (Run # 10).

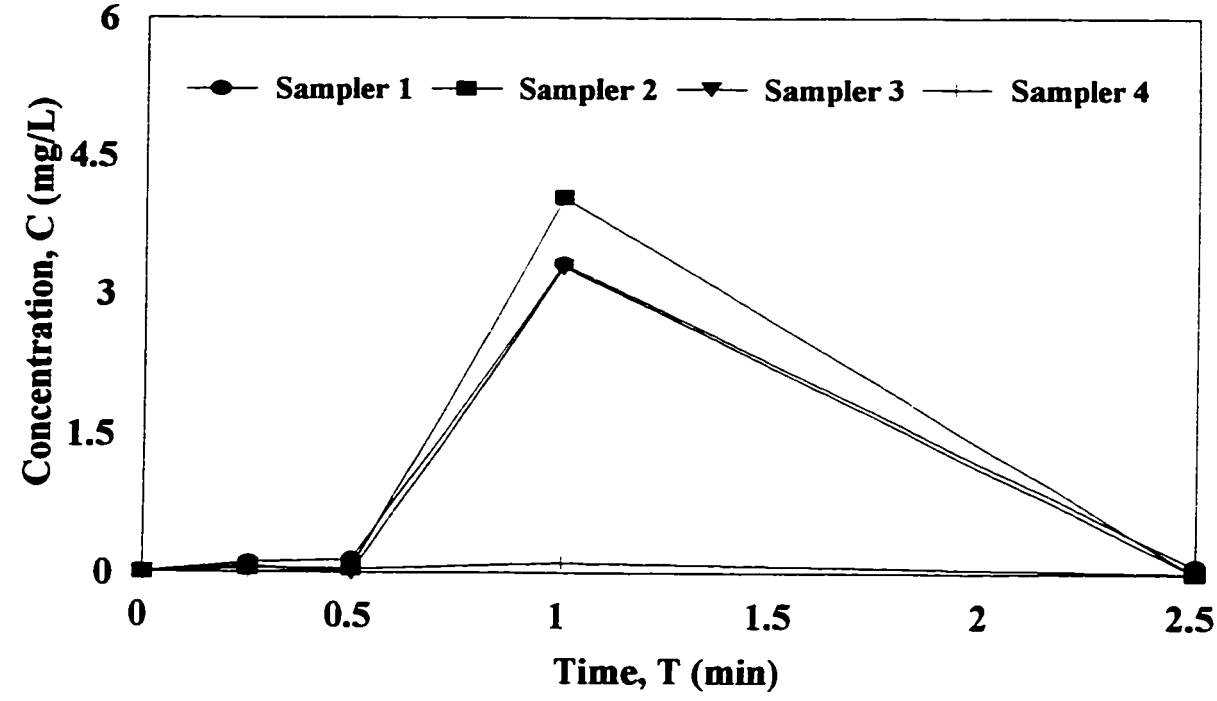

(a) Upstream

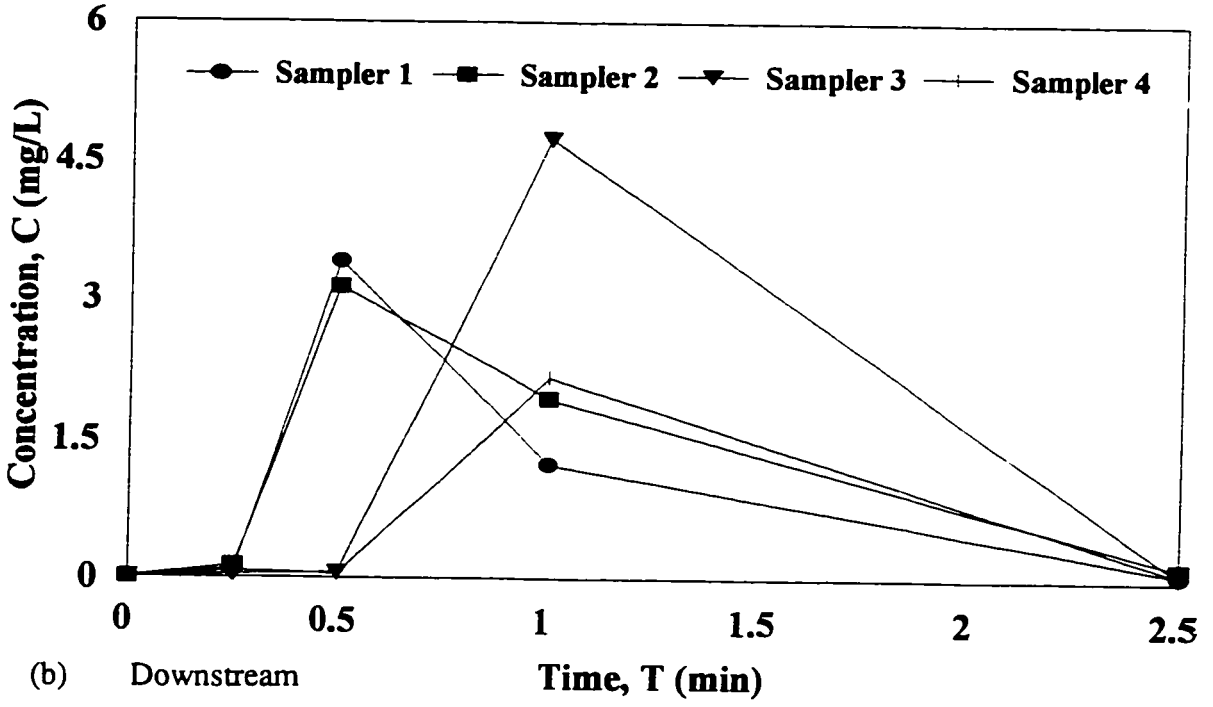

(b) Downstream

Figure 6.26 Cross-Stream Variation of Concentration with Time at Different Sampling Points, (Run # 13).

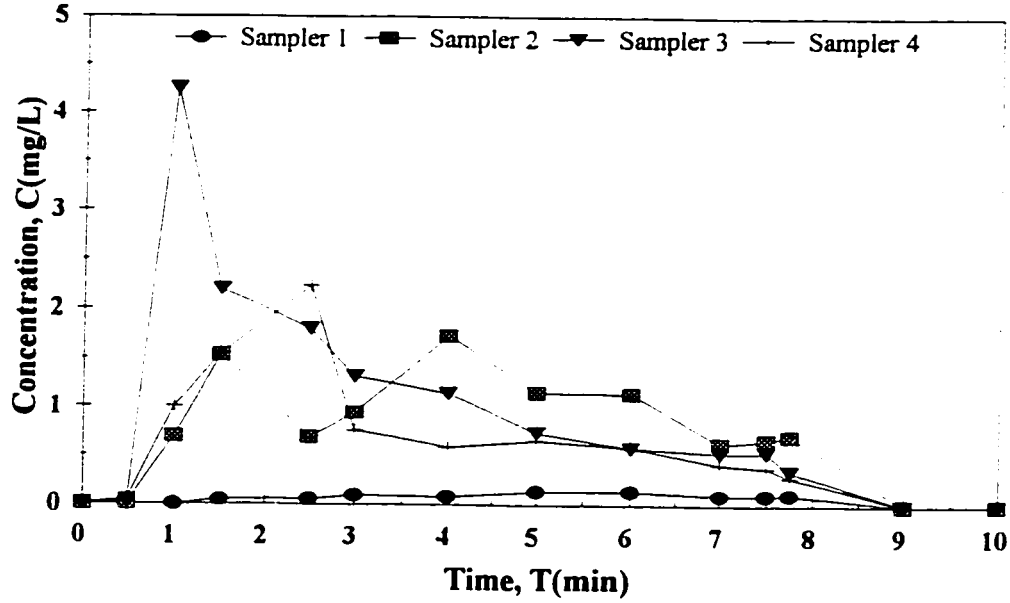

(a) Upstream

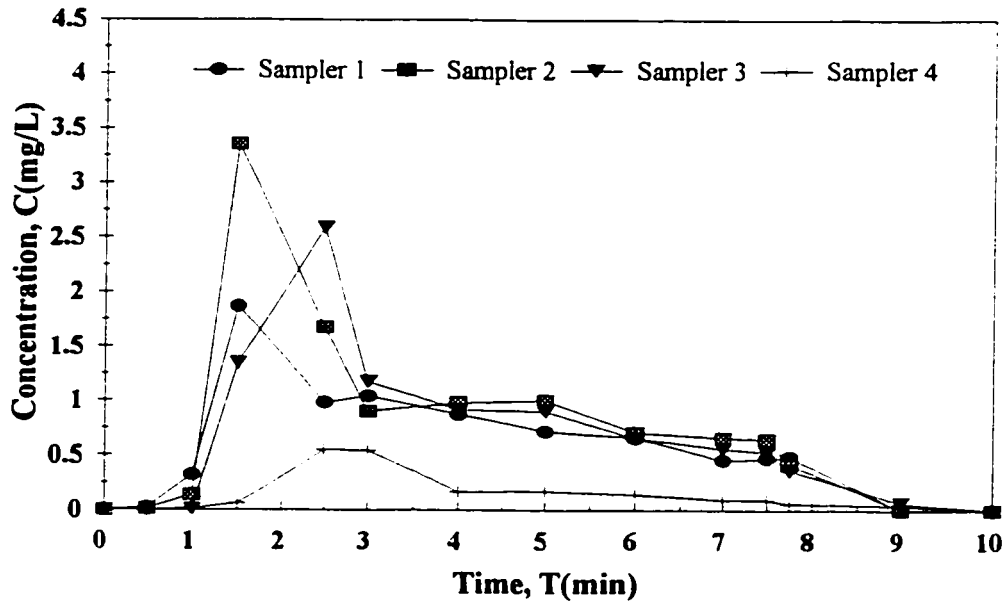

(b) Downstream

Figure 6.27 Cross-Stream Variation of Concentration with Time at Different Sampling Points, (Run # 15).

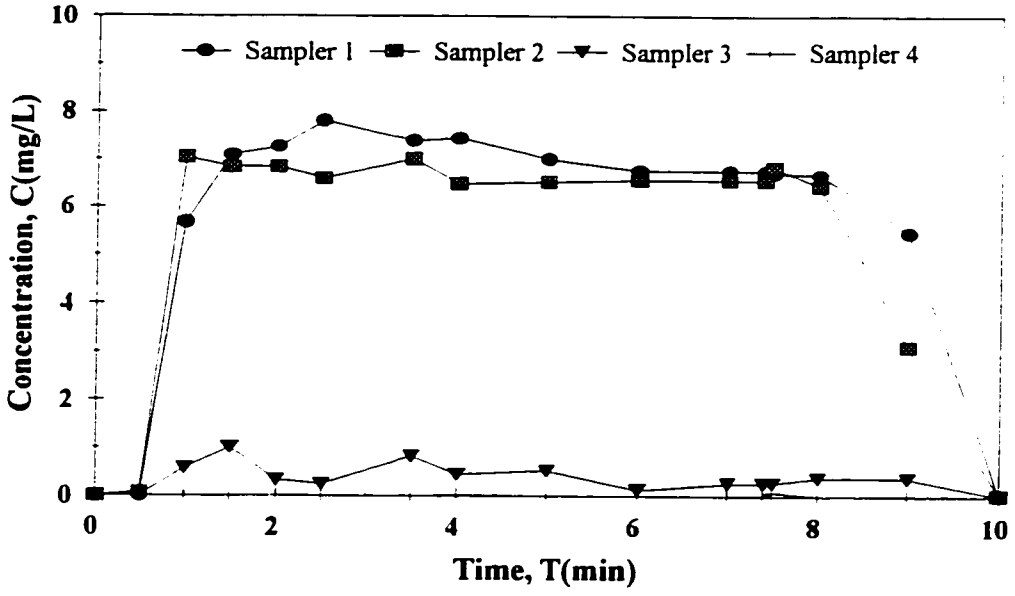

(a) Upstream

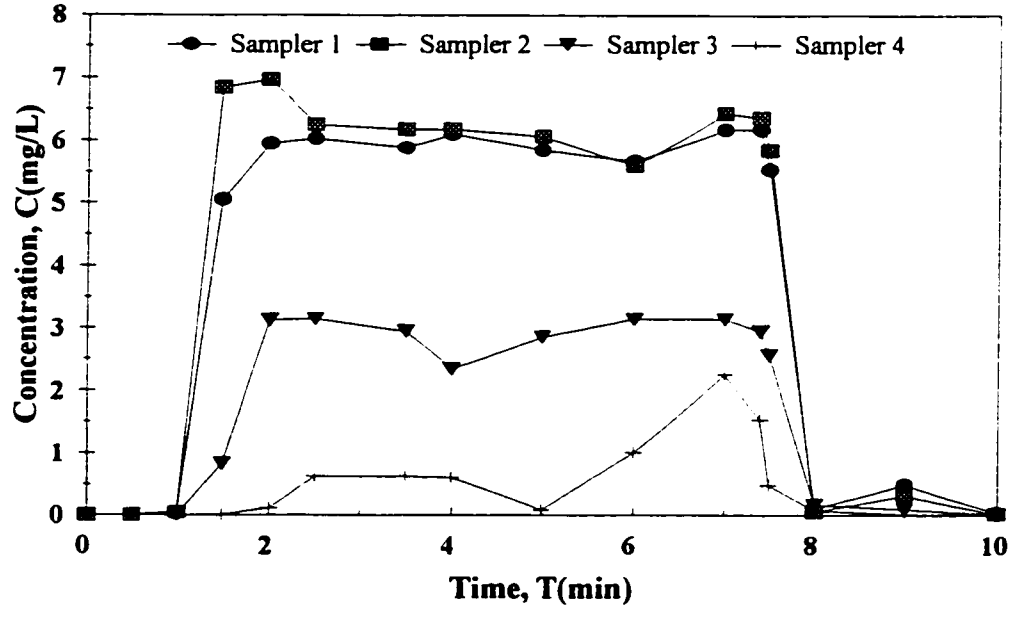

(b) Downstream

Figure 6.28 Cross-Stream Variation of Concentration with Time at Different Sampling Points, (Run # 20).

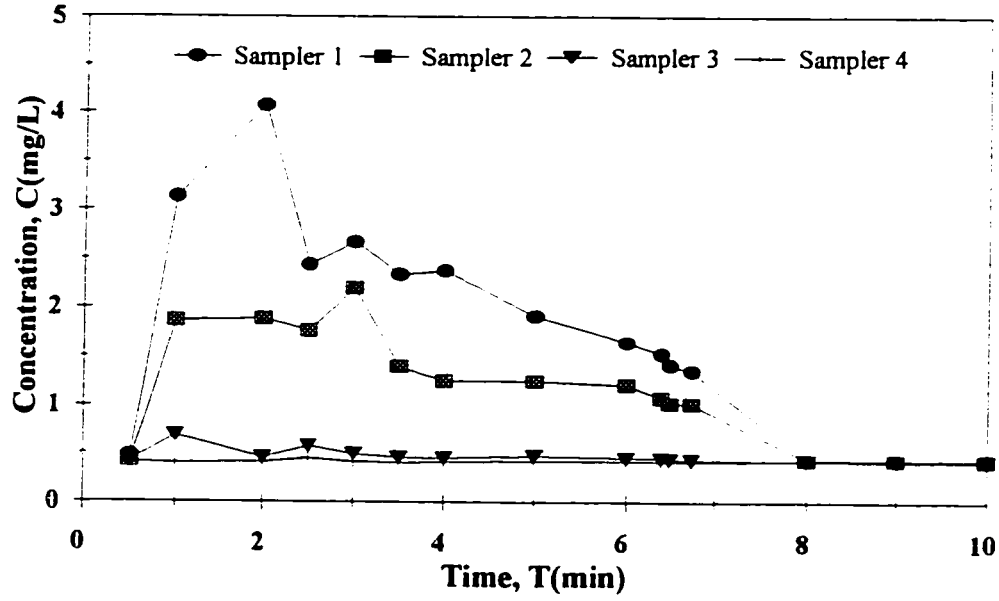

(a) Upstream

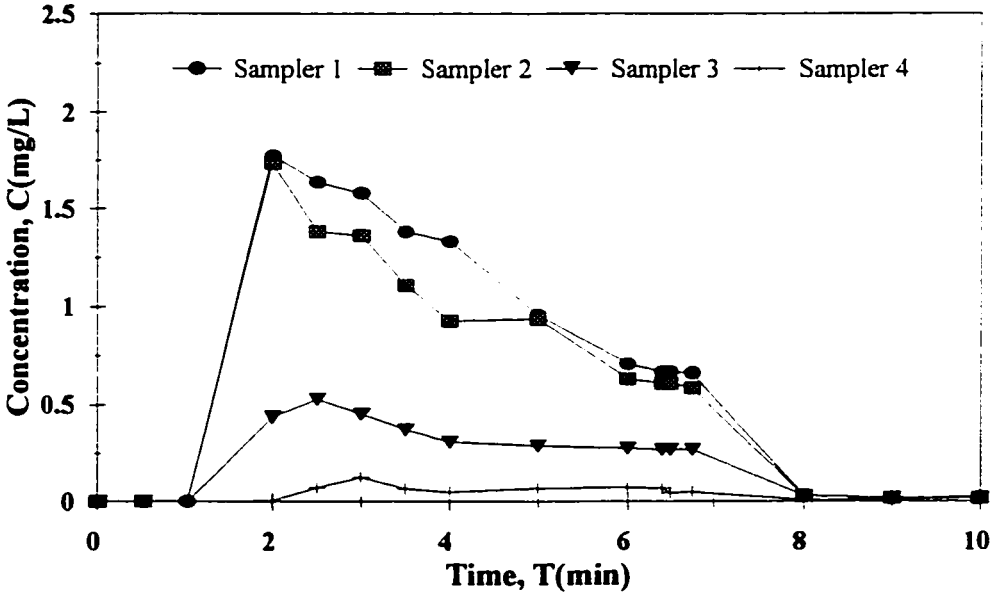

(b) Downstream

Figure 6.29 Cross-Stream Variation of Concentration with Time at Different Sampling Points, (Run # 21).

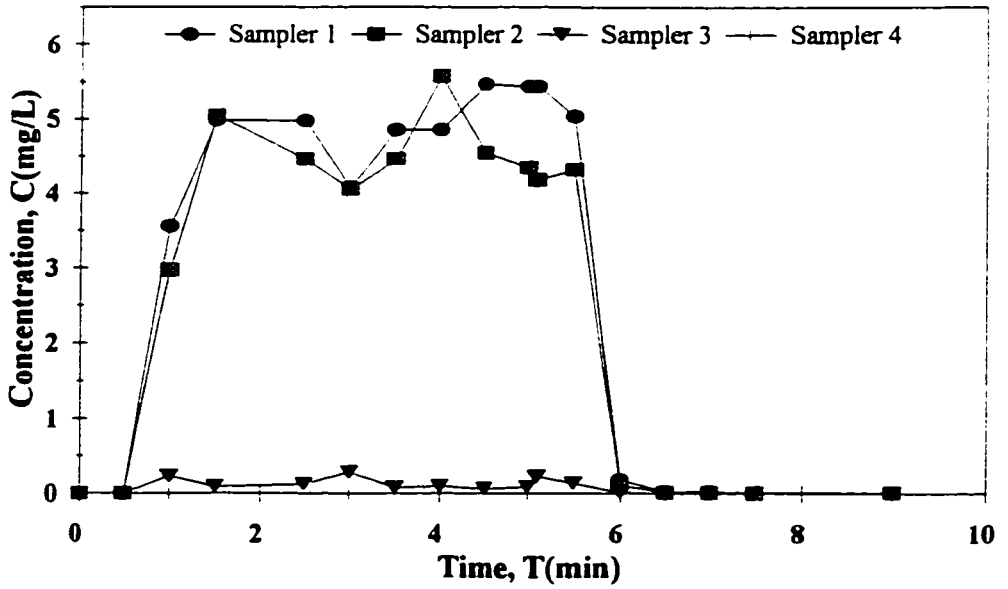

(a) Upstream

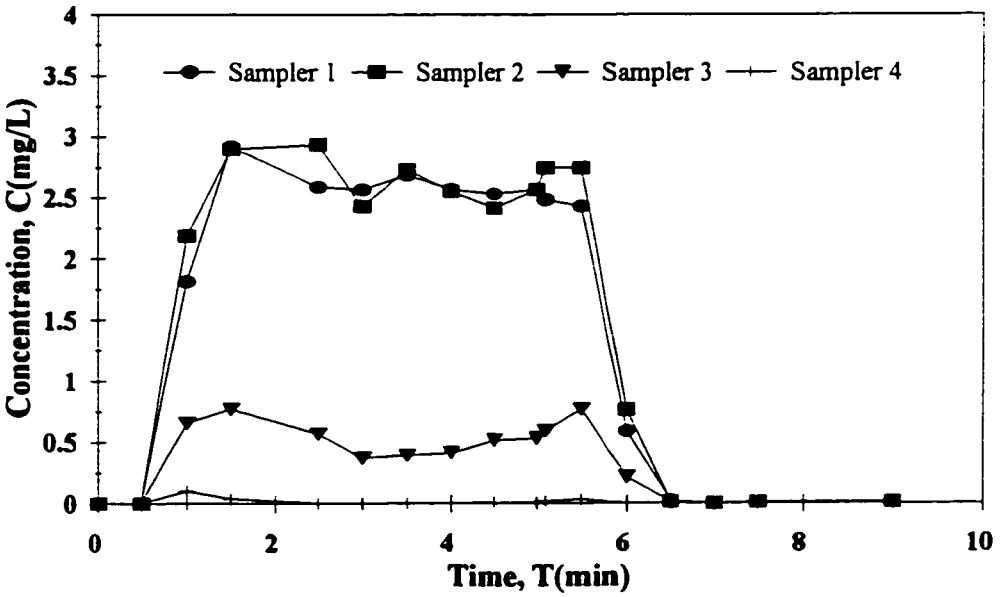

(b) Downstream

Figure 6.30 Cross-Stream Variation of Concentration with Time at Different Sampling Points, (Run # 23).

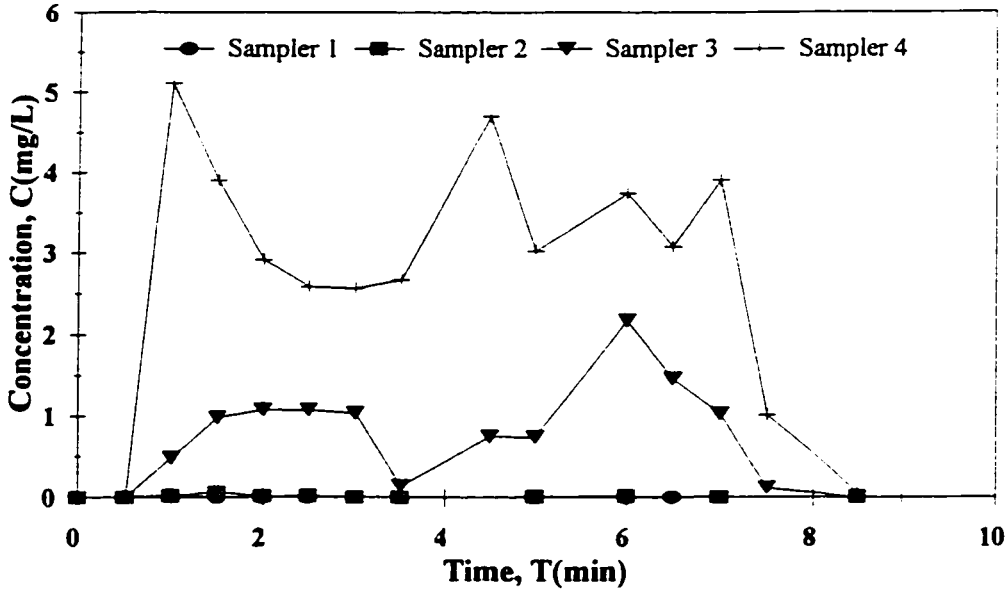

(a) Upstream

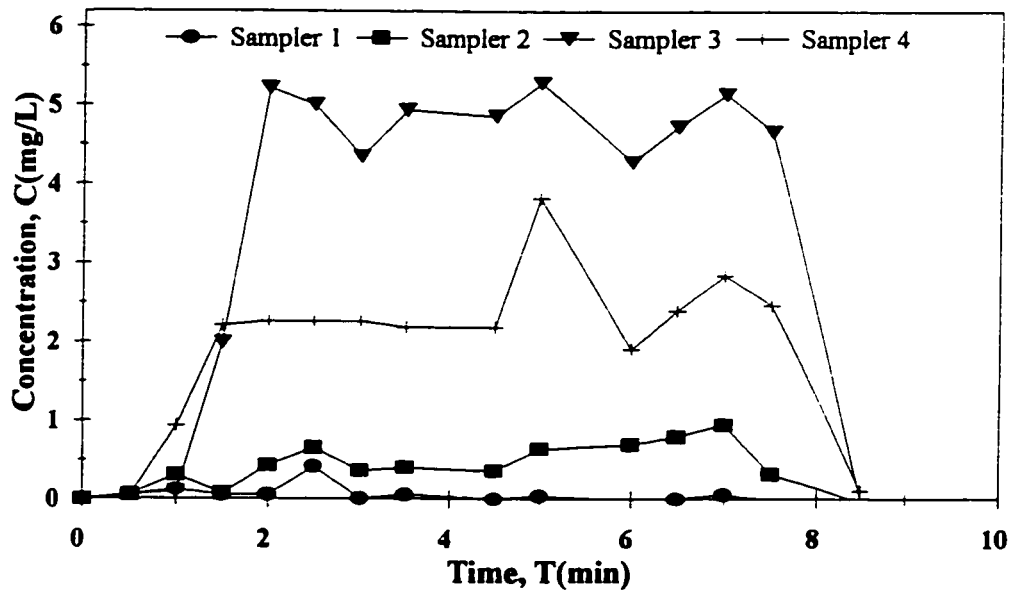

(b) Downstream

Figure 6.31 Cross-Stream Variation of Concentration with Time at Different Sampling Points, (Run # 24).

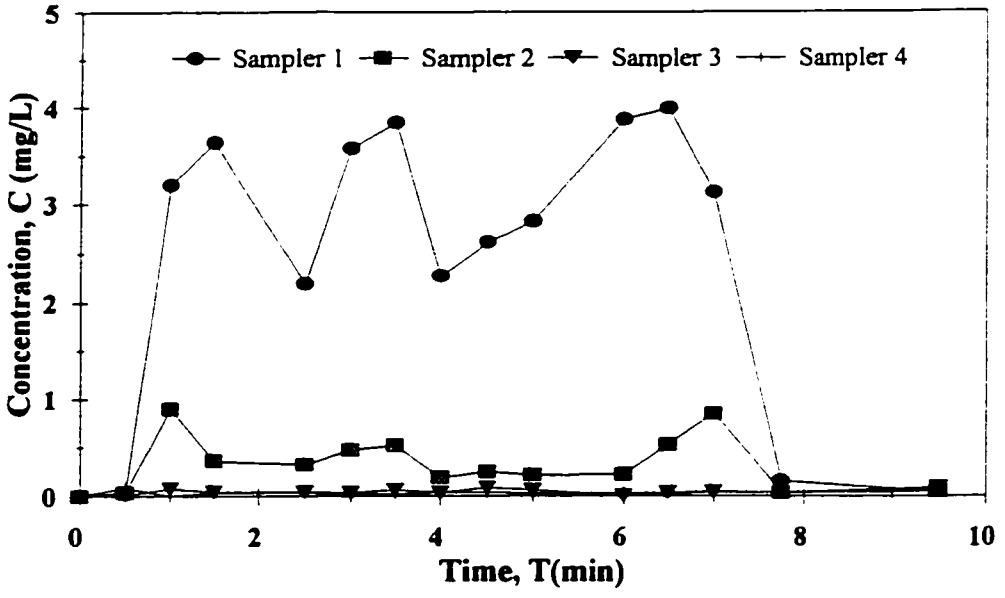

(a) Upstream

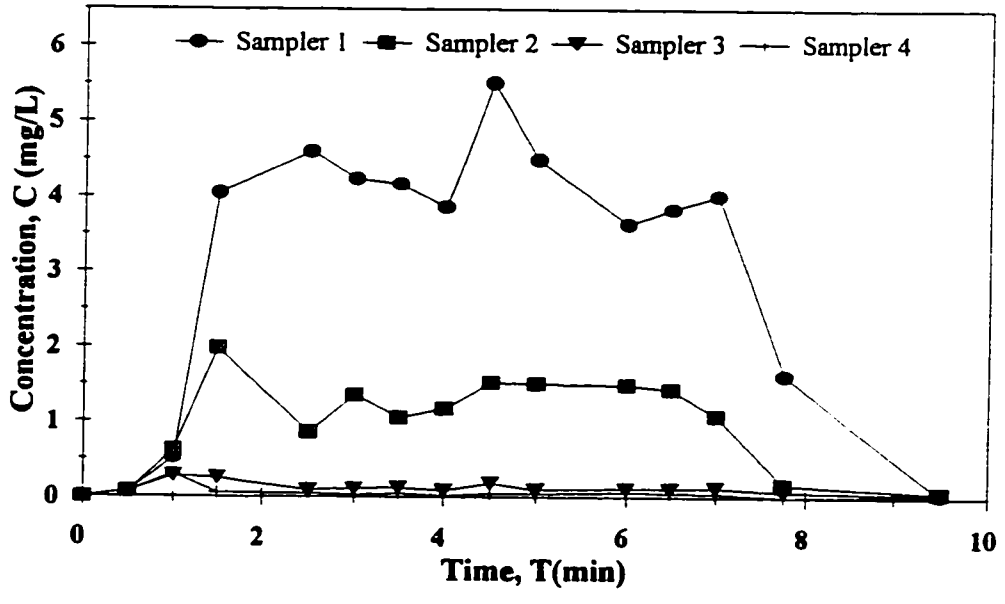

(b) Downstream

Figure 6.32 Cross-Stream Variation of Concentration with Time at Different Sampling Points, (Run # 26).

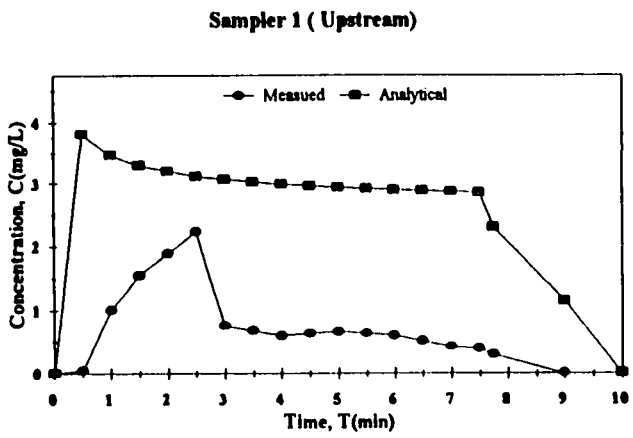

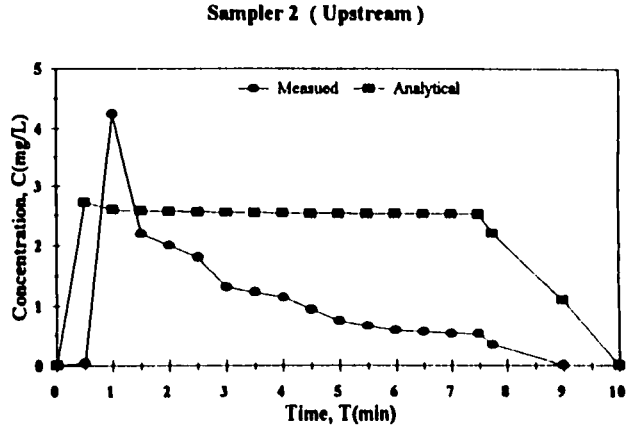

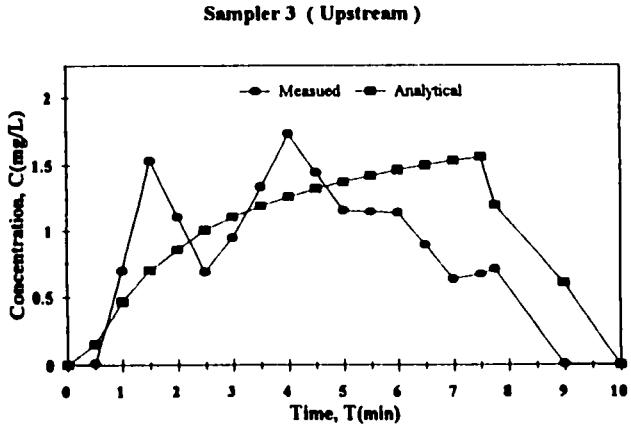

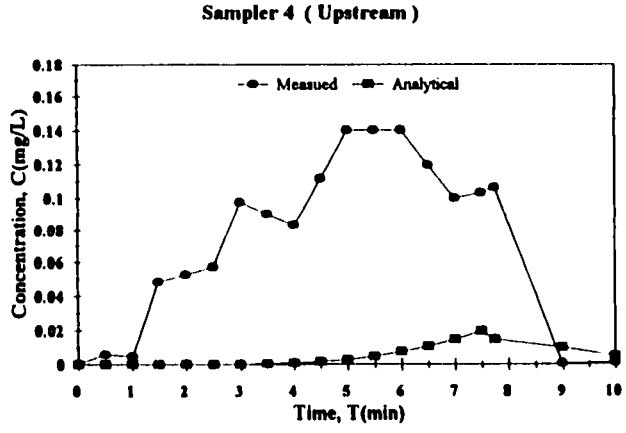

Figure 6.33 Comparison Between Closed-Form Simplified Analytical Solution with Observed Concentrations, (Run # 15, Upstream).

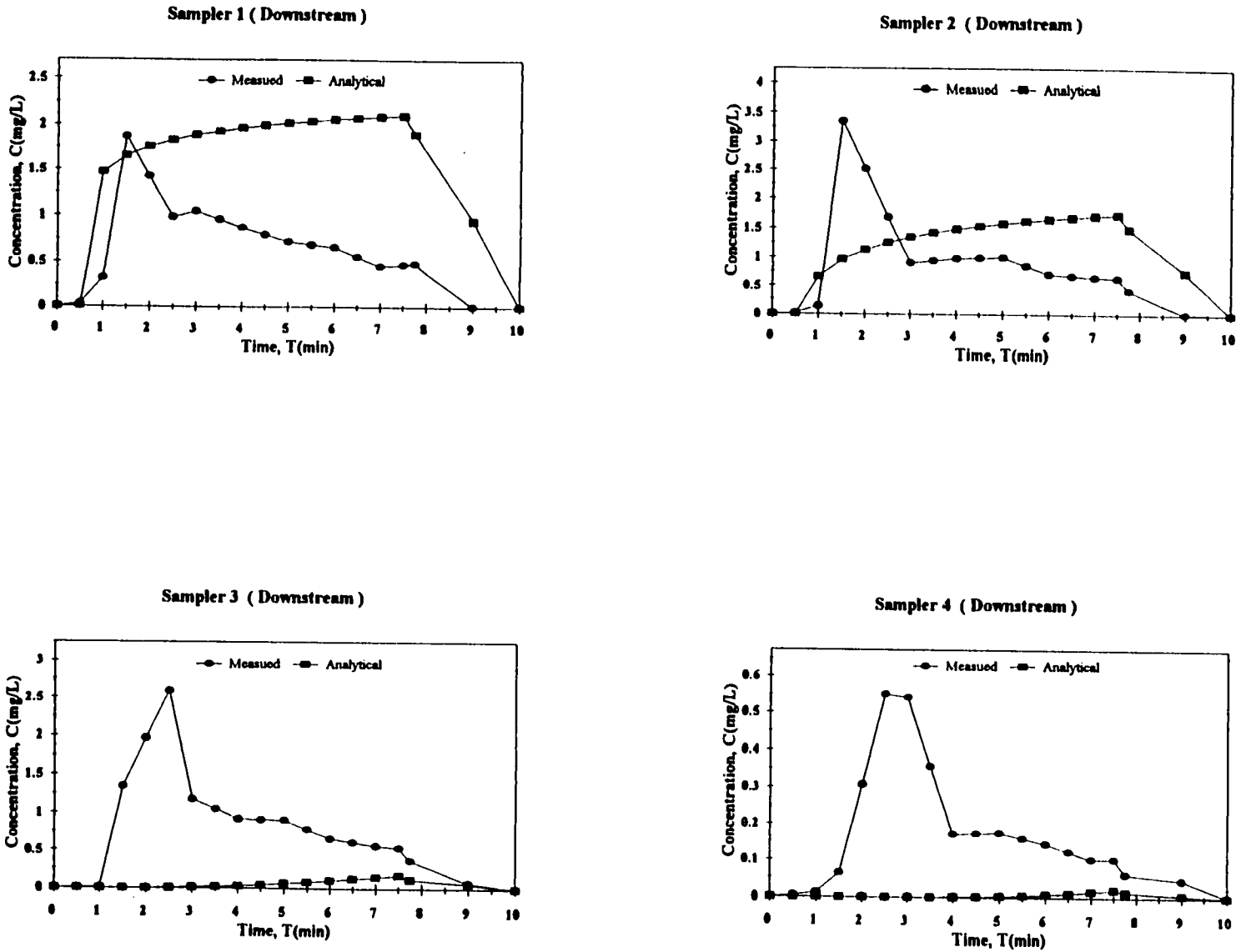

Figure 6.34 Comparison Between Closed-Form Simplified Analytical Solution with Observed Concentrations, (Run # 15, Downstream).

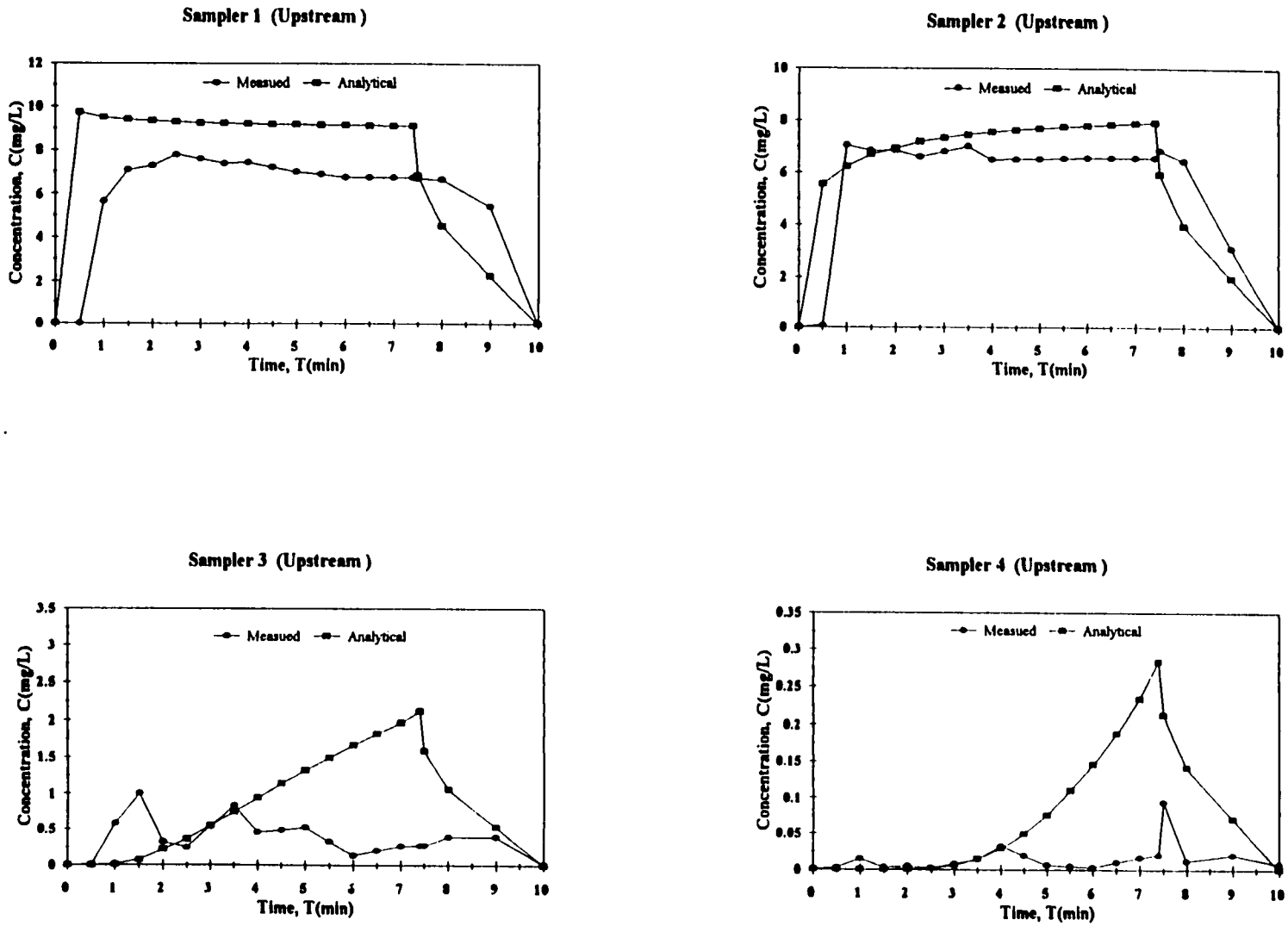

Figure 6.35 Comparison Between Closed-Form Simplified Analytical Solution with Observed Concentrations, (Run # 20, Upstream).

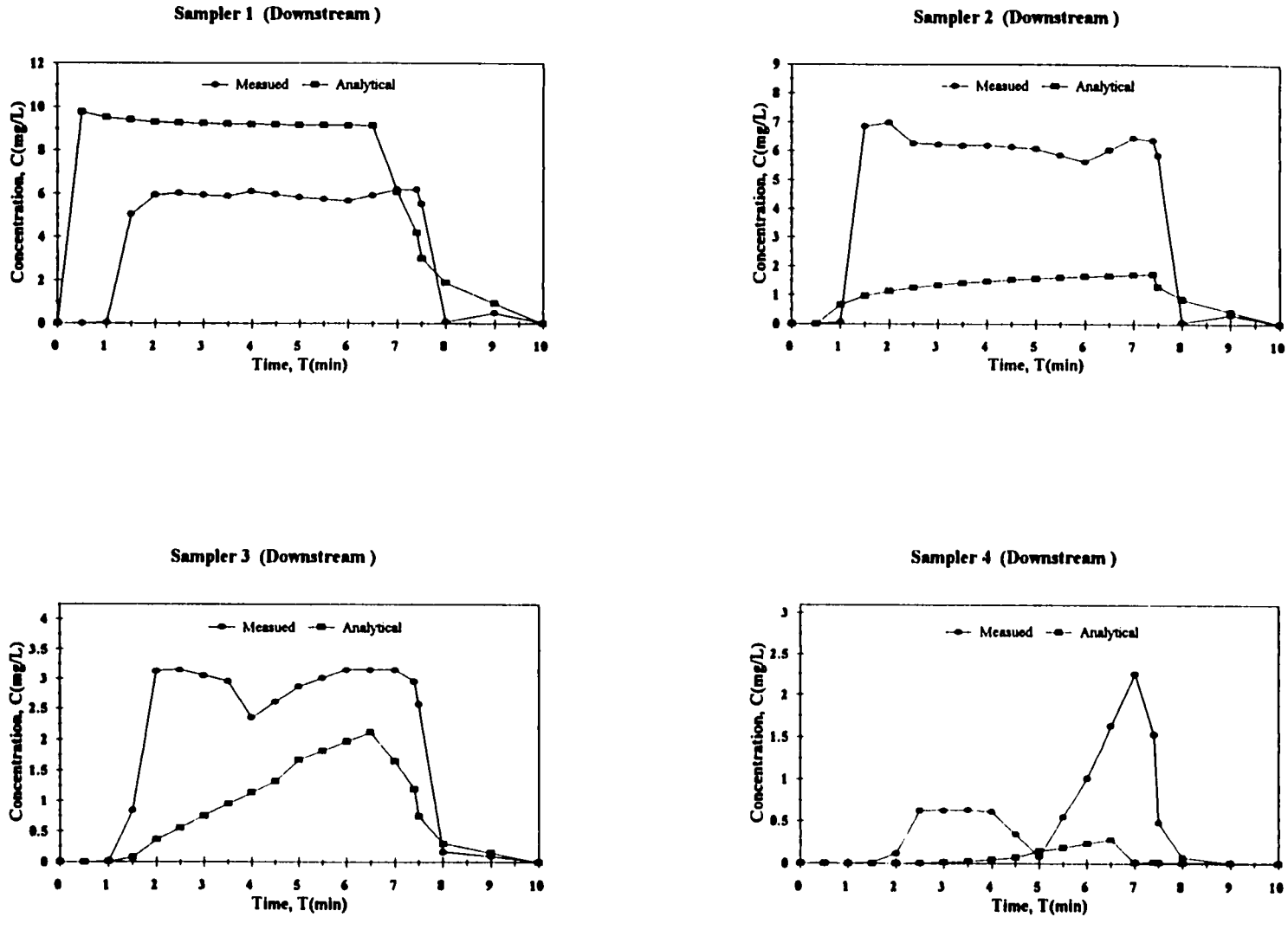

Figure 6.36 Comparison Between Closed-Form Simplified Analytical Solution with Observed Concentrations, (Run # 20, Downstream).

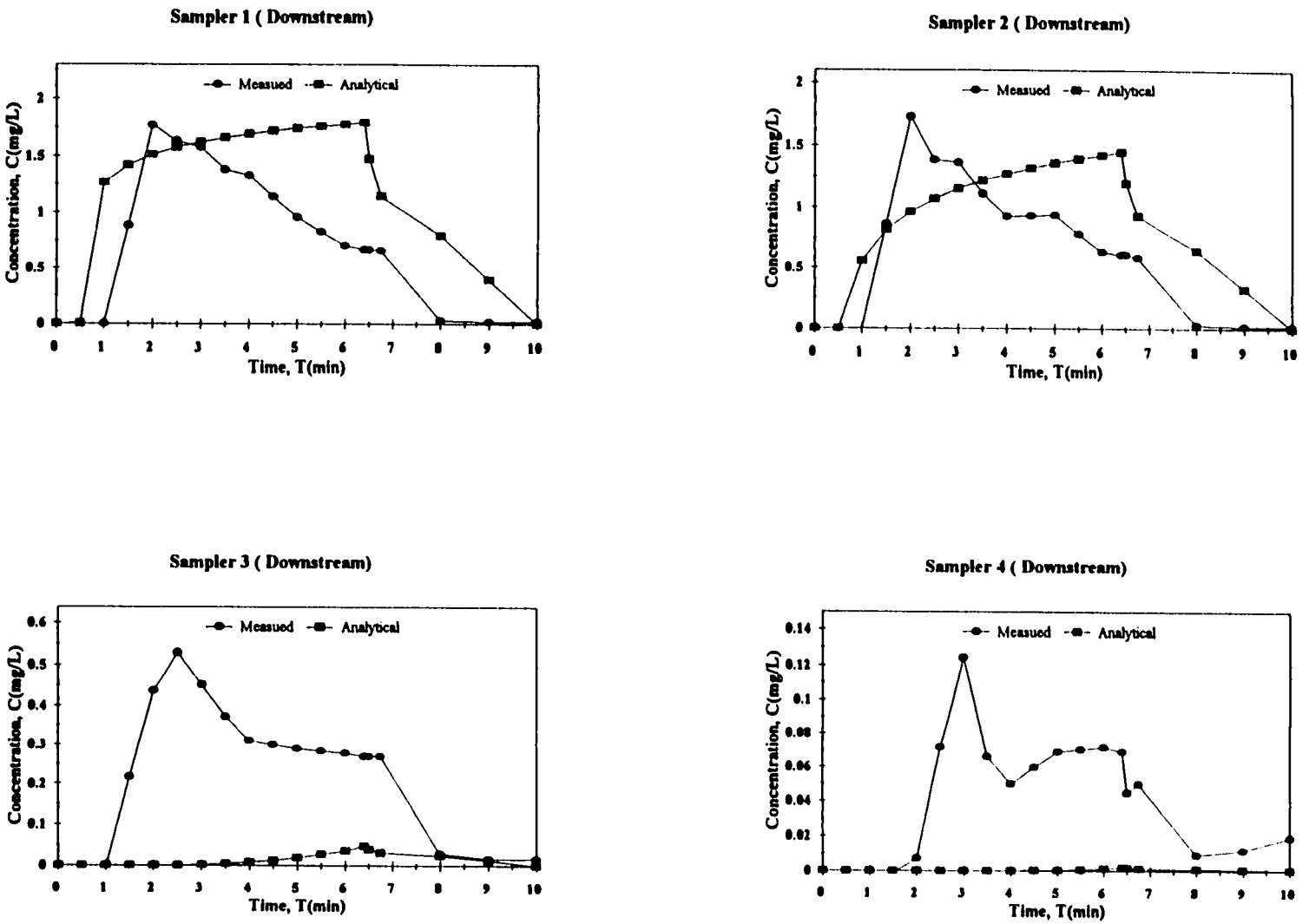

Figure 6.37 Comparison Between Closed-Form Simplified Analytical Solution with Observed Concentrations, (Run # 21, Downstream).

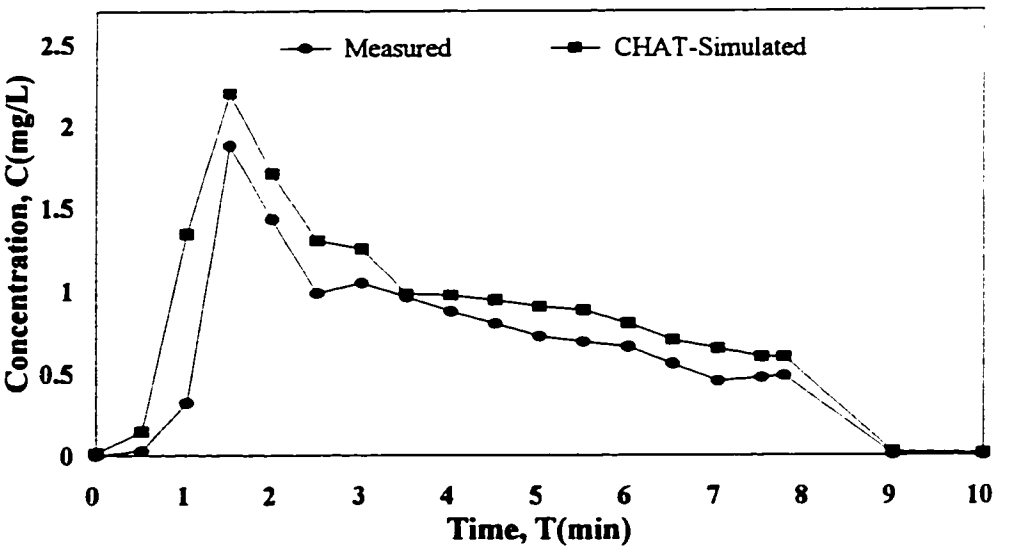

(a) Sampler 1

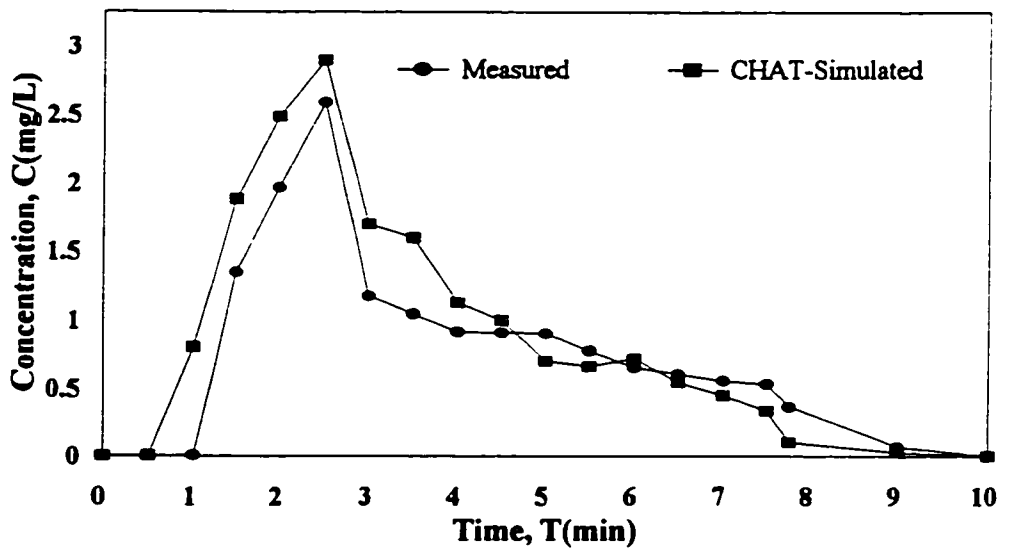

(b) Sampler 3

Figure 6.38 Observed Vs. CHAT-Simulated Concentrations, (Run # 15, Downstream).

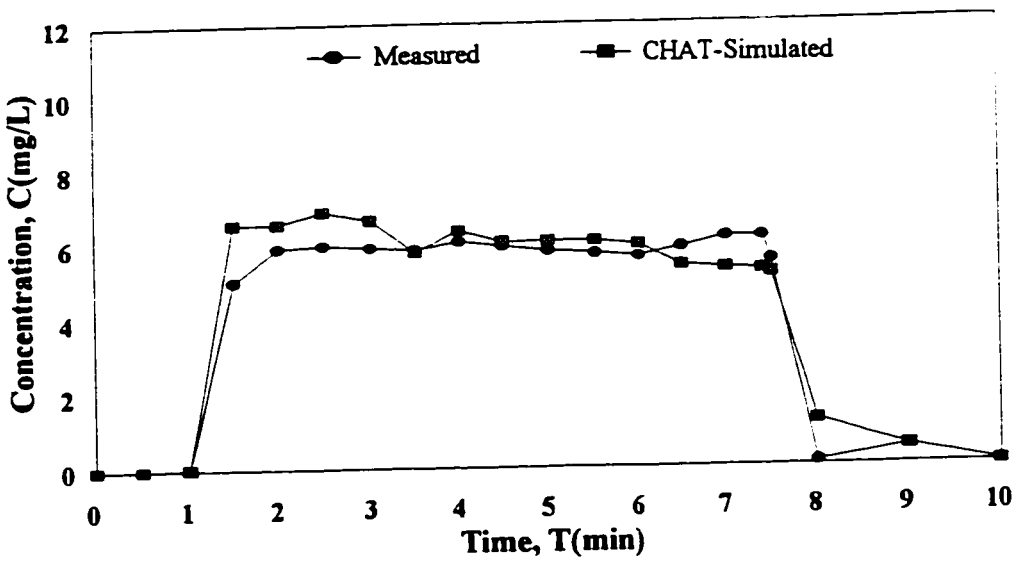

(a) Sampler 1

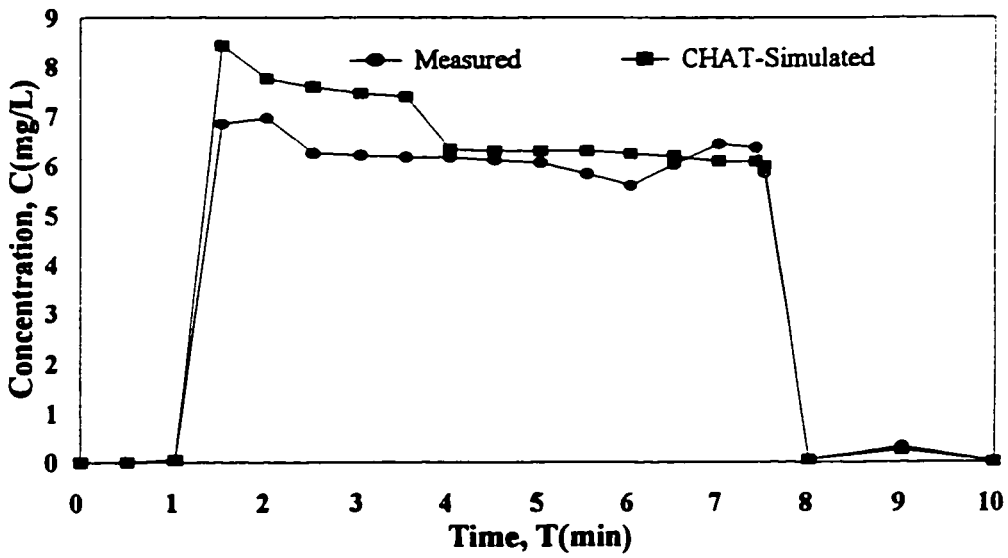

(b) Sampler 2

Figure 6.39 Observed Vs. CHAT-Simulated Concentrations, (Run # 20, Downstream).

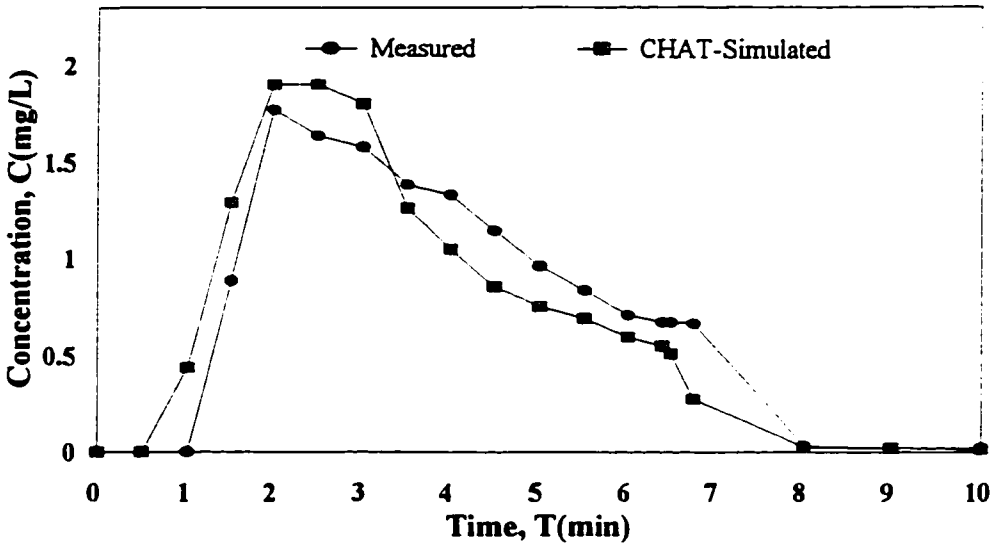

(a) Sampler 1

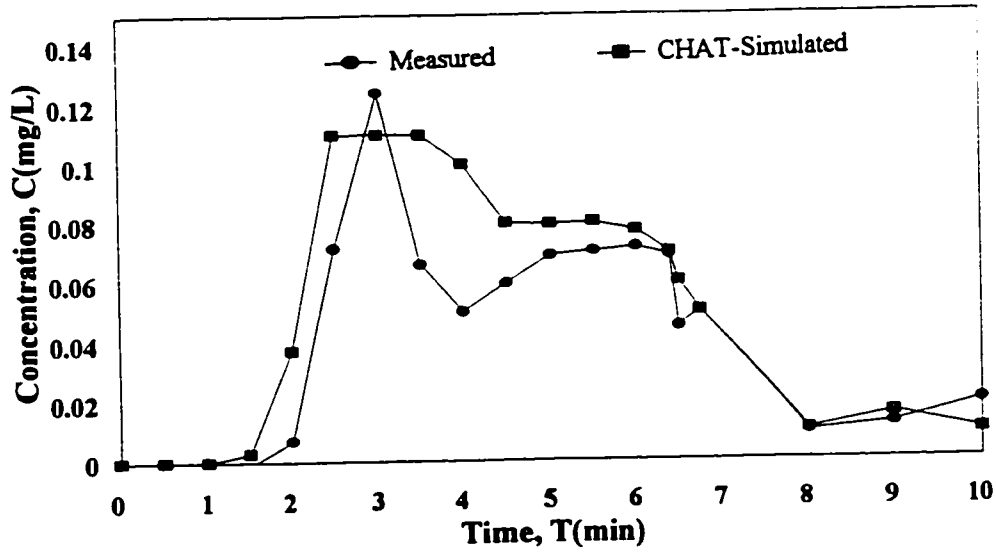

(b) Sampler 4

Figure 6.40 Observed Vs. CHAT-Simulated Concentrations, (Run # 21, Downstream).

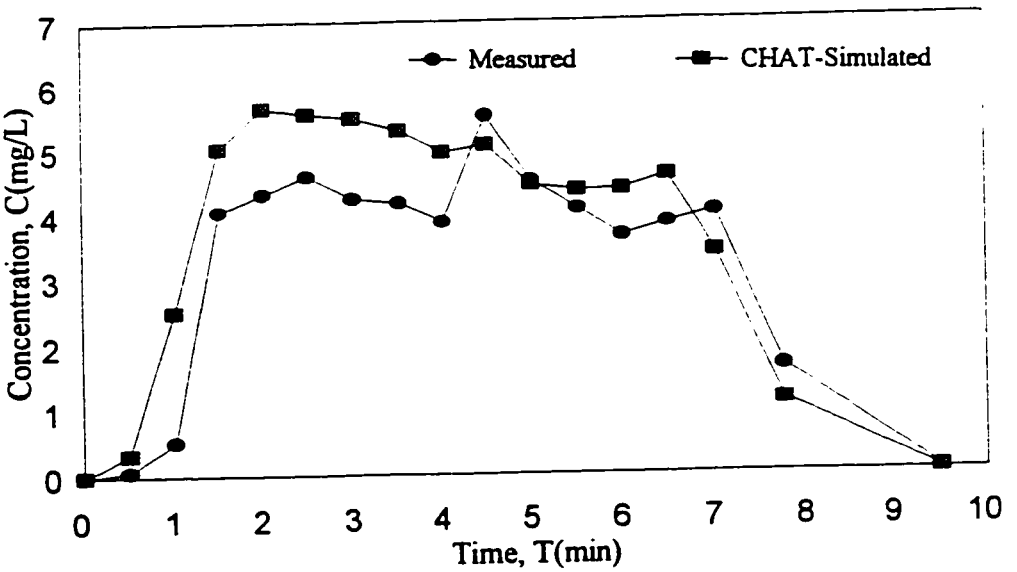

(a) Sampler 1

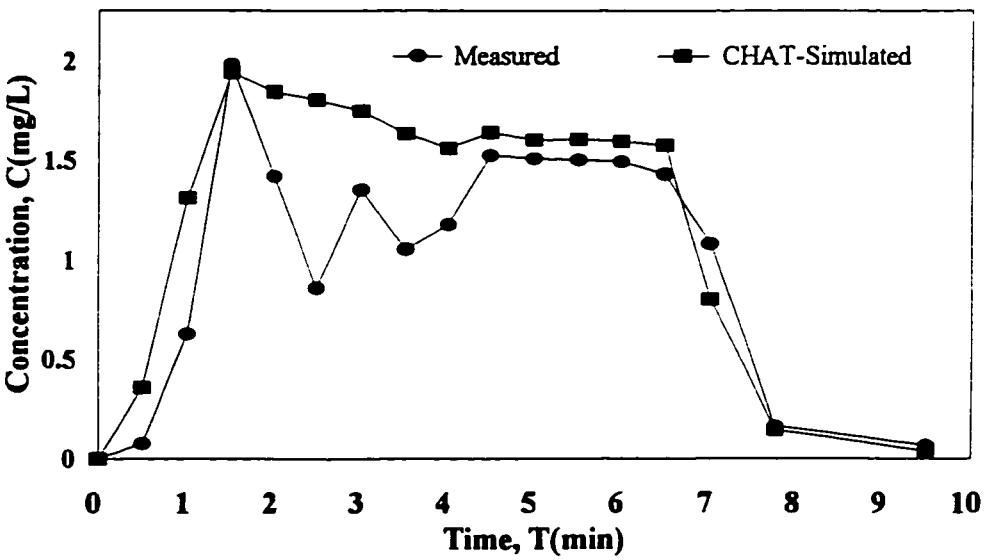

(b) Sampler 2

Figure 6.41 Observed Vs. CHAT-Simulated Concentrations, (Run # 26, Downstream).

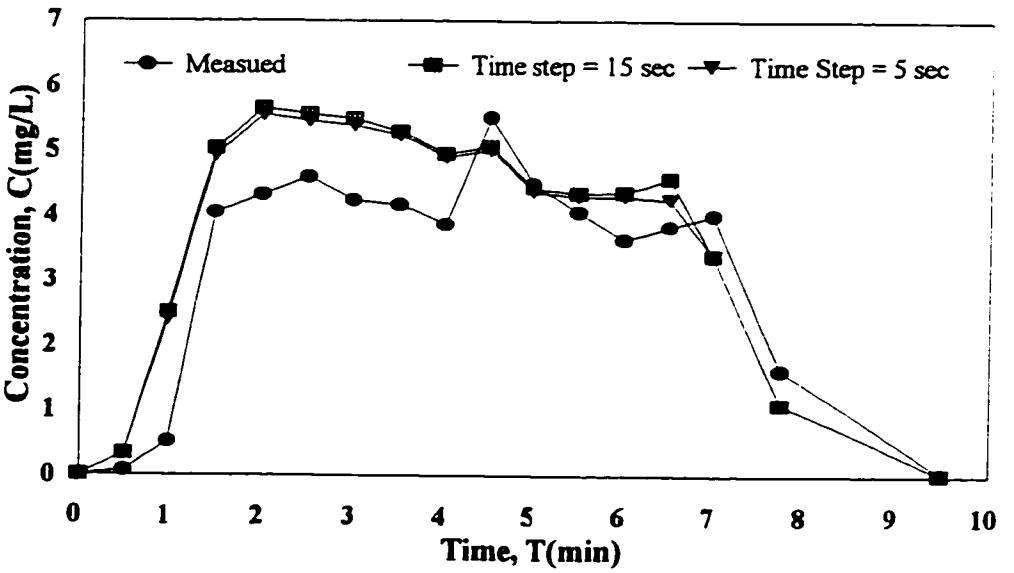

Figure 6.42 Effect of Time Step Variation on Simulated Concentrations, (Run # 26).

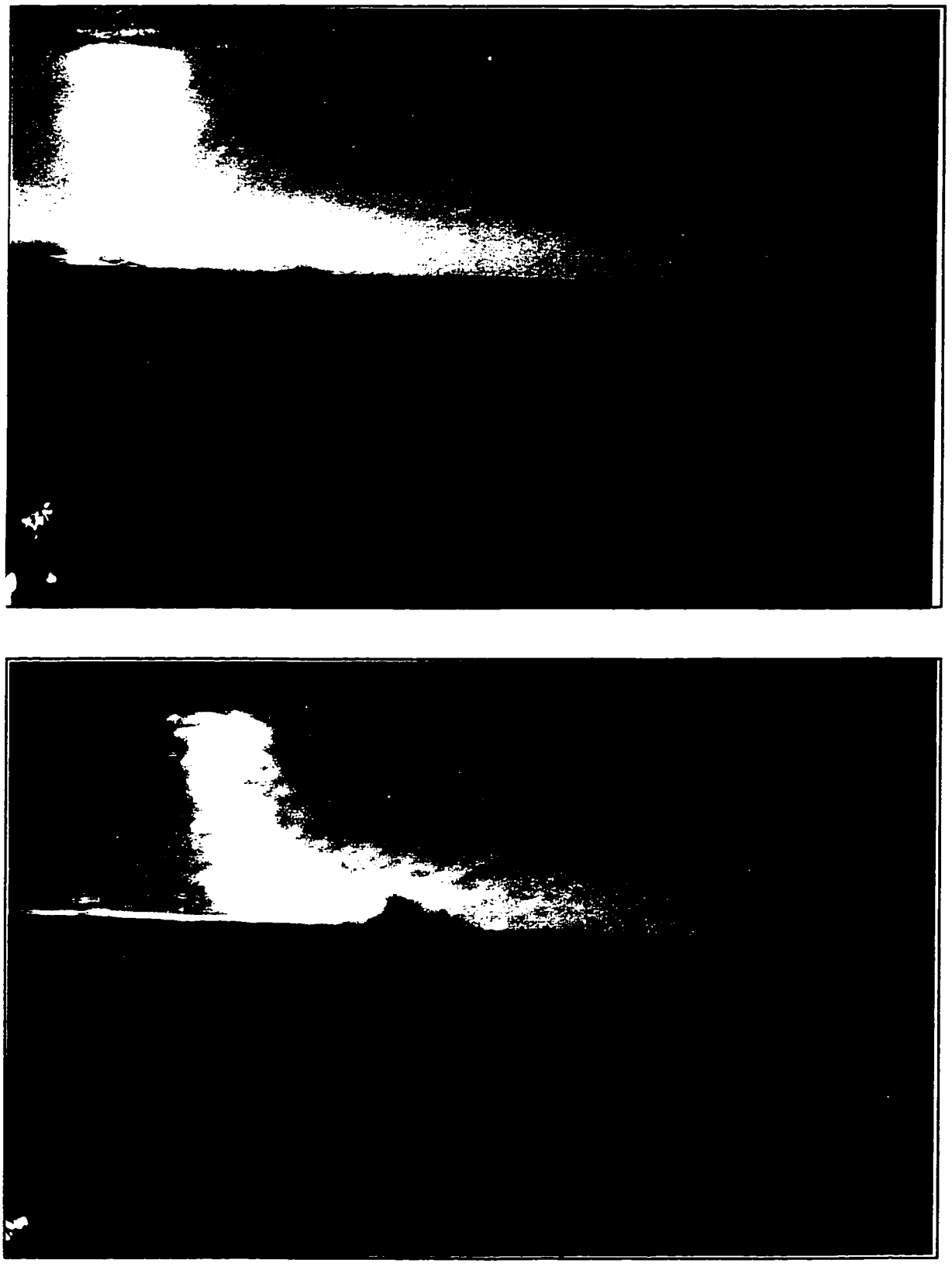

Plate 6.1 Spreading of Dye-Tracer After Main-Channel Injection.

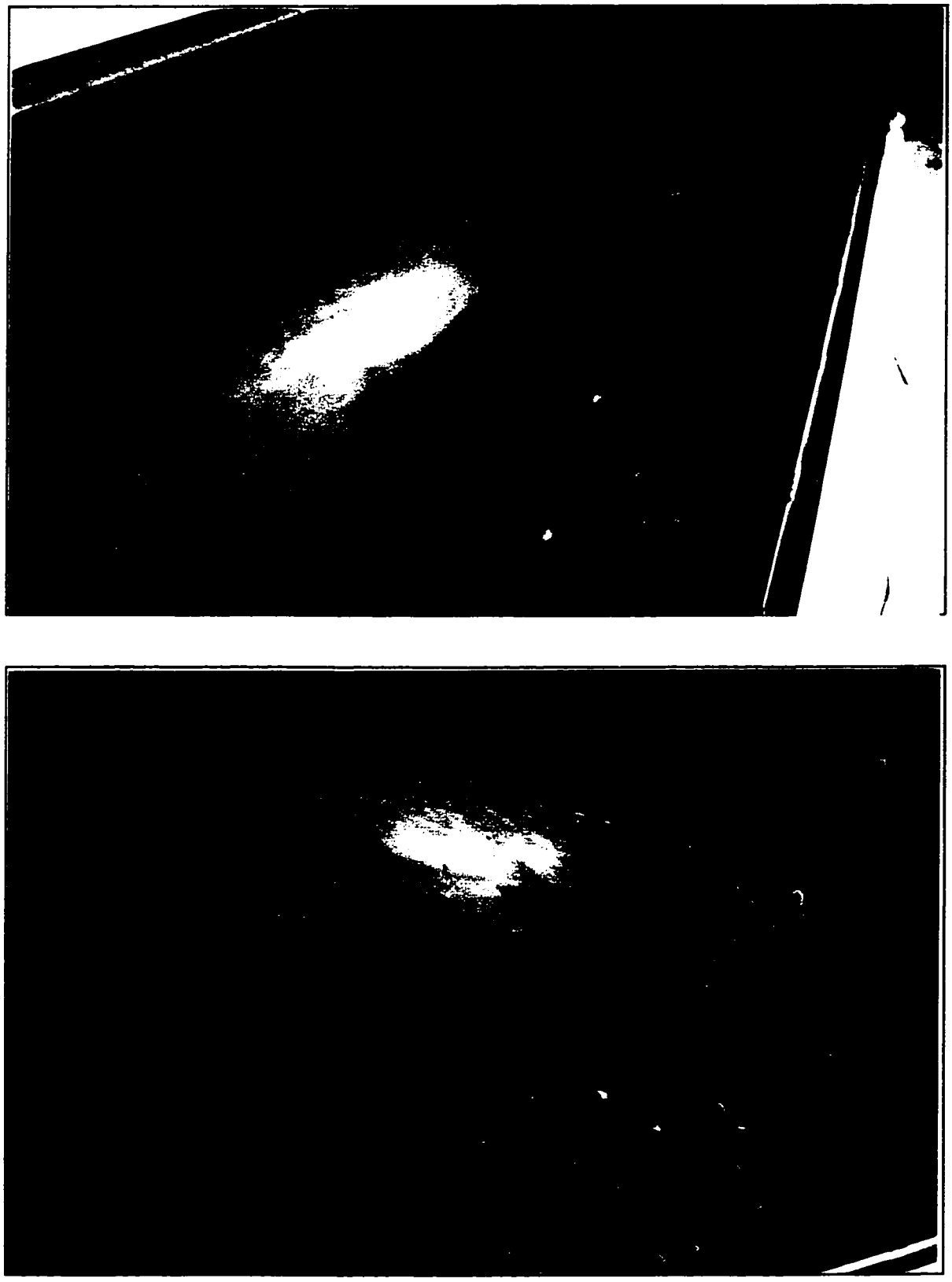

Plate 6.2 Fluctuation of Dye-Spreading Over the Junction.

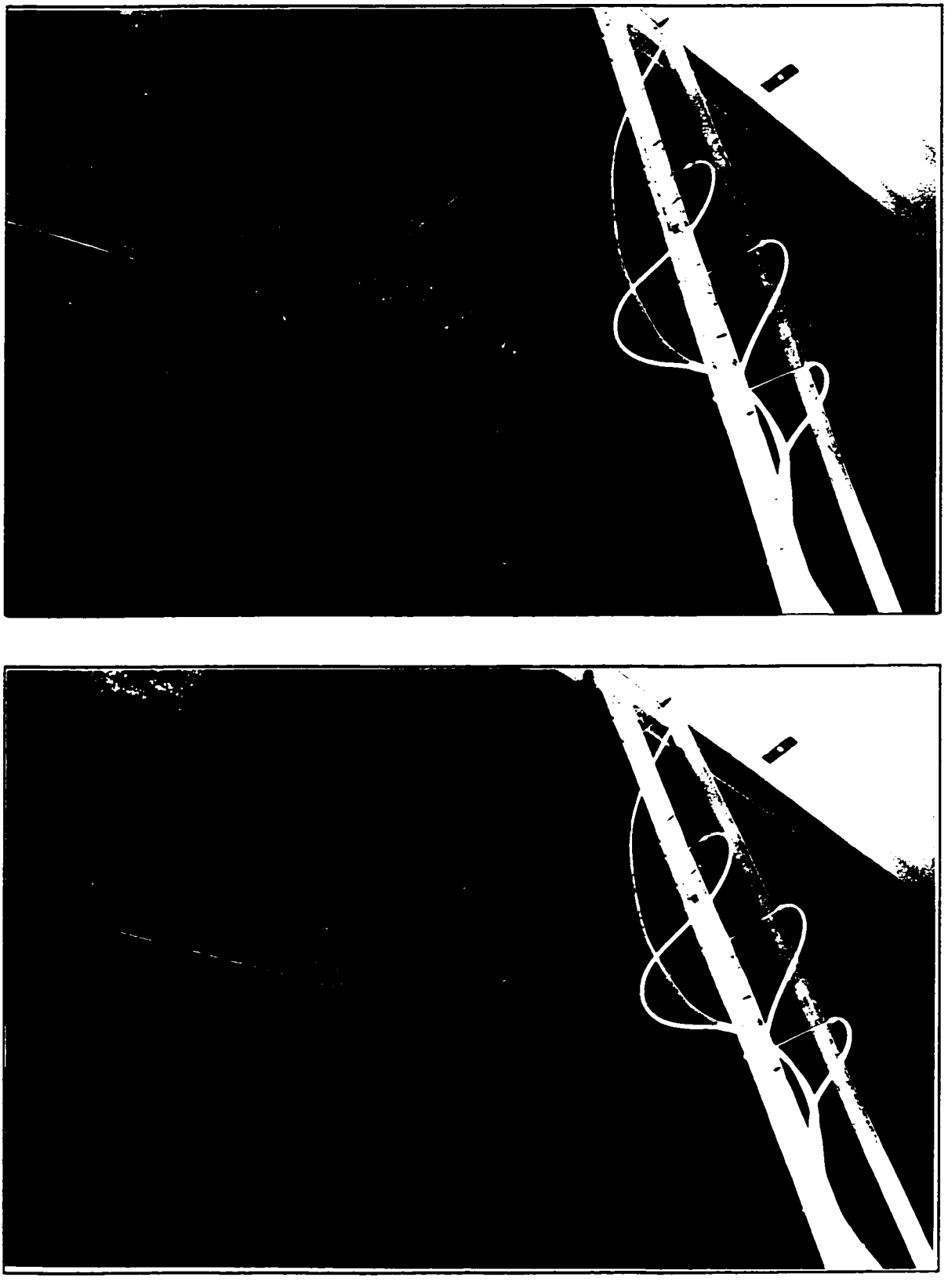

Plate 6.3 Fluctuation of Dye Near the Sampling Tubes.

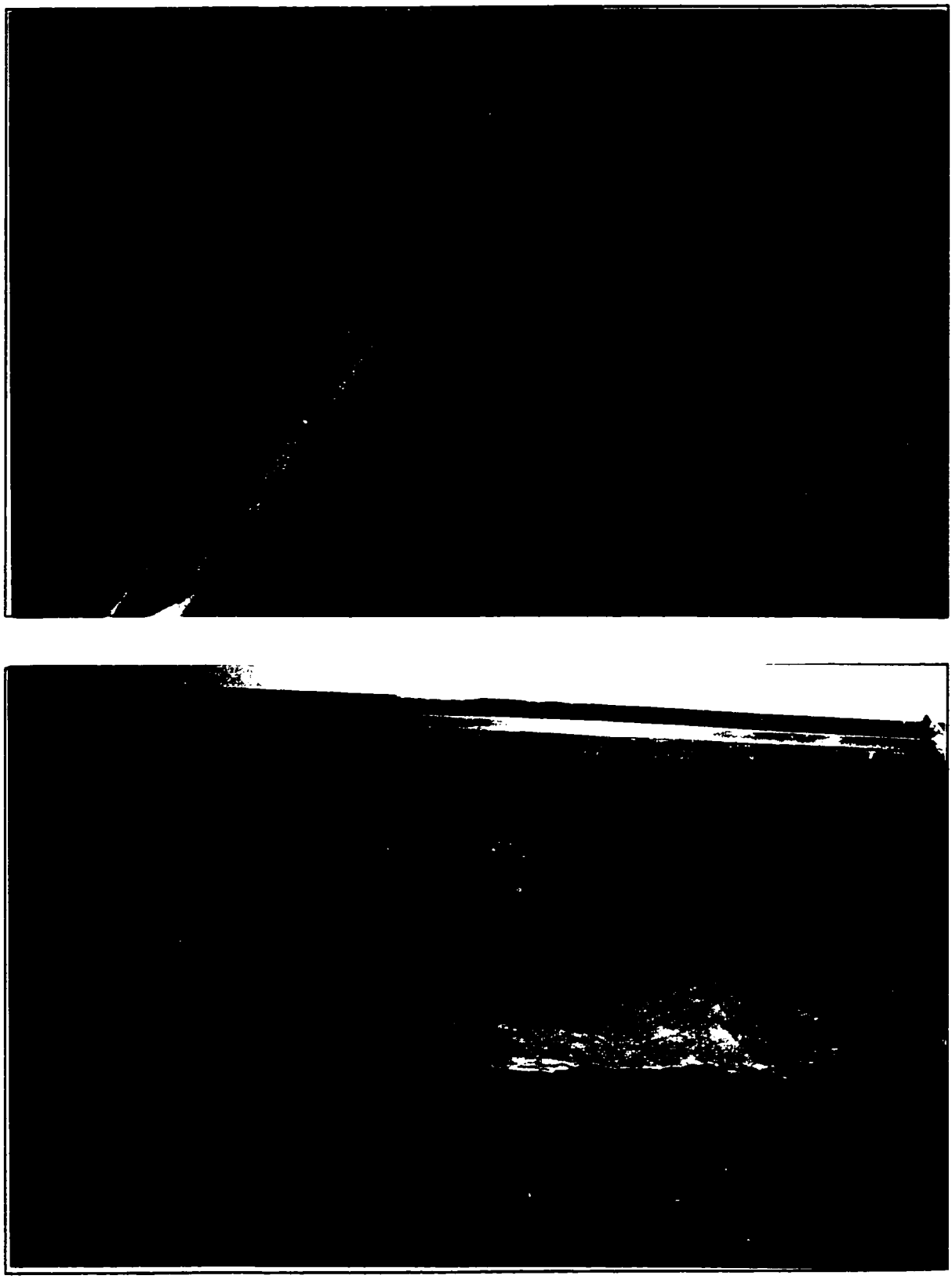

Plate 6.4 Dye Injection and Spreading Over the Flood Plain.

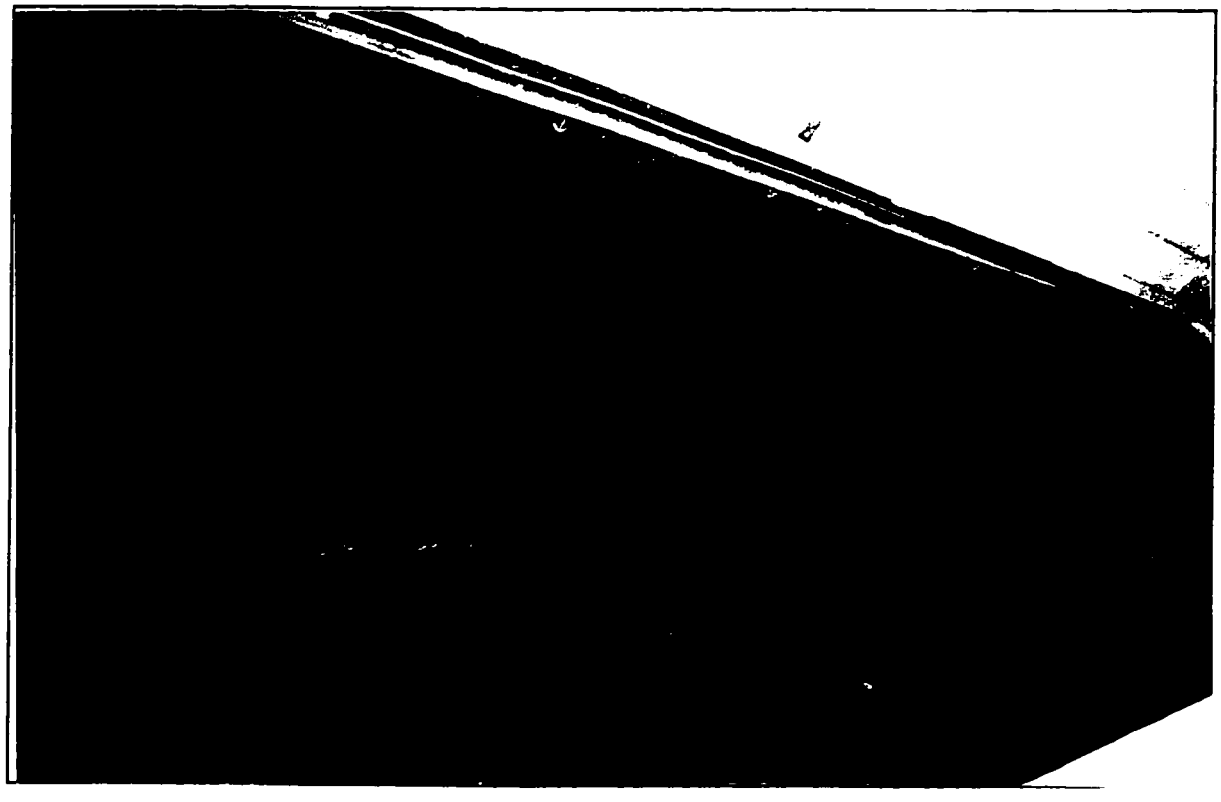

Plate 6.5 Dye Spreading from the Flood Plain to the Main Channel.

CHAPTER SEVEN

CONCLUSIONS AND RECOMMENDATIONS

7.1 CONCLUSIONS

A mathematical model, (CHAT: Compound-channel Hydraulics And transport), to simulate the transport of inert pollutants in open channel flow. The well-known advection-diffusion PDE is used to model the concentration distribution of inert pollutant transport in compound open channels. The flow and transport equations are integrated over the depth and modified to allow for compound channel effects. A 2-D FD model has been developed to solve the equations. Data for the verification of CHAT is obtained through dye-tracer experiments performed in a large channel of the Hydraulics Laboratory, University of Ottawa. The experiments include measurements of dye concentrations downstream of steady-injection *point* sources. CHAT was found to be a useful tool for predicting the concentration of an inert pollutant downstream of a source. Model calibration was performed using sets of measured dye concentrations and velocities. Comparison between measured and predicted concentration curves shows a reasonable level of agreement in the general curve shape, peak concentration, and time to peak. Due to the 3-D nature of the flow, mixing phenomena is very distinct in compound open channels. A number of modifications were made to the laboratory data set to improve the efficiency and the ability to converge to a solution. It can

be stated that on the whole a good agreement between measured and calculated values is obtained.

Analytical solutions do not exist for the *complete* set of (3-D) Navier-Stokes equations as well as the advection-diffusion equation. Also, numerical solutions of these equations in their complete form is very difficult to accomplish. The difficulties include, among other things: the complexities in defining river boundaries and geometry. It can be argued that a 3-D model is required for accurate simulation of a compound flow field. However, the effort and cost of developing a 3-D model would generally outweigh the improvement gained over a dedicated 2-D model.

The present research investigates the numerical modelling aspects of steady flow in compound channels, with special interest in the transport of inert pollutants therein. This is examined through the development of a 2-D FD mathematical model CHAT to solve the flow and transport equations for open channels having compound cross-sections. Data for verifying and validating CHAT was obtained through dye-tracer experiments performed in a large concrete channel of the Hydraulics Laboratory, University of Ottawa. The experiments included measurements of dye concentrations downstream of a *slug* injection or steady-injection *point* source. A number of questions, regarding the model and the processes it simulates, were also addressed.

The development of CHAT is based on the following assumptions:

- The fluid density is constant, hydrostatic pressure distributions are valid, and relatively uniform bottom slopes exist.

- The eddy viscosity model, which is simpler than the k-ϵ model and gives better agreement in results, (Radojkovic and Djordjevic, 1985), is used to account for compound channel effects.

- The pollutant is assumed to be uniformly mixed over the depth. This holds true in most channels having relatively large width-to-depth ratios.

- The stream velocity has two components. First, a component u along the longitudinal axis of the stream or channel. Second, a component v along the transverse direction of the stream or channel, which is taken to be perpendicular to the longitudinal axis.

- The pollutant undergoes no exchange with the bed. This excludes sedimentation problems from consideration.

- The pollutant is conservative or inert. Thus, concentrations change only by dilution and not due to any decay or generation in the flow field.

Based on these applications, the following were the main conclusions:

- Given the alternating implicit-explicit nature of the numerical solution scheme, time steps were selected based on *accuracy* as well as *stability*. The same time step and grid size were used in the solution of the continuity and momentum equations as well as the advection-diffusion equation.

- Calibration of CHAT was performed by applying it to the experimental data set.

- Decreased main channel flow velocities (produced by LMT) at low flood plain depths were observed in this study. It is noticed that for small flood plain depths, there is a sharp discontinuity of velocity at the junction of the main channel and the flood plain due to strong LMT effects.

- As the flood plain depth increases, the LMT effect gradually diminishes, resulting in a smoother transition of velocity from the deep section of the channel to the flood

plain.

- From the measurements, it is apparent that at low flood plain depth part of the flood plain area acts as a storage section. However, as d/D increases beyond 0.35, the main channel and the flood plains combined can be treated as a *single* unit.

- Proper transverse mixing did not occur in the channel. Also, longitudinal and transverse dispersion of the dye was largely a function of the position of the injection point.

- Dye concentrations were considerably over-predicted by eqs. 5-1 to 5-3, which represent simplified analytical closed-form solutions.

- The time step variation had minimal effect on the stability of the numerical scheme used in the modeling exercise.

- Different *goodness-of-fit* criteria were used in evaluating the model results based on comparisons with the observed data.

- Comparison between measured and predicted concentration curves by CHAT shows a good level of agreement in the general shape, peak concentrations and time to peak. CHAT slightly over-estimated observed peak concentrations.

7.2 RECOMMENDATIONS FOR FUTURE RESEARCH

- Although river flows are a 3-D phenomenon, CHAT was based on a DA version of the continuity, momentum and advection-diffusion equations. It is recommended to extend the present research to develope a full 3-D model for simulating pollutant

transport in compound channels..

- Another approach to a 3-D analysis would be to extend CHAT to simulate the flow in a *multi-layer* process. This results in a *2-D layered-model*, which is a close approximation to the difficult to solve 3-D version of the equations.

- CHAT used the constant eddy viscosity approach. The validity of using the DA k-ϵ turbulence model should be examined.

- Available models quantify LMT, based on steady-state flow conditions. This mechanism should be investigated experimentally under unsteady flow conditions.

- CHAT was used to simulate inert pollutant transport in compound channels flows. It is recommended to modify the structure of the model to allow for (i) other types of pollutants that may decay, and (ii) for a number of different pollutants to be included.

- CHAT was validated by applying it to data collected under nearly uniform flow conditions. The model should be validated for unsteady flow conditions, which will require a modified channel flow delivery system.

- CHAT is applicable to channels with rigid boundaries. Further research effort is required to develop a similar mobile-bed model.

CHAPTER EIGHT

REFERENCES

[1] Abbott, M.B., 1976, *Computational Hydraulics: A Short Pathology,* Journal of Hydraulic Research, V. 14, No. 4, pp. 271-285.

[2] Abbott, M.B., 1976, *Discussion of Review of Models of Tidal Waters by J.B. Hinwood and I.G. Wallis,* Journal of the Hydraulics Division, ASCE, Vol. 102, No. HY8, pp. 1145-1148.

[3] Abbott, M.B.; and Ionescu, F., 1967, *On the Numerical Computation of Nearly Horizontal Flows,* Journal of the Hydraulic Research, Vol. 5, No. 2, pp. 97-117.

[4] Ahsan, A. K. M. Quamrul; Bruno, Michael S, 1989, *Three-Dimensional Modelling of Pollutant Transport,* Proceedings, Estuarine and Coastal Modelling, Newport, RI, Publ by ASCE, Boston Society of Civil Engineers Sect, Boston, MA, USA, pp. 462-471.

[5] Aitken, A.P., 1973, *Assessing Systematic Errors in Rainfall-Runoff Models,* Journal of Hydrology, 20:121-36.

[6] Al-Kadi, Bashir Thabit; Fattah, Qais Nuri, 1991, *Unsteady Transport of Pollutants in Rivers due to Pulse Disposal,* Water Science and Technology, Vol. 23, No. 1-3, pp. 191-200.

[7] Al-Masri, N.; Musa, S.A.; Ameer, W. Abdul, 1989, *Prediction Models of Various Pollutants in the River Tigris at Baghdad,* J. Environ Sci Health, Part A, Vol. A24, No. 1, pp. 23-38.

[8] Al-Soufi, Riyadh W., 1991, *Predicting the Generation and Transport of Pollutants by the Watershed Hydrologic System Model,* Proceedings, ICEP, International Conference on Environmental Pollution, Publ by Inderscience Enterprises Ltd, World Trade Center Bldg, Geneva Aeroport 15, Switz. pp. 888-895.

[9] Amein, M., 1968, *An Implicit Method for Natural Flood Routing,* Water Resources Research, Vol. 4, No. 4, pp. 719-726.

[10] Amein, M., 1966, *Streamflow Routing On Computer By Characteristics,* Water Resources Research, Vol. 2, No. 1, pp. 123-130.

[11] Amein, M., and Chu, H.L., 1975, *Implicit Numerical Modelling Of Unsteady Flows,* Journal of the Hydraulics Division, ASCE, Vol. 101, No. HY6, pp. 717-1451.

[12] Amein, M.; and Fang, C., 1970, *Implicit Flood Routing In Natural Channels,* Journal of the Hydraulic Division, ASCE, No. HY12, pp. 2481-2500.

[13] Amorocho, J.; and Strelkoff, T.S., 1965, *Hydraulic Transients In The California Aqueduct,* Report No. 2, Paper No. 1008, Department of Water Science and Engineering, University of California at Davis.

[14] Aragon, A.B.; Lafuente, J.G.C.; and Comendador, M. S., 1969, *Study on the Pollution of the River Duero and its Principal Tributaries,* Agua. Barcelona, Suppl. No. 4:109-116.

[15] Armstrong, N.E.; and Gloyna, E.F., 1968, *Ecological Aspects of Stream Pollution,* Hidrotehnica, Gospodarirea Apelor, Meteorologia, Bucharest, pp. 83-95.

[16] Arnold, U.; Pasche, E.; and Riouve, G., 1985, *Mixing in Rivers with Compound Cross-section,* Proc. 21st Congress of IAHR, Melbourne, Vol. 2, pp. 167-172.

[17] ASCE Task Committee on Turbulence Models in Hydraulic Computations, 1988, Turbulence Modelling of Surface Water Flow and Transport, Journal of Hydraulic Engineering, ASCE, Vol. 114, No. 9.

[18] ASCE Task Committee on Verification of Models of Hydrologic Transport and Dispersion, 1987, *Performance Evaluation of Surface Water Transport and Dispersion Models,* Journal of Hydraulic Engineering, ASCE, Vol. 113, No. 8, August, pp. 961-980.

[19] Bagdasar'yan, G. A., 1968, *Investigation of River Water for Enteroviruses,* Hyg. and San. Translation of Gigienaii Sanitariia, Moscow, 33(10-12):134-135.

[20] Baltzer, R.A.; and Lai, C., 1968, *Computer Simulation Of Unsteady Flows In Water-Ways,* Journal Of The Hydraulic Division, ASCE, Vol. 94, No. HY4, pp. 1083-1117.

[21] Barrett, M.J.; and Mollowney, B.M., 1972, *Pollution Problems in Relation to the Thames Barrier,* Phil. Trans. R. Soc., London, A., 272.

[22] Bates, P.D.; Malcolm, G.A.; Baird, L., Walling, D.E.; and Simm, D., 1992, *Modeling Floodplain Flows Using Two-Dimensional Finite Element Model,* Earth Surface Processes and Landforms, Vol. 17, pp. 575-588.

[23] Bensabat, J.; Zeitoun, D. G., 1990, *Least-Squares Procedure for the Solution of Transport Problems,* International Journal for Numerical Methods in Fluids, Vol. 10, No. 6, pp. 623-636.

[24] Benque, J.P.; Cunge, J.A.; Feuillet, J.; Hauguel, A.; and Holly, F.M., 1982, *New Method for Tidal Current Computation,* Journal of the Waterway, Port, Coastal and Ocean Division, ASCE, Vol. 108, No. WW3, pp. 396-417.

[25] Bhowmik, N.G.; and Demissie, M., 1982, *Carrying Capacity of Flood Plains,* Journal of the Hydraulics Division, ASCE, No. HY3, March, pp. 443-453.

[26] Bird, Sandra Lee; Holley, E. R., 1985, *Evaluation of a Two-Dimensional Model for Transport of a slug Release in a Meandering Channel,* Tech Rep Univ Tex Austin Central Research Water Resources, CRWR, 92 pp.

[27] Boss Corporation and Brigham Young University, 1992, *Boss FASTTABS,* User's Manual.

[28] Brown, V.M.; Shurben, D.G.; and Shaw, D., 1970, *Studies on Water Quality and the Absence of Fish from Some Polluted English Rivers,* Water Research, Pergamon, 4(5):363-382.

[29] Brooks, A.N.; and Hughes, T.J.R., 1982, *Streamline Upwind Petrov Galerkin Formulations for Convection Dominated Flows with Particular Emphasis on the Incompressible Navier-Stokes Equations,* Computer Methods in Applied Mechanics and Engineering, Vol.32, pp.199-259.

[30] Burdiyan, B.G., 1968, *Contamination of the Ob-Irtysh Basin,* Underwater Naturalist 5(2):18-21.

[31] Buscemi, P.A., 1969, *Chemical and Detrital Features of Palouse River, Idaho, Runoff Flowage,* Oikos 20(1):119-127.

[32] Cadena, Fernando, 1989, *Numerical Approach to Solution of Pollutant Transport Models Using Personal Computers,* CoED, Computers in Education Division of ASEE, Vol. 9, No. 2, pp. 34-36.

[33] Casulli, Vincenzo; Bertolazzi, Enrico; Cheng, Ralph T., 1993, *Three-Dimensional Model for Accurate Simulation of Shallow Water Flow,* Proceedings, National Conference on Hydraulic Engineering, San Francisco, CA, Publ by ASCE, New York, NY, USA, pp. 1988-1993.

[34] Chatila, J.G., and Townsend, R.D., 1996, *Discharge Estimation Methods in Compound Channels flows*, Canadian Water Resources Journal, Vol. 2.

[35] Chatila, J.G., and Townsend, R.D., 1995, *Modelling Flood Plain Conveyance in Compound Channel Flows*, Canadian Journal for Civil Engineering, Vol. 23, No.4.

[36] Chatila, J.G., 1992, *Application and Comparison of Dynamic Routing Models for Unsteady Flows in Simple and Compound Channels*, M.A.Sc. Thesis, Civil Engineering Department, University of Ottawa, Ottawa, Ontario.

[37] Chaudhry, H.M. (1993), *Open-Channel Flow*, Prentice Hall Inc., N.J.

[38] Chau, K., 1991, *Numerical Modelling of Pollutant Transport in Estuaries*, ASCE, Engineering Mechanics Specialty Conference on Mechanics Computing in 1990's and Beyond, Publ by ASCE, New York, NY, USA, pp. 494-498.

[39] Chaudhry, Y.M.; and Contactor, D.N., 1973, *Application of Implicit Method to Surges in Channels*, Water Resources Research, Vol. 9, No. 6, pp. 1605-1612.

[40] Chen, Y.H., and Simon, D.B., 1975, *Mathematical Modelling of Alluvial Channels*, Symp. on Modelling Techniques, ASCE, New York, N.Y., pp. 466-483.

[41] Chow, V.T., 1964, *Handbook of Applied Hydrology*, McGraw Hill Book Co., New York, U.S.A.

[42] Chow, V.T., 1959, *Open Channel Hydraulics*, McGraw Hill Book Co., New York, U.S.A.

[43] Christensen, B. A., 1986, *Marina Design and Evvironmental Concern*, Ports '86, Proceedings, Specialty Conference on Innovations in Port Engineering and Development in the 1990's, Oakland, CA, Publ by ASCE, New York, NY, pp. 307-322.

[44] Cleary, R. W., and Adrian, D.D., 1973, *New Analytical Solutions for Dye Diffusion Equations*, Journal of the Environmental Engineering Division, Proceedings ASCE, Vol. 99, No. EE3, pp. 213-227.

[45] Cokljat, D; Younis, BA, 1995, *Compound-channel flows:A parametric study using Reynolds-stress transport closure*, J.HYDRAUL. RES., vol.33, no.3, pp. 307-320

[46] Cooley, R.L., and Moin, S.A., 1976, *Finite Element Solution of Saint-Venant Equations*, Journal of the Hydraulics Division, ASCE, Vol. 102, No. HY6, pp. 759-775.

[47] Costa, J. R.; Young, P.; French, P., 1987, *Aggregated Dead Zone (ADZ) Interactive Water Quality Model For The Ave River*, Water Science and Technology, Vol. 19, No. 7,

[48] Cruffs, R.W., 1965, *Cross-Channel Transfer of Linear Momentum in Smooth Rectangular Channels*, Geological Survey Water-Supply Paper, 1592-B.

[49] Cunge, J.A., 1975, *Rapidly Varying Flow in Power and Pumping Canals*, in: K. Mahmood and V. Yevjevich (Editors), Unsteady Flow in Open Channels, Vol. II, Chapter 14, pp. 539-586, Water Resources Publications, Fort Collins, Colorado.

[50] Cunge, J.A., 1966, *Etude d'un Schema de Differences Finies Applique a l'Integration Numerique d'un Certain Type d'Equation Hyperbolique d'Ecoulement*, Thesis, Grenoble University, France.

[51] Cunge, J.A.; Holly, F.M. Jr.; and Verwey, A., 1986,

[52] Cunge, J.A.; Holly, F.M. Jr.; and Verwey, A., 1980, *Practical Aspects of Computational River Hydraulics*, Pitman, London.

[53] Cunge, J.A; and Wegner, M., 1964, *Integration Numerique des Equations D'Ecoulement De Barre de Saint-Venant Par Un Schema Implicite De Differences Finies*, La Houille Blanche, Grenoble, France, No. 1, pp. 33-39.

[54] Dronkers, J.J., 1969, *Tidal Computations for Rivers, Coastal Areas, and Seas*, Journal of the Hydraulics Division, ASCE, Vol. 95, No. HY1, pp. 29-77.

[55] Datsenko, Yuri; Edelstein, Konstantin; Ivanenko, Sergei; Kochurov, Alexander, 1993, *Simulation of the Propagation of Conservative Contamination*, Proceedings, Symposium on Engineering Hydrology, San Francisco, CA, Publ by ASCE, New York, NY, USA. pp. 497-502.

[56] Dawdy, D.R., and O'Donnell, T., 1965, *Mathematical Model of Catchment Behaviour*, Journal of the Hydraulics Division, Proceedings of ASCE, Vol. 91, No. HY4, pp. 123-137.

[57] De Long , L.L., 1989, *Mass Conservation: 1-D Open Channel Flow Equations*, Journal of the Hydraulic Engineering, Vol. 115, No. 2, pp.263-269.

[58] De Saint Venant, A.J.C. Barre', 1871, *Théorie du mouvement non-permanent des Eaux avec Application aux crues des Rivieres et a l'introduction des Mareées dans leur lit, (Theory of Unsteady Water Flow, with Apllication to River Floods and to Propagation of Tides in River Channels)*, Comptes Rendus, Vol. 73, Academy Science, Paris, pp. 148-154, 237-240.

[59] Diskin, M.H., and Simon, E., 1977, *A Procedure for the Selection of Objective Functions for Hydrologic Simulation Models*, Journal of Hydrology, 34(1/2):129-49.

[60] Djordjevic, S., 1993, *Mathematical Model of Unsteady Transport and its Experimental Verification in a Compound Open Channel Flow*, Journal of Hydraulic Research, Vol. 31, No. 2, pp. 229-248.

[61] Dracos, T., and Hardegger, P., 1987, *Steady Uniform Flow in Prismatic Channels with Flood Plains," Journal of Hydraulic Research*, Vol. 25, No. 2, pp. 169-185.

[62] Elder, J.W., 1959, The Dispersion of Marked Fluid in Turbulent Shear Flow, Journal of Fluid Mechanics, Vol. 5, No. 4, pp. 544-560.

[63] Falconer, R. A., 1992, *Coastal Pollution Modelling: Hydrodynamic Tidal Models*, Proceedings, Institution of Civil Engineers, Water Maritime and Energy, Vol. 96, No. 3, pp. 183-185.

[64] Fischer, H. B.; List, E. J.; Koh; R. C. Y., Imberger, J.; and Brooks, N. H., 1979, *Mixing in Inland and Coastal Waters*, Academic Press, New York.

[65] Fischer, H.B.; and Holley, E.R., 1971, *Analysis of the Use of Distorted Hydraulic Models for Dispersion Studies*, Water Resources Res., 7(1), pp. 46-51.

[66] Fischer, H.B., 1966, *Longitudinal Dispersion in Laboratory and Natural Streams*, Report No. KH-R-12, W.M. Keck Laboratory of Hydraulics and Water Resources, California Institute of Technology, Pasadena.

[67] Fletcher, A.G.; and Hamilton, W.S., 1967, *Flood Routing In Irregular Channel*, Journal of the Engineering Mechanics Division, ASCE, Vol. 93, No. EM3, pp. 45-62.

[68] Fletcher, R. and Powell, M.J.D., 1963, *A Rapidly Convergent Descent Method for Minimization*, Computer Journal, 6(2):163-86.

[69] Fread,D.L., 1974, *Numerical Properties Of Implicit Four-Point Finite Difference Equations Of Unsteady Flow*, NOAA Technical Memorandum NWS HYDRO 18, NOAA, pp. 88.

[70] Froehlich, D.C., 1989, *Finite Element Surface Water Modelling System: Two-Dimensional Flow in a Horizontal Plane*, Users Manual, U.S. Federal Highway Administration, report No. FHWA-RD-88-177.

[71] Fuller, G.W.; and McClintock, J.R., 1926, *Solving Sewage Problems*, McGraw-Hill, New York.

[72] Forsius, J., 1984, *Computing Unsteady Flow and racer Movement in a River,* Vesientutkimuslaitoksen Julk 60, pp. 3-21.

[73] Garrison, J.M., Granju, J.P., and Price, J.T., 1969, *Unsteady Flow Simulation in Rivers and Reservoirs,* Journal of the Hydraulics Division, ASCE, Vol. 95, No. HY5, pp.1559-1576.

[74] Gray, H.F., 1940, *Sewerage in Ancient and Medieval Times,* sewage Wks. J., 12, pp. 939-946.

[75] Gray, William G. (Ed.), 1986, *Physics-Based Modelling of Lakes, Reservoirs, and Impoundments,* Phys-Based Model of Lakes, Reservoirs, and Impoundments, Publ by ASCE, New York, NY, USA, 308p.

[76] Gunaratnam, D.J.; and Perkins, F.E., 1970, *Numerical Solution of Unsteady Flows in Open Channels,* Hydrodynamic Laboratory Report 127, Department of Civil Engineering, Massachusetts Institute of Technology, Cambridge, Massachusetts.

[77] Hayter, Earl J.; Pakala, Chalam V, 1988, *Three-Dimensional Modelling of Cohesive Sediments and Pollutants in Surface Waters,* Proceedings, National Conference on Hydraulic Engineering, Colorado Springs, CO, Publ. by ASCE, New York, NY, USA, pp. 236-241.

[78] Hicks, F.E.; and Steffler, P.M., 1992, *Characteristic Dissipative Galerkin Scheme for Open Channel Flow,* Journal of Hydraulic Engineering, ASCE, Vol. 118, pp. 37-352.

[79] Hicks, F.E.; and Steffler, P.M., 1990, *Finite Element Modeling of Open Channel Flow,* Department of Civil Engineering, University of Alberta, Technical Report (WRE 90-6).

[80] Hinwood, J.B., and Wallis, I.G., 1975-a, *Classification of Models of Tidal Waters,* Journal of the Hydraulics Division, ASCE, Vol. 101, No. HY10, pp. 1315-1331.

[81] Hinwood, J.B., and Wallis, I.G., 1975-b, *Review of Models of Tidal Waters,* Journal of the Hydraulics Division, ASCE, Vol. 101, No. HY11, pp. 1405-1421.

[82] Hirch, C., 1988, *Numerical Computation of Internal and External Flows,* John Wiley and Sons. Vols. 1 and 2.

[83] Hoffman, J.D., 1993, *Numerical Methods for Engineers and Scientists,* McGraw-Hill, Mechanical Engineering Series.

[84] Holly, F.M. Jr; Nerat, G, 1983, *Field calibration of sream-tube dispertion model,* J. HYDRAUL. ENG., vol.109,no.11,pp. 1455-1470

[85] Holly, F.M. Jr., 1985, *Dispersion in Rivers and Coastal Waters-1. Physical Principles and Dispersion Equations,* Developments in Hydraulic Research-3, Ed. by P. Novak, Elsier Applied Science, London, pp. 1-37.

[86] Holly, F.M. Jr.; and Cunge, J.A., 1975, *Prediction of Time-Dependent Mass Dispersion in Natural Streams,* Proceedings of Modelling 75, ASCE Hydraulics Division, February.

[87] Holly, F.M. Jr.; Preissmann, A., 1977, *Accurate Calculation of Transport in Two Dimensions,* Journal of the Hydraulics Division, Proceedings ASCE, Vol. 103, No. HY11, pp. 1259-1277.

[88] Holly, F.M. Jr.; Usseglio-Polatera, J.M., 1984, *Dispersion Simulation in Two-Dimensional Tidal Flow,* Journal of the Hydraulic Engineering, ASCE, Vol. 110, No. 7, pp. 905-926.

[89] Ibbitt, R.P., and O'Donnell, T., 1971, *Fitting Methods for Conceptual Catchment Models,* Journal of the Hydraulics Division, Proceedings of ASCE, Vol. 100, No. HY7, pp. 005-1109.

[90] Isaacson, E., Stoker, J.J., and Troesch, A., 1954, *Numerical Solution of Flood Prediction and River Regulation Problems,* Report II, Courant Institute Of Mathematical Science, No. IMM 205.

[91] Isaacson, E.; Stoker, J.J.; and Troesch, A., 1958, *Numerical Solution Problems in Rivers,* Journal of the Hydraulics Division, ASCE, Vol. 84, No. HY5, pp. 1-18.

[92] Januszewski, U., 1980, *Automatische Eichung Fur ein-und zweidimensionale hydrodynamisch-numerische Flachwassermodelle,* Dissertation Uni. Hannover, Fortschr.-Ber. VDI-Zeitschriften, Reihe 4, Nr. 58.

[93] Jirka, Gerhard H.; Akar, Paul J, 1993, *Density Currents in Pollutant Transport and Mixing,* Proceedings, National Conference on Hydraulic Engineering. Part 1, San Francisco, CA, Publ by ASCE, New York, NY, USA, pp. 838-844.

[94] Johnson, B.H., 1974, *Unsteady Flow Computations on the Ohio-Cumberland-Tennessee-Mississippi River System,* Technical Report H-74-8, Hydraulics Laboratory, Waterways Experiment Station, U.S. Army Corps of Engineers.

[95] Johnson, J., 1933, *Reminiscences of 45 years as a River Inspector,* J. Inst. Se. Purif., 1, pp. 17-19.

[96] Johnston, P.R., and Pilgrim, D.H., 1976, *Parameter Optimization for Watershed Models,* Water Resources Res., Vol. 12 No. 3.

[97] Karasev, I.F., 1969, *Influence of Banks and Flood Plain on Channel Conveyance*, Soviet Hydrology: Selected Papers, Issue No. 5, pp. 429-442.

[98] Keller, R. J. and Rodi, W., 1984, *Prediction of Two-dimensional Flow Characteristics in Complex Channel Cross-sections*, Proc. International Conference on Hydraulic Engineering Software, Portoroz, Yugoslavia, Elsevier, pp. 3-3 to 3-14.

[99] Kimura, I., 1988, *Aquatic Pollution Problems in Japan*, Aquatic Toxicology, 11, pp. 287-301.

[100] King, I.P.; and Norton, W.R., 1986, *Finite Element Model for Two-Dimensional Depth Averaged Flow*, RMA-2V, Version 3.3b, Resources Management Associates, Lafayette, CA.

[101] Kolovopoulos, P., 1990, *Streamflow Modelling*, Report 7, Water Systems Research Group, University of the Witwatersrand, Johannesburg.

[102] Komatsu, T.; Holly, F. M. Jr.; Nakashiki, N.; and Ohgushi, K., 1985, *Numerical Calculation of Pollutant Transport in One and two Dimensions*, Journal of Hydroscience and Hydraulic Engineering, Vol. 3, No. 2, pp. 15-30.

[103] Krishnappan, B.G.; and Lau, Y.L., 1986, *Turbulence Modelling of Flood Plain Flows*, Journal of Hydraulic Engineering, ASCE, Vol. 112, No. 4, pp. 251-266.

[104] Krishnappan, B.G., and Lau, Y.L., 1977, *Transverse Mixing in Meandering Channels with Varying Bottom Topography*, Journal of Hydraulic Research, 15(4), pp. 351-369.

[105] Lafe, Olu, 1986, *Pollutant Transport in Surface Flows - A New Boundary Element Approach*, Proceedings, International Conference on Water Quality Modelling in the Inland Natural Environment, Bournemouth, Engl, pp. 449-456.

[106] Lai, C., 1986, *Numerical Modelling of Unsteady Open-Channel Flow*, Advances in Hydroscience, Vol. 14, B.C.Yen, ed., Academic Press, Orlando, Fl, pp. 161-333.

[107] Lai, C., 1965-a, *Flows Of Homogeneous Density In Tidal Reaches: Solution By The Method Of Characteristics*,Open-File Report, United States Department of the Interior, Geological Survey, Washington, D.C.

[108] Lai, C., 1965-b, *Flows Of Homogeneous Density In Tidal Reaches: Solution By The Implicit Method*, Open-File Report, United States Department of the Interior, Geological Survey, Washington, D.C.

[109] Lam, D.C.L., 1975, *Computer Modelling of Pollutant Transports in Lake Erie*, Mathematical Models for Environmental Problems, edited by C.A. Brebbia, Proceedings of the International Conference held at the University of Southampton, England, pp. 237-251.

[110] Land, L.F., 1978, *Unsteady Solute-Transport Simulation in Stream flow Using a Finite-Difference Model*, USGS Water Resource Investigations, 78-18, NSTL Station, Mississippi 39529.

[111] Lau, Y.L, and Krishnappan, B.G., 1981, *Modeling Transverse Mixing in Natural Streams*, Journal of Hydraulics Division, ASCE, Vol. 107, No. HY2, pp. 209-226.

[112] Lau, Y.L, and Krishnappan, B.G., 1977, *Transverse Dispersion in Rectangular Channels*, Journal of Hydraulics Division, Vol. 103, No. HY10, pp. 1173-1189.

[113] Lax, P.D., 1954, *Weak Solutions of Non-Linear Hyperbolic Equations and Their Numerical Computations*, Comm. Pure and Appl. Math. Vol. 2, pp. 159-193.

[114] Leclerc, M.; Bellemare, J.; Dumas, G.; and Dhatt, G., 1990, *A Finite Element Model of Estuarian and River Flows with Moving Boundaries*, Advances in Water Resources, Vol. 13, No. 4, pp. 158-168.

[115] Lee, J.K.; and Froehlich, D.C., 1986, *Review of Literature on the Finite-Element Solution of the Equations of Two-Dimensional Surface-Water Flow in the Horizontal Plane*, U.S. Geological Survey, Circular 1009.

[116] Liggett, J.A., 1987, *Forty Years of Computational Hydraulics--1960-2000*, Proceedings of the 1987 National Conference on Hydraulic Engineering, Hydraulic Engineering, Edited by Robert M. Ragan, pp. 1124-1133.

[117] Liggett, J.A., 1968, *Mathematical Flow Determination in Open Channels*, ASCE-Proc., Journal of Engineering Mechanics Division, Vol. 94, No. EM4, pp. 947-963.

[118] Liggett, J.A., and Cunge, J.A., 1975, *Numerical Methods of Solution of the Unsteady Flow Equations in Open Channels*, Unsteady Flow in Open Channels, K. Mahmood and V. Yavjevich, Eds. Vol. 1, Water Resources Publications, Fort Collins, Colorado, pp. 89-182

[119] Liggett, J.A., and Woolhiser, D.A., 1967, *Difference Solutions Of The Shallow-Water Equations*, Journal Of The Engineering Mechanics Division, ASCE, Vol. 93, No. EM2, Proc. Paper 5189.

[120] Lin, B; Shiono, K, 1995, *Numerical modelling of solute transport in compound channel flows*, J.HYDRAUL. RES., vol.33, no.6, pp.773-788

[121] Maier-Reimer, E., 1982, *On Tracer Methods in Computational Hydrodynamics*, Engineering Applications of Computational Hydraulics, Vol. 1, Edited by M.B. Abbott and J.A. Cunge, pp. 198-217.

[122] Martin, B., 1974, *Numerical Representations which Model Properties of the Solution to the Diffusion Equation*, Journal of Computational Physics, Vol. 17, pp. 358-383.

[123] McCorquodale, John A.; Ibrahim, Kamal; Hamdy, Yousry, 1986, *Fate and Transport Modelling of Perchloroethylene in the St. Clair River*, Water Pollution Research Journal of Canada, Vol. 21 No. 3, pp. 398-410.

[124] Meissner, U.; Narten, M.; and Ratke, R., 1982, *Numerical Models and Their Calibration for the Analysis of Flow and Heat Transport Problems in Rivers*, Proc. 4th Int. Symp. on Finite Element Methods in Flow Problems, Chuo University, Tokyo, Japan, edited by Tadahiko Kawai, pp. 595-601.

[125] Ming, J., 1992, *A Random Differential Equation Model For Predicting Water Quality*, Journal of Hydraulic Engineering, Vol.1, pp. 299-310.

[126] Moeller, Jeffrey, C.; Adams, E. Eric, 1994, *Comparison of Eulerian-Lagrangian, random walk and hybrid methods of modelling pollutant transport*, Proceedings, 3rd International Conference on Estuarine and Coastal Modelling III, Oak Brook, IL, Publ by ASCE, New York, NY, USA. pp. 609-623.

[127] Mollowney, B.M., 1975, *Solution of the Advective-Diffusion Equation by the Method of Moving Coordinate Systems with Particular Reference to the Modelling of Estaurine Pollution*, Mathematical Models for Environmental Problems, edited by C.A. Brebbia, Proceedings of the International Conference held at the University of Southampton, England, pp. 313-327.

[128] Mollowney, B.M., 1973, *One-Dimensional Models of Estaurine Pollution*, In Mathematical and Hydraulic Modelling of Estaurine Pollution, Edited by A.L.H. Gameson, Water Pollution Research Technical Paper, No. 13, H.M. Stationary Office, London.

[129] Myers, W.R.C., 1978, *Momentum Transfer in Compound Channels*, Journal of Hydraulic Research, Vol. 16, No. 2, pp. 139-150.

[130] Nelder, J.A., and Mead, R., 1965, *Simplex Method for Function Minimization*, Computer Journal, Vol. 7, No. 4, pp.308-313.

[131] Neuman, S.P., 1980, *Adjoint-State Finite Element Equations for Parameter Estimation*, Proc. 3rd Int. Conf. Finite Element Methods in Water Resources, Mississippi University, USA., pp. 595-601.

[132] Nicollet, G.; and Uan, M., 1979, *Ecoulements permanents a surface libre en fits composes*, La Houille Blanche, No. 1, pp. 21-30.

[133] Naot, D.; Nezu, I.; and Nakagawa, H., 1993, *Hydrodynamic Behaviour of Compound Rectangular open Channels*, Journal of Hydraulic Engineering, ASCE, Vol. 119, pp. 390-408.

[134] Naot, D.; Nezu, I.; and Nakagawa, H., 1993 *Calculation of compound-open-channel flow*, J. HYDRAUL.RES.,vol.34,no.3, pp. 381-394, 1996

[135] Noye, B.J.; Hayman, K.J., 1993, *Implicit Two-Level Finite-Difference Methods for the Two-Dimensional Diffusion Equation*, International Journal of Computer Mathematics, Vol. 48, No. 3-4, pp. 219-227.

[136] Okoye, J.K., 1970, *Characteristics of Transverse Mixing in Open Channel Flows*, Report KH-R-23, California Institute of Technology, Pasadena.

[137] Pasche, E., Rouve, G. and Evers, P., 1985, *Flow in Compound Channels with Extreme Flood-Plain Roughness*, Proc. 2Ist Congress of International Association for Hydraulic Research, Melbourne, Australia, Vol. 3, pp. 383-389.

[138] Paulson, A.J.; Curl, H.C.; and Feely, R.A., 1989, *Estimates of Trace Metal Inputs from Non-point Source Discharged into Estauries*, Marine Pollution Bulletin, Vol. 20, No. 11, pp. 549-555.

[139] Pezzinga, G, 1994, *Velocity distribution in compound channel flows by numerical modeling*, J. HYDRAUL. ENG., vol. 120,no.10,pp.1176-1198

[140] Platzman, G.W., 1959, *A Numerical Computation of the Surge of 26 June 1954 on Lake Michigan*, Geophysics, Vol. 6, No. 3-4.

[141] Ponce, V.M.; Indlekofer, H.; and Simons, D.B., 1978, *Convergence of Four-Point Implicit Water Wave Models*, Journal of the Hydraulics Division, Proc. ASCE, Vol. 104, No. HY7, pp.947-958.

[142] Posey, C.J., 1967, *Comparison of Discharge Including Over-Bank Flow*, Civil Engineering, Vol. 37, No. 4, pp. 62-63.

[143] Pasuhn, A. 1992, *Fundamentals of Hydraulic Engineering*, Oxford Press.

[144] Prinos, P.; and Townsend, R., 1984, *Comparison of Methods for Predicting Discharge in Compound Open Channels*, Advances in Water Resources, Vol. 7, pp. 180-187.

[145] Preissman, A., 1961, *Propagation des Inntumescences Dans les Cammaux et les Rivieres*, le Congress de L'Association Francaise de Calcule, Grenoble, France, pp. 433-442.

[146] Prinos, P.; and Townsend, R., 1983, *Estimating Discharge in Compound Open Channels*, Proceedings of the Canadian Hydrotechnical Conference, Vol. 1, Ottawa, Canada, pp. 129-146.

[147] Radojkovic, M. and Djordjevic, S.,1985, *Computation of Discharge Distribution in Compound Channels*, Proc. 21st Congress of International Association for Hydraulic Research, Melbourne, Australia, Vol. 3, pp. 367-371.

[148] Rajar, R., 1990, *Three-Dimensional Mathematical Model of Currents and of Transport of Pollutants in the Adriatic*, Computational Methods in Surface Hydrology, Proc., 8 Int Conf Comput Method Water Resour, Publ by Springer-Verlag Berlin, Dept ZSW, Berlin 33, GER, pp. 57-62.

[149] Rajaratnam, N. and Ahmadi, R., 1981, *Hydraulics of Channels with Flood-plains*, Journal of Hydraulic Research, Vol. 19, No. 1, pp. 43-60.

[150] Rajaratnam, N.; and Ahmadi, R., 1979, *Interaction Between Main Channel and Flood Plain Flows*, Journal of the Hydraulic Division, ASCE, pp. 573-588.

[151] Rastogi, A. K.; and Rodi, W., 1978, *Predictions of Heat and Mass Transfer in Open Channels*, Journal of the Hydraulics Division, ASCE, Vol. 104, No. HY3, pp. 397-420.

[152] Ren, W.M.; Ghiaasiaan, S.M.; Abdel-Khalik, S.I., 1994, *GT3F: An Implicit Finite-Difference Computer Code for Transient Three-Dimensional Three-Phase Flow, Part II: Applications*, Numerical Heat Transfer, Part B: Fundamentals, Vol. 25, No. 1, pp. 21-38.

[153] Ren, W. M.; Ghiaasiaan, S.M.; Abdel-Khalik, S.I., 1994-b, *GT3F: An Implicit Finite-Difference Computer Code for Transient Three-Dimensional Three-Phase Flow Part I: Governing Equations and Solution Scheme*, Numerical Heat Transfer, Part B: Fundamentals, Vol. 25, No. 1, pp. 1-20.

[154] Richtmyer, R.D., 1962, *A Survey of Difference Methods for Non-Steady Fluid Dynamics*, NCAR Technical Notes 63-2, National Centre for Atmospheric Research, Boulder, Colorado.

[155] Richtmyer, R.D., and Morton, K.W., 1957, *Difference Methods for Initial Value Problems*, Interscience Publishers, New York, Second Edition.

[156] Rodi, W., 1984, *Turbulence Models and Their Application in Hydraulics-A State of the Art Review*, Second Edition, IAHR, Delft.

[157] Rodi, W., 1980, *Turbulence Models and Their Application in Hydraulics: A State-of-the-Art Review*, International Association for Hydraulic Research Book Publication, Delft.

[158] Rouse, H., 1959, *Advanced Mechanics of Fluid*, Wiley, New York.

[159] Sauvaget, P., 1985, *Dispersion in Rivers and Coastal Waters-2. Numerical Computation of Dispersion*, Developments in Hydraulic Research-3, Ed. by P. Novak, Elsier Applied Science, London, pp. 39-78.

[160] Savant, S. Anne; Reible, Danny D.; Thibodeaux, Louis J., 1986, *Modelling Convective Transport in River Sediments*, Proceedings, American Chemical Society, Division of Environmental Chemistry 192nd National Meeting, Anaheim, CA, USA, Vol. 26 No. 2, pp. 36-39.

[161] Schumann, A. H.; Koncsos, L.; Schultz, G. A., 1991, *Estimation of Dissolved Pollutant Transport to Rivers from Urban Areas: A Modelling Approach*, IAHS, International Association of Hydrological Sciences No. 203, pp. 267-276.

[162] Sellin, R. H., 1964, *A Laboratory Investigation into the Interaction between the Flow in the Channel of a River and that over its Flood-plain*, La Houille Blanche, Grenoble, France, No 7, pp. 793-802.

[163] Seo, W., 1990, *Laboratory and Numerical Investigation of Longitudinal Dispersion in Open Channels*, Water Resources Bulletin, Vol. 26, No. 5, pp. 811-822.

[164] Shiono, K.; and Knight, D.W., 1991, *Turbulent Open Channel Flows with Variable Depth Across the Channel*, Journal of Fluid Mechanics, Vol. 222, pp. 617-646.

[165] Simons, T. J.; Lam, D. C. L., 1986, *Documentation of a Two-Dimensional X-Y Model Package for Computing Lake Circulations and Pollutant Trasports*, Phys-Based Model of Lakes, Reservoirs, and Impoundments, Publ by ASCE, New York, NY, USA, pp. 258-308.

[166] Soulis, J.V., 1992, *Computation of Two-Dimensional Dam-Break Flood Flows*, International Journal for Numerical Methods in Fluids, Vol. 14, pp. 631-664.

[167] Stoker, J.J., 1957, *Water Waves*, Interscience.

[168] Stoker, J.J., 1953, *Numerical Solution of Flood Prediction and River Regulation Problems, I: Derivation of Basic Theory and Formulation of Numerical Methods of Attack,* New York University, Institute of Mathematical Sciences, Report No. IMM-200.

[169] Streeter, V.L., 1948, Fluid Dynamics, McGraw-Hill, New York.

[170] Strelkoff, T., and Amorocho, J., 1965, *Gradually Varied Unsteady Flow In A Controlled Canal System,* Proceedings, International Association For Hydraulic Research, Eleventh International Congress, Leningrad, No. 3.16,8 pp. Also, Vol. VI, Transactions of the Congress (I.A.H.R.XI Congress), Discussion, pp. 317-320.

[171] Stronach, J. A.; Murthy, C. R.; Murty, T. S, 1992, *Pollutant Transport Modelling in Large River Plumes,* Proceedings, 2nd International Conference on Estuarine and Coastal Modelling, Tampa, FL, Publ by ASCE, New York, NY, USA, pp. 759-770.

[172] Swanson, J. , Craig; Howlett, Eoin; Mendelsohn, Daniel, L, 1992, *PC-Based Integrated Water Quality Impact and Analysis System,* Proceedings, 2nd International Conference on Estuarine and Coastal Modelling, Tampa, FL, Publ by ASCE, New York, NY, USA, pp. 489-500.

[173] Sweerts, J. -P. R. A.; Koeze, R. D.; de Nijs, A. C. M.; Knoop, J. M.; Behrendt, H.; van Pagee, J. A, 1992, *Pollutants Transport and Management of the River Rhine,* European Water Pollution Control, Vol. 2, No. 3, pp. 42-47.

[174] Taylor, G.I., 1954, *The Dispersion of Matter in Turbulent Flow through a Pipe,* Proc. R. Soc., London, pp. 446-468.

[175] Thatcher, M.L.; and Harleman, D.R.F., 1972, *Mathematical Model for the Prediction of Unsteady Salinity Intrusion in Estauries,* Dept. Civil eng., Ralph M. Parsons Lab., Water Resources Hydrodyn., Report No. 144, pp.232.

[176] THOMAS,TG; WILLIAMS, JJR, 1995, *Large eddy simulation of a symmetric trapezoidal channel at a Reynolds number of 430,000,* J. HYDRAUL. RES./J.RECH. HYDRAUL., vol. 33, no.6,pp. 825-842

[177] Tingsanchali, T.; and Ackermann, N.L., 1976, *Effects of Overbank Flow in Flood Computations,* Journal Of The Hydraulics Division, ASCE, Vol. 102, No. HY7, pp. 1013-1025.

[178] Tominaga, A.; and Nezu, I., 1991, *Turbulent Structure in Compound Open Channel Flows,* Journal of Hydraulic Engineering, ASCE, Vol. 117, pp. 21-41.

[179] Tsanis, I.K., and Wu, J., 1992, *Transport and Dispersion of Pollutants in a Distorted Model of the Windermere Basin,* Proceeding, Annual Conference of the Canadian Society for Civil Engineers, Quebec City, P.Q., pp. 35-44.

[180] Vasil'ev, A. A., 1987, *Numerical Calculation of Pollutant Transport in Rivers,* Soviet Meteorology and Hydrology (English Translation of Meteorologiya i Gidrologiya), No. 7, pp. 80-86.

[181] Verboom, G.K., 1975, *The Advection-Dispersion Equation for an AN-Isotropic Medium Solved by Fractional-Step Methods,* Mathematical Models for Environmental Problems, edited by C.A. Brebbia, Proceedings of the International Conference held at the University of Southampton, England, pp. 299-312.

[182] Vicens, G.J., Rodriguez-Itrube, I., and Schaake, J.C., 1975, *Bayesian Framework for the Use of Regional Information in Hydrology,* Journal of Water Resources Res., Vol. 11, No. 3, pp.405-414.

[183] Walters, R.A., 1983, *Numerically Induced Oscillations in Finite Element Approximations to Shallow Water Equations,* International Journal for Numerical Methods in Fluids, Vol. 3, pp. 591-604.

[184] Walters, R.A.; and Cheng, T., 1980, *Accuracy of an Estuarine Hydrodynamic Model Using Smooth Elements,* Water Resources Research, Vol. 16, No. 1, pp. 187-195.

[185] Wang, T.; Lenahan, R.; Kanik, M.; Teneyck, J., 1986, *Removal of Trichloroethylene (TCE) Contaminated Groundwater and Impacts of Contaminants Discharged to the Main Canal and Indian River Estuary, Florida, USA,* Water Science and Technology, Vol. 4-5, pp. 52.

[186] Webel, G., and Schatzmann, M., 1980, *The Role of Bed Roughness in Turbulent Diffusion and Dispersion,* Theme D, International Symposium River Engineering and its Interaction with Hydrological and Hydraulic Research, IAHR, Belgrade.

[187] Wormleaton, A. J.; and Merret, D.J., 1990, *An Improved Method of Calculation for Steady Uniform Flow in Prismatic Main Channel/ Flood Plain Sections,* Journal of Hydraulic Research, Vol. 28, No. 2, pp. 157-174.

[188] Wormleaton, A. J., Allan, J., and Hadjipanos, P., 1982, *Discharge Assessment In Compound Channel Flow,* Journal Of The Hydraulics Division, ASCE, Vol. 108, No. HY9, pp. 975-994.

[189] Wright, R.R.; and Carstens, H.R., 1970, *Linear Momentum Flux To Overbank Sections,* Journal of the Hydraulic Division, ASCE, Vol. 96, No. HY9, pp. 1781-1793.

[190] Wright, L., 1960, *Clean and Decent: the Fascinating History of the Bathroom and the Water Closet*, Routledge and Kegan Paul, London.

[191] Yang, J.C.; and Hsu, E.L., 1991, *On the Use of the Reach-Back Characteristics Method for Calculation of Dispersion*, International Journal for Numerical Methods in Fluids, Vol. 12, No. 3, pp. 225-235.

[192] Yang, J.C.; Lee, H.P.; Chang, J.H., 1992, *Pollutant Transport Modelling for a Complex River System*, 4th Int Conf Hydraul Eng Software HYDROSOFT/92, Publ by Computational Mechanics Inc, Billerica, MA, USA. pp. 48-60.

[193] Yeh, G.T., and Tsai, Y.J., 1976, *Analytical Three-Dimensional Transient Modelling of Effluent Discharges*, Water Resources Research, Vol. 12, No. 3, pp. 533-540.

[194] Yen, C.L., and Overton, D.E., 1973, *Shape Effects On Resistance In FloodPlain Channels*, Journal Of The Hydraulic Division, ASCE, Vol. 99, No.HY1, pp. 219-238.

[195] Young, P. C.; Wallis, S. G., 1986, *Aggregated Dead Zone (ADZ) Model for Dispersion in Rivers*, Proceedings, International Conference on Water Quality Modelling in the Inland Natural Environment, Bournemouth, Engl, pp. 10-13.

[196] Zheleznyakov, G.V., 1971, *Interaction of Channel and Floodplain Streams*, Proceedings, Fourteenth International Conference of the International Association for Hydraulic Research, Paris, France.

[197] Zheleznyakov, G.V., 1965, *Relative Deficit of Mean Velocity of Instable River Flow; Kinematic Effect in River Beds with Floodplains*, Proceedings of the Eleventh International Conference of the International Association for Hydraulic Research, Leningrad, U.S.S.R.

[198] Zhou, D.H.; Shen, H.W.; Tabios, G.Q.; Lai, J.S.; and Tan, W.Y., 1994, *Finite Volume Two-Dimensional Unsteady-Flow Model for River Basins*, Journal of Hydraulic Engineering, ASCE, Vol. 120, No. 7, pp. 863-883.

APPENDIX A

GOVERNING EQUATIONS FOR THE FLOW PROBLEM

The derivation of the basic differential equations begins from the general equations of continuity and motion for an incompressible fluid in classical hydrodynamics, (Streeter, 1948; Rouse, 1959). These equations, which are referred to as the Navier-Stokes equations, are derived in 3-D.

A.1 EQUATION OF CONTINUITY

The equation of continuity, or conservation of mass, is derived from the principle that matter is neither created nor destroyed in the flow through an infinitesimal control volume. With reference to an elementary control volume as shown in the definition sketch of figure A.1, the faces are parallel to a Cartesian set of axes (x,y,z), having its centre at point (x,y,z) and its dimensions as Δx, Δy, and Δz. The velocity vector has the components u, v, and w along the x, y, and z directions respectively. With ***no restrictions made regarding the nature of the fluid*** and applying the mass balance principle:

'ate of inflow - rate of outflow = rate of accumulatio **(A-1)**

In the x-direction:

$$\textit{Rate of inflow} = \left[\rho u - \frac{\partial (\rho u)}{\partial x}\,\frac{\Delta x}{2}\right] \Delta y\ \Delta z \qquad \textbf{(A-2)}$$

where ρ = fluid density.

$$\textit{Rate of outflow} = \left[\rho u + \frac{\partial (\rho u)}{\partial x}\,\frac{\Delta x}{2}\right] \Delta y\ \Delta z \qquad \textbf{(A-3)}$$

Substituting eq. (A-2) and (A-3) in eq. (A-1), neglecting the higher order terms and simplifying gives:

$$\textit{Net rate of storage in } x = -\frac{\partial (\rho u)}{\partial x}\ \Delta x\ \Delta y\ \Delta z \qquad \textbf{(A-4)}$$

In the same manner, the corresponding net change in the y-direction is:

$$\textit{Net rate of storage in } y = -\frac{\partial (\rho v)}{\partial y}\ \Delta x\ \Delta y\ \Delta z \qquad \textbf{(A-5)}$$

and in the z-direction is:

$$\textit{Net rate of storage in } z = -\frac{\partial (\rho w)}{\partial z}\ \Delta x\ \Delta y\ \Delta z \qquad \textbf{(A-6)}$$

Hence, the total net mass storage per unit of time is:

$$-\left[\frac{\partial (\rho u)}{\partial x} + \frac{\partial (\rho v)}{\partial y} + \frac{\partial (\rho w)}{\partial z}\right] \Delta x\ \Delta y\ \Delta z$$

However, this rate must also equal the rate of change of storage given by:

$$\frac{\partial}{\partial t} (\rho \, \Delta x \, \Delta y \, \Delta z)$$

where t = time.

Since Δx, Δy, and Δz are independent of time then:

$$\frac{\partial}{\partial t} (\rho \, \Delta x \, \Delta y \, \Delta z) = \frac{\partial \rho}{\partial t} \Delta x \, \Delta y \, \Delta z \qquad \textbf{(A-9)}$$

Consequently (combining above expressions):

$$\frac{\partial \rho}{\partial t} \Delta x \, \Delta y \, \Delta z =$$

$$- \left[\frac{\partial (\rho u)}{\partial x} + \frac{\partial (\rho v)}{\partial y} + \frac{\partial (\rho w)}{\partial z} \right] \Delta x \, \Delta y \, \Delta z \qquad \textbf{(A-10)}$$

Dividing by the volume ($\Delta x \Delta y \Delta z$) of the control volume and rearranging gives the continuity equation in cartesian coordinates as:

$$\frac{\partial \rho}{\partial t} + \frac{\partial (\rho u)}{\partial x} + \frac{\partial (\rho v)}{\partial y} + \frac{\partial (\rho w)}{\partial z} = 0 \qquad \textbf{(A-11)}$$

For a fluid with constant density eq. A-11 reduces to:

$$\frac{\partial u}{\partial x} + \frac{\partial v}{\partial y} + \frac{\partial w}{\partial z} = 0 \qquad \textbf{(A-12)}$$

A.2 EQUATIONS OF MOTION

The equations of motion, or the dynamic or conservation of momentum equations, are based on Newton's Second Law of motion. It is important to determine the forces that act to change the motion of an infinitesimal control body as it passes a particular point. Of similar importance is to determine the acceleration of the infinitesimal control body at the same instant. Figure A-2 shows the surface forces on an elementary control volume of a fluid element in cartesian coordinates at the instant when its centre is at the point (x,y,z). The element is bounded by orthogonal planes normal to the axes of coordinates and its dimensions are Δx, Δy, and Δz. Three types of forces can be considered, namely, (i) forces due to normal stresses, (ii) forces due to tangential stresses, and (iii) body forces (distinguished from the foregoing surface surface). Body forces are usually distributed through the volume of the element and act through the centre. They are proportional to the mass. Body forces per unit mass are always parallel to the axes repectively. In their simplest form, they represent the components of the weight with respect to an arbitrary system of coordinates. The symbol σ is used for normal stress and τ for tangential stress. Since the tangential stresses may act in two rectilinear directions in each of three orthogonal planes, six intensities must be distinguished at the centroid: τ_{xy}, τ_{yx}, τ_{yz}, τ_{zy}, τ_{zx}, and τ_{xz}. A double script convention is used to identify stress components; the first subscript indicates the direction of the normal to the surface on which the stress component acts, and the second the direction of the component. A stress component is positive if it has the same sense and direction as the normal to that surface (tensile). In the general case there are nine stress components, as follows:

$$\begin{bmatrix} \sigma_{xx} & \tau_{xy} & \tau_{xz} \\ \tau_{yx} & \sigma_{yy} & \tau_{yz} \\ \tau_{zx} & \tau_{zy} & \sigma_{zz} \end{bmatrix}$$

Summing moments of the stresses tending to accelerate the element in the angular sense about

a centroidal axis normal to the xy-plane would give, (figure A-3):

$$(\tau_{xy}\ \Delta y\ \Delta z)\ \Delta x\ -\ (\tau_{yx}\ \Delta x\ \Delta z)\ \Delta y\ =\ \frac{dI}{dt} \qquad \textbf{(A-13)}$$

where I = angular momentum. The angular momentum depends on the density, volume, and the square of an effective radius of gyration. As the sides of the element become smaller, the right-hand side of the above equation tends to zero more rapidly than the left-hand side. Therefore:

$$(\tau_{xy}\ \Delta y\ \Delta z)\ \Delta x\ -\ (\tau_{yx}\ \Delta x\ \Delta z)\ \Delta y\ =\ 0 \qquad \textbf{(A-14)}$$

Simplifying and rearranging gives: $\tau_{xy} = \tau_{yx}$. By similar reasoning the following can be obtained: $\tau_{yz} = \tau_{zy}$ and $\tau_{zx} = \tau_{xz}$.

Binder (1958) showed that the total shear stresses are expressed as:

$$\begin{aligned}
\tau_{xy} &= \tau_{yx} = \mu\left[\frac{\partial v}{\partial x} + \frac{\partial u}{\partial y}\right] \\
\tau_{yz} &= \tau_{zy} = \mu\left[\frac{\partial w}{\partial y} + \frac{\partial v}{\partial z}\right] \\
\tau_{zx} &= \tau_{xz} = \mu\left[\frac{\partial u}{\partial z} + \frac{\partial w}{\partial x}\right]
\end{aligned} \qquad \textbf{(A-15)}$$

With reference to figure A-2, summing the forces in the x-direction gives:

$$F_x = \left[\frac{\partial \sigma_{xx}}{\partial x} + \frac{\partial \tau_{zx}}{\partial z} + \frac{\partial \tau_{yx}}{\partial y}\right] \Delta x\ \Delta y\ \Delta z \qquad \textbf{(A-16)}$$

and the resultant surface force per unit volume at the point (x,y,z) is:

$$f_x = \frac{\partial \sigma_{xx}}{\partial x} + \frac{\partial \tau_{xy}}{\partial y} + \frac{\partial \tau_{xz}}{\partial z} \qquad \textbf{(A-17)}$$

In a similar manner:

$$f_y = \frac{\partial \tau_{xy}}{\partial x} + \frac{\partial \sigma_{yy}}{\partial y} + \frac{\partial \tau_{yz}}{\partial z}$$

$$f_z = \frac{\partial \tau_{xz}}{\partial x} + \frac{\partial \tau_{yz}}{\partial y} + \frac{\partial \sigma_{zz}}{\partial z} \qquad \textbf{(A-18)}$$

It can be concluded that the force per unit volume in a particular direction consists of gradients of the stress components which act in that direction. As far as the normal stresses are concerned, Binder (1958) showed that:

$$\sigma_{xx} = - P + 2 \mu \frac{\partial u}{\partial x}$$

$$\sigma_{yy} = - P + 2 \mu \frac{\partial v}{\partial y} \qquad \textbf{(A-19)}$$

$$\sigma_{zz} = - P + 2 \mu \frac{\partial w}{\partial z}$$

where P = fluid pressure. For a condition where the body is in a generally stressed case the following can be written for a unit volume of fluid in the x-, y-, and z-directions, respectively:

$$\rho \frac{Du}{Dt} = \rho F_x + \frac{\partial \sigma_{xx}}{\partial x} + \frac{\partial \tau_{yx}}{\partial y} + \frac{\partial \tau_{zx}}{\partial z} \qquad \textbf{(A-20)}$$

$$\rho \frac{D v}{D t} = \rho F_y + \frac{\partial \tau_{xy}}{\partial x} + \frac{\partial \sigma_{yy}}{\partial y} + \frac{\partial \tau_{zy}}{\partial z} \qquad \textbf{(A-21)}$$

$$\rho \frac{D\ w}{D\ t} = \rho\ F_z + \frac{\partial \tau_{xz}}{\partial x} + \frac{\partial \tau_{yz}}{\partial y} + \frac{\partial \sigma_{zz}}{\partial z} \qquad \textbf{(A-22)}$$

where: F_x, F_y and F_z = body forces per unit mass in the x, y and z directions respectively. If u changes by Δu in time Δt as the fluid element travels then:

$$\Delta\ u = \frac{\partial u}{\partial t}\ \Delta t + \frac{\partial u}{\partial x}\ \Delta x + \frac{\partial u}{\partial y}\ \Delta y + \frac{\partial u}{\partial z}\ \Delta z \qquad \textbf{(A-23)}$$

and in the limit as Δx, Δy and Δz tend to zero:

$$\frac{Du}{Dt} = \frac{\partial u}{\partial t} + u\ \frac{\partial u}{\partial x} + v\ \frac{\partial u}{\partial y} + w\ \frac{\partial u}{\partial z} \qquad \textbf{(A-24)}$$

Applying Newton's Second Law of motion, neglecting higher order terms, rearranging and simplifying (manipulating eq. A-13 to A-24) gives the 3-D equations of motion:

$$\frac{\partial u}{\partial t} + u\ \frac{\partial u}{\partial x} + v\ \frac{\partial u}{\partial y} + w\ \frac{\partial u}{\partial z} = F_x - \frac{1}{\rho}\ \frac{\partial P}{\partial x} + \nu\ \nabla^2 u \qquad \textbf{(A-25)}$$

$$\frac{\partial v}{\partial t} + u\ \frac{\partial v}{\partial x} + v\ \frac{\partial v}{\partial y} + w\ \frac{\partial v}{\partial z} = F_y - \frac{1}{\rho}\ \frac{\partial P}{\partial y} + \nu\ \nabla^2 v \qquad \textbf{(A-26)}$$

$$\frac{\partial w}{\partial t} + u\ \frac{\partial w}{\partial x} + v\ \frac{\partial w}{\partial y} + w\ \frac{\partial w}{\partial z} = F_z - \frac{1}{\rho}\ \frac{\partial P}{\partial z} + \nu\ \nabla^2 v \qquad \textbf{(A-27)}$$

where ν = fluid kinematic viscosity, and

$$\nabla^2 = \frac{\partial^2}{\partial x^2} + \frac{\partial^2}{\partial y^2} + \frac{\partial^2}{\partial z^2}$$

The fluid flow in a river is 3-D and time-dependent. Hydrostatic pressures can be ordinarily assumed in the case of a tranquil river flow because this type of flow is horizontal. In addition, only shear stresses from horizontal velocity components are important. In the classical approach, it is further assumed that gross motions only are considered and the effects of small-scale velocity fluctuation are aggregated into shear stress terms. Furthermore, it will be assumed that the mass densities of the substances transported in the river are very small compared to the density of water. In such a case, the density of water is considered constant in the whole region under investigation and is not influenced in time and/or space by changes in the mass density of the transported substances.

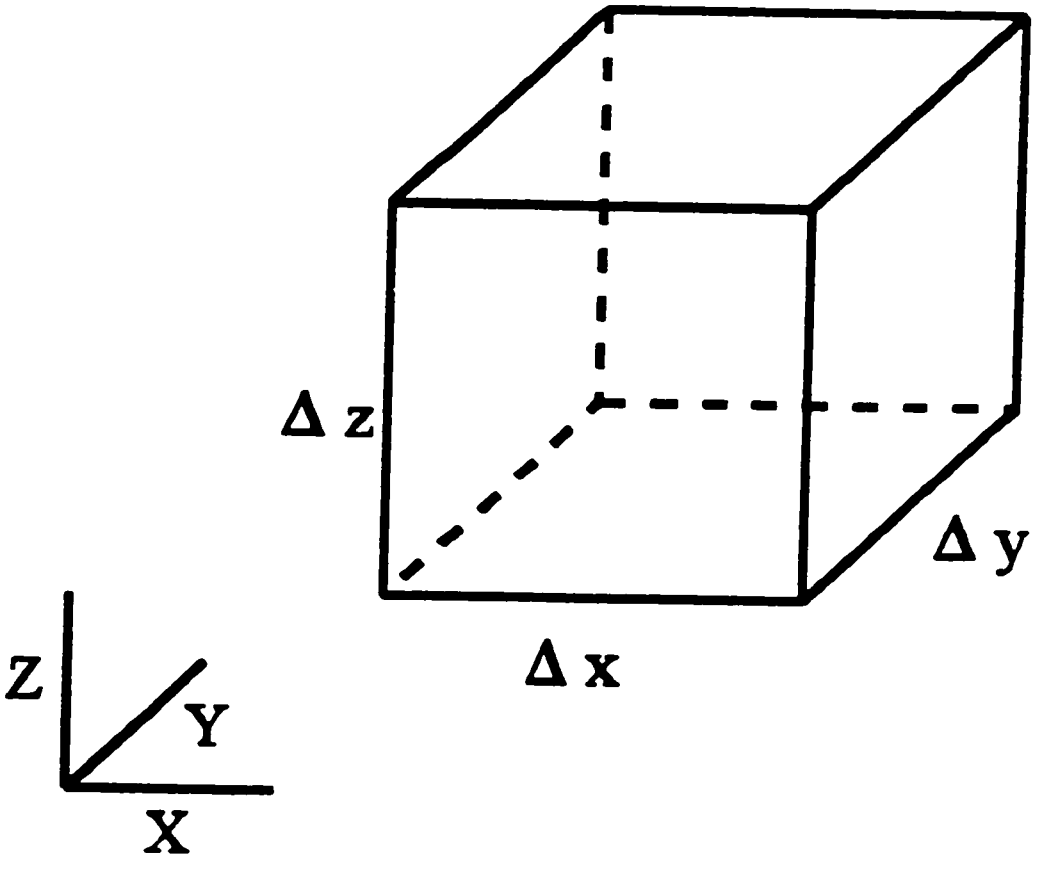

Figure A-1 Definition Sketch of an Elementary Control Volume.

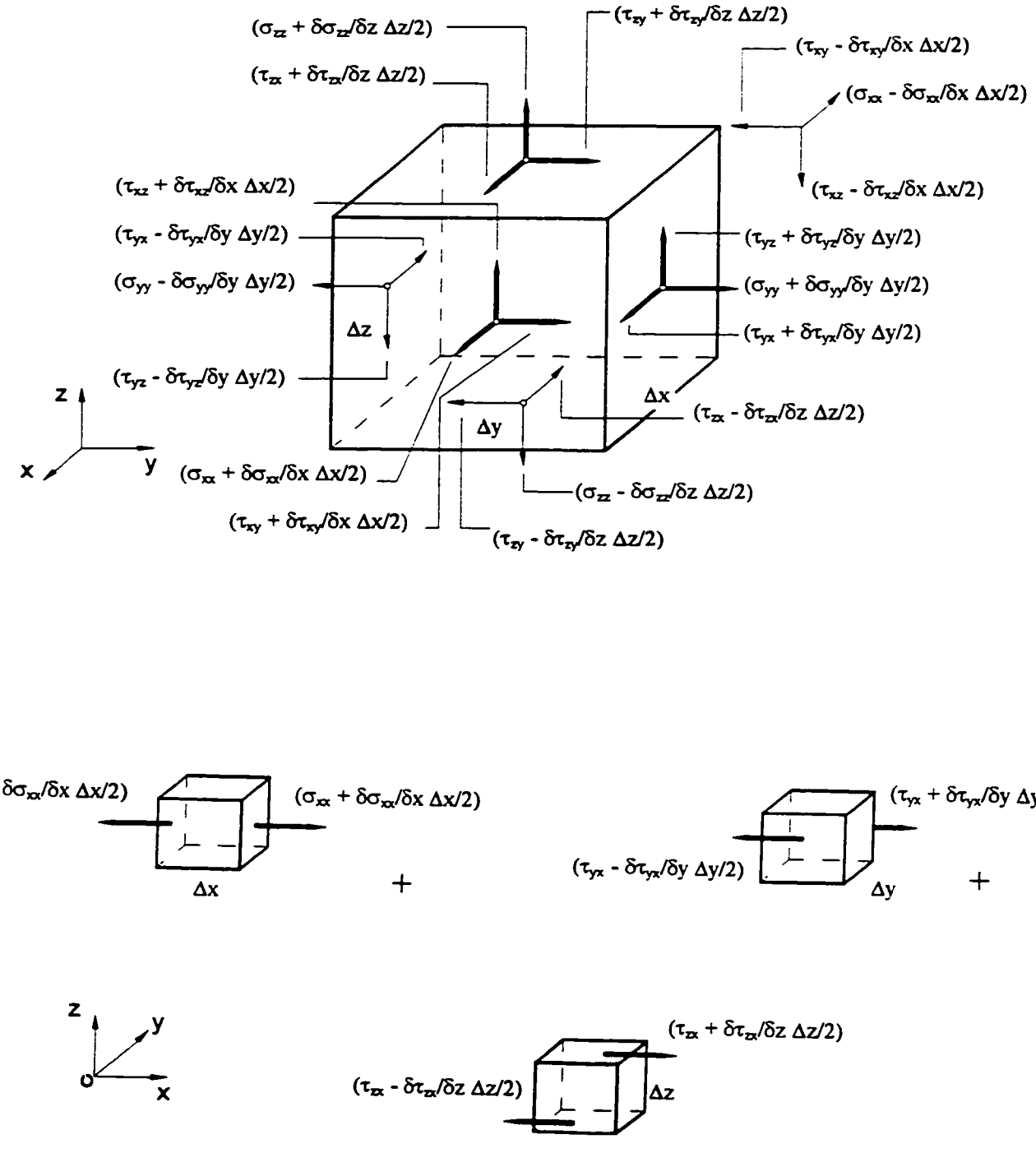

Figure A-2 Surface Forces on Elementary Control Volume.

APPENDIX B

MATHEMATICAL FORMULATION OF THE TRANSPORT PROBLEM

B.1 INTRODUCTION

Physical hydraulic models are generally more expensive than computer models. However, for some situations they may have a great advantage over computer models, especially for 3-D flows. In a sense a hydraulic model can educate the investigator about various phenomena at the time that a computer model can not handle all large scale phenomena in 3-D, often with transients. Hydraulic models have their limitations too. The scaling is done by the Froude law, because gravity effects including buoyancy are usually important. Consequently, the Reynolds numbers are much reduced from the prototype, altering turbulence and resistance characteristics.

The mean velocity in the cross-section V_o is related to the mean wall shear stress τ_o by the relation: $\tau_o = f \rho V_o^2 / 8$, where f is the familiar Darcy-Weisbach friction factor. For convenience, the shear velocity u_* is defined as: $u_* = \sqrt{(\tau_o/\rho)}$. For circular pipes, f may be estimated from the familiar pipe friction (or Moody) diagram. For wide open channels and other nearly-symmetric shapes, the Moody diagram may also be used when the pipe diameter

is replaced by 4 R, where R is the hydraulic radius. The mean shear stress τ_o may be found directly from the balance of forces as: $\tau_o = \rho\, g\, R\, S$, and consequently, $u_* = \sqrt{(g\, R\, S)}$.

B.2 FICK'S LAW

Fick's Law states that a flux of solute mass, that is the mass of a solute crossing a unit area per unit time in a given direction, is proportional to the gradient of solute concentration in that direction. Fick's Law is represented in 3-D by the following relationship:

$$q = - D \nabla c \qquad \textbf{(B-1)}$$

where:

q = solute mass flux vector with components in the three directions of a Cartesian coordinate system,

c = mass concentration of diffusing solute,

D = coefficient of proportionality or diffusion, (the minus sign indicates transport is from high to low concentrations), and

$$\nabla = \frac{\partial}{\partial x} + \frac{\partial}{\partial y} + \frac{\partial}{\partial z}$$

B.3 DIFFUSIVE FLUX

Starting with a certain elemental volume and applying the conservation of mass, one can obtain a second relationship in addition to Fick's Law. This relationship is true irrespective of the type of the transport process. Combining these two results leads to a partial differential equation that describes the diffusion processes.

Figure B-1 illustrates a 1-D transport process in which mass is being transferred in the x-direction. Two parallel surfaces of unit area are drawn perpendicular to the x-axis and

separated by a distance. Let c(x,t) be the mass per unit volume at the point x at time t. Then, there is a mass $c(x,t)\Delta x$ in the line segment bounded by the parallel planes. Since molecules are passing in and out of the volume defined by each bounding surface, there is a time rate of change of mass in the volume equal to:

$$\frac{\partial c}{\partial t}\,\Delta x$$

The time rate of change must be equal to the difference in the flux, or rate of passage of molecules, through each surface. Suppose the mass rate of flow across the unit surface located at x is q(x,t) then the mass rate of flow per unit area across the surface at $x+\Delta x$ is simply:

$$q(x,t) + \frac{\partial\, q(x,t)}{\partial x}\,\Delta x$$

and the difference between the two is:

$$\frac{\partial q}{\partial x}\,\Delta x$$

In order to satisfy conservation of mass, this difference must be equal to the rate of change of mass in the volume, thus equating the two gives:

$$\frac{\partial q}{\partial x} + \frac{\partial c}{\partial t} = 0 \qquad \textbf{(B-2)}$$

Substituting Fick's Law gives:

$$\frac{\partial c}{\partial t} = D\,\frac{\partial^2 c}{\partial x^2} \qquad \textbf{(B-3)}$$

Alternatively, differentiating eq. B-2 with respect to x, substituting Fick's Law and re-

arranging:

$$\frac{\partial q}{\partial t} = D \frac{\partial^2 q}{\partial x^2} \qquad \textbf{(B-4)}$$

The above equation is known as the diffusion equation, which describes how mass is transferred by Fickian diffusion processes.

The previous results can be extended to more than 1-D using a vector notation. Consider a fixed volume ψ with surface area S. The concentration of tracer mass is a function of position x and time t, so that the total mass in the volume ψ is:

$$\int_{\psi} c(x,t)\ d\psi$$

If the mass flux is q(x,t) then conservation of mass requires that:

$$\frac{\partial}{\partial t} \int_{\psi} c(x,t)\ d\psi + \int_{S} [\ q(x,t)\ .\ nn]\ dS = 0 \qquad \textbf{(B-5)}$$

where nn = unit vector normal to surface element dS. Using Green's Theorem, and noting that ψ is a fixed volume, we have:

$$\int_{\psi} [\frac{\partial c}{\partial t} + \nabla\ q]\ d\psi = 0 \qquad \textbf{(B-6)}$$

For molecular processes the flux is specified by Fick's Law and the diffusion equation in 3-D becomes:

$$\frac{\partial c}{\partial t} = D\ \nabla^2 c \qquad \textbf{(B-7)}$$

or written fully in 3-D in a Cartesian system of coordinates:

$$\frac{\partial c}{\partial t} = D \left[\frac{\partial^2 c}{\partial x^2} + \frac{\partial^2 c}{\partial y^2} + \frac{\partial^2 c}{\partial z^2} \right] \qquad \textbf{(B-8)}$$

B.4 ADVECTIVE FLUX

The above derivations are based on the assumption that the fluid is stationary and that the mass is transported by diffusion alone. However, in most cases the fluid is moving with a velocity vector **u** with components u, v, and w in the x, y, and z directions respectively. **The transport by the mean motion of the fluid is referred to as advection.** It is assumed that the transport by advection and by diffusion are separate entities and they are additive processes. This is equivalent to assuming that diffusion takes place within the moving fluid just as though the fluid were stationary.

The rate of mass transport through a unit area in the yz plane c multiplied by the component of velocity in the x direction u is the quantity uc, because this is the rate at which fluid volume passes through the unit area multiplied by the concentration of mass in that volume. The total rate of mass transport is the advective plus the diffusive fluxes:

$$q = u\,c + \left[-D \frac{\partial c}{\partial x}\right] \qquad \textbf{(B-9)}$$

which when substituted into the equation of conservation of mass in 1-D gives:

$$\frac{\partial c}{\partial t} + \frac{\partial (u\,c)}{\partial x} = D \frac{\partial^2 c}{\partial x^2} \qquad \textbf{(B-10)}$$

In a similar manner to obtaining the diffusion equation, the above equation can be extended to 3-D as:

$$\frac{\partial c}{\partial t} + \nabla(u\ c) = D\ \nabla^2 c \qquad \textbf{(B-11)}$$

Based on the equation of conservation of a fluid volume:

$$\nabla u = 0 \qquad \textbf{(B-12)}$$

then:

$$\frac{\partial c}{\partial t} + u\ \nabla\ c = D\ \nabla^2 c \qquad \textbf{(B-13)}$$

Written fully in Cartesian coordinates, the advection-diffusion equation is:

$$\frac{\partial c}{\partial t} + u\ \frac{\partial c}{\partial x} + v\ \frac{\partial c}{\partial y} + w\ \frac{\partial c}{\partial z} = D\ \left[\ \frac{\partial^2 c}{\partial x^2} + \frac{\partial^2 c}{\partial y^2} + \frac{\partial^2 c}{\partial z^2}\ \right] \qquad \textbf{(B-14)}$$

Two simple limiting solutions of the advection-diffusion equation exist in a fluid moving with a constant velocity u in the x-direction only. In the first the gradients in the y-direction are small(longitudinal):

$$\frac{\partial c}{\partial t} + u\ \frac{\partial c}{\partial x} = D\ \frac{\partial^2 c}{\partial x^2} \qquad \textbf{(B-15)}$$

and in the second the diffusive transport in the x-direction is smaller than the advective transport (transverse), so that:

$$\frac{\partial c}{\partial t} + u\ \frac{\partial c}{\partial x} = D\ \frac{\partial^2 c}{\partial y^2} \qquad \textbf{(B-16)}$$

B.5 TURBULENT FLOWS

Fischer et al. (1979) reported that the spread of the ensemble mean concentration may be described by a diffusion equation whose simplest 3-D form is:

$$\frac{\partial c}{\partial t} = \epsilon_x \frac{\partial^2 c}{\partial x^2} + \epsilon_y \frac{\partial^2 c}{\partial y^2} + \epsilon_z \frac{\partial^2 c}{\partial z^2} \qquad \textbf{(B-17)}$$

where: ϵ_x, ϵ_y, and ϵ_z = empirical mixing coefficient in the x-, y-, and z-directions respectively. Eq. B-17 is written for zero mean flow velocity, as in Taylor's analysis. If the fluid has a mean velocity it is necessary to add the advection terms.

The analogy with molecular diffusion can be taken further as follows. The equation for conservation of matter in turbulent flow, neglecting molecular diffusion and letting c be the time varying point concentration, is:

$$\frac{\partial c}{\partial t} + U' \frac{\partial c}{\partial x} + V' \frac{\partial c}{\partial y} + W' \frac{\partial c}{\partial z} = 0 \qquad \textbf{(B-18)}$$

where U', V', and W' are randomly varying velocities. If the above equation is averaged over a time long enough to average the turbulent velocity and concentration fluctuations, and if the time averages of the random velocities are zeros, then:

$$\frac{\partial \bar{c}}{\partial t} = - \frac{\partial \overline{U'c}}{\partial x} - \frac{\partial \overline{V'c}}{\partial y} - \frac{\partial \overline{W'c}}{\partial z} \qquad \textbf{(B-19)}$$

The overbar indicates the time average turbulent fluxes in the three directions. Comparing the above equation with the turbulent diffusion equation (eq. B-8) gives:

$$\overline{U'c} = -\epsilon_x \frac{\partial c}{\partial x}$$

$$\overline{V'c} = -\epsilon_y \frac{\partial c}{\partial y} \qquad \textbf{(B-20)}$$

$$\overline{W'c} = -\epsilon_z \frac{\partial c}{\partial z}$$

Comparison with Fick's law for molecular diffusion shows that ϵ_x, ϵ_y, and ϵ_z are the turbulent equivalents to the molecular diffusion coefficient. These parameters are often referred to as Fickian turbulent diffusion coefficients, or eddy diffusivities.

Thus, the general advection-diffusion equation in 3-D has the following form:

$$\frac{\partial c}{\partial t} + \frac{\partial (u\ c)}{\partial x} + \frac{\partial (v\ c)}{\partial y} + \frac{\partial (w\ c)}{\partial z} = \frac{\partial \left(\epsilon_x \frac{\partial c}{\partial x}\right)}{\partial x} + \frac{\partial \left(\epsilon_y \frac{\partial c}{\partial y}\right)}{\partial y} + \frac{\partial \left(\epsilon_z \frac{\partial c}{\partial z}\right)}{\partial z} \qquad \textbf{(B-21)}$$

The equation for the mass balance of a substance can be derived accounting for the presence of a source or sink, or if one of the constituents undergoes a certain chemical reaction and will take the following form:

$$\frac{\partial c}{\partial t} + \frac{\partial (u\ c)}{\partial x} + \frac{\partial (v\ c)}{\partial y} + \frac{\partial (w\ c)}{\partial z} - \frac{\partial \left(\epsilon_x \frac{\partial c}{\partial x}\right)}{\partial x} - \frac{\partial \left(\epsilon_y \frac{\partial c}{\partial y}\right)}{\partial y} - \frac{\partial \left(\epsilon_z \frac{\partial c}{\partial z}\right)}{\partial z} = \pm r\ c \pm s \qquad \textbf{(B-22)}$$

where:

r = reaction coefficient, and

s = sources or sinks present.

The first term on the left hand side of eq. B-22 expresses the rate of change of the mass concentration with time. The next three terms represent the advective transport, and the last three terms express the turbulent diffusive transport. Furthermore, the right hand side of eq. B-22 represents the rate of production or decay of the substance and the presence of any sources or sinks. The 3-D mass balance equation (eq. B-22) of a certain pollutant can be reduced into a 1- or 2-D form. In this instance, the following sections will discuss the advantages and limitations of using 1- or 2-D analogies.

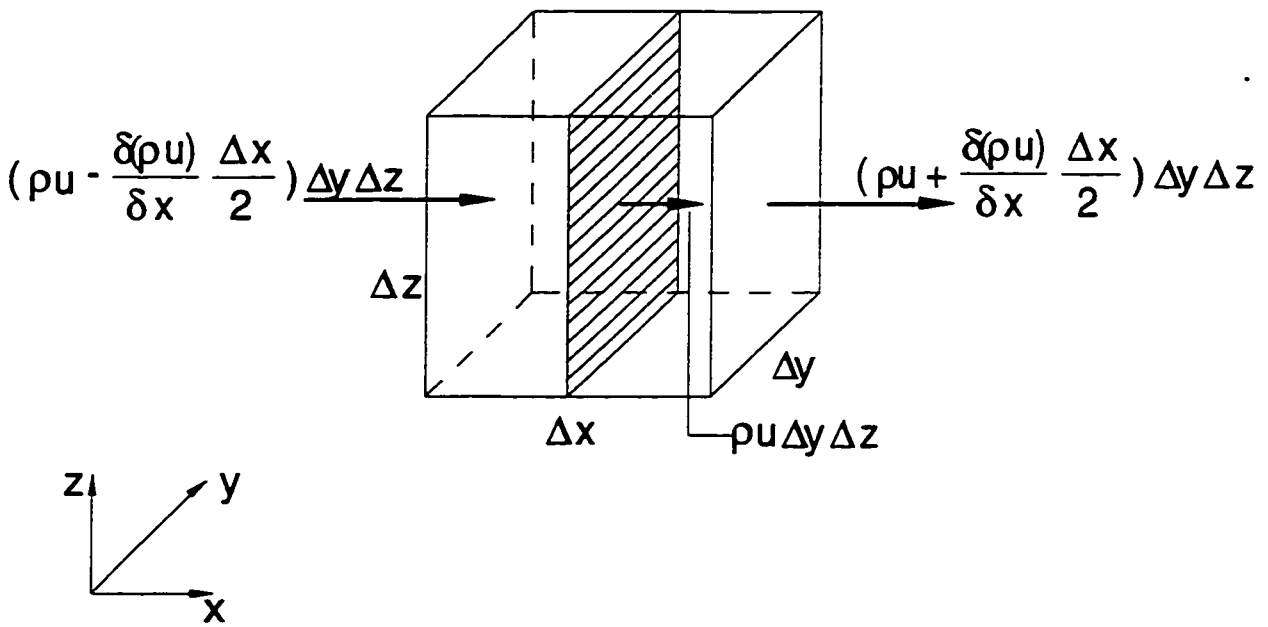

Figure B-1 1-D Transport Process in the x-Direction.

APPENDIX C

STATISTICAL CRITERIA FOR MODEL EVALUATION

C.1 INTRODUCTION

The representation of a hydraulic phenomenon by some mathematical relationships (or models) inevitably introduces some degree of inaccuracy. Other inaccuracies occur when representing the system of mathematical equations by FD and in producing the results. It is generally accepted that no single simulation model output will be identical in all respects to the physical phenomenon it aims to represent. However, it is required that this output be sufficiently close to its physical counterpart in order for the model simulation to be considered acceptable.

The principle of *goodness-of-fit* is a measure of the degree to which the output conforms to the corresponding observed data. *Goodness-of-fit* techniques may range from purely subjective graphical (visual) methods to purely objective techniques using mathematical and statistical relationships. These relationships usually portray the difference between simulated and observed variables.

Prior to any calibration or model application, the user should establish criteria for comparing simulated and observed variables. However, if too many criteria are used and are frequently switched, the assessment of the model performance becomes difficult. For example, if the model is intended to design sewers, then the primary variable of interest is the peak flow and calibration would be best made on a comparison between modelled and observed peak flows. On the other hand, in designing a storm detention basin, run-off volumes and possibly the hydrograph shape are important and calibration must be based on a comparison of simulated and observed volumes and hydrograph shapes. In a hydrodynamic flood routing and pollutant transport application, both the peak flow rates (or peak depths) and hydrograph shapes would be the criteria for comparison in the modelling exercise, in addition to pollutant concentration values in a water quality application.

C.2 GRAPHICAL METHOD

Related to model simulation assessment is the graphical method for calibration. It consists of plotting the observed and simulated hydrographs on the same graph. A visual comparison is then made of peak flows and hydrograph shapes. The importance of the graphical method should not be overlooked. Although subjective, it provides a rough appreciation of the model capabilities. Johnston and Pilgrim (1976) emphasized the importance of subjective impressions, based on the fact that even the choice of the form of a statistical fitting technique is still a subjective decision.

With a good understanding of the physical problem (and the effect of each model parameter on the simulation), the user can re-adjust parameters to obtain a better fit. Even though time consuming, this method is very instructive to the model user and helps in understanding the model performance under different conditions. This methodology is often used when there is only a limited number of measured events. However, it is usually thought to be highly subjective and difficult when comparing the performance of similar models. In these instances the user can only resort to statistical *goodness-of-fit* techniques.

C.3 STATISTICAL *GOODNESS-OF-FIT* TECHNIQUES

While the graphical calibration method is often referred to as a *trial and error* procedure, statistical *goodness-of-fit* techniques are more often associated with automatic optimization of parameters. A statistical goodness-of-fit procedure implies a method to measure, in some way, the deviation of a simulated output to that observed; the measurement thus obtained being an end in itself. On the other hand, a statistical fitting procedure employs this measure of deviation of the simulated output to assist in the calibration process; the objective being a simulated output more closely resembling that observed.

Statistical fitting procedures were used by Dawdy and O'Donnel (1965) to demonstrate the usefulness of automatic optimization for parameter calibration. Automatic optimization means systematic adjustment of model parameters, or sets of parameters, in such a way that the corresponding model output agrees more closely with the observed data after the adjustment. In this context, the statistical *goodness-of-fit* equation is called an objective function. For example, let G(x) be an objective function of the error in a model prediction which results from x_1, x_2, x_3, ..., x_n model input parameters. It would be required to minimize (or optimize) the value of G(x) by assigning a suitable choice of values to the individual elements in the vector x. A search must be employed to determine the location of the overall global minimum over the surface where G(x) is defined.

Several search methods are available. Nelder and Mead (1965) used the *Direct Search Simplex* method, whereas Fletcher and Powell (1963) used the *Steepest Descent* procedure. The optimization (or minimization) of the objective function G(x) can be achieved by changing several values of x until no significant reduction of the G(x)-value is recognized. Therefore, the goal of calibration would be to find the combination of model parameters that would minimize the objective function.

Different objective functions would ordinarily give more weight to a certain aspect of

disagreement between observed and simulated results. In general, the choice and role of the objective functions are aspects which offer serious difficulties to the model user. In a comparative study, Diskin and Simon (1977) concluded that the choice of the most appropriate objective function must be based on the nature of the problem to which the model is to be applied. Furthermore, this study favoured the consideration of more than one objective function when assessing the *goodness-of-fit* of a particular model for a given application. Ibbitt and O'Donnell (1971) expressed similar sentiments with regard to statistical fitting procedures. Aitken (1973) stated that the simulation model should have the ability to reproduce the mean and standard deviation of the observed values.

Goodness-of-fit equations for comparing two sets of data are often manifested in the following form:

$$\textit{Residual} = (\textit{Observed value}) - (\textit{Simulated value}) \qquad \textbf{(C-1)}$$

C.3.1 Sum of Squares (SS) Criteria

One of the most widely used objective functions for model comparison studies or model calibration and parameter optimization is the sum of squares criterion:

$$G = \sum_{i=1}^{n} [\, q_o(t) - q_s(t)]_i^2 \qquad \textbf{(C-2)}$$

where:

G = sum of squares criterion,

$q_o(t)$ = observed peak value of a property at time t,

$q_s(t)$ = simulated peak value of a property at time t, and

n = number of coordinates in the hydrograph under consideration.

Clarke (1973) criticized the use of the sum of squares criterion unless consideration was given to the statistical properties of the residuals themselves. He based his criticism on

the fact that minimizing the least squares objective function was applied to simulations where the underlying assumptions, with regard to the statistical properties of the residuals, were seldom valid. In spite of the shortcomings of the sum of squares criteria, it has been widely used for model comparison and calibration.

C.3.2 Nash and Sutcliffe (N & S) Method

Nash and Sutcliffe (1970) used a dimensionless objective function that measured the efficiency of a model. It has the following form:

$$R^2 = \frac{F_o^2 - F^2}{F_o^2} \qquad \text{(C-3)}$$

where:

R = model efficiency parameter,

$$F^2 = \sum_{i=1}^{n} [q_o(t) - q_s(t)]_i^2$$

$$F_o^2 = \sum_{i=1}^{n} [q_o(t) - \bar{q}]_i^2$$

and $\bar{q}$ = the mean of observed values.

Nash and sutcliffe (1970) defined R^2 as the *index of agreement* and F_o^2 as the *initial variance.* The index of agreement would have a value of one for a perfect fit. In fact, dividing F_o^2 by the number of coordinates of the corresponding hydrograph would produce the variance of the observed data. The criticism of the SS and N & S criteria was based on the fact that a measure of accuracy should not be dependent on the number of hydrograph coordinates considered in the analysis.

C.3.3 Root Mean Square Error (RMSE) Method

To overcome the dilemma of the dependency of the objective function on the number of hydrograph coordinates, other accuracy measures, such as RMSE, were proposed in the literature. RMSE takes the following form:

$$RMSE = \{ \frac{1}{n} \sum_{i=1}^{n} [q_o(t) - q_s(t)]^2 \}^{\frac{1}{2}} \qquad \text{(C-4)}$$

RMSE was used by Patry and Marino (1983) to assess the performance of a non-linear functional run-off model as a criterion for comparison of hydrographs. The RMSE is a dimensional objective function with the dimensions of flow rate (or depth when comparing stage hydrographs, or concentration when comparing pollutographs).

C.3.4 Wood's Objective Function Method

Another criterion in hydrograph comparison and fitting assessment was proposed by Wood et al. (1974). His objective function has the following form:

$$G = \sum_{i=1}^{n} \{ \frac{q_o(t) - q_s(t)}{[q_o(t)]^b} \}_i^c \qquad \text{(C-5)}$$

where G = Wood's objective function and exponents b and c are referred to as *control parameters* (determined by trial and error procedures). These parameters govern the optimization strategy.

C.3.5 Standard Error of Estimate (SEE) Method

Another objective function was introduced which was not affected by the number of ordinates of the corresponding hydrographs or the record length. This statistic (SEE) was

dimensional with the dimensions of the property under consideration. SEE is defined as:

$$SEE = \{ \frac{1}{n - 2} \sum_{i=1}^{n} [q_o(t) - q_s(t)]^2 \}^{\frac{1}{2}} \quad \text{(C-6)}$$

C.3.6 Reduced Error of Estimate (REE) Method

REE, which was proposed by Manley (1977), has the following form:

$$REE = \{ \frac{\sum_{i=1}^{n} [q_o(t) - q_s(t)]^2}{\sum_{i=1}^{n} [q_o(t) - \bar{q}]^2} \}^{\frac{1}{2}} \quad \text{(C-7)}$$

This method has a major drawback, in that it emphasizes errors associated with large values of the property more than a sequence of errors at low values.

C.3.7 Proportional Error of Estimate (PEE) Method

To avoid the drawback of REE, Manley (1978) proposed this alternative method. The PEE method takes the following form:

$$PEE = \{ \frac{\sum_{i=1}^{n} [q_o(t) - q_s(t)]^2}{[\sum_{i=1}^{n} q_o(t)]^2} \}^{\frac{1}{2}} \quad \text{(C-8)}$$

C.4 RANDOM AND SYSTEMATIC ERRORS

The *goodness-of-fit* criteria perviously discussed involves residuals which may be either *random* or *systematic* in form. As the name implies, *random* error means that the model does not show any general trend of under- or over-estimation of values. On the other hand, a *systematic* error implies that the sign of the error persists over successive time

intervals. Aitken (1973) was the first to recognize the importance of systematic errors in assessing model performance and that existing criteria did not account much for these errors. This meant that, while one could obtain the optimal (minimum) value of an objective function, still the model performance was not satisfactory. This would happen when large positive errors counter-balance large negative errors. Hence, the overall calibration results would be misleading.

C.5 DETECTION OF SYSTEMATIC ERRORS

C.5.1 Aitken's Methods

To overcome the aforementioned shortcoming, Aitken (1973) proposed three different methods:

1- A simple sign test which compared the number of runs of positive and negative errors to the expected number of such runs.

2- A coefficient of determination, (CD), defined as:

$$CD = \frac{F_o^2 - \sum_{i=1}^{n} [\, q_o(t) - q_s(t)]_i^2}{F_o^2} \qquad \text{(C-9)}$$

where $q_s(t)$ = simulated value of a property at time t, obtained from the regression line of $q_o(t)$ on $q_s(t)$.

3- A residual mass curve coefficient, (RMCC), defined as:

$$RMCC = \frac{\sum_{i=1}^{n} (D_c - \overline{D}_c)_i^2 - \sum_{i=1}^{n} (D_c - D_e)_i^2}{\sum_{i=1}^{n} (D_c - \overline{D}_c)_i^2} \qquad \text{(C-10)}$$

where:

D_c = departure from the mean for the observed residual mass curve,

D_c = mean of departures from the mean for the observed mass curve, and

D_e = departure from the mean of estimated or simulated mass curve.

According to Aitken (1973), as the statistic measures the relationship between property sequence and not simply individual properties, it should indicate the presence of systematic errors. Hughes (1982) made use of the coefficient of efficiency (Nash and Sutcliffe, 1970), the coefficient of determination, and the residual mass curve coefficient in model calibration.

C.5.2 Coefficient of Persistence (CP)

Wallis and Todini (1975) pointed out the shortcoming of RMCC and proposed CP as another measure of accuracy. This coefficient is defined as:

$$CP = \sum_{i=1}^{k} \frac{A_i^2}{F^2} \qquad \text{(C-11)}$$

where:

k = number of positive and negative runs, and

A = individual area of each segment of deviation.

Eq. C-11 squares areas of segments of deviation created by numbers of consecutive

residuals of the same sign. Thus, the resulting CP value indicates a persistent over- or under-estimation of prediction. The term *coefficient of persistence* is possibly a misnomer as the CP value is not dimensionless, but has the dimensions of (time)^2.

C.6 SUMMARY AND RECOMMENDATIONS

When only limited data are available, the graphical calibration and validation (trial and error) technique is fairly efficient. On the other hand, depending on the type of model application, different measures of accuracy, or deviation between simulated and observed variables, can be adopted; such as:

$$\% \text{ Error in simulated peak value} = \frac{q_s(t) - q_o(t)}{q_o(t)} \times 10 \qquad \text{(C-12)}$$

Another criterion, based on Aitken's (1973) assertion that any model should be capable of reproducing the mean of the observed values, was considered. This was:

$$\% \text{ Error in mean value} = \frac{\bar{q}_s - \bar{q}}{\bar{q}} \times 100 \qquad \text{(C-13)}$$

where q_s = the mean simulated value of a property.

When a large amount of observed data is available, a more comprehensive, systematic and detailed calibration effort is required. This form of calibration would largely depend on the choice of the objective function used in the automatic calibration process. The selection of the objective function should consider possible measures of accuracy that would not depend on the number of hydrograph ordinates considered in the analysis. This is especially true when comparison of the performance of different models, based on a relatively large number of events, is involved.

C.6.1 Dimensional, Ordinate dependent, Shape Factors

The sum of squares and the sum of absolute residuals were considered adequate indications for comparison of simulated and observed data having the same number of ordinates. However, to compare the performance of different models, based on several events, it seemed reasonable to compare the following criteria:

1- Total overall sum of squared residuals (TSSR):

$$TSSR = \sum_{j=1}^{m} \{ \sum_{i=1}^{n_j} [q_{ot} - q_{st}]_i^2 \}_j \qquad \text{(C-14)}$$

where:

q_{ot} = observed value of a property at time t,

q_{st} = simulated value of a property at time t,

n_j = number of ordinates in event j, and

m = number of events.

2- Total overall sum of absolute deviations (TSAR):

$$TSAR = \sum_{j=1}^{m} \{ \sum_{i=1}^{n_j} | q_o(t) - q_s(t) |_i \}_j \qquad \text{(C-15)}$$

In some instances, the percentage error in simulated volume may indicate good agreement between simulated and observed total volumes, whereas the shapes of the respective hydrographs may be considerably different. This difference can be defined as:

$$\overline{A} = \sum_{i=1}^{n} \left| \frac{(Residual)_i + (Residual)_{i+1}}{2} \Delta t \right|_i \qquad \text{(C-16)}$$

where:

A = sum of absolute areas of divergence between the two hydrographs, and

Δt = time step.

3- Total overall sum of absolute areas of divergence (TSAA):

$$TSAA = \sum_{j=1}^{m} \overline{A}_j \qquad \textbf{(C-17)}$$

where A_j = sum of absolute areas of divergence from event j.

C.6.2 Dimensional, Ordinate Independent, Shape Factors

1- The sum of squared residuals (S^2):

$$S^2 = \frac{1}{n} \sum_{i=1}^{n} [\, q_o(t) - q_s(t)]_i^2 \qquad \textbf{(C-18)}$$

S^2 can be defined as the variance. The standard deviation is obtained by taking the square root of the variance.

2- The mean deviation for one event (MD) is defined as:

$$MD = \frac{1}{n} \sum_{i=1}^{n} | \, q_o(t) - q_s(t) \, |_i \qquad \textbf{(C-19)}$$

3- The sum of absolute area of divergence for one event is (A/n), where n is defined as the number of ordinates in that event.

Because of its simplicity, the coefficient of efficiency proposed by Nash and Sutcliffe (1970) had an appealing aspect. The proportional error of estimate (Manley, 1978) is also attractive as it gives equal weight to equal proportional errors rather than to equal absolute errors.

C.7 CONCLUSIONS

No single statistical goodness-of-fit criterion is sufficient to assess adequately the measure of fitness between simulated and observed hydrographs. Ultimately, the selected objective function should depend on the objective of the modelling exercise, as different criteria are weighted in favour of different hydrograph variables.

For the present research, different statistical *goodness-of-fit* techniques were employed to evaluate the performance and validation of the new hydrodynamic model. The graphical assessment technique was employed occasionally. Simulated results were compared with observed data on the same graphs and a visual check was performed. This method gives a good appreciation of the effect of parameter variation on model performance. However, it may be misleading on some occasions when a visual check is made for the rising and recession parts of the hydrograph. A visual check may appear to have an excellent fit, but the actual relative error at a particular point might rise to 30 % in some instances.

Statistical *goodness-of-fit* techniques used in this research to evaluate model performance included: sum of squares criteria, Nash and Sutcliffe (N & S) method, RMSE, SEE, REE, and PEE. An alternative method, which determined the relative percent error at every point of the simulated hydrograph, is relied on. Absolute values of the corresponding relative percent errors at every point are then summed to give the total absolute percent relative error or the total absolute relative error (TARE). In general, hydrographs with the least total absolute relative errors would give the best-fit. Therefore, except for N&S criteria which should approach 1, the goal is to minimize the objective function to obtain the best-fit hydrograph.

IMAGE EVALUATION TEST TARGET (QA-3)

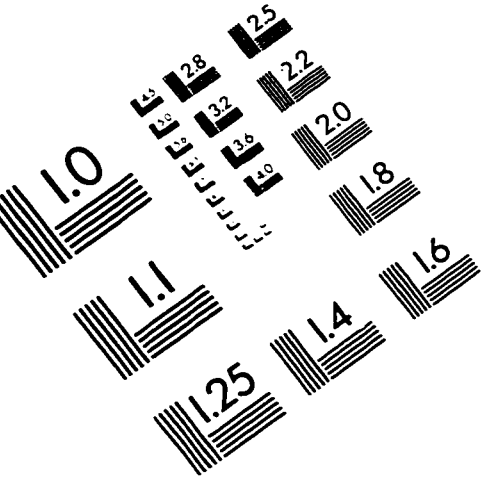

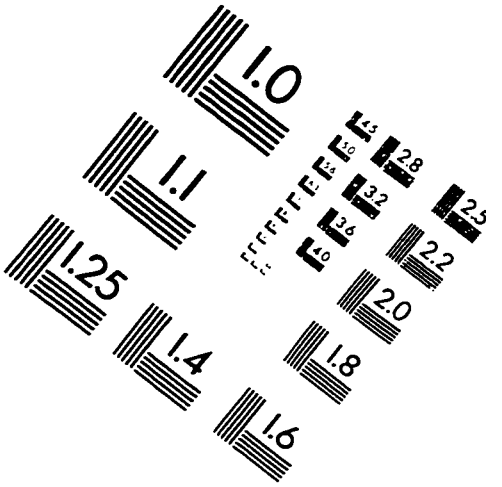

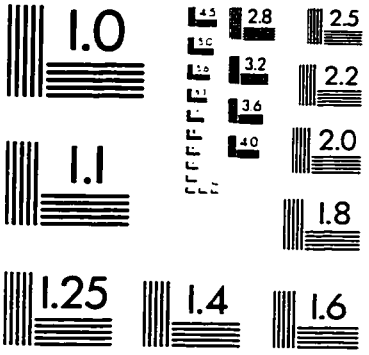

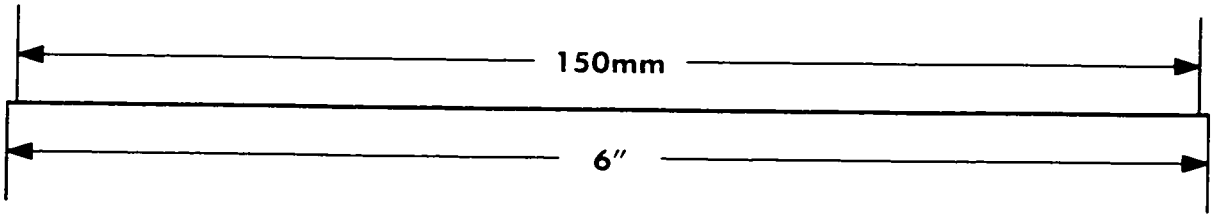

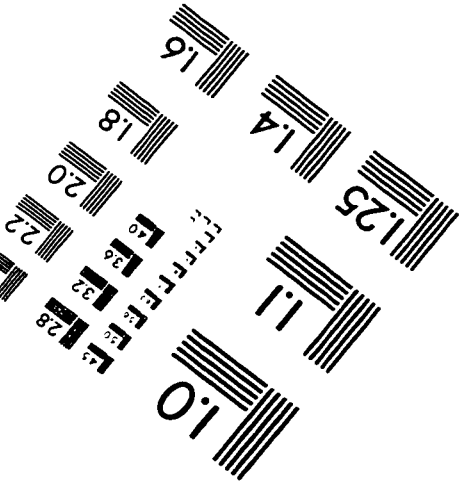

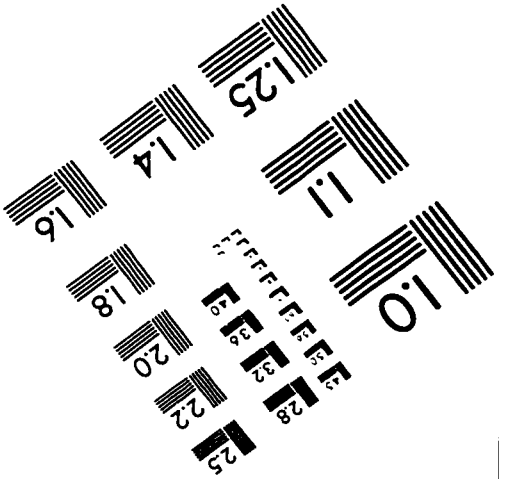

APPLIED IMAGE, Inc
1653 East Main Street
Rochester, NY 14609 USA
Phone: 716/482-0300
Fax: 716/288-5989